The effect of gender on *Helicobacter pylori* and gastric cancer

by

Alexander Sheh

B.S., Biological Engineering (2003)
Cornell University

Submitted to the Department of Biological Engineering
in Partial Fulfillment of the Requirements for the Degree of

Doctor of Philosophy Degree in Biological Engineering

at the

Massachusetts Institute of Technology

June 2011

© 2011 Massachusetts Institute of Technology
All rights reserved

Signature of Author _____

Department of Biological Engineering
Division of Comparative Medicine
April 11, 2011

Certified by _____

James G. Fox
Professor, Department of Biological Engineering
Director, Division of Comparative Medicine
Thesis Co-supervisor

Accepted by _____

Forest M. White
Co-chairman, Department Committee on Graduate Students
Associate Professor of Biological Engineering

A thesis advisory committee consisting of the following members has examined this doctoral thesis:

David B. Schauer
Professor, Department of Biological Engineering and Division of Comparative Medicine
Thesis Co-supervisor

Leona D. Samson
Director, Center for Environmental Health Sciences
Professor of Toxicology, and Biological Engineering
American Cancer Society Research Professor
Committee Chair

Andrew Camilli
Investigator, Howard Hughes Medical Institute
Professor of Molecular Biology and Microbiology at Tufts University School of Medicine

Jacquin C. Niles
Pfizer-Laubach Career Development Assistant Professor of Biological Engineering

The effect of gender on *Helicobacter pylori* and gastric cancer
By Alexander Sheh

Submitted to the Department of Biological Engineering on
April 11, 2011, in Partial Fulfillment of the Requirements for the Degree of
Doctor of Philosophy Degree in Biological Engineering

ABSTRACT

Gastric cancer is the 2nd leading cause of cancer death worldwide and the 4th most commonly diagnosed cancer worldwide. *Helicobacter pylori* infection is the major risk factor of gastric cancer, and as such, this bacterium has been classified as a type 1, or definite, carcinogen by the International Agency for Research on Cancer. *H. pylori* infects the gastric mucosa of more than half of the world's population and promotes gastric carcinogenesis by inducing chronic inflammation. Over decades of persistent *H. pylori* infection and chronic inflammation, the stomach goes through a well characterized pathological progression involving chronic gastritis, atrophy, intestinal metaplasia, dysplasia, and ultimately cancer. Interestingly, there are strong gender differences in the development of gastric cancer, as men are twice as likely to develop the disease than women. Given the importance of *H. pylori* and chronic inflammation in gastric carcinogenesis, this thesis investigated the role of gender in modulating host immune responses to *H. pylori*. The aims of this thesis explored 1) the effect of gender on *H. pylori*'s ability to induce mutations and 2) the effect of estrogen and the anti-estrogen, Tamoxifen, on *H. pylori*-induced gastric cancer. For the first aim, the *gpt* delta mouse model, a murine mutational analysis model, was used to study chronic infection with *H. pylori*. Increased frequency of point mutations was observed in infected female mice at 12 months post infection. These mutations

were not observed in infected male mice. Further analysis revealed that *H. pylori* induced a greater immune response in female mice in this model, as measured by increased severity of gastric lesions, decreased bacterial counts and the higher levels of Th1 antibodies for *H. pylori*. The spectra of mutations pointed towards oxidative damage as the underlying cause of induction. This study revealed that gender differences in mutagenesis were mediated by the severity and duration of the immune response.

In the second aim, 17β-estradiol prevented the formation of gastric cancer in the INS-GAS mouse model, which develops gastric cancer in a male-predominant manner. Unexpectedly, this study led to the discovery that Tamoxifen may act as an agonist in this model of gastric cancer, as it was able to prevent gastric cancer using mechanisms similar to 17β-estradiol. Both compounds downregulated pathways associated with cellular movement and cancer. CXCL1, a murine homolog of IL-8, was downregulated by treatment at both local and systemic levels, which led to a decreased neutrophilic infiltrate. 17β-estradiol and Tamoxifen mediated the disruption of a positive feedback loop coupling CXCL1 secretion with neutrophil recruitment, which dampened the activation of proinflammatory and oncogenic pathways, leading to protection against gastric cancer. In conclusion, these studies provide further insight into the role of gender modulation of host immune response in *H. pylori*-induced mutagenesis and carcinogenesis.

Thesis Co-supervisor: James G. Fox
Title: Professor, Department of Biological Engineering
Director, Division of Comparative Medicine

Thesis Co-supervisor: David B. Schauer

Title: Professor, Department of Biological Engineering and Division of Comparative Medicine

Acknowledgements

This thesis is dedicated in loving memory of David Schauer, a mentor and friend.

First and foremost, I'd like to thank God for bringing me to MIT and for His providence and sustenance during this PhD. He has also provided me with great colleagues and friends for whom I am deeply grateful. To my two wonderful advisors, David Schauer and James Fox, I am thankful for the ways that you complemented each other in mentoring an inexperienced graduate student. I will always recall your patience and investment of time in my work, and your meaningful contributions and insights that made it all possible. Thank you for allowing me to sample a wide swath of the research related to *H. pylori* pathogenesis but also for teaching me to focus and distill the relevant questions when necessary. I am appreciative of my many colleagues in DCM and the Schauer lab who were always attentive for discussions on research, life and family.

I'd also like to thank a lot of good friends that I've made throughout my time at MIT. To Abhinav Arneja, Bonnie Huang, Brandon Kwong, Carol Koh, James Mutamba, Megan McBee, Mike Murrell, Nidhi Shrivastav, and Ta-Chun Hang, thanks for lots of good times at lunch, coffee and otherwise discussing intricacies of science, movies and every other topic. You've all helped me become a better scientist and friend. Finally, to my loving wife, Karen, our son, Nicholas, and our child-to-be, I love you all so much. Your love helped me through this. I am truly blessed.

Table of Contents

List of Figures and Tables

Chapter 1: Introduction

1.1 Gastric cancer

Overview. Cancer is the leading cause of deaths worldwide, accounting for 7.6 million deaths worldwide (13% of all deaths) in 2008[1]. In 2008, there were 989,000 cases of gastric cancer diagnosed and 738,000 gastric cancer associated deaths, making gastric cancer the fourth most common cancer and the second leading cause of cancer death[1]. The high mortality to incidence ratio (0.75) is due in part to the lack of clinical symptoms in most cases of early gastric cancer, which makes screening and treatment difficult. At diagnosis, gastric cancer is usually at an advanced stage, making prognosis poor and the overall 5-year survival rate less than 25%[2].

Up until 1985, gastric cancer was the number one cause of cancer deaths worldwide[3]. At the time, the causes and pathogenesis of stomach cancer were not well understood, but for reasons unknown, a gradual decline in the incidence of gastric cancer had been observed over the last several decades. Improvements in sanitation and nutrition are believed to have contributed by increasing the amount of fresh fruits and vegetables available and by decreasing dietary salt intake. In the field of medicine, the development of endoscopies allowed for better management of precancerous lesions. However, it was the discovery in 1982 of a curved bacillus in the stomachs of patients with gastritis and peptic ulcers that revolutionized our understanding of the etiology and pathogenesis of gastric cancers[4]. This bacillus named, *Helicobacter pylori*, was recognized in 1994 by the International Agency for Research on Cancer (IARC) as a class I, or definite, carcinogen, for its role in the development of gastric cancer[5]. *H. pylori* was one of the first infectious agents recognized as a potential carcinogen. For their seminal discovery, Robin Warren and Barry Marshall were awarded the Nobel Prize in Medicine

in 2005. The decline in *H. pylori* infection, resulting from increased sanitation, improved nutrition, the common usage of antibiotics and changes in family structures due to modern life, is thought to be one of the main reasons for the decreased incidence of gastric cancer[6]. Nevertheless, despite falling incidence rates, the total number of new gastric cancer cases and deaths continues to increase worldwide due to overall population growth and aging in high-risk areas.

Epidemiology. Marked differences in gastric cancer incidence are observed based on geographical location, ethnicity and gender. Over 70% of cases occur in developing nations. 50% of cases worldwide occur in Eastern Asia, with a majority of them in China, Japan and South Korea. Western industrialized nations like the United States have relatively low gastric cancer incidence rates. In the United States, gastric cancer-related incidence and mortality have been reduced approximately 50% since 1975[1,7]. Not surprisingly, in 2008, Eastern Asia, including Japan, China, Korea and Mongolia, has the highest mortality rates (28.1 per 100,000 men and 13.0 per 100,000 women), while North America, including Canada and the United States, has the lowest (2.8 and 1.5 per 100,000 men and women, respectively)[1]. Other gastric cancer "hot spots" include Central and Eastern Europe, as well as Central and South America. In contrast, Australia, Africa, Southern Asia, Western Europe and North America are areas of low risk (Figure 1.1). Interestingly, country of birth is a better predictor of gastric cancer risk than country of current residence. Immigrants from regions with high gastric cancer risk to regions with lower gastric cancer risk have an intermediate risk of gastric cancer but have higher risk compared to second-generation immigrants[8-9].

Despite the aforementioned influence of location, gastric cancer incidence and mortality differed significantly among different ethnic groups. In the United States between 2003-2007, the highest annual incidence rates were observed among Asian/Pacific Islanders (17.5 per 100,000 men and 10.0 per 100,000 women), followed by blacks (16.7 per 100,000 men and 8.6 per 100,000 women), Hispanics (14.8 per 100,000 men and 9.1 per 100,000 women), American Indians and Alaska Natives (15.5 per 100,000 men and 7.3 per 100,000 women), and whites (9.6 per 100,000 men and 4.7 per 100,000 women)[10]. Gastric cancer mortality rates, in the United States during the same period, mostly paralleled the trends observed for gastric cancer incidence with rates being highest among black Americans (10.7 per 100,000 men and 5.0 per 100,000 women), followed by Asian/Pacific Islanders (9.4 per 100,000 men and 5.6 per 100,000 women), American Indian/Alaska native (9.2 per 100,000 men and 4.2 per 100,000 women), Hispanic (8.0 per 100,000 men and 4.6 per 100,000 women), and white Americans (4.6 per 100,000 men and 2.4 per 100,000 women)[10].

However, irrespective of location and ethnicity, men are twice as likely as women to develop gastric cancer with age-standardized incidence rates ranging from 3.9 in Northern Africa to 42.4 in Eastern Asia for men and from 2.2 in Southern Africa to 18.3 in Eastern Asia for women[10-11]. The pattern of the M/F incidence of gastric cancer is a global phenomenon, equally seen in populations with high and low risk for gastric cancer (Figure 1.2). This remains one of the unresolved epidemiological questions as this sexual dimorphism has not been explained by putative risk factors such as smoking, alcohol and obesity[12]. However, epidemiological evidence points to the protective role of female hormones[13] and we are just starting to study this using in vivo models[14-15]. The question of gender is central to the work of this thesis and will be

examined in the context of mutagenesis in Chapter 2 and carcinogenesis in Chapter 3.

Pathology. Approximately 90% of gastric cancers are adenocarcinomas, malignant epithelial tumors that arise from the gastric glandular epithelium[16]. Adenocarcinomas, referred to as gastric cancer in this work, can be further subdivided by anatomical site and histologic type. Anatomically, gastric cancers are categorized as cardia and non-cardia. Cardia adenocarcinomas are more similar pathologically and epidemiologically to esophageal adenocarcinomas, and are not the focus of this work, as their development may be associated with the absence of *H. pylori*[6]. Most non-cardia gastric cancers originate in the antrum, exhibit a male-predominant pattern and are associated with chronic *H. pylori* infections. Histologically, gastric cancers are classified as either diffuse- or intestinal-type adenocarcinomas[17]. Diffuse-type gastric cancer is present in younger populations and is prevalent in both men and women, while the intestinal-type gastric cancer is most commonly associated with high risk populations and elderly men. Diffuse-type adenocarcinomas are characterized by poorly-differentiated cells without glandular structures and a distinct progression of precancerous lesions leading to cancer has not been identified[17-18]. Furthermore, diffuse-type gastric cancers can be familial in distribution as germline mutations leading to reduced E-cadherin (CDH1) have been associated with this histologic type[19]. In contrast, intestinal-type adenocarcinomas have well-differentiated neoplastic cells connected by tubules and glands similar to those observed in normal intestinal mucosa. This intestinal phenotype preserve cell polarity, partially due to the action of E-cadherin[18]. No germline mutations have been associated with this form of gastric cancer. The intestinal-type gastric cancer is associated with tissues with chronic inflammation, and follow a clear disease progression described by Correa's model of gastric carcinogenesis[20].

Briefly, Correa's model characterized the series of sequential lesions that lead to gastric cancer. The stages of the precancerous cascade are normal stomach, chronic active nonatrophic gastritis, multifocal atrophic gastritis, intestinal metaplasia (complete, followed by incomplete), dysplasia and ultimately invasive carcinoma (Figure 1.3)[20]. This work focuses on non-cardia, intestinal-type gastric adenocarcinomas, which represent the most common form of gastric cancer worldwide.

Mutations associated with gastric cancer. Data from literature examining mutations in gastric cancer as well as the sequencing efforts of the Cancer Genome Project is compiled in the Catalogue of Somatic Mutations in Cancer (COSMIC). COSMIC lists the genes most frequently mutated as well as the type of mutations seen in these mutations[21-23]. According to COSMIC data, the top ten mutated genes found in gastric cancer samples are TP53, KRAS, CTNNB1, APC, PIK3CA, CDH1, CDKN2A, PTEN, MSH6 and FBXW7 (http://www.sanger.ac.uk/genetics/CGP/cosmic/ accessed on 2/22/2011). Analysis of the mutational spectra of gastric cancer shows that G:C>A:T (mostly at CpG sites) transitions are the most common mutation observed, followed by A:T>G:C transitions and G:C>T:A transversions[22]. These mutations can be induced by reactive oxygen and nitrogen species (RONS)[24], such as nitric oxide[25]. RONS are constantly released by inflammatory cells in response to *H. pylori* infection.

Etiology. The role of *H. pylori* infection in gastric carcinogenesis has been established through epidemiological[26-28] and experimental evidence[29-30]. *H. pylori* promotes precancerous lesions and the development of gastric cancer by inducing a chronic inflammatory state. The association of cancer with inflammation has been recognized since 1863 when Virchow

detected leukocytes in neoplastic tissues[31]. The causal relationship between RONS produced by inflammatory cells and DNA damage that leads to cancer is now widely accepted[32]. The combination of DNA damage, increased cell proliferation, deregulation of apoptosis and tissue remodeling that occurs during chronic inflammation increases the risk of neoplasia[33]. These processes are largely regulated by proinflammatory cytokines, chemokines and growth factors that are part of the inflammatory environment. This model of persistent *H. pylori* infection leading to chronic inflammation and cancer is supported by chronic viral (hepatitis B-induced liver cancer) and parasitic (Schistosomiasis-induced bladder cancer) infections[34-35].

Fifty percent of the world population is infected with *H. pylori,* but only a small fraction (1-2%) develops multifocal atrophic gastritis which leads to gastric cancer. The majority of infected individuals present no clinical symptoms of infection while 5-15% of infected individuals develop peptic duodenal ulcers (Figure 1.4)[36-37]. Duodenal ulcers are characterized by antral predominant nonatrophic gastritis which may reduce the risk of gastric cancer[38]. While *H. pylori* infection drives gastric carcinogenesis, the outcome of infection is modulated by the virulence of the bacterial strain, the genetic susceptibility of the host and the external environment.

1.2 *Helicobacter pylori*

Overview. The first well-documented report of spiral-shaped bacteria in human stomachs was by Bizzozero in 1893[39]. Early reports linking these microorganisms to gastritis, and even carcinomas, were dismissed as the bacteria were not found by others and were considered contaminants, as bacteria were not expected to survive in the acidic gastric environment[40-42].

The field stagnated until 1982 when Marshall and Warren "rediscovered" unidentified curved bacilli in gastric biopsies associated with active, chronic gastritis[4]. Later, Marshall fulfilled Koch's postulates by developing gastritis after swallowing a pure culture of *H. pylori*[43]. *H. pylori*'s ability to persist for years in the human gastric mucosa was demonstrated in another experiment involving self-induced infection, which required antibiotics to eradicate the bacterium[44]. Within the last several decades, investigators around the world have proven that *H. pylori* is the causative agent of gastritis, ulcers, gastric mucosa-associated lymphoid tissue lymphoma and gastric cancer in humans and laboratory animal models[45].

Epidemiology. While 50% of the world's population is infected with *H. pylori*, prevalence differs dramatically between developing (>80%) and developed (<40%) nations[46]. *H. pylori* is the most common bacterial infection worldwide. Bacterial phylogenetic studies demonstrate that *H. pylori* has infected humans for at least 58,000 years, before humans migrated out of Africa[47]. Currently, *H. pylori* incidence has been estimated at 1-3% in developed nations and 3-10% in developing nations[48-49]. *H. pylori* infection is usually acquired in childhood and normally persists for life within the gastric mucosa[6]. In recent years, *H. pylori* prevalence worldwide has been decreasing coinciding with better hygiene and improved socioeconomic status, particularly in the industrialized world[46].

The mechanism of *H. pylori* transmission remains largely unknown. The bacterium is almost exclusively found in humans and some nonhuman primates with no known reservoirs of *H. pylori* in the environment, which makes direct person-to-person transmission the most likely method of infection. The fecal-oral (e.g. fecal contamination in institutions), oral-oral (e.g. premastication of food) and gastric-oral (e.g. iatrogenic infection or vomitus) routes have been

proposed but conclusive evidence is not yet available[46]. There is a strong association of *H. pylori* infection with family size, as intra-familial transmission is facilitated by increased number of siblings, possibly due to reinfection among children[6].

Virulence factors. *H. pylori* is a microaerophilic, gram-negative, curved rod with multiple flagella that is capable of persistently infecting the harsh gastric environment. The bacterium's success is due largely to an array of virulence factors that have adapted to the stomach for millennia. The first obstacle the bacteria have to overcome is navigating the acidic lumen of the stomach and finding its niche in the gastric mucosa. To survive the acid pH, *H. pylori* utilizes urease to convert gastric urea into ammonia and CO_2 which may form a protective layer of ammonia to neutralize the acid adjacent to the bacteria[50]. A second mechanism which utilizes an α-carbonic anhydrase takes the CO_2 produced and converts it to HCO_3^{2-} which helps maintain the periplasmic pH of the bacteria around 6.1[51]. In order to escape the lumen, *H. pylori* swims following gradients of carbonate and urea secreted by gastric epithelia to chemotactically find the mucin layer. Mutants deficient in chemotaxis (*cheW* mutant) or sensing gradients (*TlpB* mutant), as well as mutants deficient in motility (nonflagellated mutants and flagellated but nonmotile mutants), do not infect the gastric mucosa at all or are outcompeted by wild-type counterparts[52-54]. Once in the mucin layer, *H. pylori*'s adhesins mediate persistent infection by binding sulfated mucin sugars or epithelial cells to prevent the sloughing of the bacterium. The best characterized adhesin is BabA which binds Lewis B antigens on epithelial cells. An allele of BabA, *babA2*, has been strongly associated with worse clinical outcomes[55]. Other known *H. pylori* adhesins include SabA, SabB, OipA, AlpA and AlpB[46].

The final set of virulence factors have perhaps been the most studied as they are the genes associated with *H. pylori* pathogenicity and epithelial cell damage.

Damaging epithelial cells or destabilizing tight junctions is believed to release nutrients and substrates required by the bacteria to survive[56]. The most important virulence factors in this set are CagA, VacA, HP-NAP, and LPS. Recently, a prospective study conducted in Spain demonstrated that infection with *H. pylori* strains harboring CagA and VacA s1/m1 was associated with the development of gastric preneoplastic lesions (Odds ratio of 4.80, 95% CI 1.71–13.5) compared to *H. pylori*-infected individuals without these virulence factors[57]. The cytotoxin-associated gene A (CagA) is part of the *H. pylori* Cag pathogenicity island (CagPAI) which contains 31 genes required for the assembly and function of a type IV secretion system. CagA is a bacterial effector protein injected into the cytoplasm of gastric epithelial cells that can be phosphorylated by human kinases and directly interferes with signaling networks inducing changes in morphology and IL-8 secretion (Figure 1.5)[58]. *H. pylori* strains possessing CagA, specifically CagA variants common in East Asia, are believed to increase the risk of gastric cancer[58]. VacA, or vacuolating cytotoxin A, produces large acidified vacuoles in epithelial cells in vitro, which leads to cell death. Epithelial cell vacuoles are derived from late endosomes and lysosomes, affecting endocytosis. VacA also forms membrane channels through the epithelial layer, increasing its permeability[46]. The activity of the s1/m1 type of VacA is strongly correlated with increased *H. pylori* pathogenicity in Western populations[46]. HP-NAP is the *H. pylori* neutrophil activation protein that specifically targets and activates neutrophils, presumably to increase epithelial damage[59]. *H. pylori*'s LPS, or lipopolysaccharide, is interesting as it poorly elicits an inflammatory response, as *H. pylori*'s LPS moeities mimic the Lewis antigens x and y on

gastric epithelial cells. This immune mimicry might have two distinct objectives: 1) limit specific immune responses to *H. pylori,* or 2) elicit immune responses against gastric epithelial cells to further destabilize epithelial polarity[46]. All together, *H. pylori* has evolved to infect the gastric niche and utilizes the appropriate combination of virulence factors to transform the environment for its survival. Determining the role of virulence factors in different strains of *H. pylori* is the purpose of experiments using *H. pylori* microarrays that are introduced in Appendix A.

Diagnosis and Treatment. The methods for diagnosing *H. pylori* infection include urea breath testing, serology, fecal antigen tests, histology and culture. Urea breath testing is the least invasive and works by detecting the activity of *H. pylori*'s urease. Patients swallow urea labeled with a carbon isotope and breathe into a tube that detects the presence of labeled carbon dioxide, which would be produced by the decomposition of urea. Serological tests detect specific antibodies against *H. pylori*, but cannot definitively determine active infection as antibodies can be produced for years after clearance. Fecal antigen tests use *H. pylori*-specific antibodies to detect *H. pylori* antigen. Both histology and culture are used as the gold standard of detection but are the most invasive as they require an endoscopy[46].

The current treatment of *H. pylori* in symptomatic carriers is eradication of the bacteria. Antimicrobial therapy to eradicate *H. pylori* consists of triple or quadruple therapy as individual antibiotics are not as effective in the gastric niche. Triple therapy incorporates two antibiotics, usually clarithromycin and amoxicillin, with a bismuth compound or a proton pump inhibitor, while quadruple therapy has both the bismuth compound and the proton pump inhibitor[46]. However, these therapies have shown suboptimal results in some studies leading to concerns

of antibiotic resistant strains[60]. Due to *H. pylori*'s association with gastric cancer, wide-scale eradication and vaccines have been proposed to prophylactically prevent gastric cancer. Early stage eradication of *H. pylori* prevents gastric cancer[61], and reduces atrophy and physiological alterations to the stomach that allow colonization by other microbiota, which may be involved in gastric carcinogenesis[62-66]. The possibility of developing antibiotic resistant strains and the possible relationship between *H. pylori* eradication and development of proximal gastric cancer and esophageal cancer have quelled discussions advocating *H. pylori* eradication in asymptomatic carriers worldwide. Efforts to develop a *H. pylori* vaccine have produced mixed results[60]. However, a viable solution is aggressive screening by X-ray or endoscopy and eradication of the bacteria in symptomatic carriers in high-risk regions. These methods have proven effective in Japan, a nation with one of the highest incidence rates of gastric cancer, as they have also experienced the worldwide decrease in gastric cancer incidence and increased their overall 5 year survival rate[67]. From 1962 to 1992, Japan doubled the overall 5 year survival of gastric cancer patients from 20% to 40% by detecting stomach cancer at the localized stage and surgically removing cancerous tissues[60].

1.3 Host factors

Although *H. pylori* is the major causative agent of gastric cancer, the host plays an important role in the progression of gastric cancer through its response to the bacterium[68]. There is a two- to three-fold increase in gastric cancer risk in individuals with blood relatives with gastric cancer, and 10% of gastric cancer cases show familial clustering[69]. While *H. pylori* infection is likely to be transmitted throughout a family, controlling for *H. pylori* infection indicated that a family

history of gastric cancer is still a risk factor for disease. These families have been shown to have increased susceptibility to *H. pylori* and its associated precancerous lesions which suggest a strong host component in disease development[70]. As *H. pylori* pathogenesis is mediated through chronic inflammatory processes, the modulation of the host's immune response may affect disease development and will be discussed below.

The adaptive immune response. The current model of persistent *H. pylori* infection leading to a chronic inflammatory state that causes gastric cancer (through DNA damage, errors in replication due to hyperproliferative conditions or recruitment of oncogenic bone-marrow derived cells) is largely dependent on the host's specific immune response to the bacterium[68]. In response to initial *H. pylori* infection, circulating phagocytic cells including neutrophils, macrophages and monocytes are recruited to the site of infection by the cytokine/chemokine system and the complement system (Figure 1.6). However, failure to eradicate the bacteria by the innate immune response and its associated acute inflammation lead to the recruitment of T and B lymphocytes and more macrophages, signaling the involvement of the adaptive immune system and the establishment of chronic inflammation. Following their recruitment, immature helper T cells (Th0) are activated by *H. pylori* antigens expressed on antigen presenting cells (APCs) and differentiate into several subtypes, including Th1, Th2 and the more recently discovered Th17 cells, which secrete different sets of cytokines that modulate the type of immune response (Figure 1.6). Broadly, Th1 cells secrete IL-2 and IFN-γ, increase proinflammatory cues and are associated with macrophage activation. Th2 cells secrete IL-4, IL-5, and IL-10, increase antiinflammatory cues and stimulate B cell responses. Th17 cells secrete IL-17 and IL-22, also increase proinflammatory cues and are associated with neutrophil

recruitment and inflammatory disorders. By mechanisms incompletely understood, *H. pylori* infection promotes a strong Th1 and Th17 proinflammatory response[71]. Historically, Th1 responses have been shown to mediate *H. pylori*-associated gastritis[71-75], but there is increasing recognition of the role of Th17 cells in *H. pylori* pathogenesis[76-77]. However, due to the recent discovery of Th17, its contributions have not been as thoroughly studied. Based on the Th1/Th2 model of *H. pylori* pathogenesis, the proinflammatory Th1, and possibly now Th17, cytokines promote gastritis, while Th2 cytokines, and possibly T regulatory cells that counteract Th17 actions, protect against gastric inflammation. The importance of T cells, particularly Th1 cells, in the development of *Helicobacter*-induced gastric disease has been demonstrated in mouse models lacking functional lymphocytes and utilizing adoptive transfer to investigate the effect of specific T cell subsets[74,78-79]. Furthermore, different mouse models of *Helicobacter* spp. infection demonstrate the importance of Th1/Th2 responses, as C57BL/6 mice which are susceptible to gastric atrophy caused by *H. pylori* have stronger Th1 responses while BALB/c mice which are less susceptible to gastric atrophy mount Th2 responses[68]. These models will be further discussed in the section on "Mouse models of *H. pylori* infection" as the effects of the immune response in the context of gender of great importance to this thesis.

As differences in the host's T cell response affect the outcome of *H. pylori* infection, it has been hypothesized that modulating the host's response might exacerbate or ameliorate gastric disease. Coinfection with *Heligmosomoides polygyrus*, a murine parasite, and *Helicobacter felis*, a gastric Helicobacter, decreased Th1-associated cytokines and antibodies to *H. felis* leading to attenuated gastritis and less severe premalignant lesions[80]. Coinfection with *Helicobacter bilis*, an enterohepatic helicobacter that subclinically infects numerous strains of

mice, also attenuated *H. pylori* induced gastritis in C57BL/6 mice[81]. The opposite effect was observed by modulating the host's response using a parasite that induces a strong Th1 response, such as *Toxoplasma gondii*. Coinfection with *T. gondii* exacerbated *H. felis* infection leading to increased morbidity[82]. These results support the "African enigma," the hypothesis that the low incidence of gastric cancer observed in some developing nations is due to the immunomodulating effect of coinfections leading to Th2 responses[83]. This effect has been observed in a study involving a coastal population and an Andean population in Colombia with vastly different incidences in gastric cancer[84]. While *H. pylori* prevalence (>90%) was similar, the coastal population had a lower incidence of gastric cancer which was associated with coinfection with enteric helminths and a systemic Th2 response to *H. pylori*, unlike the Andean population that experience a higher incidence of gastric cancer, had fewer parasites and a systemic Th1 response[84].

Inflammation, oxidative stress and DNA repair. T helper cells create an environment that recruits and activates the appropriate inflammatory cells to deal with specific antigens. T helper cells direct the immune response through the secretion of specific cytokines. *H. pylori*-infected gastric epithelium has increased levels of IL-1β, IL-2, IL-6, IL-8 and TNFα, which is a potent proinflammatory combination characterized by the predominance of phagocytes[85]. IL-1β promotes a strong proinflammatory response and inhibits gastric acid secretion[70]. IL-8, a neutrophil activating chemokine, is strongly induced by *H. pylori*[85-86]. After following cytokine and chemokine gradients to the site of infection, phagocytes have two functions: a) eradicate *H. pylori* and b) repair the tissue. To eradicate *H. pylori*, phagocytes utilize lysosomal proteins, such as proteases, lysozymes, and myeloperoxidases. Myeloperoxidases produce superoxide

(O_2^-), a precursor of peroxide (H_2O_2) and hypochlorous acid. Monocytes and macrophages release nitric oxide (NO) which also forms peroxynitrite ($OONO^-$). Lysosomal proteins and RONS released during *H. pylori* infection damage adjacent tissues and are the main source of epithelial damage. To accomplish the goal of repairing the tissue, phagocytes secrete cytokines and growth factors to recruit more inflammatory cells and initiate wound healing responses, such as proliferation, ECM degradation, angiogenesis, etc. required to return the tissue to homeostasis[33]. As *H. pylori* persistently infects the stomach, the proinflammatory and wound healing responses are not shut down and over time can promote cancer.

Another way in which the host can modulate the inflammatory response is through host genetics. The association of single nucleotide polymorphisms (SNPs) of inflammation-related genes with increased risk of gastric cancer highlights the importance of inflammation and oxidative stress in *H. pylori* driven carcinogenesis[87-88]. SNPs have been associated with increased susceptibility to *H. pylori* infection, *H. pylori*-induced gastric atrophy and gastric cancer. SNPs in many inflammatory mediators, such as IL-1β, IL-1RN2, IL-10, IL-8, CXCR2 (IL-8RB) , IL-4, COX2, TNF, iNOS, and IFNGR2, are relevant in gastric carcinogenesis as they further alter the balance of both Th cells and phagocytes (Table 1.1). The associations of IL1β-31*C and -511*T with increased risk of gastric atrophy and cancer in Western populations were among the first discovered[70]. Studies in East Asian populations have associated SNPs in the IL-1 family with increased gastric cancer risk[89-91]. Polymorphisms in the promoter region of IL-8 (IL-8 -251 T to A) have been associated with increased gastric cancer risk[92-93]. The role of CXCL1, a murine homolog of IL-8, in *H. pylori* induced carcinogenesis will be discussed in Chapter 3.

DNA repair enzymes may play an important role in reducing *H. pylori*-related

carcinogenesis by decreasing oxidative DNA damage. *H. pylori*-induced chronic inflammation increases DNA damage, double-strand breaks and DNA fragmentation in the gastric mucosa through the effect of oxidative stress and RONS[94-97]. RONS cause DNA damage via multiple mechanisms such as direct base oxidation, nucleoside deamination, and the formation of etheno adducts by lipid peroxidation[24,32,98-99]. *H. pylori* gastritis selectively increases the activity of DNA damage and repair proteins, such as Ku, poly (ADP-ribosyl) polymerase, 8-hydroxyguanine glycosylase (OGG1), and MSH2, in human gastric mucosa[96]. Studies of SNPs in genes related to DNA repair, such as MGMT, and OGG1, have not always demonstrated clear links with gastric cancer[87-88,100]. MGMT, also known as O^6-methylguanine-DNA methyltransferase, repairs DNA adducts such as O^6-methylguanine and O^4-methylthymine[101-102], and its inactivation by promoter hypermethylation has been associated with increased gastric cancer risk[103-104]. MGMT Ile143Val polymorphism was associated with increased gastric cancer risk, but only in patients with low intake of fruits and vegetables[100]. Polymorphisms of OGG1, or 8-oxoguanine DNA glycosylase, cause the accumulation of 8-oxo-dG during *H. pylori* gastritis, but their association with increased gastric cancer risk is still controversial[105-107]. Given their role in repairing DNA damage induced by *H. pylori*, DNA repair proteins may greatly influence *H. pylori* carcinogenesis.

Gender. Men experience higher rates of infection and its associated mortality than women. Normal immune responses are sexually dimorphic with a heightened inflammatory response in women compared to men. This greater inflammatory response in women provides advantages during infection, sepsis and trauma but makes women more susceptible to autoimmune diseases[108]. Epidemiological and immunological evidence suggests that the menstrual cycle,

pregnancy and menopausal status influence the etiology and progression of chronic inflammatory diseases, such as gastric cancer and rheumatoid arthritis, which suggests the importance of female sex hormones[109-110]. Hormone therapies in men and women are also associated with decreased gastric cancer risk[13]. Postmenopausal hormone replacement therapy (HRT) may lower the rate of gastrointestinal cancer, particularly colonic cancer[111-113]. Prostate cancer patients treated with estrogen had a decreased risk of gastric cancer[110]. Additionally, the usage of anti-estrogen therapy, particularly the breast cancer drug Tamoxifen, is linked with increased incidence rates of gastrointestinal malignancies. Considerable evidence exists that Tamoxifen, a mixed agonist/antagonist of estrogen signaling, is associated with protection against breast cancer, but also increases the risk of endometrial cancers[114-115]. However, Tamoxifen treatment and its association with gastrointestinal cancers, and gastric cancer in particular, is not clear; one study reports no effect[115] while others demonstrate Tamoxifen treatment with increased risk[116-118].

A review of the effects of estrogens on inflammation indicate that estrogens, of which 17β-estradiol or E2 is the most important, decrease the apoptosis of immune cells, inhibit reactive oxygen species formation, and inhibit nitric oxide production in the presence of inflammatory stimuli[108]. Another mechanism by which estrogens may affect chronic inflammatory diseases is by directly affecting the secretion of cytokines by T cells, B cells and macrophages. Generally E2 in premenopausal women favors the downregulation of T cell-dependent immunity. Periovulatory to pregnancy levels of E2 promotes IL-4, IL-10 and IFN-γ secretion from CD4+ T cells while inhibiting the production of TNFα. Furthermore, mouse studies demonstrate that high concentrations of E2 increase Th2 and T regulatory transcription

factors, thus increasing the antiinflammatory response. In contrast, B cell antibody secretion is normally stimulated by E2 in pre- and post-menopausal women. Furthermore, very high levels of E2 inhibit the secretion of IL-1β and TNFα, while lower levels stimulated both cytokines demonstrating the importance of E2 levels in shaping the inflammatory response[108]. As estrogens can strongly decrease T cell-dependent immunity and the proinflammatory cytokine environment, the role of estrogens in gastric cancer is further explored in Chapter 3.

1.4 Environmental factors

The sharp decrease in the incidence and mortality of gastric cancer in developed countries suggest that the environment is a third factor to consider in the etiology of gastric cancer. As mentioned previously, second-generation immigrants had a reduction in gastric cancer risk compared to first-generation immigrants indicating that the environment can be more important that host genetics and bacterial factors (assuming intra-familial transmission of *H. pylori*)[9]. Diet and lifestyle have been associated with increased gastric cancer risk. High salt consumption and low intake of fresh fruits and vegetables are independent dietary factors that increase gastric cancer risk[119]. Of these dietary factors, the intake of high levels of dietary salt has been studied most extensively due to the association of high incidences of gastric cancer to countries with high salt intake, which is thought to promote further injury to the stomach[120-121]. Animal models assessing the role of high salt in gastric pathology have yielded mixed results[66,122] Smoking also increases gastric cancer risk[123]. Associations between meat consumption or alcohol and gastric cancer are not as clear[119,124]. Additionally, the impact of

long-term proton pump inhibitors in gastric carcinogenesis is now being probed, as proton pump inhibitors have been linked to precancerous lesions and cancer in rodents[125-126]

1.5 Mouse models of *H. pylori* infection

Many animal models, such as neonatal gnotobiotic piglets, Macaca species and Mongolian gerbils, have been utilized to model *H. pylori* infection in humans[127-129]. However, the mouse is the most widely used animal model in *H. pylori* studies due to its myriad advantages, such as well-documented immune responses, the sequencing of its genome, availability of reagents and transgenic mice and low cost relative to other models. Early *H. pylori* experiments with mice did not lead to persistent colonization in wild-type strains leading to the use of athymic, or nude mice[130] or other *Helicobacter* spp., most notably *H. felis*[131]. *H. felis* infection of C57BL/6 mice causes oxyntic atrophy and gastric cancer by 15 months post-infection (MPI)[132-133]. The first reports of successful adaptation of *H. pylori* to the mouse model came from Italy in the mid-1990's[134-136], but they were superseded by the adaptation of the cagPAI+ Sydney strain, or SS1, which has become the standard for *H. pylori* mouse studies due to its ability to persistently infect many inbred mouse strains, such as C57BL/6, BALB/c, DBA/2 and C3H/He[137]. As mentioned previously, SS1 elicits a robust chronic active gastritis in C57BL/6 mice accompanied by a Th1 immune response while BALB/c mice develop less pathology accompanied by a Th2 response due to host strain differences (e.g. differences in phospholipase A_2 secretion)[132,138-139]. Each system has particular differences that must be considered in order to address the right biological questions. For example, in C57BL/6 mice, females have a stronger inflammatory

response compared to males leading to increased gastritis and cell proliferation, which is an important factor to consider when determining the interpretation of data such as histopathological scores[140]. These differences in the models are useful in determining how changes in the immune response and gender affect the formation of gastric lesions. Nevertheless, *H. pylori* infection alone does not reliably induce gastric cancer in either of these strains[138]. Limitations associated with the murine model are differences in gastric architecture, the lack of *H. pylori*-associated ulcers and gastric cancer in some models, and the presence of *Lactobacillus* spp. in the proximal murine stomach, which are not found in the human stomach[46]. However, new murine models that more closely recreate conditions in humans continue to progress. For example, the development of *H. pylori*-induced gastric cancer has been documented in male hypergastrinemic INS-GAS FVB mice at 7 MPI[141] and C57BL/6 × 129S6/SvEv (B6129) mice at 15 MPI[122]. Using two of these models, this thesis probes the interactions between gender and immune response in gastric mutagenesis using C57BL/6 mice (Chapter 2) and the role estrogens and innate immunity in gastric carcinogenesis in INS-GAS mice (Chapter 3).

1.6 Transgenic mouse mutation systems

Murine mutational analysis systems are mouse models used to detect somatic mutations and assess the mutagenicity of chemical, biological or physical agents. These in vivo models use reporter genes to detect mutations under the assumption that damage to reporter genes are indicative of mutations to the host genome. Based on the origin of their reporter genes, murine mutational analysis systems are classified as endogenous or exogenous systems.

Endogenous systems include the *Dlb-1* mouse assay, the *Aprt* mouse assay, the pink-eyed unstable (p^{un}) mouse assay and the mammalian spot assay[142]. Exogenous systems include the Big Blue® assay, Muta ™Mouse assay and the *gpt* delta assay[143]. The main advantage of the endogenous systems is that the reporter genes are host genes that are expressed in their native chromosomal conformation[142]. This allows the induction of mutations in active genes which can often be assessed in vivo. In the *Dlb-1*, p^{un}, and mammalian spot models, assessment of the induction of mutations can be done visually by examining changes on the fur or staining in tissue samples. An exception is the *Aprt* system which requires in vitro culture but also allows sequencing of mutations[144-145]. However, a limitation of endogenous systems is that they can only detect mutations in certain cell types. In contrast, exogenous, or transgenic, systems express the reporter genes in every cell of the body which permits the detection of mutations in any organ. Transgenic systems insert multiple tandem copies of lambda phage carrying a reporter gene like *lacI, lacZ* or *gpt* to detect mutations ex vivo[143]. After extracting the DNA, lambda phage is repackaged, and used to infect *Escherichia coli*. *E. coli* expresses the transgene providing a readout indicating mutations in the transgene. The genes can be isolated and sequenced to determine the exact mutational spectra. The drawbacks of this method are that the reporter genes are 1) not actively expressed in the mouse and 2) are prokaryotic with differences in methylation and nucleotide composition. Furthermore, the ex vivo expression makes the reporter genes susceptible to further mutations outside the mouse.

Different transgenic systems have been used to measure the induction of mutations caused by chronic inflammation, including *H. pylori*, in the gastrointestinal tract[146-149]. The Big Blue® assay, Muta ™Mouse assay and the *gpt* delta assay are attractive candidates to study *H.*

pylori pathogenesis as they are available on the C57BL/6 background which develops precancerous lesions in response to *H. pylori* infection. As these three transgenic systems utilize similar mechanisms to report mutations, the *gpt* delta assay will be utilized to further describe the methods. The *gpt* delta transgenic mouse was developed to allow the detection of point mutations by the inactivation of *gpt*, or guanine phosphoribosyltransferase, activity under 6-thioguanine (6-TG) selection[150]. Importantly, in contrast to other transgenic systems, the *gpt* delta mouse can also measure deletions less than 10kb in size using Spi^- selection[150].

The 456 bp *gpt* gene encodes the Gpt enzyme which adds activated ribose-5-phosphate to guanine bases creating guanine monophosphate in the purine salvage pathway. Gpt can also salvage 6-TG but the product is toxic to the cell[143]. Using this principle, *E. coli* infected with plasmids expressing a functional *gpt* cannot grow on minimal media plates with 6-TG, whereas plasmids with inactivated, or mutant, *gpt* will form colonies. The *gpt* gene was inserted into a plasmid construct flanked by *lox* sites. After murine genomic DNA is isolated, the phage DNA is rescued and packaged into phage particles that transduce *E. coli* expressing Cre recombinase. Cre acts upon the *lox* sites allowing the propagation of the plasmid. The plasmid also carries the CAT gene which confers resistance to chloramphenicol (Cm). Using Cm alone or Cm and 6-TG selection, the total number of *E. coli* expressing the plasmid and the total number of *E. coli* expressing the plasmid with a mutated *gpt* gene can be calculated. 6-TG resistant colonies are then cultured and a 739 bp DNA product containing the *gpt* gene is amplified by PCR. This product can then be sequenced to determine the mutational spectra. Mutations are classified as transitions, transversions, deletions, insertions or complex (multiple changes).

The Spi$^-$ assay selects for lambda phage that are not sensitive to interference from prophage P2. Induction of wild-type lambda phage on *E. coli* carrying prophage P2 results in the host's death and inhibition of phage replication, which makes lambda phage sensitive to P2 interference, or Spi^{+151}. However, deficiency in both *red* and *gam* gene function, along with *chiC* expression, confer phages with resistance to P2's interference, or a Spi$^-$ phenotype, and importantly do not immediately kill *E. coli* allowing phage propagation. The lambda phage in the *gpt* delta mouse incorporates the *red*, *gam* and *chiC* elements. When *gpt* delta mice are exposed to agents that cause deletions capable of inactivating both *red* and *gam*, the recovered lambda phage are Spi$^-$ which allows them to form plaques on a lawn of *E. coli* carrying P2. Using strains of *E. coli* with and without P2, the total number of lambda phage with *red* and *gam* inactivation and the total number of lambda phage recovered can be determined. Mutated phage can be recovered and passaged to determine the location of the deletion by a combination of PCR and sequencing. Due to its ability to determine the mutagenic potency of infectious agents in the stomach, I utilized the *gpt* delta mouse model on a C57BL/6 background to determine the role of *H. pylori* in the induction of gastric mutations in Chapter 2.

1.7 References

1. Ferlay, J.*, et al.* Estimates of worldwide burden of cancer in 2008: GLOBOCAN 2008. *Int J Cancer* (2010).
2. Chan, A.O., Wong, B.C. & Lam, S.K. Gastric cancer: past, present and future. *Can J Gastroenterol* **15**, 469-474 (2001).
3. Pisani, P., Parkin, D.M. & Ferlay, J. Estimates of the worldwide mortality from eighteen major cancers in 1985. Implications for prevention and projections of future burden. *Int J Cancer* **55**, 891-903 (1993).
4. Marshall, B.J. & Warren, J.R. Unidentified curved bacilli in the stomach of patients with gastritis and peptic ulceration. *Lancet* **1**, 1311-1315 (1984).
5. Schistosomes, liver flukes and Helicobacter pylori. IARC Working Group on the Evaluation of Carcinogenic Risks to Humans. Lyon, 7-14 June 1994. *IARC Monogr Eval Carcinog Risks Hum* **61**, 1-241 (1994).
6. Blaser, M.J. Hypothesis: the changing relationships of Helicobacter pylori and humans: implications for health and disease. *J Infect Dis* **179**, 1523-1530 (1999).
7. Parkin, D.M., Stjernsward, J. & Muir, C.S. Estimates of the worldwide frequency of twelve major cancers. *Bull World Health Organ* **62**, 163-182 (1984).
8. Coggon, D., Osmond, C. & Barker, D.J. Stomach cancer and migration within England and Wales. *Br J Cancer* **61**, 573-574 (1990).
9. Kolonel, L.N., Nomura, A.M., Hirohata, T., Hankin, J.H. & Hinds, M.W. Association of diet and place of birth with stomach cancer incidence in Hawaii Japanese and Caucasians. *Am J Clin Nutr* **34**, 2478-2485 (1981).
10. Altekruse, S.F.*, et al.* SEER Cancer Statistics Review, 1975-2007. (National Cancer Institute, Bethesda, MD, 2010).
11. Sipponen, P. & Correa, P. Delayed rise in incidence of gastric cancer in females results in unique sex ratio (M/F) pattern: etiologic hypothesis. *Gastric Cancer* **5**, 213-219 (2002).
12. Lindblad, M., Rodriguez, L.A. & Lagergren, J. Body mass, tobacco and alcohol and risk of esophageal, gastric cardia, and gastric non-cardia adenocarcinoma among men and women in a nested case-control study. *Cancer Causes Control* **16**, 285-294 (2005).
13. Chandanos, E. & Lagergren, J. Oestrogen and the enigmatic male predominance of gastric cancer. *Eur J Cancer* **44**, 2397-2403 (2008).
14. Ohtani, M.*, et al.* Protective role of 17 beta -estradiol against the development of Helicobacter pylori-induced gastric cancer in INS-GAS mice. *Carcinogenesis* **28**, 2597-2604 (2007).
15. Ohtani, M.*, et al.* 17β-estradiol suppresses Helicobacter pylori-induced gastric pathology in male hypergastrinemic INS-GAS mice. *Carcinogenesis* (Submitted 2010).
16. Kumar, V., Abbas, A.K., Fausto, N. & Aster, J. *Robbins and Cotran Pathologic Basis of Disease*, (Saunders Elsevier, Philadelphia, PA, 2010).
17. Lauren, P. The two histological main types of gastric carcinoma: diffuse and so-called intestinal-type carcinoma. An attempt at a histo-clinical classification. *Acta Pathol Microbiol Scand.* **64**, 31-49 (1965).
18. Correa, P. Human gastric carcinogenesis: a multistep and multifactorial process--First American Cancer Society Award Lecture on Cancer Epidemiology and Prevention. *Cancer Res* **52**, 6735-6740 (1992).

19. Guilford, P*., et al.* E-cadherin germline mutations in familial gastric cancer. *Nature* **392**, 402-405 (1998).
20. Correa, P., Haenszel, W., Cuello, C., Tannenbaum, S. & Archer, M. A model for gastric cancer epidemiology. *Lancet* **2**, 58-60 (1975).
21. Futreal, P.A*., et al.* A census of human cancer genes. *Nat Rev Cancer* **4**, 177-183 (2004).
22. Greenman, C*., et al.* Patterns of somatic mutation in human cancer genomes. *Nature* **446**, 153-158 (2007).
23. Bamford, S*., et al.* The COSMIC (Catalogue of Somatic Mutations in Cancer) database and website. *Br J Cancer* **91**, 355-358 (2004).
24. De Bont, R. & van Larebeke, N. Endogenous DNA damage in humans: a review of quantitative data. *Mutagenesis* **19**, 169-185 (2004).
25. Wink, D.A*., et al.* DNA deaminating ability and genotoxicity of nitric oxide and its progenitors. *Science* **254**, 1001-1003 (1991).
26. Nomura, A*., et al.* Helicobacter pylori infection and gastric carcinoma among Japanese Americans in Hawaii. *N Engl J Med* **325**, 1132-1136 (1991).
27. Parsonnet, J., Friedman, G.D., Orentreich, N. & Vogelman, H. Risk for gastric cancer in people with CagA positive or CagA negative Helicobacter pylori infection. *Gut* **40**, 297-301 (1997).
28. Forman, D*., et al.* Association between infection with Helicobacter pylori and risk of gastric cancer: evidence from a prospective investigation. *BMJ* **302**, 1302-1305 (1991).
29. Watanabe, T., Tada, M., Nagai, H., Sasaki, S. & Nakao, M. Helicobacter pylori infection induces gastric cancer in mongolian gerbils. *Gastroenterology* **115**, 642-648 (1998).
30. Wang, T.C*., et al.* Synergistic interaction between hypergastrinemia and Helicobacter infection in a mouse model of gastric cancer. *Gastroenterology* **118**, 36-47 (2000).
31. Balkwill, F. & Mantovani, A. Inflammation and cancer: back to Virchow? *Lancet* **357**, 539-545 (2001).
32. Dedon, P.C. & Tannenbaum, S.R. Reactive nitrogen species in the chemical biology of inflammation. *Arch Biochem Biophys* **423**, 12-22 (2004).
33. Coussens, L.M. & Werb, Z. Inflammation and cancer. *Nature* **420**, 860-867 (2002).
34. IARC. Schistosomes, liver flukes and Helicobacter pylori. IARC Working Group on the Evaluation of Carcinogenic Risks to Humans. Lyon, 7-14 June 1994. *IARC Monogr Eval Carcinog Risks Hum* **61**, 1-241 (1994).
35. Chen, C.J. & Chen, D.S. Interaction of hepatitis B virus, chemical carcinogen, and genetic susceptibility: multistage hepatocarcinogenesis with multifactorial etiology. *Hepatology (Baltimore, Md* **36**, 1046-1049 (2002).
36. Kuipers, E.J*., et al.* Long-term sequelae of Helicobacter pylori gastritis. *Lancet* **345**, 1525-1528 (1995).
37. de Vries, A.C. & Kuipers, E.J. Helicobacter pylori infection and nonmalignant diseases. *Helicobacter* **15 Suppl 1**, 29-33 (2010).
38. Hansson, L.E*., et al.* The risk of stomach cancer in patients with gastric or duodenal ulcer disease. *N Engl J Med* **335**, 242-249 (1996).
39. Bizzozero, G. Ueber die schlauchformigen drusen des magendarmkanals und die beziehungen ihres epithels zu dem oberflacheepithel der schleimhaut. *Arch. Mikr. Anat.* **42**, 82 (1893).

40. Doenges, J.L. Spirochetes in the gastric glands of macacus rhesus and of man without related diseases. *Arch. Pathol.* **27**, 469-477 (1939).
41. Kreinitz, W. Ueber das Auftreten von Spirochaeten verschiedener Form im Mageninhalt bei Carcinoma ventriculi. *Dtsch Med Wochenschr* **32**, 872 (1906).
42. Palmer, E.D. Investigation of the gastric mucosa spirochetes of the human. *Gastroenterology* **27**, 218-220 (1954).
43. Marshall, B.J., Armstrong, J.A., McGechie, D.B. & Glancy, R.J. Attempt to fulfil Koch's postulates for pyloric Campylobacter. *Med J Aust* **142**, 436-439 (1985).
44. Morris, A. & Nicholson, G. Ingestion of Campylobacter pyloridis causes gastritis and raised fasting gastric pH. *Am J Gastroenterol* **82**, 192-199 (1987).
45. Houghton, J., Fox, J.G. & Wang, T.C. Gastric cancer: laboratory bench to clinic. *J Gastroenterol Hepatol* **17**, 495-502 (2002).
46. Kusters, J.G., van Vliet, A.H. & Kuipers, E.J. Pathogenesis of Helicobacter pylori infection. *Clin Microbiol Rev* **19**, 449-490 (2006).
47. Linz, B*., et al.* An African origin for the intimate association between humans and Helicobacter pylori. *Nature* **445**, 915-918 (2007).
48. Graham, D.Y*., et al.* Epidemiology of Helicobacter pylori in an asymptomatic population in the United States. Effect of age, race, and socioeconomic status. *Gastroenterology* **100**, 1495-1501 (1991).
49. Parsonnet, J. The incidence of Helicobacter pylori infection. *Aliment Pharmacol Ther* **9 Suppl 2**, 45-51 (1995).
50. Bauerfeind, P., Garner, R., Dunn, B.E. & Mobley, H.L. Synthesis and activity of Helicobacter pylori urease and catalase at low pH. *Gut* **40**, 25-30 (1997).
51. Wen, Y., Feng, J., Scott, D.R., Marcus, E.A. & Sachs, G. The HP0165-HP0166 two-component system (ArsRS) regulates acid-induced expression of HP1186 alpha-carbonic anhydrase in Helicobacter pylori by activating the pH-dependent promoter. *J Bacteriol* **189**, 2426-2434 (2007).
52. Williams, S.M*., et al.* Helicobacter pylori chemotaxis modulates inflammation and bacterium-gastric epithelium interactions in infected mice. *Infect Immun* **75**, 3747-3757 (2007).
53. Croxen, M.A., Sisson, G., Melano, R. & Hoffman, P.S. The Helicobacter pylori chemotaxis receptor TlpB (HP0103) is required for pH taxis and for colonization of the gastric mucosa. *J Bacteriol* **188**, 2656-2665 (2006).
54. Ottemann, K.M. & Lowenthal, A.C. Helicobacter pylori uses motility for initial colonization and to attain robust infection. *Infect Immun* **70**, 1984-1990 (2002).
55. Gerhard, M*., et al.* Clinical relevance of the Helicobacter pylori gene for blood-group antigen-binding adhesin. *Proc Natl Acad Sci U S A* **96**, 12778-12783 (1999).
56. Tan, S., Tompkins, L.S. & Amieva, M.R. Helicobacter pylori usurps cell polarity to turn the cell surface into a replicative niche. *PLoS Pathog* **5**, e1000407 (2009).
57. Gonzalez, C.A*., et al.* Helicobacter pylori cagA and vacA Genotypes as Predictors of Progression of Gastric Preneoplastic Lesions: A Long-Term Follow-Up in a High-Risk Area in Spain. *Am J Gastroenterol* (2011).
58. Hatakeyama, M. Helicobacter pylori CagA -- a bacterial intruder conspiring gastric carcinogenesis. *Int J Cancer* **119**, 1217-1223 (2006).

59. Evans, D.J., Jr*., et al.* Characterization of a Helicobacter pylori neutrophil-activating protein. *Infect Immun* **63**, 2213-2220 (1995).
60. Thun, M.J., DeLancey, J.O., Center, M.M., Jemal, A. & Ward, E.M. The global burden of cancer: priorities for prevention. *Carcinogenesis* **31**, 100-110 (2010).
61. Lee, C.W*., et al.* Helicobacter pylori eradication prevents progression of gastric cancer in hypergastrinemic INS-GAS mice. *Cancer Res* **68**, 3540-3548 (2008).
62. Lofgren, J.L*., et al.* Lack of commensal flora in Helicobacter pylori-infected INS-GAS mice reduces gastritis and delays intraepithelial neoplasia. *Gastroenterology* **140**, 210-220 (2011).
63. Mowat, C*., et al.* Omeprazole, Helicobacter pylori status, and alterations in the intragastric milieu facilitating bacterial N-nitrosation. *Gastroenterology* **119**, 339-347 (2000).
64. Stark, C.A*., et al.* Effects of omeprazole and amoxycillin on the human oral and gastrointestinal microflora in patients with Helicobacter pylori infection. *J Antimicrob Chemother* **38**, 927-939 (1996).
65. Adamsson, I., Edlund, C. & Nord, C.E. Impact of treatment of Helicobacter pylori on the normal gastrointestinal microflora. *Clin Microbiol Infect* **6**, 175-177 (2000).
66. Kato, S*., et al.* High salt diets dose-dependently promote gastric chemical carcinogenesis in Helicobacter pylori-infected Mongolian gerbils associated with a shift in mucin production from glandular to surface mucous cells. *Int J Cancer* **119**, 1558-1566 (2006).
67. Inoue, M. & Tsugane, S. Epidemiology of gastric cancer in Japan. *Postgrad Med J* **81**, 419-424 (2005).
68. Fox, J.G. & Wang, T.C. Inflammation, atrophy, and gastric cancer. *J Clin Invest* **117**, 60-69 (2007).
69. Koh, T.J. & Wang, T.C. Tumors of the stomach. in *Sleisinger & Fordtrans' gastrointestinal and liver disease: pathophysiology, diagnosis, management* (eds. Feldman, M., Friedman, L. & Sleisinger, M.) 829-855 (W.B. Saunders Co., Philadelphia, Pennsylvania, 2002).
70. El-Omar, E.M*., et al.* Interleukin-1 polymorphisms associated with increased risk of gastric cancer. *Nature* **404**, 398-402 (2000).
71. O'Keeffe, J. & Moran, A.P. Conventional, regulatory, and unconventional T cells in the immunologic response to Helicobacter pylori. *Helicobacter* **13**, 1-19 (2008).
72. Karttunen, R. Blood lymphocyte proliferation, cytokine secretion and appearance of T cells with activation surface markers in cultures with Helicobacter pylori. Comparison of the responses of subjects with and without antibodies to H. pylori. *Clin Exp Immunol* **83**, 396-400 (1991).
73. Mohammadi, M., Czinn, S., Redline, R. & Nedrud, J. Helicobacter-specific cell-mediated immune responses display a predominant Th1 phenotype and promote a delayed-type hypersensitivity response in the stomachs of mice. *J Immunol* **156**, 4729-4738 (1996).
74. Eaton, K.A., Mefford, M. & Thevenot, T. The role of T cell subsets and cytokines in the pathogenesis of Helicobacter pylori gastritis in mice. *J Immunol* **166**, 7456-7461 (2001).
75. Mohammadi, M., Nedrud, J., Redline, R., Lycke, N. & Czinn, S.J. Murine CD4 T-cell response to Helicobacter infection: TH1 cells enhance gastritis and TH2 cells reduce bacterial load. *Gastroenterology* **113**, 1848-1857 (1997).

76. Caruso, R., Pallone, F. & Monteleone, G. Emerging role of IL-23/IL-17 axis in H pylori-associated pathology. *World J Gastroenterol* **13**, 5547-5551 (2007).
77. Zhang, J.Y*., et al.* Induction of a Th17 cell response by Helicobacter pylori Urease subunit B. *Immunobiology* (2010).
78. Eaton, K.A., Ringler, S.R. & Danon, S.J. Murine splenocytes induce severe gastritis and delayed-type hypersensitivity and suppress bacterial colonization in Helicobacter pylori-infected SCID mice. *Infect Immun* **67**, 4594-4602 (1999).
79. Roth, K.A., Kapadia, S.B., Martin, S.M. & Lorenz, R.G. Cellular immune responses are essential for the development of Helicobacter felis-associated gastric pathology. *J Immunol* **163**, 1490-1497 (1999).
80. Fox, J.G*., et al.* Concurrent enteric helminth infection modulates inflammation and gastric immune responses and reduces helicobacter-induced gastric atrophy. *Nat Med* **6**, 536-542 (2000).
81. Lemke, L.B*., et al.* Concurrent Helicobacter bilis infection in C57BL/6 mice attenuates proinflammatory H. pylori-induced gastric pathology. *Infect Immun* **77**, 2147-2158 (2009).
82. Stoicov, C*., et al.* Coinfection modulates inflammatory responses and clinical outcome of Helicobacter felis and Toxoplasma gondii infections. *J Immunol* **173**, 3329-3336 (2004).
83. Holcombe, C. Helicobacter pylori: the African enigma. *Gut* **33**, 429-431 (1992).
84. Whary, M.T*., et al.* Intestinal helminthiasis in Colombian children promotes a Th2 response to Helicobacter pylori: possible implications for gastric carcinogenesis. *Cancer Epidemiol Biomarkers Prev* **14**, 1464-1469 (2005).
85. Suerbaum, S. & Michetti, P. Helicobacter pylori infection. *N Engl J Med* **347**, 1175-1186 (2002).
86. Crabtree, J.E*., et al.* Interleukin-8 expression in Helicobacter pylori infected, normal, and neoplastic gastroduodenal mucosa. *J Clin Pathol* **47**, 61-66 (1994).
87. Hamajima, N., Naito, M., Kondo, T. & Goto, Y. Genetic factors involved in the development of Helicobacter pylori-related gastric cancer. *Cancer Sci* **97**, 1129-1138 (2006).
88. Gonzalez, C.A., Sala, N. & Capella, G. Genetic susceptibility and gastric cancer risk. *Int J Cancer* **100**, 249-260 (2002).
89. Hamajima, N. Persistent Helicobacter pylori infection and genetic polymorphisms of the host. *Nagoya journal of medical science* **66**, 103-117 (2003).
90. Liou, J.M*., et al.* IL-1B-511 C-->T polymorphism is associated with increased host susceptibility to Helicobacter pylori infection in Chinese. *Helicobacter* **12**, 142-149 (2007).
91. Seno, H*., et al.* Novel interleukin-4 and interleukin-1 receptor antagonist gene variations associated with non-cardia gastric cancer in Japan: Comprehensive analysis of 207 polymorphisms of 11 cytokine genes. *J Gastroenterol Hepatol* **22**, 729-737 (2007).
92. Lu, W*., et al.* Genetic polymorphisms of interleukin (IL)-1B, IL-1RN, IL-8, IL-10 and tumor necrosis factor {alpha} and risk of gastric cancer in a Chinese population. *Carcinogenesis* **26**, 631-636 (2005).
93. Taguchi, A*., et al.* Interleukin-8 promoter polymorphism increases the risk of atrophic gastritis and gastric cancer in Japan. *Cancer Epidemiol Biomarkers Prev* **14**, 2487-2493

(2005).
94. Baik, S.C.*, et al.* Increased oxidative DNA damage in Helicobacter pylori-infected human gastric mucosa. *Cancer research* **56**, 1279-1282 (1996).
95. Papa, A.*, et al.* Role of Helicobacter pylori CagA+ infection in determining oxidative DNA damage in gastric mucosa. *Scand J Gastroenterol* **37**, 409-413 (2002).
96. Jang, J.*, et al.* Malgun (clear) cell change in Helicobacter pylori gastritis reflects epithelial genomic damage and repair. *Am J Pathol* **162**, 1203-1211 (2003).
97. Arabski, M.*, et al.* DNA damage and repair in Helicobacter pylori-infected gastric mucosa cells. *Mutation research* **570**, 129-135 (2005).
98. Burney, S., Caulfield, J.L., Niles, J.C., Wishnok, J.S. & Tannenbaum, S.R. The chemistry of DNA damage from nitric oxide and peroxynitrite. *Mutat Res* **424**, 37-49 (1999).
99. Bartsch, H. & Nair, J. Potential role of lipid peroxidation derived DNA damage in human colon carcinogenesis: studies on exocyclic base adducts as stable oxidative stress markers. *Cancer Detect Prev* **26**, 308-312 (2002).
100. Huang, W.Y.*, et al.* Selected DNA repair polymorphisms and gastric cancer in Poland. *Carcinogenesis* **26**, 1354-1359 (2005).
101. Singer, B. & Hang, B. What structural features determine repair enzyme specificity and mechanism in chemically modified DNA? *Chemical research in toxicology* **10**, 713-732 (1997).
102. Sandercock, L.E.*, et al.* Mutational-reporter transgenes rescued from mice lacking either Mgmt, or both Mgmt and Msh6 suggest that O6-alkylguanine-induced miscoding does not contribute to the spontaneous mutational spectrum. *Oncogene* **23**, 5931-5940 (2004).
103. Oue, N.*, et al.* Promoter methylation status of the DNA repair genes hMLH1 and MGMT in gastric carcinoma and metaplastic mucosa. *Pathobiology* **69**, 143-149 (2001).
104. Oue, N.*, et al.* Promoter hypermethylation of MGMT is associated with protein loss in gastric carcinoma. *International journal of cancer* **93**, 805-809 (2001).
105. Hanaoka, T.*, et al.* hOGG1 exon7 polymorphism and gastric cancer in case-control studies of Japanese Brazilians and non-Japanese Brazilians. *Cancer Lett* **170**, 53-61 (2001).
106. Izzotti, A.*, et al.* Interplay between Helicobacter pylori and host gene polymorphisms in inducing oxidative DNA damage in the gastric mucosa. *Carcinogenesis* **28**, 892-898 (2007).
107. Farinati, F.*, et al.* Oxidative DNA damage in gastric cancer: CagA status and OGG1 gene polymorphism. *Int J Cancer* **123**, 51-55 (2008).
108. Straub, R.H. The complex role of estrogens in inflammation. *Endocr Rev* **28**, 521-574 (2007).
109. Cutolo, M. & Wilder, R.L. Different roles for androgens and estrogens in the susceptibility to autoimmune rheumatic diseases. *Rheum Dis Clin North Am* **26**, 825-839 (2000).
110. Lindblad, M., Ye, W., Rubio, C. & Lagergren, J. Estrogen and risk of gastric cancer: a protective effect in a nationwide cohort study of patients with prostate cancer in Sweden. *Cancer Epidemiol Biomarkers Prev* **13**, 2203-2207 (2004).
111. Newcomb, P.A. & Storer, B.E. Postmenopausal hormone use and risk of large-bowel cancer. *J Natl Cancer Inst* **87**, 1067-1071 (1995).
112. Nanda, K., Bastian, L.A., Hasselblad, V. & Simel, D.L. Hormone replacement therapy and

the risk of colorectal cancer: a meta-analysis. *Obstet Gynecol* **93**, 880-888 (1999).
113. Pukkala, E., Tulenheimo-Silfvast, A. & Leminen, A. Incidence of cancer among women using long versus monthly cycle hormonal replacement therapy, Finland 1994-1997. *Cancer Causes Control* **12**, 111-115 (2001).
114. White, I.N. Anti-oestrogenic drugs and endometrial cancers. *Toxicol Lett* **120**, 21-29 (2001).
115. Curtis, R.E., Boice, J.D., Jr., Shriner, D.A., Hankey, B.F. & Fraumeni, J.F., Jr. Second cancers after adjuvant tamoxifen therapy for breast cancer. *J Natl Cancer Inst* **88**, 832-834 (1996).
116. Rutqvist, L.E.*, et al.* Adjuvant tamoxifen therapy for early stage breast cancer and second primary malignancies. Stockholm Breast Cancer Study Group. *J Natl Cancer Inst* **87**, 645-651 (1995).
117. Matsuyama, Y.*, et al.* Second cancers after adjuvant tamoxifen therapy for breast cancer in Japan. *Ann Oncol* **11**, 1537-1543 (2000).
118. Chandanos, E.*, et al.* Tamoxifen exposure and risk of oesophageal and gastric adenocarcinoma: a population-based cohort study of breast cancer patients in Sweden. *Br J Cancer* **95**, 118-122 (2006).
119. Tsugane, S. & Sasazuki, S. Diet and the risk of gastric cancer: review of epidemiological evidence. *Gastric Cancer* **10**, 75-83 (2007).
120. Tsugane, S. Salt, salted food intake, and risk of gastric cancer: epidemiologic evidence. *Cancer Sci* **96**, 1-6 (2005).
121. Joossens, J.V.*, et al.* Dietary salt, nitrate and stomach cancer mortality in 24 countries. European Cancer Prevention (ECP) and the INTERSALT Cooperative Research Group. *Int J Epidemiol* **25**, 494-504 (1996).
122. Rogers, A.B.*, et al.* Helicobacter pylori but not high salt induces gastric intraepithelial neoplasia in B6129 mice. *Cancer Res* **65**, 10709-10715 (2005).
123. IARC. Tobacco Smoke and Involuntary Smoking. *IARC Monographs* **83**(2004).
124. Terry, M.B., Gaudet, M.M. & Gammon, M.D. The epidemiology of gastric cancer. *Semin Radiat Oncol* **12**, 111-127 (2002).
125. Gillen, D. & McColl, K.E. Problems associated with the clinical use of proton pump inhibitors. *Pharmacol Toxicol* **89**, 281-286 (2001).
126. Fox, J.G. & Kuipers, E.J. Long-term proton pump inhibitor administration induces atrophic corpus gastritis and promotes adenocarcinoma development in Mongolian gerbils infected with Helicobacter pylori. *Gut* (2011).
127. Krakowka, S., Morgan, D.R., Kraft, W.G. & Leunk, R.D. Establishment of gastric Campylobacter pylori infection in the neonatal gnotobiotic piglet. *Infect Immun* **55**, 2789-2796 (1987).
128. Shuto, R., Fujioka, T., Kubota, T. & Nasu, M. Experimental gastritis induced by Helicobacter pylori in Japanese monkeys. *Infect Immun* **61**, 933-939 (1993).
129. Tsuda, M.*, et al.* Essential role of Helicobacter pylori urease in gastric colonization: definite proof using a urease-negative mutant constructed by gene replacement. *European journal of gastroenterology & hepatology* **6 Suppl 1**, S49-52 (1994).
130. Karita, M., Kouchiyama, T., Okita, K. & Nakazawa, T. New small animal model for human gastric Helicobacter pylori infection: success in both nude and euthymic mice. *Am J Gastroenterol* **86**, 1596-1603 (1991).

131. Lee, A., Fox, J.G., Otto, G. & Murphy, J. A small animal model of human *Helicobacter pylori* active chronic gastritis. *Gastroenterology* **99**, 1315-1323 (1990).
132. Wang, T.C*., et al.* Mice lacking secretory phospholipase A2 show altered apoptosis and differentiation with *Helicobacter felis* infection. *Gastroenterology* **114**, 675-689 (1998).
133. Cai, X*., et al.* Helicobacter felis eradication restores normal architecture and inhibits gastric cancer progression in C57BL/6 mice. *Gastroenterology* **128**, 1937-1952 (2005).
134. Ghiara, P*., et al.* Role of the Helicobacter pylori virulence factors vacuolating cytotoxin, CagA, and urease in a mouse model of disease. *Infect Immun* **63**, 4154-4160 (1995).
135. Marchetti, M*., et al.* Development of a mouse model of Helicobacter pylori infection that mimics human disease. *Science* **267**, 1655-1658 (1995).
136. Cellini, L*., et al.* Coccoid Helicobacter pylori not culturable in vitro reverts in mice. *Microbiol Immunol* **38**, 843-850 (1994).
137. Lee, A*., et al.* A standardized mouse model of Helicobacter pylori infection: introducing the Sydney strain. *Gastroenterology* **112**, 1386-1397 (1997).
138. Thompson, L.J*., et al.* Chronic Helicobacter pylori infection with Sydney strain 1 and a newly identified mouse-adapted strain (Sydney strain 2000) in C57BL/6 and BALB/c mice. *Infect Immun* **72**, 4668-4679 (2004).
139. Panthel, K., Faller, G. & Haas, R. Colonization of C57BL/6J and BALB/c wild-type and knockout mice with Helicobacter pylori: effect of vaccination and implications for innate and acquired immunity. *Infect Immun* **71**, 794-800 (2003).
140. Court, M., Robinson, P.A., Dixon, M.F., Jeremy, A.H. & Crabtree, J.E. The effect of gender on Helicobacter felis-mediated gastritis, epithelial cell proliferation, and apoptosis in the mouse model. *J Pathol* **201**, 303-311 (2003).
141. Fox, J.G*., et al.* Helicobacter pylori-associated gastric cancer in INS-GAS mice is gender specific. *Cancer Res* **63**, 942-950 (2003).
142. Reliene, R. & Schiestl, R.H. Mouse models for induced genetic instability at endogenous loci. *Oncogene* **22**, 7000-7010 (2003).
143. Nohmi, T., Suzuki, T. & Masumura, K. Recent advances in the protocols of transgenic mouse mutation assays. *Mutat Res* **455**, 191-215 (2000).
144. Stambrook, P.J*., et al.* APRT: a versatile in vivo resident reporter of local mutation and loss of heterozygosity. *Environ Mol Mutagen* **28**, 471-482 (1996).
145. Chen, J*., et al.* Identification of a single missense mutation in the adenine phosphoribosyltransferase (APRT) gene from five Icelandic patients and a British patient. *Am J Hum Genet* **49**, 1306-1311 (1991).
146. Jenks, P.J., Jeremy, A.H., Robinson, P.A., Walker, M.M. & Crabtree, J.E. Long-term infection with Helicobacter felis and inactivation of the tumour suppressor gene p53 cumulatively enhance the gastric mutation frequency in Big Blue transgenic mice. *J Pathol* **201**, 596-602 (2003).
147. Touati, E*., et al.* Deficiency in OGG1 protects against inflammation and mutagenic effects associated with H. pylori infection in mouse. *Helicobacter* **11**, 494-505 (2006).
148. Touati, E*., et al.* Chronic Helicobacter pylori infections induce gastric mutations in mice. *Gastroenterology* **124**, 1408-1419 (2003).
149. Sato, Y*., et al.* IL-10 deficiency leads to somatic mutations in a model of IBD. *Carcinogenesis* **27**, 1068-1073 (2006).

150. Nohmi, T.*, et al.* A new transgenic mouse mutagenesis test system using Spi- and 6-thioguanine selections. *Environ Mol Mutagen* **28**, 465-470 (1996).
151. Bregegere, F. Bacteriophage P2-lambda interference. III. Essential role of an early step in the initiation of lambda replication. *J Mol Biol* **122**, 113-125 (1978).
152. Hatakeyama, M. SagA of CagA in Helicobacter pylori pathogenesis. *Curr Opin Microbiol* **11**, 30-37 (2008).
153. Correa, P., Camargo, M.C. & Piazuelo, M.B. Overview and Pathology of Gastric Cancer. in *The Biology of Gastric Cancers* (eds. Wang, T.C., Fox, J.G. & Giraud, A.S.) (Springer Science + Business Media, LLC, New York, NY, 2009).

1.8 Tables and Figures

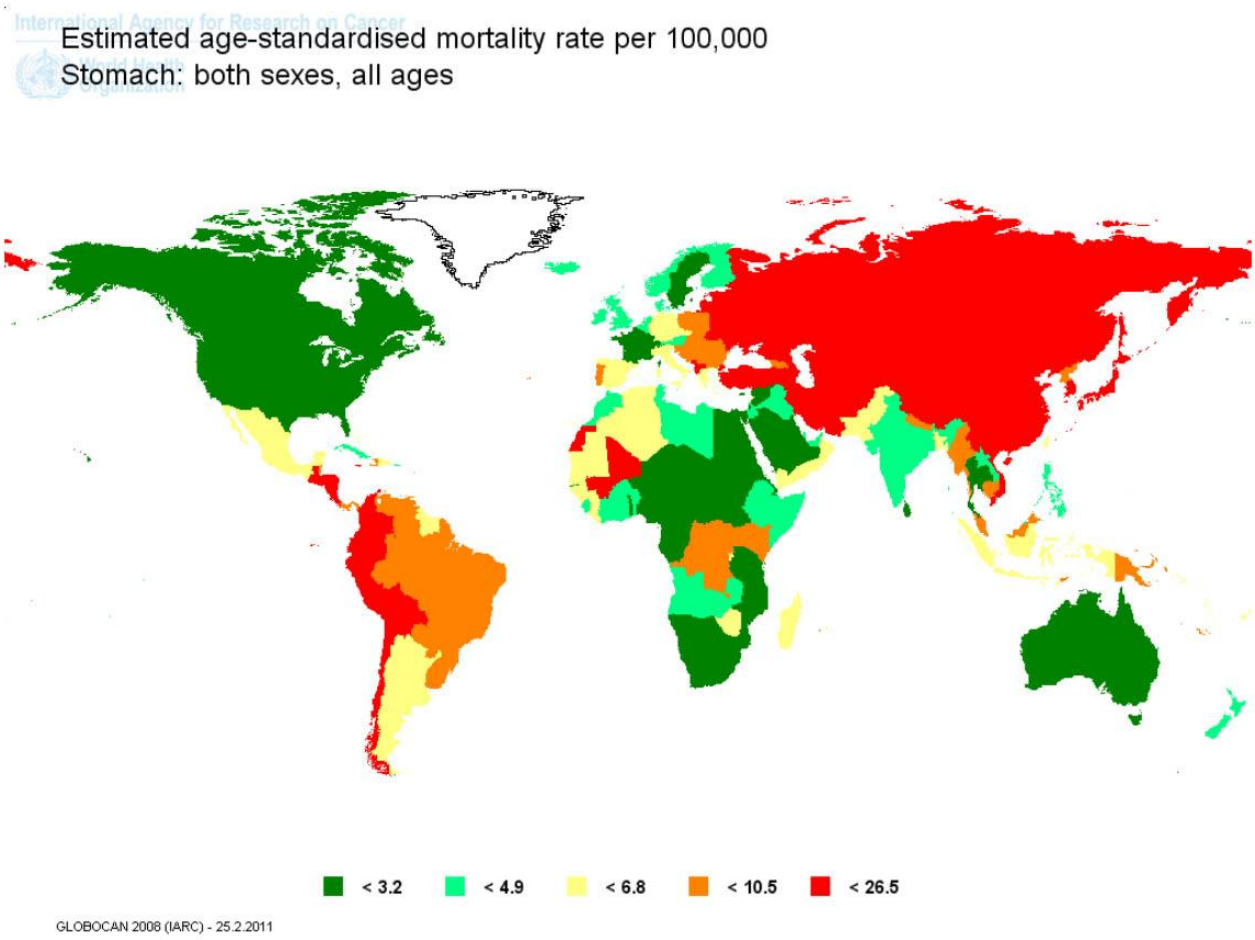

Figure 1.1. Mortality rates of gastric cancer in 2008 for men and women. Higher mortality rates are observed in Eastern Asia, Russia, Central America and the Pacific coast of South America. Lower mortality rates are observed in Western Europe, North America, Africa and Australia.

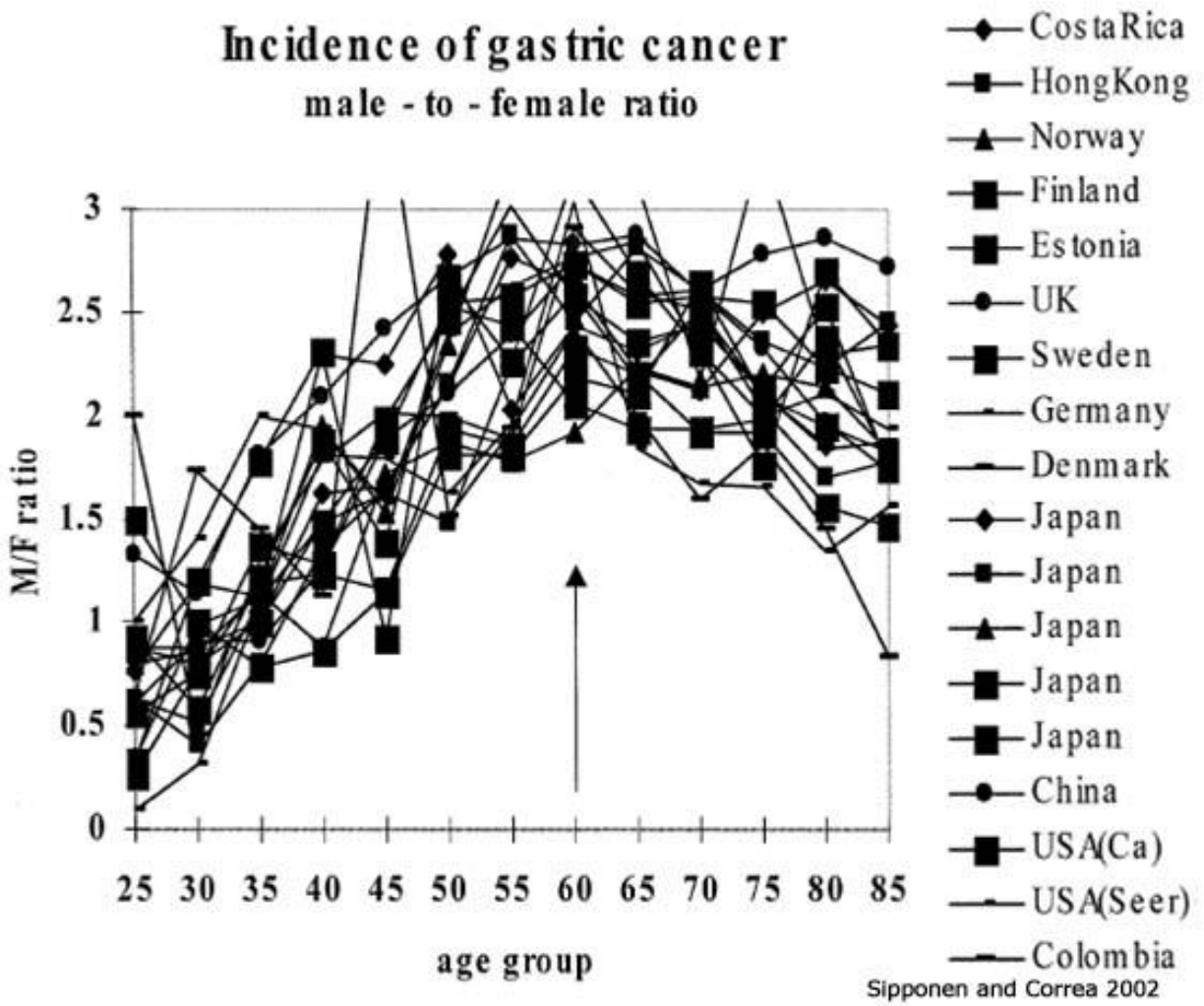

Figure 1.2. Age-standardized incidence rates of gastric cancer demonstrate a sexual dimorphism with men twice as likely as women of developing gastric adenocarcinomas. This survey compared epidemiological data from 18 surveys in 13 countries. The 13 countries encompass a wide range of geographical locations with varying incidences of gastric cancer demonstrating that the male predominance is a global phenomenon[11].

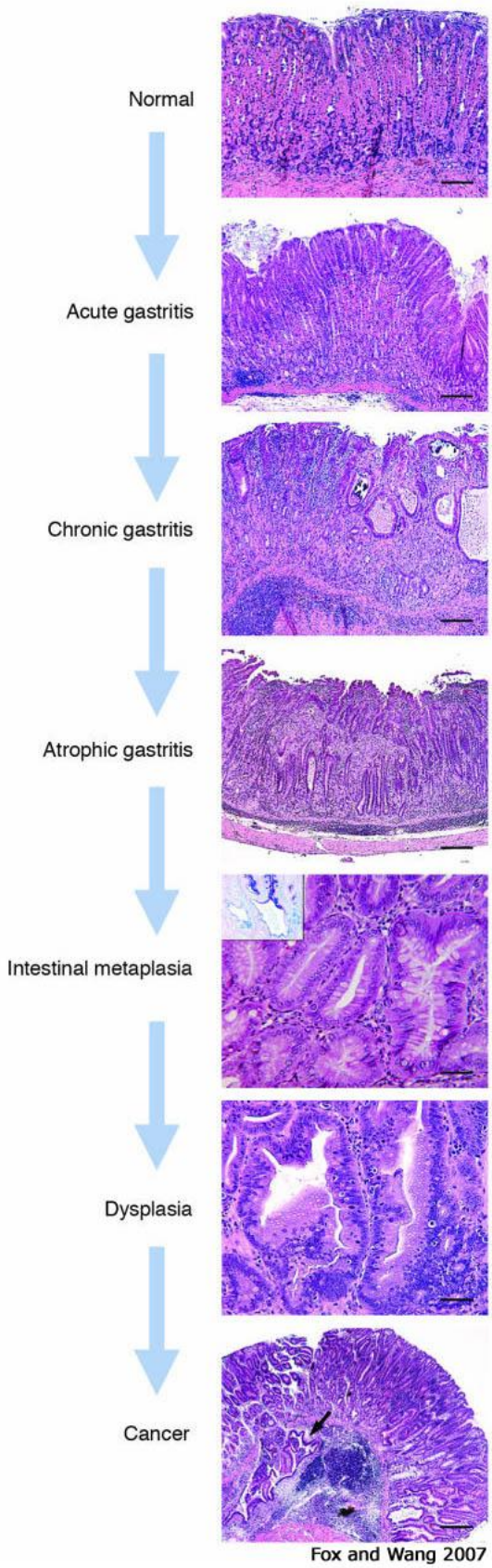

Figure 1.3. Histological progression of *Helicobacter*-induced gastric cancer in mouse model. Normal represents histology of the gastric body prior to infection. Acute gastritis results after *Helicobacter* infection with infiltration of lymphocytes and neutrophils. Subsequently, chronic gastritis ensues with moderate to severe inflammation with epithelial defects. Atrophic gastritis includes the loss of oxyntic parietal and chief cells. The next step, intestinal metaplasia, is the change of the gastric epithelia to an intestinal phenotype with columnar elongation, and increased mucins. High-grade glandular dysplasia is characterized by irregular size and shape, infolding, branching and cell piling, and marked cellular and nuclear atypia. Gastric intraepithelial neoplasia with intramucosal invasion (arrow) is classified as cancer. Scale bars: 160 µm (first panel); 400 µm (second through fourth panels); 80 µm (fifth panel; inset, original magnification, ×400); 40 µm (sixth panel); 800 µm (seventh panel)[68].

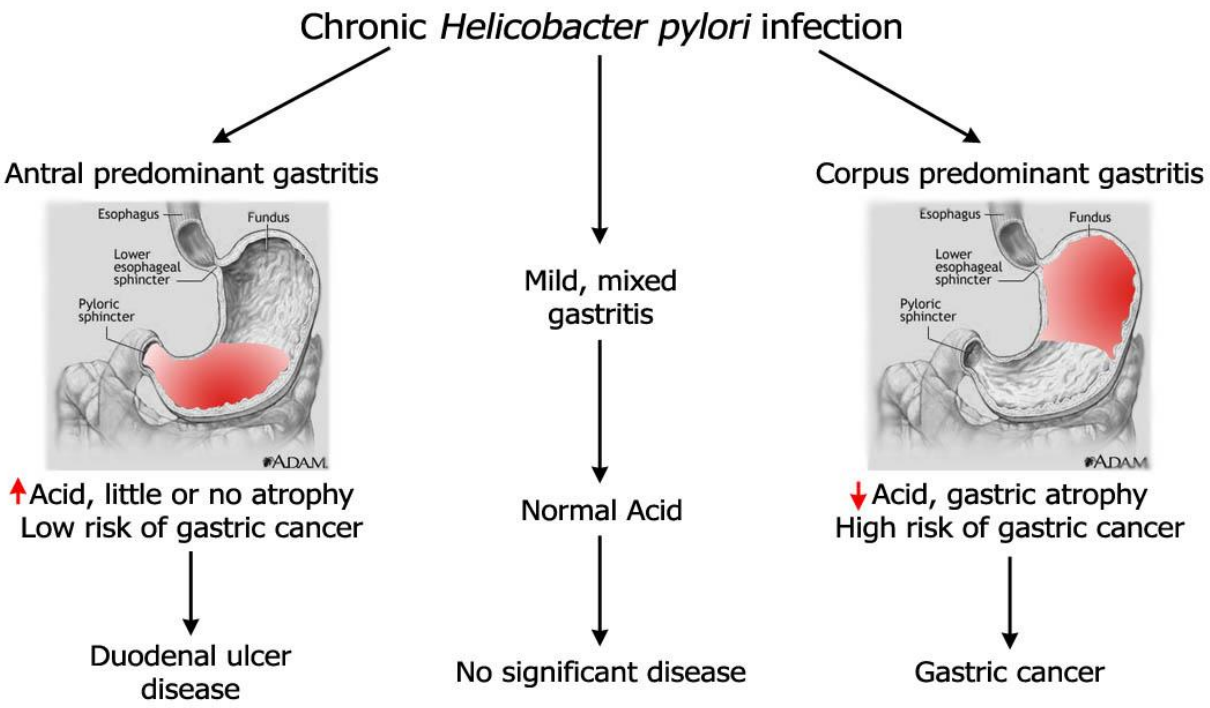

Figure 1.4. Divergent responses to *H. pylori* infection lead to three major clinical outcomes. The majority of *H. pylori* infected individuals do not develop overt clinical symptoms. Duodenal ulcers are observed in 5-15% of patients while 1-2% of infected individuals develop gastric cancer[36-37].

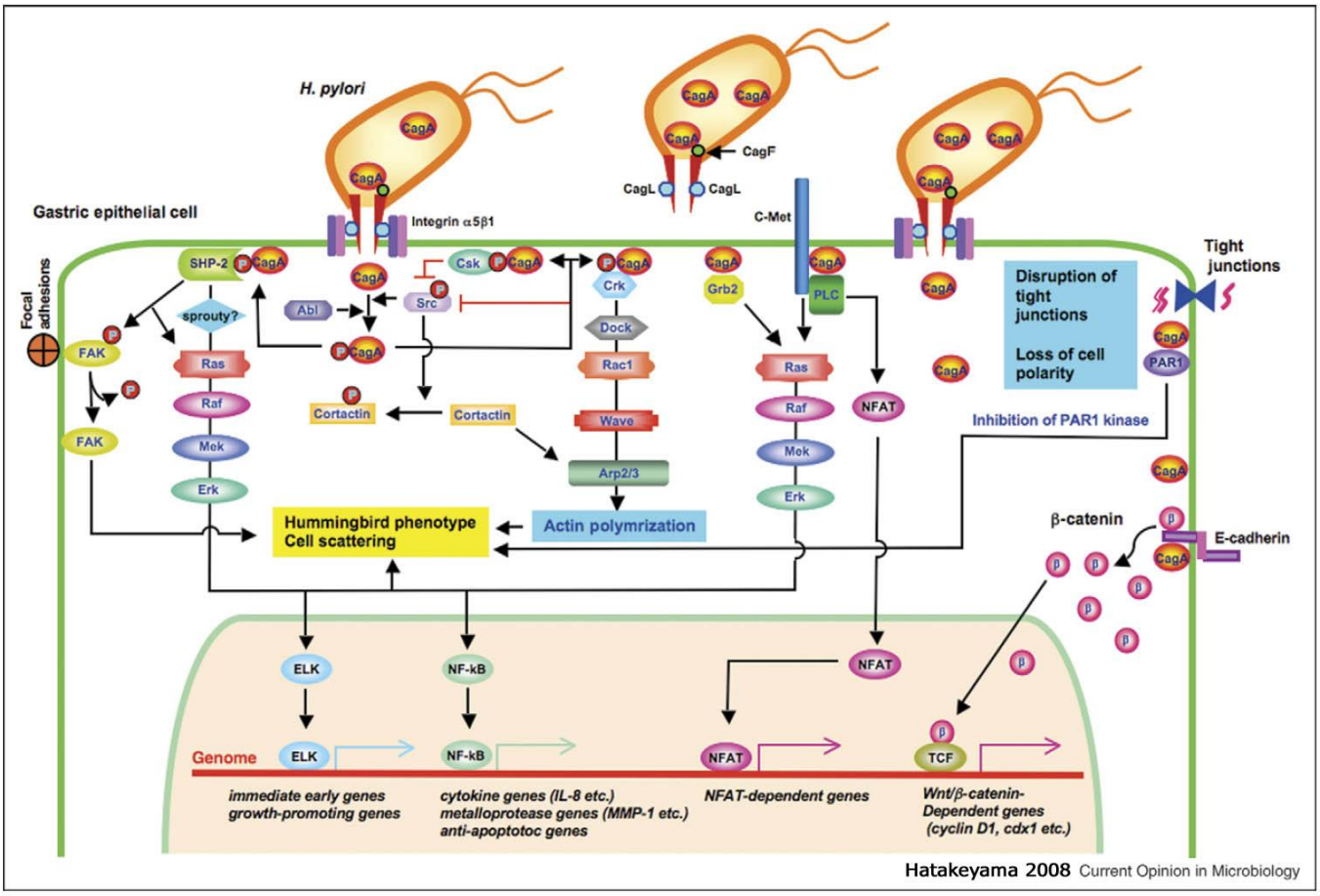

Figure 1.5. Effects of CagA translocation on host epithelial cells. After being tyrosine-phosphorylated, CagA can interact with member of the c-Met signaling pathway including SHP-2, Csk, Crk. CagA also mediates cell junction disruption by affecting PAR1 kinase and E-cadherin. Destabilization of E-cadherin leads to deregulated Wnt/β-catenin signaling[152].

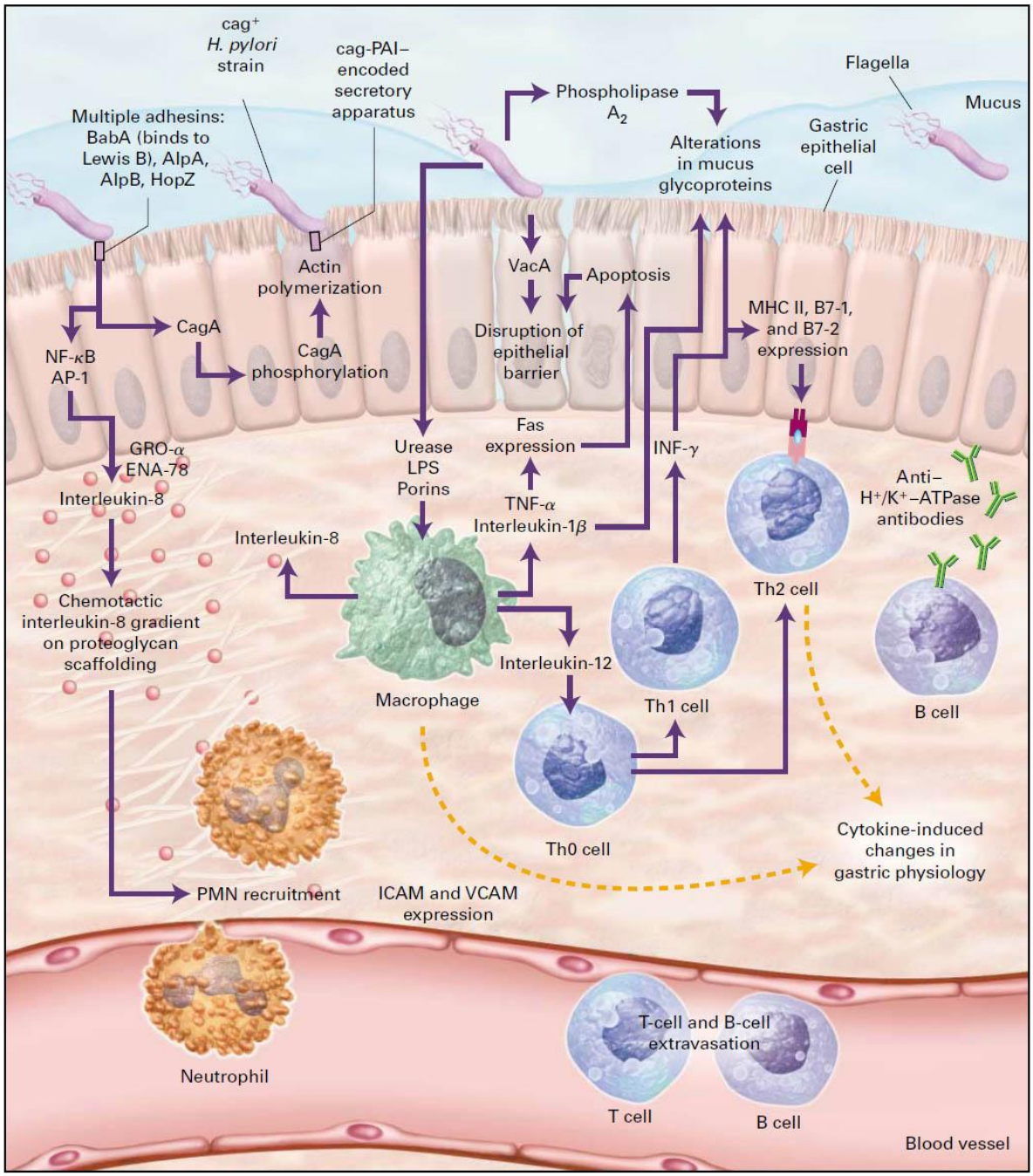

Figure 1.6. Host responses to *H. pylori* infection. After encountering *H. pylori,* epithelial cells create a chemotactic gradient leading to the recruitment of neutrophils. Subsequently, macrophages and lymphocytes arrive at the site of infection and proinflammatory cytokines are released[85].

Polymorphisms in genes related to processes relevant to gastric carcinogenesis

Process	Gene and variant
Protection of gastric mucosa against damaging agents	*MUC1* *MUC6* *TFF2*
Inflammatory response	*IL1B (−31T>C, −511C>T, +3954C>T)* *IL1RN*2* *IL10 (−1082G>A, −819C>T)* *IL8 (−51T>A, +396T>G, +781C>T)* *IL8RB (+785T>C, +1208C>T, +1440G>A)* *IL4-590 C>T* *TNF (−308G>A, −238G>A)* *COX-2 (PTG52-1195G>A, -765G>C)* *iNOS (NOS2A 150C>T, -2445C>G)* *CD14-260C>T* *IFNGR2 Ex7-128 C>T* *HLA class I gene* *HLA class II gene*
Ability to detoxify carcinogens (Phase I and II enzymes)	*CYP2E-1053C>T (RsaI)* *GSTM1* null *GSTT1* null *GSTM3*B (IVS6del3)* *GSTP1 1578A>G (I105V)* *NAT1*10 (1088T>A, 1095C>A)* *NAT2*
Protection against oxidative damage and other inductors of DNA damage	Oxidative damage: *MTHFR (677C>T* and *1298A>C)* *MTHFD (1958G>A* and *401T>C)* DNA repair: *XRCC1 26304C>T (R194W) 28152G>A (R399Q)* *OGG1 S326C* Oncogenes and tumor suppressor genes: *MYCL1 (previous symbol: L-myc) EcoRI* *TP53 codon 72*
Cell proliferation ability/cell differentiation/ cell homeostasis	*Cyclin D1 870A>G* *PGC* *CDH1-160C>A* *EGF* promoter *(61A>G, −1380A>G, −1744G>A)* *TGFB1-509C>T* *TGFBR2-875A>G* *JWA-76G >C*

Abbreviations: TFF: trefoil peptides; TNF: tumor necrosis factor; COX2: cyclooxygenase 2; iNOS: inducible nitric oxide synthase; IFNGR2: interferon gamma receptor 2; GST: glutathione S-transferase; NAT: N-acetyl transferase; MTHFR: 5,10-methylenetetrahydrofolate reductase; MTHFD: methylenetetrahydrofolate dehydrogenase; XRCC1: x-ray repair cross complementing group 1; OGG1: 7,8-dihydro-8-oxoguanine-DNA glycosylase; TP53: tumor protein 53; PGC: pepsinogen C; CDH1: E-cadherin; EGF: epidermal growth factor; TGFB: transforming growth factor beta; TGFBR2: TGFB receptor II.

Correa et al. 2009

Table 1.1. Polymorphisms in genes that have been studied for association with gastric cancer (Note: not all SNPs presented in the table have effects on gastric cancer)[153].

Chapter 2: Mutagenic potency of *Helicobacter pylori* in the gastric mucosa of mice is determined by sex and duration of infection

A version of this chapter has been previously published and is reprinted here with the permission of the publisher:

Sheh, A., Chung Wei Lee, Kenichi Masumura, Barry H. Rickman, Takehiko Nohmi, Gerald N. Wogan, James G. Fox, and David B. Schauer. Mutagenic potency of Helicobacter pylori in the gastric mucosa of mice is determined by sex and duration of infection. *Proc Natl Acad Sci U S A* 107, 15217-15222 (2010).

ABSTRACT

Helicobacter pylori is a human carcinogen, but the mechanisms evoked in carcinogenesis during this chronic inflammatory disease remain incompletely characterized. We determined whether chronic *H. pylori* infection induced mutations in the gastric mucosa of male and female *gpt* delta C57BL/6 mice infected for 6 or 12 mo. Point mutations were increased in females infected for 12 mo. The mutation frequency in this group was 1.6-fold higher than in uninfected mice of both sexes ($P < 0.05$). A:T-to-G:C transitions and G:C-to-T:A transversions were 3.8 and 2.0 times, respectively, more frequent in this group than in controls. Both mutations are consistent with DNA damage induced by oxidative stress. No increase in the frequency of deletions was observed. Females had more severe gastric lesions than males at 6 mo postinfection (MPI; $P < 0.05$), but this difference was absent at 12 MPI. In all mice, infection significantly increased expression of *IFNγ*, *IL-17, TNFα,* and *iNOS* at 6 and 12 mo, as well as *H. pylori*–specific IgG1 levels at 12 MPI ($P < 0.05$) and IgG2c levels at 6 and 12 MPI ($P < 0.01$ and $P < 0.001$). At 12 MPI, IgG2c levels in infected females were higher than at 6 MPI ($P < 0.05$) and also than those in infected males at 12 MPI ($P<0.05$). Intensity of responses was mediated by sex and duration of infection. Lower *H. pylori* colonization indicated a more robust host response in females than in

males. Earlier onset of severe gastric lesions and proinflammatory, Th1-biased responses in female C57BL/6 mice may have promoted mutagenesis by exposing the stomach to prolonged oxidative stress.

2.1 Introduction

Acting through multiple, complex mechanisms that are incompletely understood, chronic inflammation is a significant risk factor for several major human malignancies, including stomach cancer. Chronic inflammation induced by *Helicobacter pylori* infection increases lifetime risk of developing gastritis, duodenal and gastric ulcers, mucosa-associated lymphoid tissue lymphoma, mucosal atrophy, and gastric carcinoma (1, 2). Indeed, *H. pylori* has been classified by International Agency for Research on Cancer as a group I human carcinogen on the basis of its impact on gastric cancer incidence, the second most frequent cause of cancer-related death worldwide (3). Among postulated mechanisms through which infection may contribute to increased cancer risk are overproduction of reactive oxygen and nitrogen species (RONS) by inflammatory cells, and the consequent induction of mutations critical for tumor initiation in cells of inflamed tissues (4). The inflammatory response to infection results in increased production of RONS, including superoxide ($O_2^{-\cdot}$), hydrogen peroxide (H_2O_2), nitric oxide (NO), peroxynitrite (ONO_2^-), and nitrous anhydride (N_2O_3), in vitro (5, 6) and in vivo (7–9). *H. pylori* can also directly activate RONS-producing enzymes, such as inducible NO synthase (iNOS) and spermine oxidase, in gastric epithelial cells, causing DNA damage and apoptosis (5, 6). Chronic inflammatory states increase levels of DNA adducts, such as etheno adducts, 8-oxoG, and other mutagenic precursors, in vitro and in vivo (10–12), but tend not to alter the frequency of deletions (13). RONS also can damage DNA indirectly by creating adduct-forming electrophiles via lipid peroxidation (14, 15). RONS have been shown to induce mutations in *H. pylori* by inducing a hypermutation state in the bacteria (16).

A widely used experimental model is the *H. pylori* SS1-infected C57BL/6 mouse, which is susceptible to chronic infection and develops robust gastritis and premalignant lesions similar to those occurring in humans (17, 18). To date, limited investigation has focused on genetic damage associated with infection in these animals, but available data are still incomplete. Enhanced DNA fragmentation was observed in gastric cells of infected mice (19), in which dsDNA breaks were also detected by TUNEL assay (20, 21). Mutagenicity in reporter genes recovered from gastric DNA of male and female Big Blue transgenic mice 6mo after infection with *H. pylori* or *Helicobacter felis* has also been reported (22). In *H. pylori*-infected male mice, point mutation frequency was increased at 6 mo post infection (MPI), but decreased to control levels by 12 MPI, suggesting that the animals may have adapted to infection (22). Female mice infected with *H. felis* also had an increased frequency of point mutations at 7 MPI, compared with uninfected controls (23). Mutagenesis resulting from infection has also been associated with p53 status. Mutations were found in the *lacI* reporter genes of a small number of *H. felis*-infected female TSGp53/Big Blue mice harboring either one (p53+/−) or two (p53+/+) WT p53 alleles (23). A 2-fold increase in mutations was found in DNA from the gastric mucosa of infected p53+/+ mice, and also in uninfected p53+/− mice; the mutation frequency in infected p53+/− mice was further increased by approximately threefold. The intensity of inflammation was estimated to be significantly higher in infected p53+/− mice than in infected p53+/+ animals, and gastric epithelial proliferation was similarly increased with infection in both latter treatment groups. By contrast, in another study, infection of Big Blue transgenic mice (sex not specified) with the SS1 strain of *H. pylori* for 3.5 mo resulted in no significant increase in gastric mutations over uninfected controls (13).

We used the *gpt* delta mouse to measure the accumulation of gastric mutations associated with *H. pylori* SS1 infection in male and female animals at 6 and 12 MPI. This experimental system comprises λ-EG10–based transgenic C57BL/6 mice harboring tandem arrays of 80 copies of the bacterial *gpt* gene at a single site on chromosome 17. The model was specifically designed to facilitate the in vivo detection of point mutations by 6-thioguanine (6-TG) selection, and deletions up to 10 kb in length by selection based on sensitivity to P2 interference (Spi−) (24). When phage DNA rescued from mouse tissues is introduced into appropriate *Escherichia coli* strains, both point mutations and large deletions
can be efficiently detected (24). We also characterized histopathologic changes, expression of inflammatory cytokines, and expression of *iNOS* in gastric mucosa 6 and 12 mo after initial infection. In addition, we compared responses of male and female mice to assess the influence of sex. We found that *H. pylori* infection induced significant increases in the frequency of point mutations in the gastric mucosa of female, but not male, *gpt* delta mice. The accumulation of point mutations was therefore sex-dependent and was mediated by the duration of infection and the severity of disease.

2.2 Results and Discussion

2.2.1 Pathology, Cytokine and iNOS Expression, and Serologic Responses to *H. pylori* Infection and *H. pylori* Levels. Inflammatory histopathologic changes resulting from *H. pylori* infection were evaluated (Fig. 2.S1) and gastric histological activity index (GHAI) scores calculated, with the following results. Scores were significantly increased in infected animals of both sexes at 6 and 12 MPI (female, $P < 0.001$ and $P < 0.01$, respectively; and male, $P < 0.05$ and $P < 0.001$,

respectively; Fig. 2.1). Regarding specific types of lesions represented in the GHAI, infected females experienced higher levels of hyperplasia ($P < 0.05$), epithelial defects ($P < 0.001$), and dysplasia ($P < 0.05$) compared with infected males at 6 MPI, and thus had correspondingly higher ($P < 0.05$) GHAI scores at this time point. At 6 MPI, infected animals of both sexes displayed mild to moderate inflammation, comprised chiefly of submucosal and mucosal infiltrates of mononuclear and granulocytic cells. In addition, in infected males, mucous metaplasia, intestinal metaplasia, oxyntic gland atrophy, and hyalinosis were all significantly elevated compared with controls (all $P < 0.01$; intestinal metaplasia, $P < 0.001$); no significant increases occurred in foveolar hyperplasia, epithelial defects, or dysplasia. In infected females, inflammation ($P < 0.05$), epithelial defects ($P < 0.001$), mucous metaplasia ($P < 0.01$), hyalinosis ($P < 0.001$), as well as premalignant lesions of oxyntic gland atrophy ($P < 0.001$), intestinal metaplasia ($P < 0.05$), and dysplasia ($P < 0.05$) were significantly elevated compared with uninfected controls. At 12 MPI, there were no differences in gastric lesion severity between infected males and females; both groups had similar mucosal changes. Infected male mice at 12 MPI displayed significantly increased epithelial defects but decreased intestinal metaplasia than infected males at 6 MPI ($P < 0.01$ and $P < 0.001$).

H. pylori infection significantly increased transcription profiles at 6 and 12 MPI as follows (details in Fig. 2.S2): *IFNγ* (males, $P < 0.001$; females, $P < 0.01$ at 6 and 12 MPI); *TNF-α* (males, $P < 0.01$ at 6 and 12 MPI; females, $P < 0.01$ and $P < 0.05$); *IL-17* (males, $P < 0.05$ and $P < 0.001$; females, $P < 0.05$ and $P < 0.01$). *iNOS* expression was increased in male and female mice at 6 and 12 MPI (males, $P < 0.05$ and $P < 0.01$; females, $P < 0.01$ and $P < 0.001$) compared with

controls at 12 mo. *IL-10* expression was not significantly affected by infection in animals of either sex ($P > 0.05$).

H. pylori infection also resulted in a Th1-predominant IgG2c response in infected mice as previously reported (25, 26) (Fig. 2.2). *H. pylori*-specific IgG2c levels were higher in infected than in uninfected animals at 6 and 12 MPI ($P < 0.01$ and $P < 0.001$, respectively). At 12 MPI, infected females had significantly higher IgG2c levels than infected males ($P < 0.05$). Duration of infection also increased IgG2c levels in infected females, with higher levels noted at 12 versus 6 MPI ($P < 0.05$). *H. pylori*-specific IgG1 (Th2) levels were higher in infected than in uninfected animals at 12 MPI ($P < 0.05$). Females had higher Th1/Th2 ratios than males: at 6 MPI, 8.58 vs. 4.01; and at 12 MPI, 12.9 vs. 7.51.

We and others have demonstrated that *H. pylori* levels are inversely correlated with the degree of pathology and the immune response as measured by antibody and cytokine production (25, 27). At 6 MPI, *H. pylori* was detectable by quantitative PCR in all infected males, but not in one female. At 12 MPI, there was a salient difference in levels of *H. pylori* colonization between males and females; *H. pylori* was undetectable in four infected females, but undetectable in only one male (Fig. 2.3).

2.2.2 Frequency and Nature of Mutations. We determined the frequency of *gpt* point mutations in gastric DNA isolated from infected and uninfected mice by selection of mutants based on 6-TG resistance. Recognizing the possible confounding effect of clonal expansion of sibling mutants (i.e., jackpot mutations), we sequenced the *gpt* genes from all 566 recovered mutants. Any mutation found to duplicate another at the same site within an individual sample was excluded from subsequent frequency calculations. After this adjustment, at 12 MPI the *gpt*

mutation frequency in infected females (7.5 ± 2.0 × 10−6; $P < 0.05$) was significantly (1.6-fold) higher than that in all control animals (4.7 ± 1.1 × 10−6), whereas the frequency in infected males (6.3 ± 5.4 × 10−6; $P = 0.49$) was not. At 6 MPI, *gpt* mutation frequency in infected animals of either sex (females, 5.6 ± 2.0 × 10−6, $P = 0.72$; males, 7.2 ± 2.2 × 10−6, P=0.57) was not significantly different from that of controls (6.2± 3.0 × 10−6; Fig. 2.4).

After sequencing and accounting for clonal expansion, 236 from infected and 156 mutants from uninfected mice were used to identify effects of *H. pylori* infection on types of mutations causing loss of *gpt* function, with the results summarized in Table 2.1 and Table 2.S1. G:C-to-A:T transitions and G:C-to-T:A transversions were the most prevalent types of mutations in both infected and uninfected animals, representing 33% to 50% and 17% to 31%, respectively, of total mutations in various treatment groups; mutant frequencies varied from 2.1 to 3.0 × 10−6 in these transitions and 0.9–1.8 × 10−6 in the transversions. The 1.6-fold higher total mutations observed in infected females compared with age-matched controls at 12 MPI was attributable mainly to two types of mutations: 3.8 times more A:T-to-G:C transitions ($P < 0.05$) and 2.0 times more G:C-to-T:A transversions ($P < 0.05$). These two mutations are consistent with the expected mutational spectrum induced by RONS (28) and have been found elevated in another animal model of chronic inflammation (13). An increase in G:C-to-T:A transversions was also reported in a previous study documenting *H. pylori*-induced mutations (22).

A:T-to-G:C transitions can be formed by deamination of adenine to hypoxanthine or creation of ethenoadenine. Deamination is mediated by N2O3, the autoxidation product of NO·, which directly nitrosates primary amines on DNA bases (28, 29). Hypoxanthine resembles

guanine and mispairs with cytosine, resulting in the observed mutation. Alternatively, A:T-to-G:C transitions can also be created indirectly by lipid peroxidation by RONS, forming etheno adducts in DNA such as highly mutagenic ethenoadenine (30, 31). G:C-to-T:A transversions have also been associated with increased *iNOS* expression levels, pointing to the involvement of RONS (32). Cells cocultivated with activated macrophages predominantly develop G:C to T:A transversions caused by exposure to NO·, O2–·, and H2O2 (33). G:C-to-T:A transversions are also caused by adducts produced by oxidative stress or lipid peroxidation, such as 8-oxodG, εdC, and M1G (34,35). The presence of 8-oxodG, a major product of oxidative damage to DNA, results in mispairing of guanine with adenine during replication, thus inducing transversions (36). Although 8-oxodG is believed to be the main cause of this mutation, etheno adducts formed by lipid peroxidation may also play a significant role in mutagenesis observed in vivo (37).

Fig. 2.S3 shows the mutation spectrum detected in the *gpt* gene, of which the following features are noteworthy. In both uninfected and infected mice, hotspots occurred at nucleotides C64, G110, G115, and G418; C64, G110, and G115 are CpG sites and are known hotspots in this assay (38, 39). Hotspots occurring in infected mice were located at A8, G116, and G143; A8 and G116 were found predominantly in infected females at both 6 and 12 mo, whereas G143, located at a CpG site, was a hotspot in infected animals of both sexes. Uninfected mice had hotspots at G406, G416, and A419, one of which (G416) occurred mainly in males. Mutations in infected males were concentrated mainly in hotspots common to both uninfected and infected animals, whereas in infected females there was an increase in mutations throughout the *gpt* gene at non-G:C sites. This result suggests that the chemistry of

DNA damage in mice with a stronger host response to infection may have differed from that in mice with mild or minimal gastritis.

Mutation analysis using the Spi− assay revealed that the frequency of deletion mutations in *gpt* of gastric tissue DNA was not significantly affected by *H. pylori* infection (Fig. 2.5). Analyses of 57 samples from 32 mice showed that Spi− mutant frequencies in infected mice (females at 6 MPI, 4.8 ± 2.5 × 10−6, $P = 0.09$; females at 12 MPI, 5.0 ± 2.6 × 10−6, $P = 0.30$; males at 6 MPI, 6.3 ± 2.5 × 10−6, $P = 0.87$; and males at 12 MPI, 5.2 ± 1.4 × 10−6, $P = 0.17$) were not significantly different from those of age-matched controls at either time point (all mice at 6 MPI, 2.9 ± 1.3 × 10−6; all mice at 12 MPI, 3.6 ± 1.8 × 10−6).

Current models of inflammation-driven carcinogenesis are based on chronic inflammation inducing mutations that lead to cancer (40, 41). Female mice at 6 MPI had more hyperplasia, epithelial defects, and dysplasia than infected males and age-matched controls, but this increase in pathologic findings was not accompanied by increased frequency of mutations. This was detected only in infected female mice at 12 MPI, which had experienced more severe gastritis for a longer period, suggesting that gastritis is necessary but not sufficient to induce mutagenesis. Similarly, duration of infection in itself was insufficient, as mutation frequency was not increased in male mice at 12 MPI. Based on the GHAI, infected male mice had a weaker response at 6 MPI compared with infected females, whereas by 12 MPI, the level of pathologic process was similar in both sexes. These data suggest that the delayed onset of severe gastric lesions in males reduced the duration of their exposure to chronic gastritis, protecting them from mutagenesis, highlighting the importance of severity and duration of the inflammatory response.

Our findings agree with current paradigms for the role of inflammation in carcinogenesis (4) and with the more severe pathology induced in female versus male C57BL/6 mice infected with *Helicobacter* spp. (42). Our observations in female *gpt* delta mice are consistent with previously reported data from female C57BL/6 Big Blue mice infected with *H. felis*, which induces more severe gastritis at earlier time points than *H. pylori*, effectively increasing the amount of DNA damage inflicted after infection (23, 43, 44). The higher mutation frequency found at 7 MPI in *H. felis*-infected female C57BL/6 Big Blue mice may be comparable to that occurring at 12 MPI in female *gpt* delta mice infected with *H. pylori*, based on increased inflammation and epithelial proliferation. In contrast, another study of DNA point mutations induced by *H. pylori* in male Big Blue mice reported that, although mutant frequency was increased at 6 MPI, it returned to control levels by 12 MPI (22). The decrease between 6 and 12 MPI was accompanied by loss of *iNOS* expression and reversion of the mutation spectrum to one indistinguishable from that of uninfected mice (22). Two possible explanations for these results are that (i) the increase in mutations at 6 MPI may have reflected jackpot mutations, because clonal expansion was not assessed or (ii) loss of infection resulted in absence of *iNOS* expression and reversion of the mutation spectrum. An additional factor pertinent to comparisons of previous mutagenesis studies involving gastric infection by *Helicobacter* spp. is the endogenous *Helicobacter* status of the mouse colony (45). We recently reported that concurrent, subclinical infection in C57BL/6 mice with nongastric *Helicobacter bilis* significantly reduced *H. pylori*-associated premalignant gastric lesions at 6 and 11 MPI (46). This immunomodulatory effect could affect observed mutagenic responses, and it is unknown whether Big Blue mice used in previous studies were free of enteric *Helicobacter* spp.

Our observed sex-based effects on mutagenesis induced by *H. pylori* in mice has not been reported previously, but sex bias has been found in other responses to infection. In *H. pylori*–infected Mongolian gerbils, immune responses and cytokine production were reported to be affected by sex (47), and *H. pylori* preferentially induced cancer in male INS-GAS mice (48). Greater female susceptibility to gastric *Helicobacter* infections has been noted previously in WT C57BL/6 mice (42), whereby females infected with *H. felis* experience an earlier onset of gastric inflammation, epithelial hyperplasia, atrophy, and apoptosis (42). Mechanisms responsible for the observed sex-based effects are incompletely understood, but findings to date collectively indicate that sex is an important variable, affecting strength of the host response to *H. pylori* infection, which in turn determines disease outcome.

The typical host response to *Helicobacter* infection is a proinflammatory Th1 response that causes chronic gastritis (49, 50). However, mouse strains such as BALB/c, which mount a strong antiinflammatory Th2 humoral immune response to *H. pylori* infection, develop less severe disease (51). We have previously shown that modulation of the Th1 response by an increased Th2 response reduces pathology associated with concurrent helminth infections (27). In the current study, the immune response of females to *H. pylori* infection was biased toward a greater Th1/Th2 ratio compared with males at both 6 and 12 mo. Higher Th1/Th2 ratios reflect a stronger inflammatory response to *H. pylori* infection. Furthermore, proinflammatory Th17 cells and regulatory T cells have been recently shown to modulate host responses to *H. pylori* (52, 53). *H. pylori*-specific Th17 immunity, mediated by IL-17 (54), increases inflammation unless it is suppressed by regulatory T cells, which are up-regulated by TGF-β and IL-10 (53).

Higher levels of inflammation, epithelial defects, and atrophy were indeed observed in infected females at 6 MPI. At 12 MPI, the level of serum IgG2c was significantly elevated in infected females, reflective of increased proinflammatory cytokines in the gastric mucosa, and is consistent with the reduction in *H. pylori* colonization levels. The earlier onset of severe pathologic process caused by the Th1- and Th17-biased response to *H. pylori* was also associated with the increase in point mutations seen at 12 MPI.

In summary, we have shown that chronic *H. pylori* infection can cause premalignant gastric lesions and induce point mutations consistent with inflammatory processes. As our data are derived from analysis of nontranscribed DNA, it serves as an indicator of unbiased mutations reflecting genetic changes during the early stages of tumor initiation in inflamed tissues. At 12 mo, *H. pylori*-infected female C57BL/6 mice accumulate more inflammation-mediated point mutations compared with males as a result of a greater Th1-biased response to infection inducing earlier and more severe pathology. The sex-biased increase in premalignant gastric lesions and induction of mutations highlights the importance of taking into account sex-based effects in future studies of inflammation-driven disease.

2.3 Materials and Methods

Bacteria and Animals. *H. pylori* strain SS1 was grown on blood agar or Brucella broth with 5% FBS as described in SI Materials and Methods. Specific pathogen-free (including *Helicobacter* spp.) male and female C57BL/6 *gpt* delta mice (24) were infected by oral gavage with *H. pylori* SS1 or sham-dosed. At the indicated times, mice were euthanized, gastric tissue collected

for histopathology and DNA and RNA extraction, and sera were collected for cytokine and Ig analysis. Gastric lesions were scored for inflammation, epithelial defects, atrophy, hyperplasia, mucous metaplasia, hyalinosis, intestinal metaplasia, and dysplasia using previously published criteria (55). The GHAI is the sum of inflammation, epithelial defects, atrophy, hyperplasia, intestinal metaplasia, and dysplasia scores. A detailed description of the husbandry, treatment, and histopathology is provided in SI Materials and Methods.

DNA Isolation and in Vitro Packaging. Genomic DNA was extracted from gastric tissue using RecoverEase DNA Isolation Kit (Stratagene) following the manufacturer's recommendations. λ-EG10 phages were packaged in vitro from genomic DNA using the Transpack Packaging Extract (Stratagene) following the instructions.

***gpt* Assay and Sequencing Analysis.** The 6-TG selection assay was performed as previously described (24, 56). Briefly, phages rescued from murine genomic DNA were transfected into *E. coli* YG6020 expressing Cre recombinase. Infected cells were cultured on plates containing chloramphenicol (Cm) and 6-TG for 3 d until 6-TG–resistant colonies appeared. To confirm the 6-TG–resistant phenotype, colonies were restreaked on plates containing Cm and 6-TG. Confirmed 6-TG–resistant colonies were cultured, and a 739-bp DNA product containing the *gpt* gene was amplified by PCR. DNA sequencing of the *gpt* gene was performed by the Biopolymers Facility at Harvard Medical School (Boston, MA) with AMPure beads (Agencourt) and a 3730xL DNA Analyzer (Applied Biosystems). Sequences were aligned with the *E. coli gpt* gene (GenBank M13422.1) (57) using Geneious (Biomatters). Mutations were classified as transitions, transversions, deletions, insertions, or complex (multiple changes). Duplicate mutations at the

samesite within an individual tissue were excluded to account for clonal expansion of sibling mutations. More information on primers and methods is provided in SI Materials and Methods.

Spi– Assay. The Spi– assay was performed as described in SI Materials and Methods. Briefly, phages rescued from murine genomic DNA were transfected into *E. coli* strains with or without P2 lysogen. Infected cells were cultured overnight on λ-trypticase agar plates to allow plaque formation. The inactivation of red and gam genes was confirmed by respotting plaques on another *E. coli* strain with P2 lysogen (24).

mRNA Expression. RNA was extracted from gastric tissue and reverse transcribed to cDNA. Quantitative real-time PCR was performed using TaqMan Gene Expression Assays (Applied Biosystems). TaqMan primers and analysis methods are described in SI Materials and Methods.

***H. pylori* Detection.** *H. pylori* levels in the gastric mucosa were quantified by real-time quantitative PCR assay of gastric DNA as described in SI Materials and Methods. A threshold of 15 copies of the *H. pylori* genome was set as the lower limit for a positive sample.

Serum IgG Isotype Measurement. Sera were analyzed for *H. pylori*-specific IgG2c and IgG1 by ELISA. Additional information on the measurements is provided in SI Materials and Methods.

Statistical Analysis. Two-way ANOVA followed by Bonferroni posttests were used to analyze GHAI and mRNA expression values. Student two-tailed t-tests were used to analyze mutant and mutation frequency data and serum IgG isotypes. Poisson distribution analysis was used to determine hotspots at a 99% confidence level (58). For some analyses, age-matched controls of both sexes were grouped when no statistical differences were detected between sexes. Analyses were done with GraphPad Prism, version 4.0, or Microsoft Excel 2002. $P < 0.05$ was considered significant.

ACKNOWLEDGMENTS. We thank Sureshkumar Muthupalani for help with the histological images and Laura J. Trudel for assistance with the manuscript and figures. This study is dedicated in loving memory of David Schauer, a mentor and a friend, for his contribution in the design and analysis of this work. This work was supported by National Institutes of Health Grants R01-AI037750 and P01-CA026731 and Massachusetts Institute of Technology Center for Environmental Health Sciences Program Project Grant P30-ES02109.

2.4 References

1. Fox JG, Wang TC (2007) Inflammation, atrophy, and gastric cancer. J Clin Invest 117:60–69.
2. Suerbaum S, Michetti P (2002) *Helicobacter pylori* infection. N Engl J Med 347:1175–1186.
3. International Agency for Research on Cancer (1994) Schistosomes, liver flukes and *Helicobacter pylori*. IARC Working Group on the Evaluation of Carcinogenic Risks to Humans. Lyon, 7-14 June 1994. IARC Monogr Eval Carcinog Risks Hum 61:1–241.
4. Coussens LM, Werb Z (2002) Inflammation and cancer. Nature 420:860–867.
5. Obst B, Wagner S, Sewing KF, BeilW(2000) *Helicobacter pylori* causes DNA damage in gastric epithelial cells. Carcinogenesis 21:1111–1115.
6. Xu H, et al. (2004) Spermine oxidation induced by *Helicobacter pylori* results in apoptosis and DNA damage: Implications for gastric carcinogenesis. Cancer Res 64:8521–8525.
7. Davies GR, et al. (1994) Relationship between infective load of *Helicobacter pylori* and reactive oxygen metabolite production in antral mucosa. Scand J Gastroenterol 29:419–424.
8. Davies GR, et al. (1994) *Helicobacter pylori* stimulates antral mucosal reactive oxygen metabolite production in vivo. Gut 35:179–185.
9. Mannick EE, et al. (1996) Inducible nitric oxide synthase, nitrotyrosine, and apoptosis in *Helicobacter pylori* gastritis: Effect of antibiotics and antioxidants. Cancer Res 56:3238–3243.
10. Meira LB, et al. (2008) DNA damage induced by chronic inflammation contributes to colon carcinogenesis in mice. J Clin Invest 118:2516–2525.
11. Nair J, et al. (2006) Increased etheno-DNA adducts in affected tissues of patients suffering from Crohn's disease, ulcerative colitis, and chronic pancreatitis. Antioxid Redox Signal 8:1003–1010.
12. Zhuang JC, Lin C, Lin D, Wogan GN (1998) Mutagenesis associated with nitric oxide production in macrophages. Proc Natl Acad Sci USA 95:8286–8291.
13. Sato Y, et al. (2006) IL-10 deficiency leads to somatic mutations in a model of IBD. Carcinogenesis 27:1068–1073.
14. Bartsch H, Nair J (2004) Oxidative stress and lipid peroxidation-derived DNA-lesions in inflammation driven carcinogenesis. Cancer Detect Prev 28:385–391.
15. Nair U, Bartsch H, Nair J (2007) Lipid peroxidation-induced DNA damage in cancer prone inflammatory diseases: a review of published adduct types and levels in humans. Free Radic Biol Med 43:1109–1120.
16. Kang JM, Iovine NM, Blaser MJ (2006) A paradigm for direct stress-induced mutation in prokaryotes. FASEB J 20:2476–2485.
17. Crabtree JE, Ferrero RL, Kusters JG (2002) The mouse colonizing *Helicobacter pylori* strain SS1 may lack a functional cag pathogenicity island. *Helicobacter* 7:139–140, author reply 140–141.
18. Lee A, Mitchell H, O'Rourke J (2002) The mouse colonizing *Helicobacter pylori* strain SS1 may lack a functional cag pathogenicity island: Response. *Helicobacter* 7:140–141.
19. Miyazawa M, et al. (2003) Suppressed apoptosis in the inflamed gastric mucosa of *Helicobacter pylori*-colonized iNOS-knockout mice. Free Radic Biol Med 34:1621–1630.
20. Jang J, et al. (2003) Malgun (clear) cell change in *Helicobacter pylori* gastritis reflects epithelial genomic damage and repair. Am J Pathol 162:1203–1211.
21. Lee H, et al. (2000) "Malgun" (clear) cell change of gastric epithelium in chronic *Helicobacter pylori* gastritis. Pathol Res Pract 196:541–551.

22. Touati E, et al. (2003) Chronic *Helicobacter pylori* infections induce gastric mutations in mice. Gastroenterology 124:1408–1419.
23. Jenks PJ, Jeremy AH, Robinson PA, Walker MM, Crabtree JE (2003) Long-term infection with *Helicobacter* felis and inactivation of the tumour suppressor gene p53 cumulatively enhance the gastric mutation frequency in Big Blue transgenic mice. J Pathol 201:596–602.
24. Nohmi T, et al. (1996) A new transgenic mouse mutagenesis test system using Spi- and 6-thioguanine selections. Environ Mol Mutagen 28:465–470.
25. Ihrig M, Whary MT, Dangler CA, Fox JG (2005) Gastric *Helicobacter* infection induces a Th2 phenotype but does not elevate serum cholesterol in mice lacking inducible nitric oxide synthase. Infect Immun 73:1664–1670.
26. Lee CW, et al. (2008) *Helicobacter pylori* eradication prevents progression of gastric cancer in hypergastrinemic INS-GAS mice. Cancer Res 68:3540–3548.
27. Fox JG, et al. (2000) Concurrent enteric helminth infection modulates inflammation and gastric immune responses and reduces *Helicobacter*-induced gastric atrophy. Nat Med 6:536–542.
28. De Bont R, van Larebeke N (2004) Endogenous DNA damage in humans: A review of quantitative data. Mutagenesis 19:169–185.
29. Burney S, Caulfield JL, Niles JC, Wishnok JS, Tannenbaum SR (1999) The chemistry of DNA damage from nitric oxide and peroxynitrite. Mutat Res 424:37–49.
30. Kadlubar FF, et al. (1998) Comparison of DNA adduct levels associated with oxidative stress in human pancreas. Mutat Res 405:125–133.
31. Pandya GA, MoriyaM(1996) 1, N6-ethenodeoxyadenosine, a DNA adduct highly mutagenic in mammalian cells. Biochemistry 35:11487–11492.
32. Ambs S, et al. (1999) Relationship between p53 mutations and inducible nitric oxide synthase expression in human colorectal cancer. J Natl Cancer Inst 91:86–88.
33. Kim MY, Wogan GN (2006) Mutagenesis of the supF gene of pSP189 replicating in AD293 cells cocultivated with activated macrophages: roles of nitric oxide and reactive oxygen species. Chem Res Toxicol 19:1483–1491.
34. Dedon PC, Plastaras JP, Rouzer CA, Marnett LJ (1998) Indirect mutagenesis by oxidative DNA damage: formation of the pyrimidopurinone adduct of deoxyguanosine by base propenal. Proc Natl Acad Sci USA 95:11113–11116.
35. Jackson AL, Loeb LA (2001) The contribution of endogenous sources of DNA damage to the multiple mutations in cancer. Mutat Res 477:7–21.
36. Wood ML, Esteve A, Morningstar ML, Kuziemko GM, Essigmann JM (1992) Genetic effects of oxidative DNA damage: comparative mutagenesis of 7,8-dihydro-8-oxoguanine and 7,8-dihydro-8-oxoadenine in Escherichia coli. Nucleic Acids Res 20:6023–6032.
37. Pang B, et al. (2007) Lipid peroxidation dominates the chemistry of DNA adduct formation in a mouse model of inflammation. Carcinogenesis 28:1807–1813.
38. Masumura K, et al. (2003) Low dose genotoxicity of 2-amino-3,8-dimethylimidazo[4,5-f] quinoxaline (MeIQx) in *gpt* delta transgenic mice. Mutat Res 541:91–102.
39. Masumura K, et al. (2000) Characterization of mutations induced by 2-amino-1-methyl-6-phenylimidazo[4,5-b]pyridine in the colon of *gpt* delta transgenic mouse: novel G:C deletions beside runs of identical bases. Carcinogenesis 21:2049–2056.
40. Balkwill F, Coussens LM (2004) Cancer: An inflammatory link. Nature 431:405–406.

41. Clevers H (2004) At the crossroads of inflammation and cancer. Cell 118:671–674.
42. Court M, Robinson PA, Dixon MF, Jeremy AH, Crabtree JE (2003) The effect of gender on *Helicobacter* felis-mediated gastritis, epithelial cell proliferation, and apoptosis in the mouse model. J Pathol 201:303–311.
43. Fox JG, et al. (2002) Germ-line p53-targeted disruption inhibits *Helicobacter*-induced premalignant lesions and invasive gastric carcinoma through down-regulation of Th1 proinflammatory responses. Cancer Res 62:696–702.
44. Lee A, Fox JG, Otto G, Murphy J (1990) A small animal model of human *Helicobacter pylori* active chronic gastritis. Gastroenterology 99:1315–1323.
45. Taylor NS, et al. (1995) Long-term colonization with single and multiple strains of *Helicobacter pylori* assessed by DNA fingerprinting. J Clin Microbiol 33:918–923.
46. Lemke LB, et al. (2009) Concurrent *Helicobacter* bilis infection in C57BL/6 mice attenuates proinflammatory *H. pylori*-induced gastric pathology. Infect Immun 77:2147–2158.
47. Crabtree JE, et al. (2004) Gastric mucosal cytokine and epithelial cell responses to *Helicobacter pylori* infection in Mongolian gerbils. J Pathol 202:197–207.
48. Fox JG, et al. (2003) Host and microbial constituents influence *Helicobacter pylori*-induced cancer in a murine model of hypergastrinemia. Gastroenterology 124:1879–1890.
49. Bamford KB, et al. (1998) Lymphocytes in the human gastric mucosa during *Helicobacter pylori* have a T helper cell 1 phenotype. Gastroenterology 114:482–492.
50. Mohammadi M, Czinn S, Redline R, Nedrud J (1996) *Helicobacter*-specific cell mediated immune responses display a predominant Th1 phenotype and promote a delayed-type hypersensitivity response in the stomachs of mice. J Immunol 156:4729–4738.
51. Sakagami T, et al. (1996) Atrophic gastric changes in both *Helicobacter* felis and *Helicobacter pylori* infected mice are host dependent and separate from antral gastritis. Gut 39:639–648.
52. Lee CW, et al. (2007) Wild-type and interleukin-10-deficient regulatory T cells reduce effector T-cell-mediated gastroduodenitis in Rag2-/- mice, but only wild-type regulatory T cells suppress *Helicobacter pylori* gastritis. Infect Immun 75:2699–2707.
53. Kao JY, et al. (2010) *Helicobacter pylori* immune escape is mediated by dendritic cell induced Treg skewing and Th17 suppression in mice. Gastroenterology 138:1046–1054.
54. Xu S, Cao X (2010) Interleukin-17 and its expanding biological functions. Cell Mol Immunol 7:164–174.
55. Rogers AB, et al. (2005) *Helicobacter pylori* but not high salt induces gastric intraepithelial neoplasia in B6129 mice. Cancer Res 65:10709–10715.
56. Masumura K, et al. (1999) Spectra of *gpt* mutations in ethylnitrosourea-treated and untreated transgenic mice. Environ Mol Mutagen 34:1–8.
57. Nüesch J, Schümperli D (1984) Structural and functional organization of the *gpt* gene region of Escherichia coli. Gene 32:243–249.
58. Kim MY, Dong M, Dedon PC, Wogan GN (2005) Effects of peroxynitrite dose and dose rate on DNA damage and mutation in the *supF* shuttle vector. Chem Res Toxicol 18:76–86.

2.5 Tables and Figures

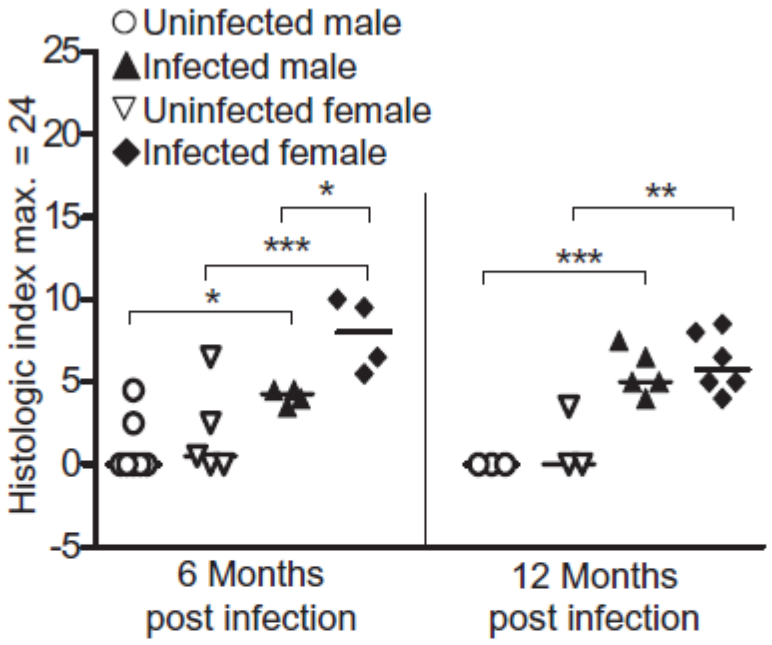

Fig. 2.1. *H. pylori* infection elicits more gastric pathologic processes in female mice at 6 mo. *H. pylori* infection increased the GHAI in both male and female C57BL/6 mice at 6 and 12 mo. At 6 mo of infection, infected females had significantly more pathologic processes than infected males. Uninfected males (○; 6 MPI, n = 7; 12 MPI, n = 3), uninfected females (▽; 6 MPI, n = 5; 12 MPI, n = 3), infected males (▼; 6 MPI, n = 4; 12 MPI, n = 5) and infected females (◆; 6 MPI, n = 4; 12 MPI, n = 6). Bar represents the mean. **P* < 0.05, ***P* < 0.01, and ****P* < 0.001.

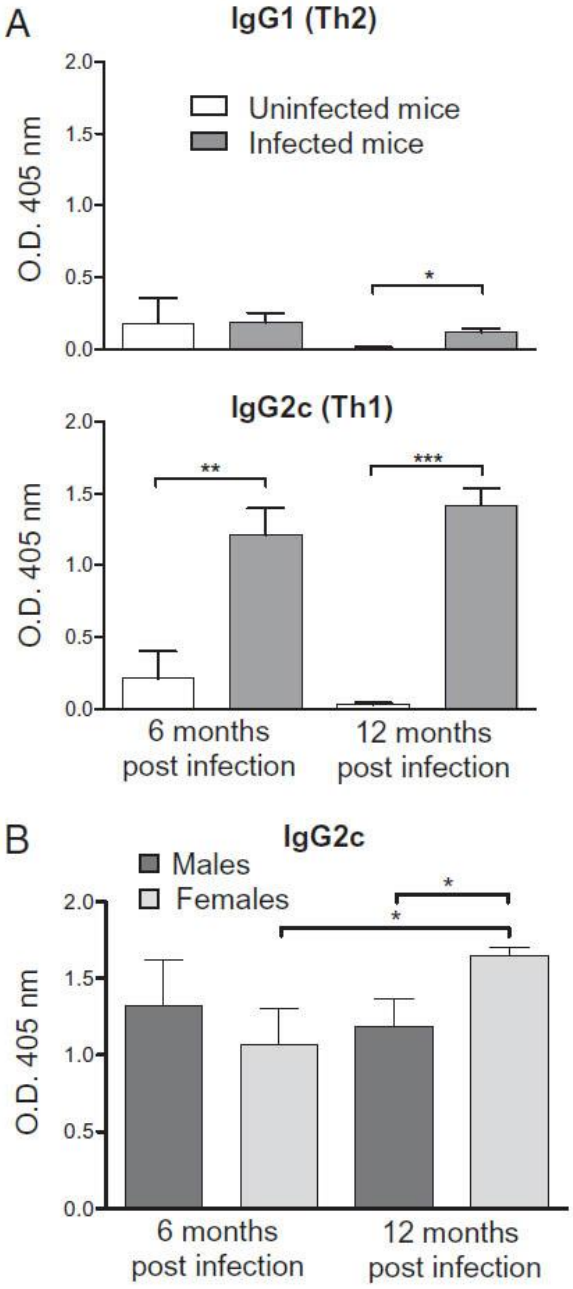

Fig. 2.2. The effect of *H. pylori* infection on *H. pylori*–specific IgG1 and IgG2c.Serum levels of IgG were measured by ELISA in uninfected and *H. pylori*–infected mice. (A) *H. pylori*–infected mice (gray bars; 6 MPI, n =9; 12 MPI, n=12) developed a greater IgG1 response after 12 mo of infection compared with uninfected mice (white bars; 6 MPI, n = 6; 12 MPI, n = 6; P < 0.05). *H. pylori*–infected mice developed a greater IgG2 response after 6and 12mo of infection ($P < 0.01$ and $P < 0.001$, respectively). (B) At 12 mo, infected female mice (light graybars; 6MPI, n=4; 12MPI, n=6) had substantially increased IgG2c compared with infected males (dark gray bars; 6 MPI, n = 5; 12 MPI, n = 6) at 12 mo and infected females at 6mo (P<0.05, both).Data are mean (SE) of mice in different treatment groups. *$P < 0.05$, **$P < 0.01$, and ***$P < 0.001$.

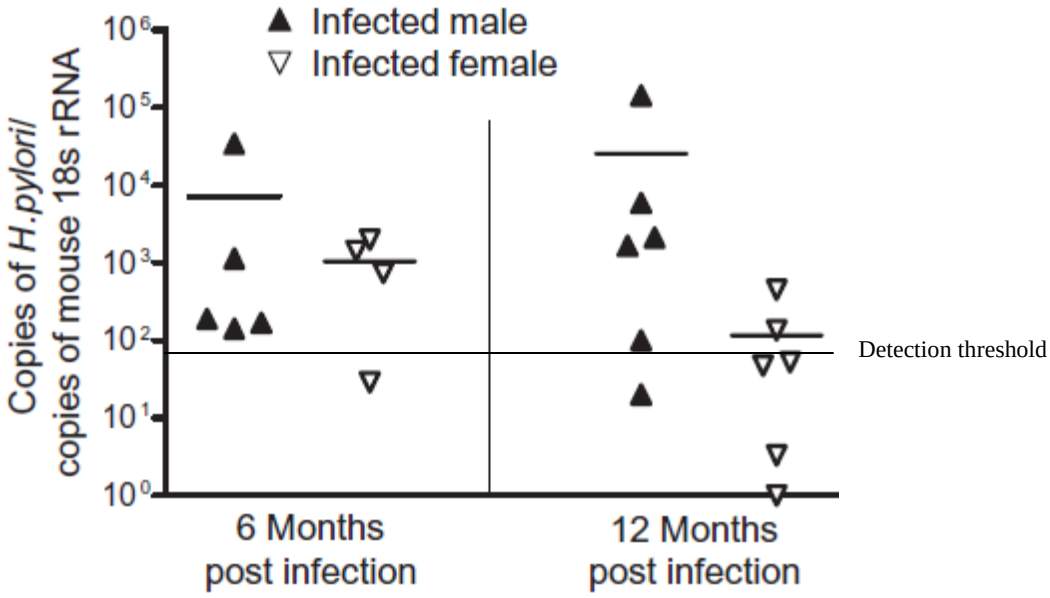

Fig. 2.3. *H. pylori* levels in the stomach were lower in infected females at 12 MPI. Values represent the number of *H. pylori* organisms per copies of mouse 18s rRNA. At 6 MPI, one infected female mouse was under the threshold of detection (15 copies of *H. pylori*). At 12 MPI, four infected females and one infected male were undetectable. Infected males (▼, 6 MPI, n = 5; 12MPI, n = 6) and infected females (▽, 6MPI, n = 4; 12MPI, n = 6). Bar represents the mean.

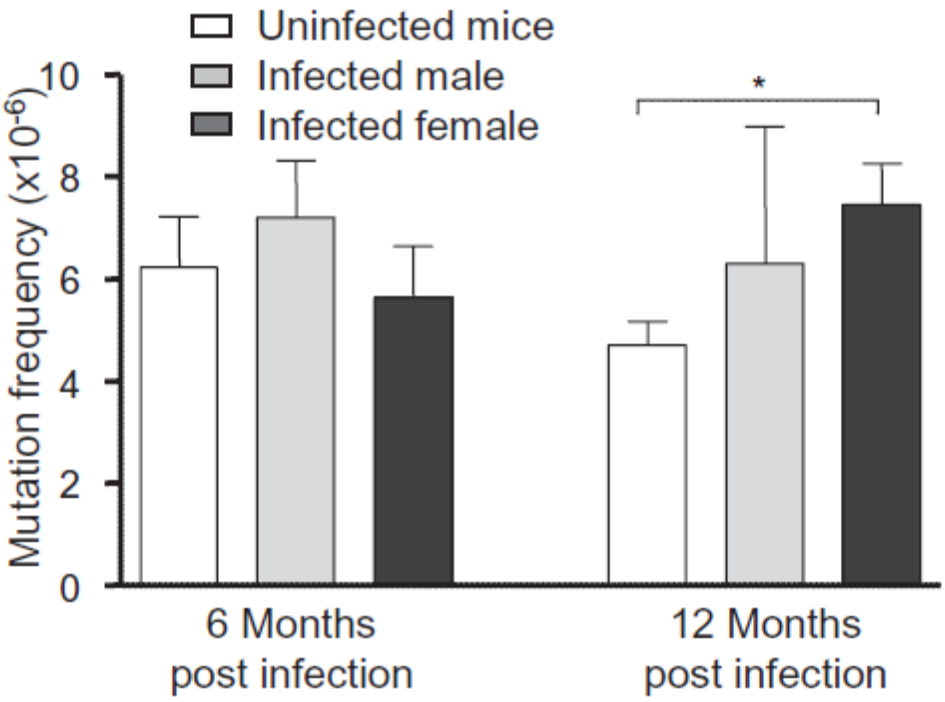

Fig. 2.4. Twelve-month infection with *H. pylori* increases the frequency of point mutations in female mice. The mutation frequency of point mutations was determined by the *gpt* assay in uninfected mice (white bars; 6 MPI, n = 13; 12 MPI, n = 15), *H. pylori*-infected males (light gray bars; 6 MPI, n = 4; 12 MPI, n = 5) and *H. pylori*-infected females (dark gray bars; 6 MPI, n = 9; 12 MPI, n = 11). Control mice of both sexes were grouped for this analysis. Data are mean (SEM) of mutation frequency of mice in different treatment groups. *$P < 0.05$.

Table 1. Twelve months of *H. pylori* infection increases the mutation frequency of A:T-to-G:C transitions and G:C-to-T:A transversions in female mice

	6 mo			12 mo		
Effect	Uninfected all (n = 6)	Infected male (n = 4)	Infected female (n = 8)	Uninfected all (n = 14)	Infected male (n = 5)	Infected female (n = 11)
Transition						
G:C to A:T	3.02 (2.07)	2.41 (2.64)	2.74 (1.07)	2.13 (0.87)	2.66 (1.70)	2.69 (0.97)
A:T to G:C	0.27 (0.61)	0.00	0.16 (0.22)	0.23 (0.19)	0.08 (0.16)	0.88 (0.59)*
Transversion						
G:C to T:A	1.30 (1.34)	1.64 (1.29)	0.89 (0.68)	0.85 (0.62)	1.69 (2.43)	1.75 (0.54)*
G:C to C:G	0.29 (0.66)	0.36 (0.71)	0.40 (0.60)	0.19 (0.27)	0.84 (1.25)	0.09 (0.14)
A:T to T:A	0.34 (0.47)	0.00	0.37 (0.37)	0.31 (0.41)	0.00	0.53 (0.89)
A:T to C:G	0.00	0.36 (0.71)	0.18 (0.22)	0.05 (0.12)	0.00	0.25 (0.46)
Deletion						
1-bp deletion	0.84 (0.94)	2.44 (3.99)	0.66 (0.43)	0.53 (0.35)	0.67 (0.54)	0.88 (0.73)
≥2-bp deletion	0.04 (0.12)	0.00	0.44 (0.57)	0.22 (0.20)	0.18 (0.36)	0.22 (0.34)
Insertion	0.00	0.00	0.08 (0.16)	0.20 (0.23)	0.00	0.11 (0.17)
Complex mutation	0.14 (0.31)	0.00	0.04 (0.08)	0.00	0.18 (0.36)	0.12 (0.29)
Total	6.23 (2.98)	7.20 (2.21)	5.95 (1.54)	4.71 (1.13)	6.29 (5.37)	7.51 (1.91)*

Data are mean (SD) of mutation frequency data from 411 mutants recovered from the *gpt* assay after excluding 155 mutants considered siblings. Control mice of both sexes were grouped for this analysis. The mutation frequency of A:T-to-G:C transitions and G:C-to-T:A transversions was significantly elevated in female mice infected with *H. pylori* for 12 mo.

*$P < 0.05$.

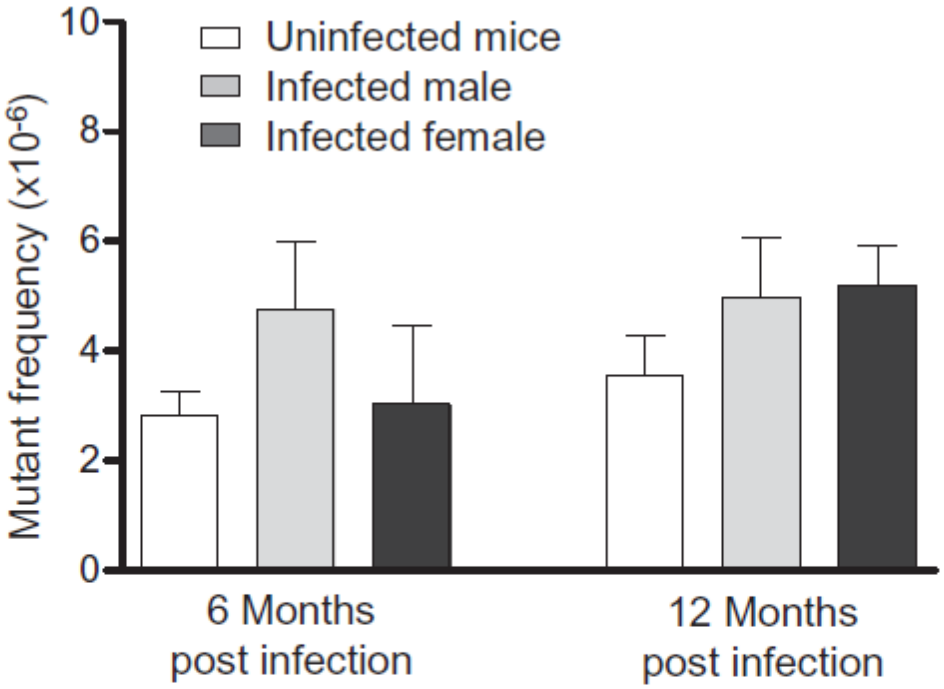

Fig. 2.5. Mutant frequency of deletions was unchanged by *H. pylori* infection. *H. pylori* infection did not alter the levels of deletions detected by the Spi− assay in uninfected mice (white bars; 6 MPI, n = 12; 12 MPI, n = 16), *H. pylori*-infected males (light gray bars; 6 MPI, n = 3; 12 MPI, n = 5) and *H. pylori*-infected females (dark gray bars; 6 MPI, n = 9; 12 MPI, n = 12). Control mice of both sexes were grouped for this analysis. Data are mean (SEM) of mutant frequency of mice in different treatment groups.

2.6 Supplemental Information

SI Materials and Methods

Bacteria and Animals. *H. pylori* strain SS1 was cultured on blood agar (TSA with sheep blood; Remel) or Brucella broth with 5% FBS under microaerobic conditions (10% H2, 10% CO2, 80% N2). Specific pathogen-free (including Helicobacter spp.) male and female C57BL/6 *gpt* delta mice (1) bred and maintained in our facilities were used. Mice were maintained in a facility accredited by the Association for Assessment and Accreditation of Laboratory Animal Care International, housed in polycarbonate microisolator cages on hardwood bedding, and provided standard rodent chow and water ad libitum. All protocols were approved by the Massachusetts Institute of Technology Committee on Animal Care.

Experimental Design. Twenty-one 6- to 8-wk-old *gpt* delta mice (11 male and 10 female) were infected by oral gavage with 0.2 mL of *H. pylori* SS1 on alternate days for a total of three doses of approximately 1 × 108 organisms per dose (2, 3). Twelve age-matched uninfected mice were dosed with 0.2 mL of tryptic soy broth. Mice were euthanized at 6 or 12 MPI. After CO2 asphyxiation, blood was immediately collected by cardiac puncture and the stomach and proximal duodenum were removed and incised along the greater curvature. For histopathologic study, linear gastric strips from the lesser curvature were fixed overnight in 10% neutral-buffered formalin, embedded, sectioned at 4-μm thickness, and stained with H&E. A board-certified comparative pathologist (B.H.R.), blinded to treatment groups, scored gastric lesions on an ascending scale of 0 to 4 for inflammation, epithelial defects, atrophy, hyperplasia, mucous metaplasia, hyalinosis, intestinal metaplasia, and dysplasia according to previously published criteria (4). A GHAI was calculated as the sum of scores for inflammation, epithelial

defects, atrophy, hyperplasia, intestinal metaplasia, and dysplasia. Hyalinosis and mucous metaplasia were excluded from the GHAI as they have been observed to develop spontaneously in mice (4, 5). Data for two infected male mice with GHAI scores of 0 were excluded from all subsequent analyses, unless specifically noted, as a result of their lack of response to infection. The remainder of the gastric tissue was snap-frozen in liquid nitrogen and stored at –70 °C for DNA and RNA analyses.

Assay for *gpt* Mutagenesis. Fifty-seven samples from 33 mice were processed according to the *gpt* delta mutagenesis procedures to determine frequencies of point mutations (6-TG selection assay) and large deletions (Spi– assay). Animals were selected for analysis based on histopathological findings, and analyses of tissues from 15 mice were repeated two or three times to verify assay reproducibility. Animals studied at 6 MPI included five uninfected males, four uninfected females, four infected males, and four infected females; those at 12 MPI were three uninfected males, three uninfected females, four infected males, and six infected females. In the 6-TG selection assay procedure, genomic DNA was extracted from gastric tissue previously kept at −70 °C using the Recoverease DNA Isolation Kit (Stratagene). The Transpack Packaging Extract (Stratagene) was used to recover λ-EG10 phages from tissue DNA, and the 6-TG selection assay was performed as previously described (1, 6). Briefly, *E. coli* expressing Cre recombinase was infected with rescued λ-EG10 phages and incubated for 72 h on selective media containing either Cm (25 μg/mL) or Cm (25 μg/mL) plus 6-TG (25 μg/mL) to select colonies possessing Cm acetyltransferase activity only (survival) or both Cm acetyltransferase activity and loss of *gpt* function (mutant). Recovered *gpt* mutants were restreaked onto

Cm and 6-TG plates for confirmation. Mutant frequency was expressed as the mutant/survivor ratio.

Confirmed 6-TG–resistant mutants were boiled and pelleted to obtain DNA template for sequencing of the *gpt* gene. A 739-bp DNA fragment containing the *gpt* gene was amplified by PCR using primers P1 (forward) 5′-TACCACTTTATCCCGCGTCAGG-3′ and primer P2 (reverse) 5′-ACAGGGTTTGGCTCAGGTTTGC-3′. PCR amplification was carried out using Vent DNA polymerase (New England Biolabs) on a DNA Engine PTC-200 (MJ Research). The reaction was started by incubation at 94 °C for 5 min, followed by 30 cycles of 30 s at 94 °C, 30 s at 56 °C, and 120 s at 72 °C and finalized by incubating at 72 °C for 5 min before storing at 4 °C (6). PCR product cleanup and DNA sequencing were performed by the Biopolymers Facility at Harvard Medical School (Boston, MA) using AMPure beads (Agencourt) and a 3730xL DNA Analyzer (Applied Biosystems) using sequencing primers A (forward) 5′-GAGGCAGTGCGTAAAAAGAC-3′ and A2 (forward) 5′-CTCGCGCAACCTATTTTCCC-3′. Sequences were aligned with the *E. coli gpt* gene (GenBank M13422.1) (7) with Geneious software (Biomatters). Mutations were individually corroborated by multiple sequence results and classified as transitions (G:C to A:T, A:T to G:C), transversions (G:C to T:A, G:C to C:G, A:T to T:A, A:T to C:G), deletions (1 bp or ≥2 bp), insertions, or complex (multiple changes). A mutation found repeated at the same site within the same sample was excluded from frequency calculations to eliminate overrepresentation caused by sibling mutations. Samples from 33 mice were sequenced. Mutation frequencies calculated for each animal and each mutation type were subjected to statistical analysis.

Spi– Assay for Large Deletions. The Spi– assay was carried out as described (1). *E. coli* strains XL-1 Blue MRA or XL-1 Blue MRA P2 lysogen were infected with phages rescued from mouse DNA and incubated for 20 min without shaking at 37 °C. The suspensions were poured on λ-trypticase agar plates (1% trypticase peptone, 0.5% NaCl, 1.2% agar), which were then incubated overnight at 37 °C to select for plaques formed in MRA P2 lawns containing phage with inactivated *red* and *gam* genes. Plaques formed in MRA lawns were counted to determine titer. Mutant phages were picked and spotted onto lawns of *E. coli* strain WL95 P2 lysogen (WL95 P2) to confirm the inactivation of *red* and *gam* genes. The mutant frequency was expressed as mutant plaque/titer ratio. *E. coli* strain LE392 was infected with recovered Spi– mutant phages to obtain phage lysates (8).

Quantitative Analysis of mRNA Expression. Total RNA was extracted from gastric tissue using TRIzol reagent (Invitrogen) and the RNeasy kit (Qiagen). cDNA was synthesized from 5 μg of total RNA with SuperScript II RT (Invitrogen). Quantitative real-time PCR was performed on cDNA using TaqMan gene expression assays (Applied Biosystems) specific for *IFN-γ* (assay Mm99999071_m1), *TNF-α* (Mm99999068_m1), *IL-10* (Mm00439616_m1), *IL-17* (Mm00439619_m1), *iNOS* (NOS2 or iNOS; Mm00440485_m1), and GAPDH (Mm99999915_g1). mRNA levels for each cytokine were normalized to the mRNA level of internal control *GAPDH* and compared with the data of uninfected mice using the ΔΔCT method (User Bulletin 2; Applied Biosystems). Data were log10-transformed for analysis.

Detection of *H. pylori* Infection by Quantitative PCR. To quantify infection levels of *H. pylori* strain SS1 within the gastric mucosa, a real-time quantitative PCR assay targeting *H. pylori urease B* was used (9, 10). DNA was extracted from gastric tissue using the High Pure PCR

Template purification kit (Roche). A standard curve was generated by using serial 10-fold dilutions of *H. pylori* SS1 genome copies (from 5 × 105 to 5), estimated from an average *H. pylori* genome size of 1.66 Mb (11, 12). Copy numbers of the gastric *H. pylori* genome were standardized using micrograms of murine chromosomal DNA determined by quantitative PCR using a mammalian 18S rRNA gene-based primer and probe mixture (Applied Biosystems) as described previously (13). A threshold of 15 copies of the *H. pylori* genome was set as the lower limit for a positive sample. Although five infected female mice and one infected male mouse had *H. pylori* levels under the established threshold, these mice had increased cytokine expression and higher GHAI scores consistent with that of mice infected with *H. pylori* and not uninfected mice. Despite the low counts, these six mice were considered infected during subsequent analyses as a result of serological and histological evidence. Conversely, the two mice with the highest number of *H. pylori* copies (one infected male at 6 MPI and one infected male at 12 MPI) had a GHAI of 0 and cytokine production similar to uninfected controls, indicating an aberrant response to infection, and they were excluded from subsequent analyses unless otherwise noted as a result of lack of pathology.

Serum IgG Isotype Measurement. Serum was analyzed for *H. pylori*-specific IgG2c and IgG1 by ELISA using an outer membrane protein preparation from *H. pylori* (SS1 strain) as described previously (14). In brief, 96-well flat-bottom plates were coated with 100 µL of antigen (10 µg/mL) overnight at 4 °C, and sera were diluted 1:100. Biotinylated secondary antibodies for detecting IgG2c and IgG1 were from clone 5.7 and A85-1 (BD Pharmingen). Incubation with extravidin peroxidase (Sigma-Aldrich) was followed by treatment with 2,2’-azino-bis (3-ethylbenzthiazoline-6-sulphonic acid) substrate (Kirkegaard and Perry Laboratories) for color

development. Optical density was recorded on a plate reader according to the manufacturer's protocol (VersaMax; Molecular Devices).

Supplemental References

1. Nohmi T, et al. (1996) A new transgenic mouse mutagenesis test system using Spi- and 6-thioguanine selections. Environ Mol Mutagen 28:465–470.
2. Fox JG, et al. (1999) High-salt diet induces gastric epithelial hyperplasia and parietal cell loss, and enhances *Helicobacter pylori* colonization in C57BL/6 mice. Cancer Res 59:4823–4828.
3. Lee A, et al. (1997) A standardized mouse model of *Helicobacter pylori* infection: Introducing the Sydney strain. Gastroenterology 112:1386–1397.
4. Rogers AB, et al. (2005) *Helicobacter pylori* but not high salt induces gastric intraepithelial neoplasia in B6129 mice. Cancer Res 65:10709–10715.
5. Kang W, Rathinavelu S, Samuelson LC, Merchant JL (2005) Interferon gamma induction of gastric mucous neck cell hypertrophy. Lab Invest 85:702–715.
6. Masumura K, et al. (1999) Spectra of *gpt* mutations in ethylnitrosourea-treated and untreated transgenic mice. Environ Mol Mutagen 34:1–8.
7. Nüesch J, Schümperli D (1984) Structural and functional organization of the *gpt* gene region of Escherichia coli. Gene 32:243–249.
8. Sambrook J, Fritsch EF, Maniatis T (1989) Molecular Cloning: A Laboratory Manual (Cold Spring Harbor Lab Press, Cold Spring Harbor, NY), 2nd Ed.
9. Fox JG, et al. (2003) Host and microbial constituents influence *Helicobacter pylori*-induced cancer in a murine model of hypergastrinemia. Gastroenterology 124:1879–1890.
10. Maurer KJ, et al. (2006) *Helicobacter pylori* and cholesterol gallstone formation in C57L/J mice: A prospective study. Am J Physiol Gastrointest Liver Physiol 290:G175–G182.
11. Alm RA, et al. (1999) Genomic-sequence comparison of two unrelated isolates of the human gastric pathogen *Helicobacter pylori*. Nature 397:176–180.
12. Tomb JF, et al. (1997) The complete genome sequence of the gastric pathogen *Helicobacter pylori*. Nature 388:539–547.
13. Whary MT, et al. (2001) Long-term colonization levels of Helicobacter hepaticus in the cecum of hepatitis-prone A/JCr mice are significantly lower than those in hepatitis resistant C57BL/6 mice. Comp Med 51:413–417.
14. Ihrig M, Whary MT, Dangler CA, Fox JG (2005) Gastric helicobacter infection induces a Th2 phenotype but does not elevate serum cholesterol in mice lacking inducible nitric oxide synthase. Infect Immun 73:1664–1670.

Supplemental images

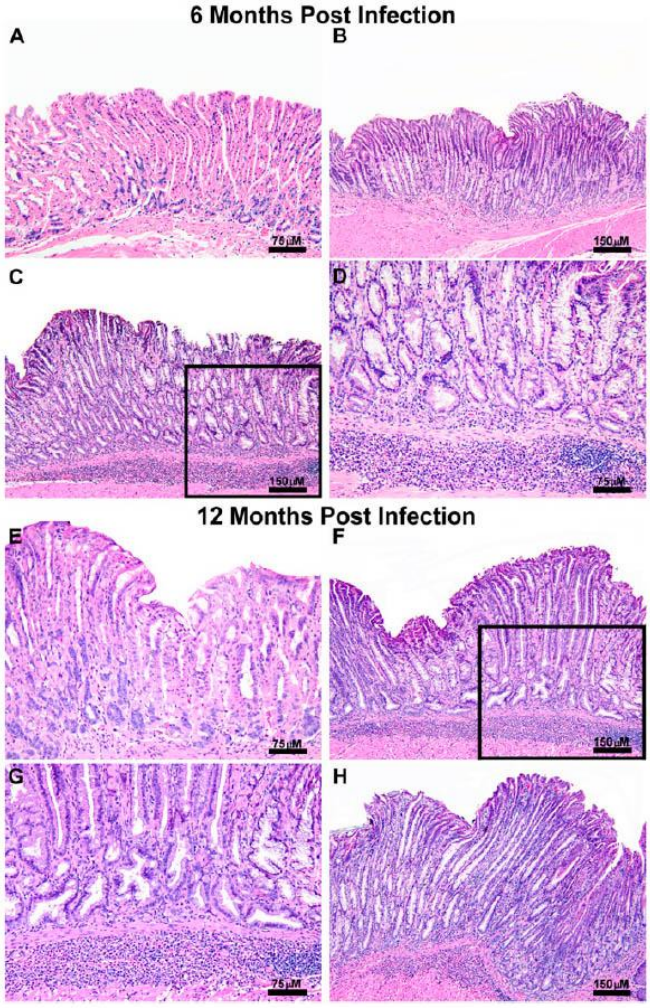

Fig. 1.S1. *H. pylori*-infected mice display significant gastric histomorphological alterations with an accelerated development of gastric pathologic processes in females. (A–D) H&E staining of gastric tissue at 6 MPI. (A) Uninfected female control shows normal gastric mucosa. (B) *H. pylori*-infected male mice exhibiting mild gastric mucosal inflammation, associated oxyntic loss, metaplasia, and mild foveolar hyperplasia. (C) *H. pylori*-infected female mice had significantly higher histological activity than uninfected mice and infected males as shown by the moderate gastric inflammation, associated oxyntic loss, glandular metaplasia, prominent epithelial defects, moderate foveolar hyperplasia, and mild dysplasia. (D) Higher magnification of C shows metaplastic glands with architectural distortion and loss of orientation (dysplasia). (E–H) H&E staining of gastric tissue at 12 MPI. (E) Uninfected male control with minimal gastric morphological changes. (F) *H. pylori*-infected male with moderate inflammation, prominent oxyntic loss, hyperplasia, metaplasia, and mild dysplasia. (G) Higher magnification of F shows metaplastic and dysplastic glands. (H) *H. pylori*-infected female had similar gastric pathological changes as male mice. (Scale bars: 75 µM in A, D, E, and G; 150 µM in B, C, F and H.)

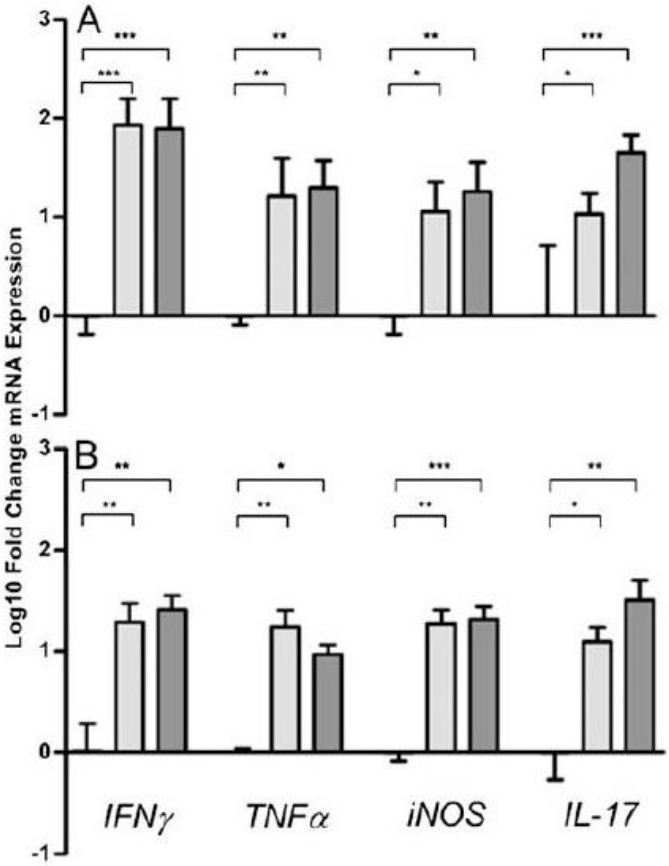

Fig. 2.S2. *H. pylori* infection increases the expression levels of *IFNγ*, *TNFα*, *iNOS*, and *IL-17. IFNγ, TNFα, iNOS*, and *IL-17* transcript levels relative to *GAPDH* in the gastric mucosa are presented in male (A) and female (B) mice. Uninfected mice at 12 mo (white bars; males, n = 3; females, n = 3) and H. pylori-infected mice at 6 mo (light gray bars; males, n = 4; females, n = 4) and 12 mo (dark gray bars; males, n = 5; females, n = 6) are presented. *H. pylori* infection increased expression of *IFNγ, TNFα, IL-17*, and *iNOS* in both sexes at 6 and 12 mo. **P* < 0.05, ***P* < 0.01, and ****P* < 0.001.

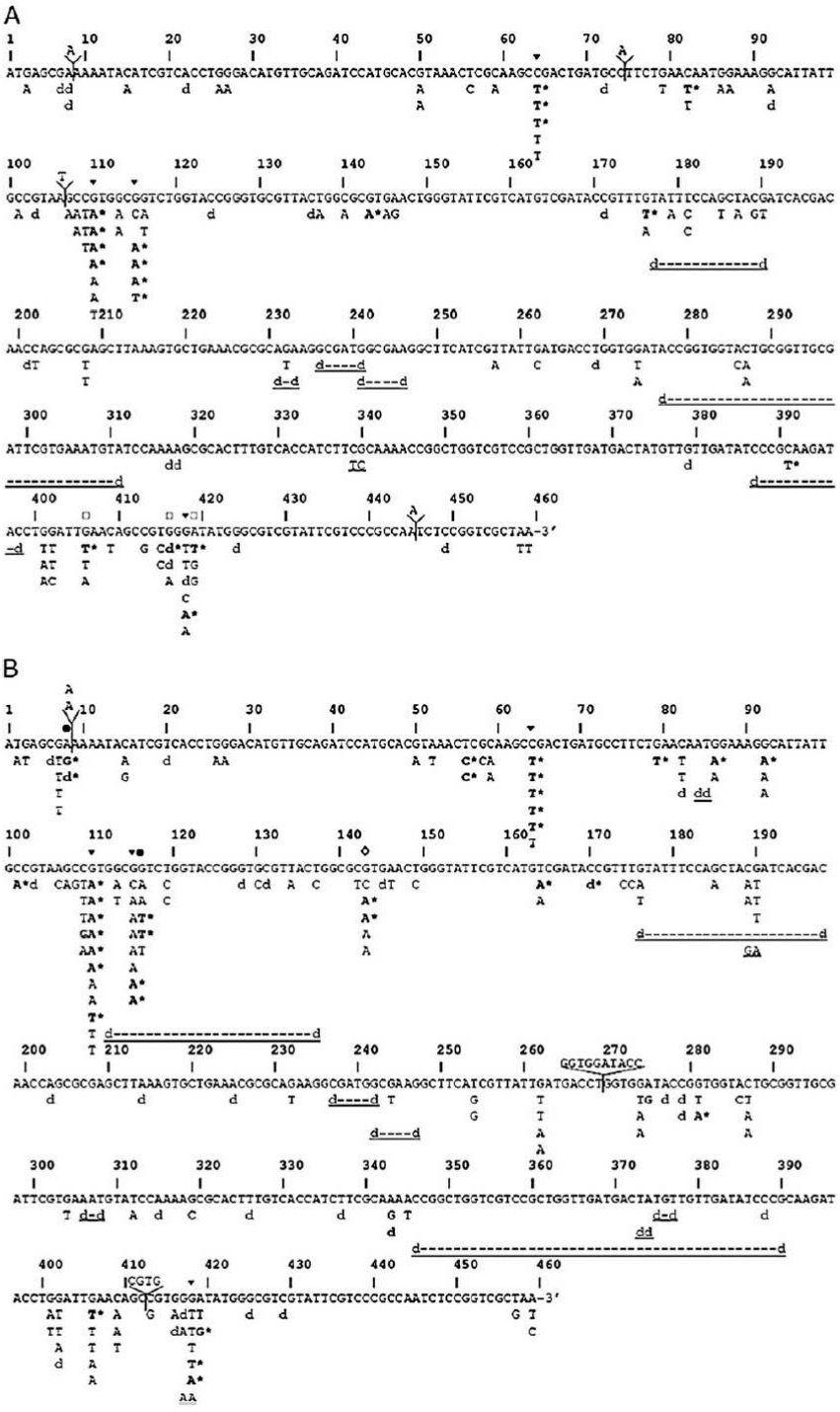

Fig. 2.S3. *H. pylori* infection targets specific hot spots in the *gpt* gene. The distribution of mutations induced in the *gpt* gene was determined by sequencing analysis of 411 mutants. Hot spots seen in uninfected and infected mice are denoted by ▼. (A) Spectra of all uninfected mice. Not shown is a complex mutation from 407 to 429. A hot spot mainly seen in uninfected males is marked by □. (B) Spectra of all infected mice. Not shown is a complex mutation from 389 to 419. Mutations at 142 and 174 were second mutations. Hot spots mainly seen in infected mice of both sexes are represented by ◇and hot spots seen mostly in infected females are marked •. N* represents 3× mutations, d represents a deletion. Underlined mutations denote a single mutation.

Table S1. Number of A:T-to-G:C transitions and G:C-to-T:A transversions in *H. pylori*–infected female mice at 12 MPI is higher than in other groups

	6 mo			12 mo		
Effect	Uninfected all (n = 6)	Infected male (n = 4)	Infected female (n = 8)	Uninfected all (n = 14)	Infected male (n = 5)	Infected female (n = 11)
Transition						
G:C to A:T	32 (50.0)	7 (43.8)	35 (42.7)	41 (41.4)	16 (48.5)	39 (33.3)
A:T to G:C	2 (3.1)	0	4 (4.9)	6 (6.1)	1 (3.0)	15 (12.8)
Transversion						
G:C to T:A	11 (17.2)	5 (31.3)	16 (19.5)	21 (21.2)	7 (21.2)	31 (26.5)
G:C to C:G	2 (3.1)	1 (6.3)	3 (3.7)	4 (4.0)	3 (9.1)	2 (1.7)
A:T to T:A	4 (6.3)	0	6 (7.3)	5 (5.1)	0	6 (5.1)
A:T to C:G	0	1 (6.3)	3 (3.7)	1 (1.0)	0	2 (1.7)
Deletion						
1-bp deletion	10 (15.6)	2 (12.5)	8 (9.8)	12 (12.1)	4 (12.1)	15 (12.8)
≥2-bp deletion	1 (1.6)	0	4 (4.9)	5 (5.1)	1 (3.0)	4 (3.4)
Insertion	0	0	2 (2.4)	4 (4.0)	0	2 (1.7)
Complex mutation	2 (3.1)	0	1 (1.2)	0	1 (3.0)	1 (0.9)
Total	64 (100)	16 (100)	82 (100)	99 (100)	33 (100)	117 (100)

Values in parentheses are percentages. The number of A:T-to-G:C transitions and G:C-to-T:A transversions was elevated in female mice infected with *H. pylori* for 12 mo. The number of mutations was determined from the sequence analysis of 411 mutants recovered from the *gpt* assay after excluding 155 mutants considered siblings. Control mice of both sexes were grouped for this analysis.

Chapter 3: 17β-estradiol and Tamoxifen prevent gastric cancer by modulating leukocyte recruitment and oncogenic pathways in *Helicobacter pylori*-infected INS-GAS male mice

Alexander Sheh, Zhongming Ge, Nicola MA Parry, Sureshkumar Muthupalani, Melissa W Mobley, Amanda McCabe, Julia E Rager, Arkadiusz R Raczynski, Rebecca C Fry, Timothy C Wang, James G Fox

Abstract

Gastric cancer (GC) is a male-predominant cancer associated with *Helicobacter pylori* infection. Epidemiological studies suggest that estrogens reduce GC risk and our previous studies demonstrated that 17β-estradiol (E2) administered prior to *H. pylori* infection in INS-GAS mice decreases GC risk. We examined the effect of E2 and the anti-estrogen, Tamoxifen (TAM), on *H. pylori*-induced gastric cancer in hypergastrinemic male and female INS-GAS mice infected with *H. pylori* SS1. Sixteen weeks after infection with *H. pylori*, mice were treated with E2, TAM, both E2 and TAM, or placebo subcutaneously implanted pellets for 12 weeks. Gastric histopathology was evaluated at 16 and 28 weeks post-infection (WPI). At 28 WPI, global gastric gene expression was evaluated, and serum inflammatory cytokines measured. At 16 WPI, *H. pylori* infection induced robust gastric pathology in mice of both genders ($P<0.001$). After 12 weeks of treatment, gastric precancerous lesions were significantly reduced in *H. pylori*-infected E2-, TAM- or dual-treated males compared to *H. pylori*-infected untreated males ($P<0.001$, 0.01 and 0.01, respectively). Forty percent of infected untreated males developed intramucosal gastric carcinoma while cancer was not detected in any group treated with E2 or/and TAM. In contrast, TAM did not alter pathology in females regardless of infection status. Infected E2 males differentially expressed 363 genes compared to infected untreated males ($Q<0.05$) while

infected TAM males differentially expressed 144 genes compared to controls (Q<0.05). Differentially expressed genes from E2 or TAM males were associated with cancer and cellular movement as determined using molecular network analysis, indicating similar mechanisms in the reduction of gastric lesions. E2 or TAM decreased expression of metastasis associated genes (*PLAUR* and *MMP10*) and increased two Wnt signaling repressors (*Fzd6* and *SFRP2*). Gastric expression of cytokines involved in cellular movement (*CXCL1* and *IL-1α*) were reduced in E2 or TAM treated males. CXCL1, a potent neutrophil and macrophage chemokine, was also decreased in the serum of infected E2 males and infected untreated females (P<0.05 and 0.001 respectively) compared to controls. A decrease in neutrophil infiltration was observed by immunohistochemistry in infected E2 and TAM males compared to untreated males (P < 0.01 and P = 0.07, respectively). Our results demonstrate that E2 and TAM downregulate CXCL1, limit recruitment of innate immune cells and therapeutically prevent *H. pylori*-induced gastric cancer.

3.1 Introduction

Acting through multiple, complex mechanisms that are incompletely understood, chronic inflammation induced by *Helicobacter pylori* is a significant risk factor for gastric adenocarcinoma (GC). Chronic inflammation induced by *H. pylori* infection increases lifetime risk of developing gastritis, duodenal and gastric ulcers, mucosa-associated lymphoid tissue (MALT) lymphoma, mucosal atrophy and gastric carcinoma [68,85]. Indeed, *H. pylori* is classified a group I human carcinogen by IARC due to its impact on gastric cancer incidence, the second most frequent cause of cancer-related death worldwide [34]. However, age-standardized and cumulative incidence rates of gastric adenocarcinoma are twice as high in men as in women with a 2.5-fold difference around age 60[11]. The age-specific pattern of the M/F gastric cancer incidence curve is a global phenomenon, equally seen in populations with high and low risk for GC. Given the high prevalence of *H. pylori* worldwide, this implies that intrinsic sex differences modulate *H. pylori*-induced carcinogenesis irrespective of other environmental factors, but the mechanisms mediating these differences are unknown.

Estrogens have been associated with the protection against GC as postmenopausal women experience an increase in GC incidence[11]. Epidemiological studies indicate that delayed onset of menopause, increased length of fertility life and hormone therapies in men and women were associated with decreased GC risk[13]. Postmenopausal hormone replacement therapy (HRT) may lower the rate of gastrointestinal cancer, particularly colonic cancer[111-113]. Prostate cancer patients treated with estrogen had a decreased risk of gastric cancer[110]. Additionally, there is epidemiological data linking the usage of anti-estrogen therapy, particularly the breast cancer drug Tamoxifen (TAM), with increased incidence rates of

gastrointestinal malignancies. Due to its suppression of estrogen receptor positive breast cancer, TAM is considered an antagonist of estrogen signaling, but considerable evidence exists demonstrating that TAM can also act as an agonist leading to increased incidence of endometrial cancers in postmenopausal women[114-115,154]. However, TAM's function in the stomach and its association with gastrointestinal cancers, and GC in particular, is not clear; one study reports no effect[115] while others have associated TAM treatment with increased risk of GC[116-118]. Due to their retrospective nature, the studies assessing the effects of estrogen and TAM on GC were unable to control for *H. pylori* infection, a major confounding factor in these studies[13,110,118].

Transgenic INS-GAS mice over-express human gastrin, a phenotype associated with increased risk for gastric glandular atrophy and cancer in humans[30,155]. INS-GAS mice infected with *H. pylori* or *H. felis* develop gastric carcinomas 28 weeks post-infection (WPI) in a male-predominant fashion[141,156].This process parallels the development of human gastric cancer after decades of chronic *H. pylori* gastritis[14,30,141,156]. Similar to human patients, INS-GAS mice progress to GC following development of gastric atrophy, hypochlorhydria, intestinal metaplasia and dysplasia[18,68,141,156]. Antibiotic eradication therapy targeting *H. pylori* in male INS-GAS mice reduced GC risk, but this effect was most pronounced with antibiotic treatment at 8 WPI compared to mice treated at 12 or 22 WPI[61,157], implying that the progression of *H. pylori* carcinogenesis may be reversible up to a point. We previously demonstrated that ovariectomized female INS-GAS mice developed *H. pylori*-induced GC whereas E2 supplementation of ovariectomized female mice was protective[14]. We also reported that E2 treatment, but not castration, prior to *H. pylori* infection attenuated gastric lesions by increasing

Foxp3+ and interleukin 10 (*IL-10*) expression and decreasing *IFN*-γ and *IL-1* expression[15].

In this study, we employed the INS-GAS mouse to determine the effects of E2 and TAM treatment on chronically *H. pylori*-infected mice and examined the mechanisms by which E2 and/or TAM affect gastric lesions in male and female mice. Following 16 weeks of sham or *H. pylori* infection, pellets containing placebo, E2, TAM, or both E2 and TAM were subcutaneously implanted in male INS-GAS mice, while placebo or TAM pellets were implanted in female mice. E2 was administered via the pellets to determine its therapeutic effect during *H. pylori* infection. We sought to clarify TAM's effects on GC incidence, expecting exacerbation of precancerous gastric lesions (TAM alone) or the blocking of E2's protective effects (E2 and TAM treatment). At 28 WPI, we characterized the effects of E2 and TAM on histopathologic changes in the stomach, serum levels of inflammatory cytokines, global gastric gene expression and gastric immune cell infiltration.

3.2 Materials and Methods

Bacteria and Mice. *Helicobacter pylori* SS1 was cultured on blood agar (TSA with sheep blood, Remel, Lenexa, KS) or Brucella broth with 5% fetal bovine serum under microaerobic conditions (10% H2, 10% CO2, 80% N2).One hundred and fifty-one (52 females, 99 males) specific pathogen-free (including Helicobacter spp.) INS-GAS mice on a FVB background were used in this study. Mice were maintained in a facility accredited by the Association for Assessment and Accreditation of Laboratory Animal Care International, housed on hardwood bedding in microisolator, solid-bottom polycarbonate cages and fed regular chow diet (Prolab RMH3000, LabDiet, Richmond, IN) and water ad libitum. All protocols were approved by the MIT

Committee on Animal Care.

Experimental design. Eight-week-old male and female mice were either infected by oral gavage with approximately 1×10^8 colony forming units of *H. pylori* SS1 (47 males and 29 females) or dosed with broth only (52 males and 23 females) on alternate days for a total of 3 doses[137,158]. At 4 and 16 weeks post-infection (WPI), 4 and 20 mice, respectively, were euthanized to confirm *H. pylori* infection by PCR. At 16 WPI, pathology was assessed to establish severity of gastritis prior to pellet implantation. The remaining mice were divided into six groups for pellet implantation: (i) untreated males (n = 23), (ii) E2-treated males (n = 21), (iii) TAM-treated males (n = 23), (iv) E2- and TAM-treated males (n = 19), (v) untreated females (n = 19), and (vi) TAM-treated females (n = 21). At 28 WPI, the mice were euthanized and the presence of pellets was confirmed. Mice missing pellets were excluded, and the following were used in subsequent analyses (i) untreated males (10 infected, 12 uninfected), (ii) E2-treated males (9 infected and 10 uninfected), (iii) TAM-treated males (7 infected and 6 uninfected), (iv) E2- and TAM-treated males (4 infected and 7 uninfected), (v) untreated females (10 infected and 9 uninfected), and (vi) TAM-treated females (9 infected and 1 uninfected). Three of 9 infected E2 males were euthanized before 28WPI due to poor body condition. These 3 mice were excluded from serum cytokine analysis.

Subcutaneous implantation of placebo, 17-β estradiol and Tamoxifen pellets. Surgical placement of pellets containing E2 or TAM was performed using sterile techniques and under general anesthesia with isoflurane. All the mice received intraperitoneal injections of 0.5 ml of warm lactated Ringer's solution prior to surgery. Time-release placebo (5 mg, 90 day release NC-111), E2 (0.25 mg, 90 day release NE-121), TAM (15 mg, 90 day release NE-361) or both E2 and

TAM pellets (Innovative Research of America, Sarasota, FL) were placed subcutaneously at 16 WPI. Skin incisions were closed using 9 mm surgical clips (MikRon Autoclip, Clay Adams, Parsippany, NJ). The E2 timed-release pellet results in a serum E2 level in the range from proestrus levels (~45 pg/ml) to slightly supraphysiological (up to 100 pg/ml) ([14]). The TAM pellet was expected to result in serum TAM level in the range of 2-3 ng/ml (Personal communication from Innovative Research of America, Sarasota, FL).

Sample collection and histological analysis. Immediately following CO_2 euthanasia, blood was collected by cardiac puncture, serum was separated and stored at -80°C. Reproductive tissues (testes and epididymis or uterus) were removed and weighed. The stomach and proximal duodenum were removed and incised along the line of the greater curvature. Luminal contents were removed and the mucosa was rinsed with sterile PBS.

Individual linear gastric strips from the lesser curvature were sectioned, flash frozen and stored at -80°C for DNA and RNA extraction. For histopathologic evaluation, linear strips extending from the squamocolumnar junction to the proximal duodenum were taken along the lesser curvature and fixed overnight in 10% neutral-buffered formalin. Tissues were routinely processed and embedded in paraffin. Four μm-thick sections were stained with hematoxylin and eosin (H&E) for microscopic examination. A board-certified comparative pathologist (N.M.P.), blinded to treatment groups, scored gastric lesions in the corpus on an ascending scale of 0 to 4 for inflammation, epithelial defects, atrophy, hyperplasia, mucous metaplasia, hyalinosis, intestinal metaplasia, and dysplasia according to previously published criteria[122]. Gastric lesions in the antrum were also scored on an ascending scale of 0 to 4 for inflammation, epithelial defects, hyperplasia and dysplasia. A dysplasia score of 3 was considered carcinoma

in situ or low-grade gastrointestinal intraepithelial neoplasia (GIN). In addition, a dysplasia score of 3.5-4 represented intramucosal carcinoma or high-grade GIN[122,159]. Both low grade and high-grade GIN were classified as gastric cancer. A gastric histologic activity index (GHAI) was calculated as the sum of scores for inflammation, epithelial defects, atrophy, hyperplasia, intestinal metaplasia, and dysplasia for the corpus and inflammation, epithelial defects, hyperplasia and dysplasia for the antrum. Hyalinosis and mucous metaplasia were excluded from the GHAI as they have been observed to develop spontaneously in mice[122,160].

Immunohistochemistry for neutrophils and macrophages. Levels of neutrophils and macrophages were quantified by immunohistochemistry as previously described ([161]) using antibodies for 1:75 myeloperoxidase (MPO) (RB-373-A; Thermo Scientific, Waltham, MA), a neutrophil-specific marker, and 1:150 F4/80 (MF48015; Caltag Laboratories, Burlingame, CA), a macrophage-specific marker, respectively, in 5 mice per group. Cells expressing MPO+ or F4/80+ were counted in the corpus at a magnification of x40. Five fields were counted per mouse and results are presented as the average number of MPO+ or F4/80+ cells/mm^2 of stomach.

Detection of *H. pylori* infection by PCR and qPCR. To confirm infection with *H. pylori* SS1 within the gastric mucosa, DNA was extracted from gastric tissue using the High Pure PCR Template purification kit (Roche). At 4 and 16 WPI, primers (CHP1: 5'-AAAGCTTTTAGGGGTGTTAGGGGTTT, CHP2: 5'-AAGCTTACTTTCTAACACTAACGC) specific for the *H. pylori ureC* gene were used to confirm infection as described previously[162]. A real-time quantitative PCR assay targeting *H. pylori* urease B was also used to quantify *H. pylori* infection levels[156,163]. A standard curve was generated by using serial 10-fold dilutions of *H. pylori* SS1 genome copies (from 5×10^6 to 50),

estimated from an average *H. pylori* genome size of 1.66 Mb[164-165]. Copy numbers of the gastric *H. pylori* genome were standardized using micrograms of murine chromosomal DNA determined by quantitative PCR using a mammalian 18S rRNA gene-based primer and probe mixture (Applied Biosystems) as described previously[166]. A threshold of 50 copies of the *H. pylori* genome was set as the lower limit of detection.

17β-estradiol serum levels. Serum E2 levels were measured using commercially available enzyme immunoassay kits (Cayman Chemical Company, Ann Arbor, MI) with a serum dilution of 1:4 and following the manufacturer's instruction. The E2 kits have a limit of detection of 6.6 pg/ml.

Analysis of mRNA expression. A longitudinal strip of gastric tissue was frozen in liquid nitrogen and stored at -80°C. Tissue was cut and weighed and total RNA was extracted using Trizol reagent (Invitrogen, Carlsbad, CA) and further cleaned up using RNase-free DNAse with an RNeasy kit (Qiagen Sciences, Germantown, MD). Quality of the RNA was determined with the Agilent 2100 Bioanalyzer using a RNA 6000 Nano total RNA Kit (Agilent Technologies, Santa Clara, CA). Total RNA was hybridized to Agilent 4x44K Whole Mouse Gene Expression Microarrays following the One-Color Microarray-Based Gene expression Analysis, Low Input Quick Amp Labeling protocol. Briefly, the method utilizes a T7 RNA polymerase that amplifies RNA to cRNA while incorporating cyanine 3-labeled CTP. Cy-3 incorporation and cRNA levels were measured with a NanoDrop ND-1000 UV-Vis Spectrophotometer (NanoDrop Technologies, Inc., Wilmington, DE). Arrays were scanned using an Agilent Microarray Scanner and data was extracted using Feature Extraction 9.1.

Processing of the raw gene expression data was performed using Partek® Genomics

Suite™ software (St. Louis, MO), where microarray data were first normalized by quantile using Robust Multi-Chip Average (RMA)[167]. Data were then filtered for expression levels above background noise (>abs[180]) which resulted in a reduction of probesets from 41,174 to 21,549. Differential gene expression was defined as a significant difference in mRNA levels between the groups compared where the following statistical requirements were set: (1) fold change of ≥ 1.5 or ≤ - 1.5; (2) p-value < 0.05 (ANOVA); and (3) a false discovery rate corrected q-value < 0.05. To control the rate of false positives, q-values were calculated as the minimum positive false discovery rate that can occur when identifying significant hypotheses[168]. Comparisons were performed between 1) infected males with placebo vs. infected males with 17-β estradiol, and 2) infected males with placebo vs. infected males with TAM. Three microarrays were hybridized for each group except for infected males with TAM (n=2).

Serum cytokine and chemokine levels. Serum protein levels of IL-1α, IL-1β, IL-2, IL-3, IL-4, IL-5, IL-6, IL-9, IL-10, IL-12 (p40), IL-12 (p70), IL-13, IL-17, Eotaxin, G-CSF, GM-CSF, IFN-γ, KC (CXCL1), MCP-1, MIP-1α, MIP-1β, RANTES and TNF-α were measured using the Bio-Plex Pro Cytokine assay (Bio-Rad Laboratories, Hercules, CA). Sera were diluted 1:4 in mouse-specific diluent and 50 µl of standard, control and serum samples were added to 96 well plate containing 50 µl of antibody coated fluorescent beads (Bio-Plex Mouse Cytokine 23-Plex Panel). Biotinylated secondary and streptavidin-PE antibodies were added to the plate and were read on the Bio-Plex array reader on the high photomultiplier tube setting with sample levels quantified using regression analysis of the standard curve. IL-9 data were not measured as insufficient counts were obtained.

Statistical analysis. Two-way analysis of variance (ANOVA) followed by Bonferroni post-tests

were used to analyze the effect of sex and 17β-estradiol and Tamoxifen on gastric lesions. Student two-tailed *t*-tests were used to analyze serum hormone differences and neutrophil and macrophage infiltration. Mann-Whitney tests were used for serum cytokine responses. Analyses were done with GraphPad Prism 5.0 (GraphPad, La Jolla, CA), or Microsoft Excel 2007 (Microsoft, Redmond, WA). *P*-values <0.05 were considered significant.

3.3 Results

3.3.1 E2 and Tamoxifen reduce reproductive tissue size and serum E2 concentrations through different mechanisms. Efficacy of the placebo, E2, TAM and dual (E2 and TAM) treatments was confirmed histopathologically and by measurement of serum E2. In male mice, E2 and dual treatment reduced the size of testes and seminal vesicles regardless of infection status. Placebo and TAM treatment had no effect on testes and seminal vesicles. E2 and dual treatment caused interstitial cystitis in male mice, which has been associated with E2[169], and TAM treatment in males caused inguinal hernias (data not shown). The ratio of reproductive tissues (testes and epididymis) to body weight was computed (Fig. 3.1). Both E2 and dual-treated mice had a significant reduction in the ratio compared to either untreated or TAM mice regardless of infection status (all $P < 0.001$, except infected TAM males vs. infected dual males $P < 0.01$). Infection status had no effect on the ratio of reproductive tissues to body weight. Serum E2 levels were significantly higher in infected E2 males (137.9 ± 29.9 pg/ml) and dual-treated males (154.0 ± 15.5 pg/ml) compared to untreated males (88.9 ± 24.7 pg/ml) ($P < 0.05$ and 0.001, respectively) (Fig. 3.2).

In female mice, TAM reduced the ratio of uterus weight to body weight compared to

untreated mice ($P < 0.001$) in infected mice, but not in uninfected mice due to decreased cohort size resulting from mice removed from the study because of pellet loss (Fig. 3.1). Infection status had no effect on the ratio of reproductive tissues to body weight. E2 was significantly reduced in infected TAM females compared to uninfected untreated females ($P < 0.001$) (Fig. 3.2).

3.3.2 E2, Tamoxifen and dual treatment prevent gastric cancer in infected males. Gastric histopathology was evaluated at 16 and 28 WPI to determine the effect of E2, TAM and dual treatment on *H. pylori* pathogenesis. *H. pylori* infection was confirmed at 4 and 16 WPI (n=14) by PCR. Randomly selected uninfected control mice across all time points were negative for infection. *H. pylori* levels were confirmed at 28 WPI by qPCR with no significant differences observed between groups (data not shown).

At 16 WPI, *H. pylori* infection induced robust gastric pathology, as quantified by the gastric histologic activity index (GHAI), in mice of both genders (M=12.2 ± 1.9, F=11.4 ± 1.2) compared to uninfected controls (M=6.5 ± 1.8, F=5.1 ± 0.5) (both $P<0.001$). At this point, both infected and uninfected male mice were divided into 4 groups: a) untreated, b) E2, c) TAM and d) dual (E2 and TAM). Infected and uninfected female mice were divided into 2 groups: a) untreated and b) TAM.

After 12 weeks of treatment, GHAI was significantly reduced in infected E2 (12.6 ± 3.7), TAM (11.9 ± 0.7) and dual males (13.9 ± 1.9) compared to infected untreated males (17.1 ± 1.2) ($P<0.001$, 0.001 and 0.01, respectively) (Fig. 3.3A and 3.3C). The reduction in overall gastric pathology demonstrated that therapeutic treatment with E2 protects the stomach from lesions caused by *H. pylori*, even after chronic inflammation has been established. Unexpectedly, TAM

was protective, indicating that TAM may be acting agonistically in this model and activating estrogen receptor locally or systemically. E2 and TAM treatment of infected male mice did not provide increased protection against gastric lesions in these mice, suggesting that the two treatments may progress through overlapping and/or nonadditive pathways. Examining the individual histologic parameters in infected males, foveolar hyperplasia and dysplasia, two precancerous lesions, were found significantly decreased in all three treated groups. A significant decrease in inflammation was seen in relation to E2 or TAM treatments alone, while epithelial defects were only significantly decreased in relation to E2 treatment (Fig. 3.4 and Supplemental Table 3.S6). Intestinal metaplasia was significantly decreased in response to either E2 or combined E2 and TAM treatments. Forty percent of infected untreated males had high-grade gastrointestinal intraepithelial neoplasia (GIN), or intramucosal carcinoma, while infected males treated with E2, TAM or both E2 and TAM had no incidence of GIN (Fig. 3.4 and Supplemental Table 3.S6). No significant difference between all treated infected male groups and the untreated infected males was observed with regard to mucous metaplasia, hyalinosis and oxyntic atrophy. While *H. pylori* pathogenesis normally occurs in the corpus in mice, E2, TAM and dual treatment (0.4 ± 0.2, 0.6 ± 0.4, 1.1 ± 0.5, respectively) also significantly reduced antral pathology compared to infected untreated males (2.5 ± 1.1) (all $P<0.001$).

Uninfected male mice treated with E2 and mice with dual treatments also had less corpus pathology (3.0 ± 1.1 and 1.8 ± 1.1, respectively) compared to uninfected untreated males (5.8 ± 1.8) ($P < 0.01$ and 0.001, respectively), but uninfected TAM treated males were not protected (4.5 ± 0.9) (Fig. 3.3A, 3.3C). In uninfected males, epithelial defects (including glandular ectasia, surface irregularities and mucosal erosions), oxyntic atrophy, and dysplasia

(characterized by loss of oxyntic cells, disorganization and branching of glands, loss of columnar glandular orientation, cell stratification, pleomorphism and atypia, as well as nuclear changes including anisokaryosis and loss of basal polarity) were all significantly decreased with E2 treatment, as well as with E2 in combination with TAM, compared to untreated males. In uninfected male mice, TAM alone produced no significant changes in any of the lesion categories. Foveolar hyperplasia was significantly decreased only as a result of combined E2/TAM treatment. There was no significant difference in any of the uninfected male groups with regard to inflammation, mucous metaplasia or intestinal metaplasia (characterized by columnar elongation of foveolar epithelium with or without interspersed goblet cells) (Fig. 3.3C). In contrast, TAM treatment in females did not alter the levels of pathology in infected or uninfected females. No significant changes in any of the lesion categories were found in any of the female groups (Fig. 3.3 and Supplemental Table 3.S6).

3.3.3 E2 and Tamoxifen decreased MPO+ neutrophils and F4/80+ macrophages in the stomach. Neutrophils expressing myeloperoxidase (MPO) were present in lower numbers in the stomach of *H. pylori*-infected, E2 or TAM treated male mice (10 ± 2 cells/40x field and 13 ± 7 cells/40x field, respectively) compared to *H. pylori* infected untreated males (21 ± 4 cells/40x field, $P<0.01$ and 0.072, respectively) (Fig. 3.5A). *H. pylori* infection increased the infiltration of neutrophils into the stomach in infected male mice compared to uninfected male mice (3 ± 2 cells/40x field, respectively, $P <0.001$) and in infected female mice compared to uninfected female mice (21 ± 6 cells/40x field vs.1 ± 2 cells/40x field, respectively, $P <0.001$) (Fig. 3.5A). Although neutrophil counts were decreased, infected male mice treated with E2 or TAM still had increased neutrophilic infiltration compared to untreated uninfected male mice ($P< 0.001$ and

P<0.05, respectively). Neutrophils infiltrating the site of infection promote chronic inflammation and contribute to the recruitment of other inflammatory cells. Interestingly, significant decreases were observed due to E2 in male mice, while decreasing trends were observed due to TAM in male mice, indicating deregulation of neutrophil recruitment through estrogen signaling.

Macrophages expressing F4/80 were present in lower numbers in the stomach of *H. pylori*-infected, E2 or TAM treated male mice (28 ± 7 cells/40x field and 27 ± 8 cells/40x field, respectively) compared to *H. pylori* infected untreated males (macrophages: 34 ± 9 cells/40x field, *P*=0.276 and 0.229, respectively) (Fig. 3.5B). *H. pylori* infection increased macrophage infiltration into the stomach in infected male mice compared to uninfected male mice (9 ± 5 cells/40x field, respectively, *P* <0.001) and in infected female mice compared to uninfected female mice (25 ± 9 cells/40x field vs. 5 ± 2 cells/40x field, respectively, *P* <0.01) (Fig. 3.5B). As seen in the neutrophil data, *H. pylori*-infected male mice treated with E2 or TAM still had greater macrophage infiltration than untreated uninfected male mice (Both *P* < 0.01). As macrophages are recruited by neutrophils, the decreased neutrophil levels may contribute to decreased macrophage numbers in E2 or TAM treated male mice.

3.3.4 E2 and Tamoxifen modulate cellular movement and immune responses responsible for cancer and chronic inflammatory diseases in infected mice. Gene expression analysis was performed on longitudinal gastric strips from *H. pylori*-infected male mice receiving placebo, E2 or TAM pellets to determine if a characteristic expression profile was observed in E2 and TAM reduction of inflammation and gastric adenocarcinoma. For this analysis, we compared the expression level of 41,000 probes and required a fold change of greater than or equal to 1.5,

ANOVA p-value < 0.05 and FDR q-value < 0.05 for significance. 363 and 144 genes were significantly different between infected males treated with E2 and infected males treated with TAM compared to infected untreated males (A complete list of genes is found in Supp. Table 3.S1A & 3.S1B). Comparison of both data sets yielded 61 commonly deregulated genes in treated mice compared to untreated mice (Supp. Table 3.S1C).

In order to identify potential biological pathways and functions affected by E2 or TAM, molecular networks containing differentially expressed genes were algorithmically constructed based on connectivity and the known relationships among proteins using Ingenuity Pathways Analysis (IPA). Genes deregulated by E2 and TAM resulted in the generation of 25 and 12 networks respectively (For the top 5 networks, see Supp. Table 3.S2A & 3.S2B). For both treatments, the most significant network was highlighted for further evaluation (Fig. 3.6). Analysis of the 61common genes between both E2 and TAM generated 7 networks (Supp. Table 3.S2C, Fig. 3.6).

Within the "molecular and cellular functions" category, cellular movement was highly associated with both data sets. Of the top 5 functions, 2 other functions were shared by both groups: cellular development, and cell-to-cell signaling and interaction (Supp. Table 3.S3B & 4.S4B). Cellular movement and cell-to-cell signaling and interaction were among the top "molecular and cellular functions" in the set of common genes (Supp. Table 3.S5B). Among the cytokines associated with cellular movement, *CXCL1*, a murine IL-8 homolog, as well as *IL-1α* and *Fosl1*, modulators of IL-8, were downregulated by E2 or TAM. E2 alone upregulated gastric expression of *CCL19* (*MIP3β*), *CCL21a*, *CXCL15* and *IL-17b* while downregulating *IL-33,* a IL-1 family cytokine. TAM alone downregulated *CCL2* (*MCP-1*), *CCL7* (*MCP-3*), and *CCL12* (*MCP-5*)

(see Supplemental Table 3.1 for a complete list). *CXCL1* was associated with the most significant networks and top biological functions in both treatment groups.

Cancer was the most associated "disease or disorder" in both datasets with 115/363 and 41/144 genes associated with E2 and TAM, respectively (Supp. Tables 3.3A & 3.4A), as well as in the dataset of overlapping genes (21/61) (Supp. Table 3.5A). Genes differentially expressed affected oncogenic processes such as tumorigenesis, hyperplasia, hyperproliferation, malignant tumors, metastasis and neoplasia. Organismal injury and abnormality was the other disease and disorder associated highly with both E2 and TAM treatments. Furthermore, diseases associated with immune and inflammatory responses were significantly changed in both treatments, e.g. cardiovascular disease, inflammatory response and hypersensitivity response. Among the genes associated with cancer, stress response genes (*DNAJA1* and *HSPA1A*), extracellular remodeling genes (*MMP10*, *PLAUR*, *SERPINE1*, and *GDF15*) and a component of the AP-1 transcription complex (*FOSL1*) were downregulated by E2 or TAM, indicative of the reduced severity of gastric lesions. E2 or TAM upregulated genes associated with the Wnt/β-catenin pathway including a phosphatase (*PPP2R2B*) and two receptors (*SFRP2* and *FZD6*). E2 alone downregulated gastric expression of additional metalloproteinases (*MMP3* and *MMP13*) while upregulating another Wnt receptor (*SFRP4*). TAM downregulated the growth factor, *IGF1*, which mediates insulin like effects (see Supplemental Table 3.1 for a complete list of genes).

3.3.5 E2 modulates inflammatory serum cytokines involved in neutrophil and macrophage chemotaxis. To determine if E2 modulated systemic responses to infection, serum cytokine protein levels were measured in both uninfected and infected mice of the following groups: untreated males, E2 males and untreated females (Fig. 3.7). Basal differences in immunity were

observed between genders as uninfected untreated females had elevated Th2 cytokines, interleukin 5 (IL-5) and IL-13, compared to uninfected untreated males ($P < 0.05$ and 0.01, respectively).

E2 treatment modulated serum cytokine responses in infected E2 males compared to infected untreated males. Systemic levels of the neutrophil chemokine, CXCL1, were decreased in both infected E2 males and infected untreated females compared to infected untreated males ($P < 0.05$ and 0.001, respectively). Furthermore, macrophage inflammatory protein 1-alpha (MIP1α or CCL3) and MIP1β (or CCL4) were both significantly higher in infected untreated females compared to infected untreated males ($P < 0.01$ and 0.05, respectively) but were not different between E2 males and untreated females, indicating a slight E2-mediated increase in MIP1α/β levels. IL-6 was increased significantly in infected males receiving E2 compared to infected untreated males ($P <0.05$).

A subset of cytokines were significantly different between genders and were not affected by E2 supplementation. IL-1β, IL-5 and monocyte chemoattractant protein-1 (MCP-1 or CCL2) were significantly decreased in either untreated or E2-treated infected males compared to infected untreated females ($P < 0.05$, 0.01, 0.05 for infected untreated male vs. infected untreated female and $P <0.05$, 0.05 and 0.05 for infected E2 male vs. infected untreated female). IL-12p70 was increased in infected untreated females compared to infected E2 males ($P < 0.05$) but not significantly compared to infected untreated males ($P = 0.08$).

3.4 Discussion

Although estrogen is hypothesized to reduce gastric adenocarcinoma in women[13] due to

its myriad of immunomodulatory effects[108], few studies involving male and female animals with a recognized sexual dimorphism in GC incidence have analyzed the role of 17β-estradiol and *H. pylori* in gastric carcinogenesis. In a short term, 6 week study, E2 treatment of ovariectomized *H. pylori* infected gerbils increased acute inflammation and epithelial cell proliferation[170]. In contrast, previous studies using ovariectomized female *H. pylori* infected INS-GAS mice demonstrated that E2 treatment of mice infected chronically for 28 weeks reduced epithelial cell proliferation, attenuated the severity of gastritis and reduced the development of GIN[14]. We hypothesized that E2 was protective due to decreases in proinflammatory mediators like *IL-1β* and *iNOS* and increases in antiinflammatory mediators like *IL-10*[14]. We also demonstrated that E2 administered prophylactically, but not castration, reduced *H. pylori* induced gastric lesions in male INS-GAS mice and was associated with an increase in gastric FoxP3+ regulatory T cells[15].

In the present study, we investigated the role of E2 and TAM in reducing GC in male and female *H. pylori* infected INS-GAS mice. Infected male mice treated with E2, TAM or both compounds experienced a significant reduction in gastric lesions with no cancer development compared to more severe lesions and a 40% incidence of gastric carcinoma in infected untreated males. Progressive *H. pylori* gastritis results from chronic inflammatory processes mediated by proinflammatory Th1 and Th17 cells[71,171]. In the present study, the attenuation of gastric lesions by E2 and TAM treatments was accompanied by a downregulation of proinflammatory cues. E2-mediated downregulation of inflammatory cues has been observed in other chronic inflammatory processes in many organs[108].

Epidemiological studies suggest that E2 decreases GC risk, and that TAM promotes GC by

antagonizing E2, presumably by competitively inhibiting binding to estrogen receptors[13,110,116-118]. However, TAM is recognized as a mixed agonist/antagonist of estrogen receptors[172-173], and the effects of TAM on *H. pylori* associated GC have not been carefully studied. Our results demonstrated that TAM may act agonistically in the stomach as it was protective in infected male mice and had no effect in female mice.

Two factors that differentiate this mouse study from epidemiological studies associating TAM to GC are menopausal status and cumulative dose. TAM-associated risk of endometrial cancers is noted mainly in postmenopausal women[154], and studies associating TAM with increased gastrointestinal cancer risk are exclusively composed of, or include a high percentage of, postmenopausal women[116-118]. It is possible that estrogen cycles in premenopausal women, or breeding age female mice as in our study, minimize the aberrant estrogen signaling promoted by TAM that leads to increases in cancer. In the context of male mice, increased estrogen signaling via E2 or TAM was protective as seen in men on HRT[110]. Additionally, human studies indicate that the cumulative dose of TAM is crucial for increasing cancer risk[115-116,174]. Breast cancer patients are prescribed a daily dose of 20mg (0.3 mg/kg for a 70 kg person) for 5 years[175]. Using TAM concentrations that inhibit breast cancer in mice[176], our mice were treated with a higher daily dose of 0.18mg (6.8 mg/kg for a 25g mouse) for 12 weeks. However, given the short lifespan of the mouse, as well as differences in drug metabolism[177-178], the murine model may not be ideal to assess longer term effects of chronic TAM treatment. While E2 and TAM mediated different systemic effects on male mice, the reduction of gastric lesions by E2, TAM and their combined use, along with the lack of increased protection with the dual treatment, suggests common and/or non-synergistic mechanisms.

A systems biology approach was used to understand the biological implications of gastric gene expression changes induced by systemic E2 and TAM treatments. Individual comparisons against infected untreated males indicated that both treatments reduced gastric pathology via common mechanisms including those affecting the movement of cells and decreasing inflammatory signals (Supp. Table 3.3 & 3.4). Our analysis highlighted the importance of decreased expression of *CXCL1*, also known as keratinocyte chemoattractant (KC) or growth-related oncogene-α (GROα), in the stomach of both E2 and TAM treated, *H. pylori* infected male mice. Moreover, serum CXCL1 protein levels were decreased in infected females and infected E2 males compared to infected untreated males. E2 also significantly decreased neutrophilic infiltration in infected male mice compared to infected untreated male mice, while a decreasing trend was observed in infected TAM male mice. Macrophages in the corpus were slightly decreased in infected E2 or TAM male mice compared to infected untreated mice.

CXCL1, the murine homolog of human IL-8, is a proinflammatory chemokine that recruits neutrophils and is upregulated in colon adenocarcinoma, atherosclerosis and cardiovascular disease[179-183]. CXCL1 mediates changes in the microenvironment that drive tumor formation[184-186]. CXCL1 and its receptor, CXCR2, which is highly expressed on neutrophils and macrophages, are important in the recruitment of immune cells. Both CXCL1-/- and CXCR2-/- mice develop fewer lesions and recruit fewer macrophages in a model of atherosclerosis[182]. Furthermore, E2 downregulates expression of both CXCL1 in endothelial cells and CXCR2 in monocytes, affecting monocyte adhesion to endothelial cells[187-188]. As E2 attenuates nuclear factor kappa beta (NF-κB) translocation[189-190], a potential mechanism by which E2 reduces CXCL1 is by blocking the NF-κB binding site upstream of CXCL1 (UCSC Genome bioinformatics).

Recent clinical and epidemiological studies link high CXCL1 expression and serum levels to gastric cancer[191-193]. A single nucleotide polymorphism in the IL-8 promoter region (IL-8 -251 T to A) that increases IL-8 protein levels is associated with increased gastric cancer risk[92-93]. In a mouse model of gastric cancer, CXCL1 was the main chemokine upregulated by K-ras overexpression, and CXCL1 mRNA levels had the highest degree of correlation with dysplasia scores[184].

A positive feedback loop couples CXCL1 secretion and neutrophil recruitment. In response to *H. pylori*-mediated CXCL1 gradients, neutrophils rapidly infiltrate the site of infection and aid in the recruitment of macrophages[194-195]. In addition to secreting more CXCL1, neutrophils induce CXCL1 expression in macrophages and gastric epithelia[196]. As CXCL1 recruits and activates inflammatory cells establishing a tumorigenic microenvironment[184], a decrease in CXCL1 levels might inhibit cancer formation by decreasing neutrophil numbers, which directly correlate with the severity of *H. pylori*-related injury[59], and by dampening local and systemic proinflammatory signals. Further studies will be required to determine how E2 or TAM initially disrupt this positive feedback loop. Although local CXCR2 expression was not altered by treatment, E2 or TAM mediated decreases in CXCL1 or CXCR2 expression in circulating neutrophils, or a decrease in epithelial CXCL1 expression, would disturb the feedback mechanism and this possibility merits further research.

Given the importance of CXCL1, we further investigated the deregulation of the gene expression of other cytokines due to E2 or TAM treatment of *H. pylori*-infected male mice as *H. pylori* infection upregulates transcripts encoding chemokines and their receptors[197-201]. E2 or TAM decreased *IL-1α* expression compared to untreated controls. *IL-1α* exacerbates chronic

inflammatory conditions, as evidenced in lipid-mediated atherogenesis[202]. E2-treated infected males had higher levels of *CCL19* and *CCL21*, both CCR7 ligands, which balance immunity and tolerance by mediating the homing of subsets of T cells and dendritic cells to lymph nodes[203]. TAM-treated infected males had decreased expression of *MCP-1, MCP-3* and *MCP-5*, which are ligands of CCR2, a receptor linked to multiple sclerosis, rheumatoid arthritis, obesity, atherosclerosis, cancer, transplant rejection and asthma[204]. Changes in the local expression of these cytokines by E2 and TAM treatment may further reduce chronic inflammatory conditions delaying tumor progression.

Systemic effects of sex and E2 treatment were explored by measuring serum cytokine levels and our results indicated additional differences in immune responses. Cytokines associated with Th2 immune responses and monocytes were elevated in female mice. Uninfected and infected females had higher levels of IL-5, which stimulates B cells and antibodies[205], compared to male counterparts. IL-13, which promotes alternative macrophage activation[206], was also higher in uninfected untreated females compared to males. Alternatively activated, or M2, macrophages promote Th2 immunity and are induced during the resolution phase of inflammation. Compared to the corresponding infected untreated males, infected untreated females also produced more monocyte chemokines (MIP1α and MIP1β) and cytokines secreted by monocyte-derived cells (IL-1β, IL-12p70 and MCP-1)[202,207]. While these strong proinflammatory cytokines have been associated with cancer[70,208-209], females had less severe disease compared to males. The attenuated gastritis noted in females in the presence of high levels of monocytes and macrophages might be mediated by increased levels of Th2 cytokines leading to the alternative activation of macrophages. E2 has been shown to increase

the number of alternatively activated macrophages and concomitantly reduce the number of classically activated macrophages and neutrophils[210]. The role of alternatively activated macrophages in stabilizing the progression of chronic inflammation in female INS-GAS mice requires further research. Surprisingly, serum IL-6 levels in infected males did not correlate with gastric cancer as noted in male-predominant liver cancer[211], as untreated infected males had lower IL-6 levels than E2 treated infected males. IL-6 has both pro- and antiinflammatory properties[209] and can be both downregulated and upregulated by E2[108,212-213], so its role in gastric cancer and the INS-GAS model requires further study.

Another mechanism by which E2 and TAM may mediate protection is by decreasing oncogenic pathways. E2 and TAM downregulated the urokinase-type plasminogen activator receptor (*PLAUR*) and two of its regulators, *GDF15* and *SERPINE1* (also known as *PAI-1*)[214-215]. *PLAUR* anchors urokinase and serves as a focal point for proteolytic activity during wound healing[216]. Increased PLAUR and PAI-1 levels are associated with pathological processes like cell invasion, metastasis, and angiogenesis, and have been associated with *H. pylori* infection as well as poor prognosis in gastric cancer patients[216-218]. As *PLAUR* is activated via β-catenin[219-220] and *H. pylori* causes nuclear accumulation of β-catenin[221-222], suppression of Wnt signaling by E2 and TAM was evaluated. E2 or TAM treated mice upregulated two Wnt signaling inhibitors, secreted frizzle-related protein 2 (*SFRP2*)[223] and Frizzled-6 (*FZD6*)[224]. sFRP-2 is modulated by E2[225-226], and inhibits β-catenin activation by specifically blocking Wnt 1 and Wnt4, but not Wnt3a[223,227-229]. sFRP-2 silencing is associated with increases in gastric cancer and other malignancies[230-234]. As increased Wnt signaling promotes cancer, our microarray data suggest that E2 and TAM treatment may in part prevent cancer by increasing Wnt antagonists and downregulating cell

invasive processes downstream of β-catenin.

Sex differences in gastric cancer incidence, the protective effect of prolonged fertility in females and the reduced risk among women taking postmenopausal hormones, are elements suggesting that sex hormones play a protective role in *H. pylori* associated gastric cancer. Our findings suggest that both E2 and TAM decrease gastric cancer by decreasing neutrophilic infiltration and attenuating the chronic inflammatory response, and by decreasing expression of Wnt/β-catenin signaling factors, important in oncogenesis. As these two mechanisms are highly interrelated, we believe that the reduction of neutrophilic infiltrate by CXCL1 reduces the exposure of the stomach to oxidative stress, a cause of DNA mutagenesis[235], decreases proinflammatory cellular infiltrates and delays the progression of gastric cancer.

3.5 References

1. Fox, J.G. & Wang, T.C. Inflammation, atrophy, and gastric cancer. *J Clin Invest* **117**, 60-69 (2007).
2. Suerbaum, S. & Michetti, P. Helicobacter pylori infection. *N Engl J Med* **347**, 1175-1186 (2002).
3. IARC. Schistosomes, liver flukes and Helicobacter pylori. IARC Working Group on the Evaluation of Carcinogenic Risks to Humans. Lyon, 7-14 June 1994. *IARC Monogr Eval Carcinog Risks Hum* **61**, 1-241 (1994).
4. Sipponen, P. & Correa, P. Delayed rise in incidence of gastric cancer in females results in unique sex ratio (M/F) pattern: etiologic hypothesis. *Gastric Cancer* **5**, 213-219 (2002).
5. Chandanos, E. & Lagergren, J. Oestrogen and the enigmatic male predominance of gastric cancer. *Eur J Cancer* **44**, 2397-2403 (2008).
6. Newcomb, P.A. & Storer, B.E. Postmenopausal hormone use and risk of large-bowel cancer. *J Natl Cancer Inst* **87**, 1067-1071 (1995).
7. Nanda, K., Bastian, L.A., Hasselblad, V. & Simel, D.L. Hormone replacement therapy and the risk of colorectal cancer: a meta-analysis. *Obstet Gynecol* **93**, 880-888 (1999).
8. Pukkala, E., Tulenheimo-Silfvast, A. & Leminen, A. Incidence of cancer among women using long versus monthly cycle hormonal replacement therapy, Finland 1994-1997. *Cancer Causes Control* **12**, 111-115 (2001).
9. Lindblad, M., Ye, W., Rubio, C. & Lagergren, J. Estrogen and risk of gastric cancer: a protective effect in a nationwide cohort study of patients with prostate cancer in Sweden. *Cancer Epidemiol Biomarkers Prev* **13**, 2203-2207 (2004).
10. White, I.N. Anti-oestrogenic drugs and endometrial cancers. *Toxicol Lett* **120**, 21-29 (2001).
11. Curtis, R.E., Boice, J.D., Jr., Shriner, D.A., Hankey, B.F. & Fraumeni, J.F., Jr. Second cancers after adjuvant tamoxifen therapy for breast cancer. *J Natl Cancer Inst* **88**, 832-834 (1996).
12. Jordan, V.C., Gapstur, S. & Morrow, M. Selective estrogen receptor modulation and reduction in risk of breast cancer, osteoporosis, and coronary heart disease. *J Natl Cancer Inst* **93**, 1449-1457 (2001).
13. Rutqvist, L.E*., et al.* Adjuvant tamoxifen therapy for early stage breast cancer and second primary malignancies. Stockholm Breast Cancer Study Group. *J Natl Cancer Inst* **87**, 645-651 (1995).
14. Matsuyama, Y*., et al.* Second cancers after adjuvant tamoxifen therapy for breast cancer in Japan. *Ann Oncol* **11**, 1537-1543 (2000).
15. Chandanos, E*., et al.* Tamoxifen exposure and risk of oesophageal and gastric adenocarcinoma: a population-based cohort study of breast cancer patients in Sweden. *Br J Cancer* **95**, 118-122 (2006).
16. Wang, T.C*., et al.* Synergistic interaction between hypergastrinemia and Helicobacter infection in a mouse model of gastric cancer. *Gastroenterology* **118**, 36-47 (2000).
17. Wang, T.C*., et al.* Pancreatic gastrin stimulates islet differentiation of transforming growth factor alpha-induced ductular precursor cells. *J Clin Invest* **92**, 1349-1356 (1993).
18. Fox, J.G*., et al.* Host and microbial constituents influence Helicobacter pylori-induced cancer in a murine model of hypergastrinemia. *Gastroenterology* **124**, 1879-1890 (2003).
19. Fox, J.G*., et al.* Helicobacter pylori-associated gastric cancer in INS-GAS mice is gender

specific. *Cancer Res* **63**, 942-950 (2003).
20. Ohtani, M.*, et al.* Protective role of 17 beta -estradiol against the development of Helicobacter pylori-induced gastric cancer in INS-GAS mice. *Carcinogenesis* **28**, 2597-2604 (2007).
21. Correa, P. Human gastric carcinogenesis: a multistep and multifactorial process--First American Cancer Society Award Lecture on Cancer Epidemiology and Prevention. *Cancer Res* **52**, 6735-6740 (1992).
22. Lee, C.W.*, et al.* Helicobacter pylori eradication prevents progression of gastric cancer in hypergastrinemic INS-GAS mice. *Cancer Res* **68**, 3540-3548 (2008).
23. Lee, C.W.*, et al.* Combination of sulindac and antimicrobial eradication of Helicobacter pylori prevents progression of gastric cancer in hypergastrinemic INS-GAS mice. *Cancer Res* **69**, 8166-8174 (2009).
24. Ohtani, M.*, et al.* 17β-estradiol suppresses Helicobacter pylori-induced gastric pathology in male hypergastrinemic INS-GAS mice. *Carcinogenesis* (Submitted 2010).
25. Fox, J.G.*, et al.* High-salt diet induces gastric epithelial hyperplasia and parietal cell loss, and enhances Helicobacter pylori colonization in C57BL/6 mice. *Cancer Res* **59**, 4823-4828 (1999).
26. Lee, A.*, et al.* A standardized mouse model of Helicobacter pylori infection: introducing the Sydney strain. *Gastroenterology* **112**, 1386-1397 (1997).
27. Rogers, A.B.*, et al.* Helicobacter pylori but not high salt induces gastric intraepithelial neoplasia in B6129 mice. *Cancer Res* **65**, 10709-10715 (2005).
28. Boivin, G.P.*, et al.* Pathology of mouse models of intestinal cancer: consensus report and recommendations. *Gastroenterology* **124**, 762-777 (2003).
29. Kang, W., Rathinavelu, S., Samuelson, L.C. & Merchant, J.L. Interferon gamma induction of gastric mucous neck cell hypertrophy. *Lab Invest* **85**, 702-715 (2005).
30. Rogers, A.B., Cormier, K.S. & Fox, J.G. Thiol-reactive compounds prevent nonspecific antibody binding in immunohistochemistry. *Lab Invest* **86**, 526-533 (2006).
31. Bergin, I.L., Sheppard, B.J. & Fox, J.G. Helicobacter pylori infection and high dietary salt independently induce atrophic gastritis and intestinal metaplasia in commercially available outbred Mongolian gerbils. *Dig Dis Sci* **48**, 475-485 (2003).
32. Maurer, K.J.*, et al.* Helicobacter pylori and cholesterol gallstone formation in C57L/J mice: a prospective study. *Am J Physiol Gastrointest Liver Physiol* **290**, G175-182 (2006).
33. Alm, R.A.*, et al.* Genomic-sequence comparison of two unrelated isolates of the human gastric pathogen Helicobacter pylori. *Nature* **397**, 176-180 (1999).
34. Tomb, J.F.*, et al.* The complete genome sequence of the gastric pathogen Helicobacter pylori. *Nature* **388**, 539-547 (1997).
35. Whary, M.T.*, et al.* Long-term colonization levels of Helicobacter hepaticus in the cecum of hepatitis-prone A/JCr mice are significantly lower than those in hepatitis-resistant C57BL/6 mice. *Comp Med* **51**, 413-417 (2001).
36. Irizarry, R.A.*, et al.* Summaries of Affymetrix GeneChip probe level data. *Nucleic Acids Res* **31**, e15 (2003).
37. Storey, J.D. The Positive False Discovery Rate: A Bayesian Interpretation and the q-Value. *The Annals of Statistics* **31**, 23 (2003).
38. Theoharides, T.C., Pang, X., Letourneau, R. & Sant, G.R. Interstitial cystitis: a

neuroimmunoendocrine disorder. *Ann N Y Acad Sci* **840**, 619-634 (1998).
39. Straub, R.H. The complex role of estrogens in inflammation. *Endocr Rev* **28**, 521-574 (2007).
40. Saqui-Salces, M.*, et al.* Effects of estradiol and progesterone on gastric mucosal response to early Helicobacter pylori infection in female gerbils. *Helicobacter* **11**, 123-130 (2006).
41. O'Keeffe, J. & Moran, A.P. Conventional, regulatory, and unconventional T cells in the immunologic response to Helicobacter pylori. *Helicobacter* **13**, 1-19 (2008).
42. Kabir, S. The Role of Interleukin-17 in the Helicobacter pylori Induced Infection and Immunity. *Helicobacter* **16**, 1-8 (2011).
43. Gottardis, M.M., Robinson, S.P., Satyaswaroop, P.G. & Jordan, V.C. Contrasting actions of tamoxifen on endometrial and breast tumor growth in the athymic mouse. *Cancer Res* **48**, 812-815 (1988).
44. Fong, C.J.*, et al.* Effects of tamoxifen and ethynylestradiol cotreatment on uterine gene expression in immature, ovariectomized mice. *J Mol Endocrinol* **45**, 161-173 (2010).
45. Rutqvist, L.E. Re: second cancers after adjuvant tamoxifen therapy for breast cancer. *J Natl Cancer Inst* **88**, 1497-1499; author reply, 1497-1499 (1996).
46. Tamaki, Y., Miyoshi, Y. & Noguchi, S. Adjuvant hormonal therapy. *Breast Cancer* **9**, 185-189 (2002).
47. Gottardis, M.M., Robinson, S.P. & Jordan, V.C. Estradiol-stimulated growth of MCF-7 tumors implanted in athymic mice: a model to study the tumoristatic action of tamoxifen. *J Steroid Biochem* **30**, 311-314 (1988).
48. Robinson, S.P., Langan-Fahey, S.M., Johnson, D.A. & Jordan, V.C. Metabolites, pharmacodynamics, and pharmacokinetics of tamoxifen in rats and mice compared to the breast cancer patient. *Drug Metab Dispos* **19**, 36-43 (1991).
49. Fromson, J.M., Pearson, S. & Bramah, S. The metabolism of tamoxifen (I.C.I. 46,474). I. In laboratory animals. *Xenobiotica* **3**, 693-709 (1973).
50. Wang, D.*, et al.* CXCL1 induced by prostaglandin E2 promotes angiogenesis in colorectal cancer. *J Exp Med* **203**, 941-951 (2006).
51. Wen, Y.*, et al.* GROalpha is highly expressed in adenocarcinoma of the colon and down-regulates fibulin-1. *Clin Cancer Res* **12**, 5951-5959 (2006).
52. Breland, U.M.*, et al.* A potential role of the CXC chemokine GROalpha in atherosclerosis and plaque destabilization: downregulatory effects of statins. *Arterioscler Thromb Vasc Biol* **28**, 1005-1011 (2008).
53. Boisvert, W.A.*, et al.* Up-regulated expression of the CXCR2 ligand KC/GRO-alpha in atherosclerotic lesions plays a central role in macrophage accumulation and lesion progression. *Am J Pathol* **168**, 1385-1395 (2006).
54. Fimmel, S., Devermann, L., Herrmann, A. & Zouboulis, C. GRO-alpha: a potential marker for cancer and aging silenced by RNA interference. *Ann N Y Acad Sci* **1119**, 176-189 (2007).
55. Okumura, T.*, et al.* K-ras mutation targeted to gastric tissue progenitor cells results in chronic inflammation, an altered microenvironment, and progression to intraepithelial neoplasia. *Cancer Res* **70**, 8435-8445 (2010).
56. Haghnegahdar, H.*, et al.* The tumorigenic and angiogenic effects of MGSA/GRO proteins in melanoma. *J Leukoc Biol* **67**, 53-62 (2000).

57. Yang, G.*, et al.* The chemokine growth-regulated oncogene 1 (Gro-1) links RAS signaling to the senescence of stromal fibroblasts and ovarian tumorigenesis. *Proc Natl Acad Sci U S A* **103**, 16472-16477 (2006).
58. Lei, Z.B.*, et al.* Effect of estradiol on chemokine receptor CXCR2 expression in rats: implications for atherosclerosis. *Acta Pharmacol Sin* **24**, 670-674 (2003).
59. Lei, Z.B.*, et al.* Regulation of growth-regulated oncogene alpha expression by estrogen in human endothelial cells. *Acta Pharmacol Sin* **22**, 1003-1006 (2001).
60. Ghisletti, S., Meda, C., Maggi, A. & Vegeto, E. 17beta-estradiol inhibits inflammatory gene expression by controlling NF-kappaB intracellular localization. *Mol Cell Biol* **25**, 2957-2968 (2005).
61. Dodel, R.C., Du, Y., Bales, K.R., Gao, F. & Paul, S.M. Sodium salicylate and 17beta-estradiol attenuate nuclear transcription factor NF-kappaB translocation in cultured rat astroglial cultures following exposure to amyloid A beta(1-40) and lipopolysaccharides. *J Neurochem* **73**, 1453-1460 (1999).
62. Junnila, S.*, et al.* Gene expression analysis identifies over-expression of CXCL1, SPARC, SPP1, and SULF1 in gastric cancer. *Genes Chromosomes Cancer* **49**, 28-39 (2010).
63. Jung, J.J.*, et al.* Chemokine growth-regulated oncogene 1 as a putative biomarker for gastric cancer progression. *Cancer Sci* **101**, 2200-2206 (2010).
64. Resnick, M.B.*, et al.* Global analysis of the human gastric epithelial transcriptome altered by Helicobacter pylori eradication in vivo. *Gut* **55**, 1717-1724 (2006).
65. Lu, W.*, et al.* Genetic polymorphisms of interleukin (IL)-1B, IL-1RN, IL-8, IL-10 and tumor necrosis factor {alpha} and risk of gastric cancer in a Chinese population. *Carcinogenesis* **26**, 631-636 (2005).
66. Taguchi, A.*, et al.* Interleukin-8 promoter polymorphism increases the risk of atrophic gastritis and gastric cancer in Japan. *Cancer Epidemiol Biomarkers Prev* **14**, 2487-2493 (2005).
67. Quiding-Jarbrink, M., Raghavan, S. & Sundquist, M. Enhanced M1 macrophage polarization in human helicobacter pylori-associated atrophic gastritis and in vaccinated mice. *PLoS One* **5**, e15018 (2010).
68. Sgouras, D.N.*, et al.* Lactobacillus johnsonii La1 attenuates Helicobacter pylori-associated gastritis and reduces levels of proinflammatory chemokines in C57BL/6 mice. *Clin Diagn Lab Immunol* **12**, 1378-1386 (2005).
69. Eck, M.*, et al.* CXC chemokines Gro(alpha)/IL-8 and IP-10/MIG in Helicobacter pylori gastritis. *Clin Exp Immunol* **122**, 192-199 (2000).
70. Evans, D.J., Jr.*, et al.* Characterization of a Helicobacter pylori neutrophil-activating protein. *Infect Immun* **63**, 2213-2220 (1995).
71. Walduck, A., Schmitt, A., Lucas, B., Aebischer, T. & Meyer, T.F. Transcription profiling analysis of the mechanisms of vaccine-induced protection against H. pylori. *FASEB J* **18**, 1955-1957 (2004).
72. Sepulveda, A.R.*, et al.* Screening of gene expression profiles in gastric epithelial cells induced by Helicobacter pylori using microarray analysis. *Aliment Pharmacol Ther* **16 Suppl 2**, 145-157 (2002).
73. Mueller, A., Merrell, D.S., Grimm, J. & Falkow, S. Profiling of microdissected gastric epithelial cells reveals a cell type-specific response to Helicobacter pylori infection.

Gastroenterology **127**, 1446-1462 (2004).
74. Kobayashi, M.*, et al.* A distinctive set of genes is upregulated during the inflammation-carcinoma sequence in mouse stomach infected by Helicobacter felis. *J Histochem Cytochem* **55**, 263-274 (2007).
75. Hofman, V.J.*, et al.* Gene expression profiling in human gastric mucosa infected with Helicobacter pylori. *Mod Pathol* **20**, 974-989 (2007).
76. Dinarello, C.A. Immunological and inflammatory functions of the interleukin-1 family. *Annu Rev Immunol* **27**, 519-550 (2009).
77. Forster, R., Davalos-Misslitz, A.C. & Rot, A. CCR7 and its ligands: balancing immunity and tolerance. *Nat Rev Immunol* **8**, 362-371 (2008).
78. Allen, S.J., Crown, S.E. & Handel, T.M. Chemokine: receptor structure, interactions, and antagonism. *Annu Rev Immunol* **25**, 787-820 (2007).
79. Takatsu, K., Kouro, T. & Nagai, Y. Interleukin 5 in the link between the innate and acquired immune response. *Adv Immunol* **101**, 191-236 (2009).
80. Martinez, F.O., Helming, L. & Gordon, S. Alternative activation of macrophages: an immunologic functional perspective. *Annu Rev Immunol* **27**, 451-483 (2009).
81. Serbina, N.V., Jia, T., Hohl, T.M. & Pamer, E.G. Monocyte-mediated defense against microbial pathogens. *Annu Rev Immunol* **26**, 421-452 (2008).
82. El-Omar, E.M.*, et al.* Interleukin-1 polymorphisms associated with increased risk of gastric cancer. *Nature* **404**, 398-402 (2000).
83. Tesch, G.H. MCP-1/CCL2: a new diagnostic marker and therapeutic target for progressive renal injury in diabetic nephropathy. *Am J Physiol Renal Physiol* **294**, F697-701 (2008).
84. Seruga, B., Zhang, H., Bernstein, L.J. & Tannock, I.F. Cytokines and their relationship to the symptoms and outcome of cancer. *Nat Rev Cancer* **8**, 887-899 (2008).
85. Gilliver, S.C. Sex steroids as inflammatory regulators. *J Steroid Biochem Mol Biol* **120**, 105-115 (2010).
86. Naugler, W.E.*, et al.* Gender disparity in liver cancer due to sex differences in MyD88-dependent IL-6 production. *Science* **317**, 121-124 (2007).
87. Gregory, M.S., Duffner, L.A., Faunce, D.E. & Kovacs, E.J. Estrogen mediates the sex difference in post-burn immunosuppression. *J Endocrinol* **164**, 129-138 (2000).
88. Kawasaki, T., Ushiyama, T., Inoue, K. & Hukuda, S. Effects of estrogen on interleukin-6 production in rheumatoid fibroblast-like synoviocytes. *Clin Exp Rheumatol* **18**, 743-745 (2000).
89. Dano, K.*, et al.* Plasminogen activation and cancer. *Thromb Haemost* **93**, 676-681 (2005).
90. Rodriguez, J.A.*, et al.* Metalloproteinases and atherothrombosis: MMP-10 mediates vascular remodeling promoted by inflammatory stimuli. *Front Biosci* **13**, 2916-2921 (2008).
91. Kenny, S.*, et al.* Increased expression of the urokinase plasminogen activator system by Helicobacter pylori in gastric epithelial cells. *Am J Physiol Gastrointest Liver Physiol* **295**, G431-441 (2008).
92. Beyer, B.C.*, et al.* Urokinase system expression in gastric carcinoma: prognostic impact in an independent patient series and first evidence of predictive value in preoperative biopsy and intestinal metaplasia specimens. *Cancer* **106**, 1026-1035 (2006).
93. Kaneko, T., Konno, H., Baba, M., Tanaka, T. & Nakamura, S. Urokinase-type plasminogen

activator expression correlates with tumor angiogenesis and poor outcome in gastric cancer. *Cancer Sci* **94**, 43-49 (2003).
94. Yang, J., Duh, E.J., Caldwell, R.B. & Behzadian, M.A. Antipermeability function of PEDF involves blockade of the MAP kinase/GSK/beta-catenin signaling pathway and uPAR expression. *Invest Ophthalmol Vis Sci* **51**, 3273-3280 (2010).
95. Mann, B.*, et al.* Target genes of beta-catenin-T cell-factor/lymphoid-enhancer-factor signaling in human colorectal carcinomas. *Proc Natl Acad Sci U S A* **96**, 1603-1608 (1999).
96. El-Etr, S.H., Mueller, A., Tompkins, L.S., Falkow, S. & Merrell, D.S. Phosphorylation-independent effects of CagA during interaction between Helicobacter pylori and T84 polarized monolayers. *J Infect Dis* **190**, 1516-1523 (2004).
97. Franco, A.T.*, et al.* Activation of beta-catenin by carcinogenic Helicobacter pylori. *Proc Natl Acad Sci U S A* **102**, 10646-10651 (2005).
98. Lee, C.S., Buttitta, L.A., May, N.R., Kispert, A. & Fan, C.M. SHH-N upregulates Sfrp2 to mediate its competitive interaction with WNT1 and WNT4 in the somitic mesoderm. *Development* **127**, 109-118 (2000).
99. Golan, T., Yaniv, A., Bafico, A., Liu, G. & Gazit, A. The human Frizzled 6 (HFz6) acts as a negative regulator of the canonical Wnt. beta-catenin signaling cascade. *J Biol Chem* **279**, 14879-14888 (2004).
100. Hayashi, K. & Spencer, T.E. WNT pathways in the neonatal ovine uterus: potential specification of endometrial gland morphogenesis by SFRP2. *Biol Reprod* **74**, 721-733 (2006).
101. Das, S.K.*, et al.* Estrogen targets genes involved in protein processing, calcium homeostasis, and Wnt signaling in the mouse uterus independent of estrogen receptor-alpha and -beta. *J Biol Chem* **275**, 28834-28842 (2000).
102. Melkonyan, H.S.*, et al.* SARPs: a family of secreted apoptosis-related proteins. *Proc Natl Acad Sci U S A* **94**, 13636-13641 (1997).
103. Kress, E., Rezza, A., Nadjar, J., Samarut, J. & Plateroti, M. The frizzled-related sFRP2 gene is a target of thyroid hormone receptor alpha1 and activates beta-catenin signaling in mouse intestine. *J Biol Chem* **284**, 1234-1241 (2009).
104. von Marschall, Z. & Fisher, L.W. Secreted Frizzled-related protein-2 (sFRP2) augments canonical Wnt3a-induced signaling. *Biochem Biophys Res Commun* **400**, 299-304 (2010).
105. Suzuki, H.*, et al.* A genomic screen for genes upregulated by demethylation and histone deacetylase inhibition in human colorectal cancer. *Nat Genet* **31**, 141-149 (2002).
106. Suzuki, H.*, et al.* Epigenetic inactivation of SFRP genes allows constitutive WNT signaling in colorectal cancer. *Nat Genet* **36**, 417-422 (2004).
107. Jost, E.*, et al.* Epigenetic inactivation of secreted Frizzled-related proteins in acute myeloid leukaemia. *Br J Haematol* **142**, 745-753 (2008).
108. Veeck, J.*, et al.* Promoter hypermethylation of the SFRP2 gene is a high-frequent alteration and tumor-specific epigenetic marker in human breast cancer. *Mol Cancer* **7**, 83 (2008).
109. Nojima, M.*, et al.* Frequent epigenetic inactivation of SFRP genes and constitutive activation of Wnt signaling in gastric cancer. *Oncogene* **26**, 4699-4713 (2007).
110. Sheh, A.*, et al.* Mutagenic potency of Helicobacter pylori in the gastric mucosa of mice is determined by sex and duration of infection. *Proc Natl Acad Sci U S A* **107**, 15217-15222

(2010).

3.6 Tables and Figures

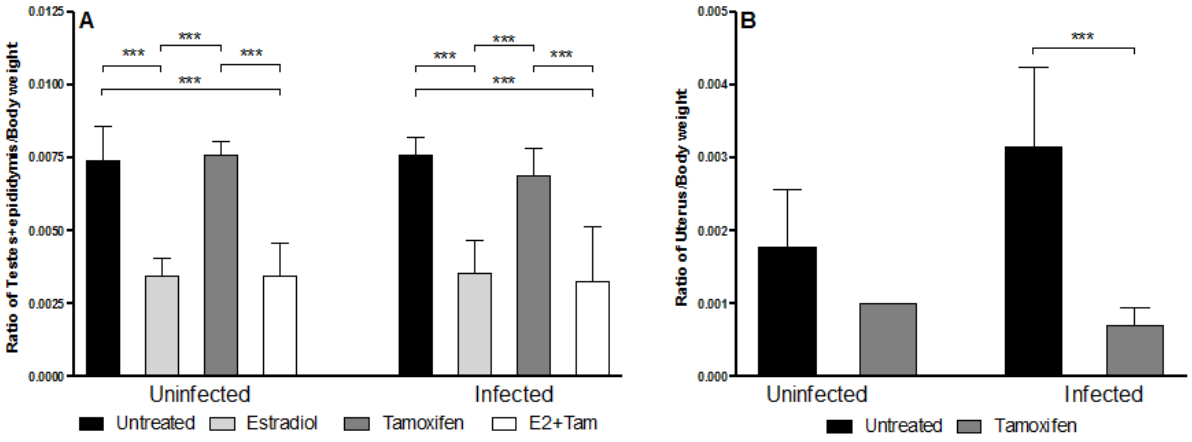

Figure 3.1. Ratios of reproductive tissues/body weight. A. After 12 weeks of hormone treatment, testes and epididymis/body weight ratios were compared in male mice showing efficacy of E2 and combination treatments compared to untreated or TAM treated mice. B. After 12 weeks of treatment, uterus/body weight ratios demonstrated the efficacy of TAM treatment. Only 1 uninfected female with TAM was available for comparison. ***P<0.001. Error bars represent SD.

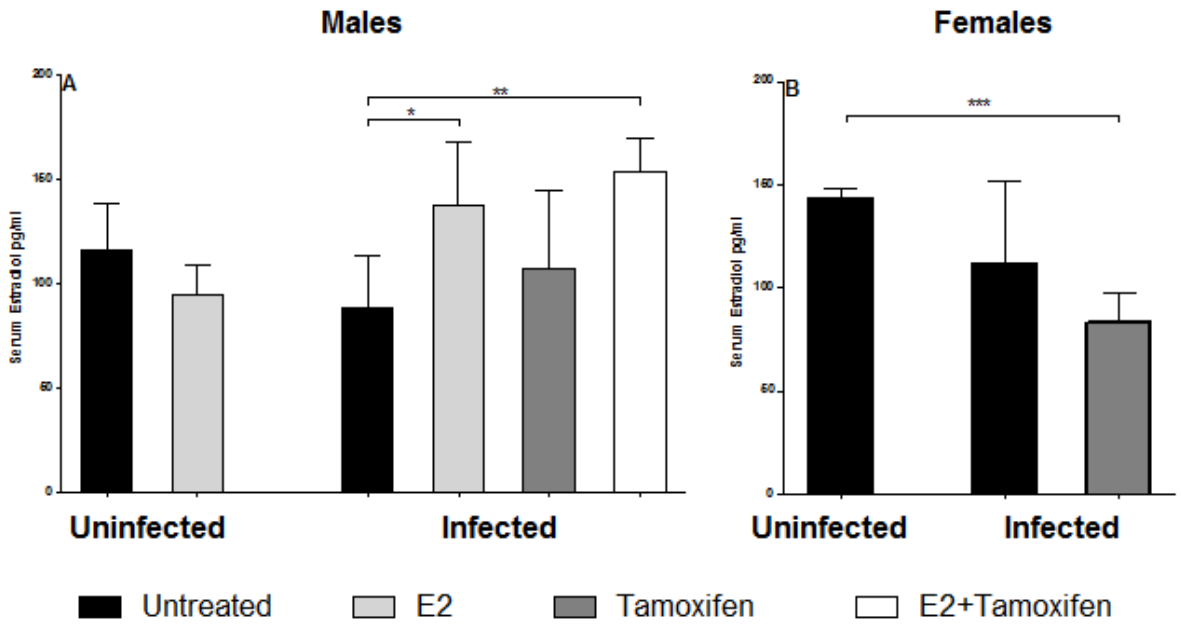

Figure 3.2. Serum E2 levels. A. Serum E2 levels were higher in *H. pylori*-infected male INS-GAS mice treated with E2 or E2 and TAM compared with untreated controls. B. Serum E2 levels in infected female mice were decreased by TAM treatment compared to uninfected untreated female mice. **P*<0.05, ***P*<0.01, ****P*<0.001. Error bars represent SD.

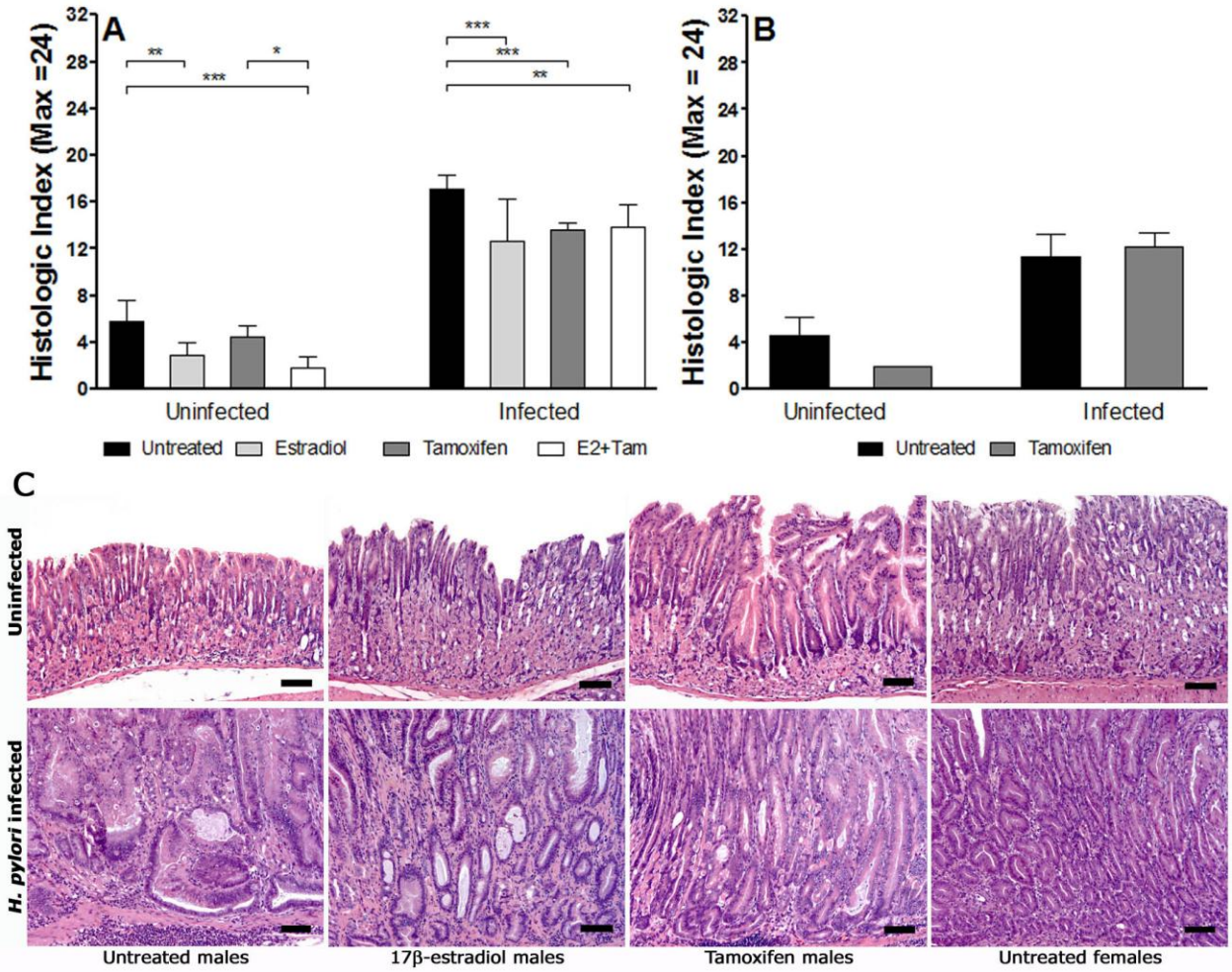

Figure 3.3. Corpus pathology after 28 weeks of *H. pylori* infection and 12 weeks of hormone treatment. A. In uninfected males, E2 and combination therapy reduced pathology compared to untreated mice. In infected male mice, E2, TAM and combination treatment reduced pathology compared to untreated mice. B. Gastric pathology in female mice was not affected by TAM treatment. **P*<0.05, ***P*<0.01, ****P*<0.001. Error bars represent SD. C. Representative H&E staining of corpus from uninfected and *H. pylori*-infected male and female mice from untreated, E2-treated or TAM-treated groups. Scale bar = 200µm.

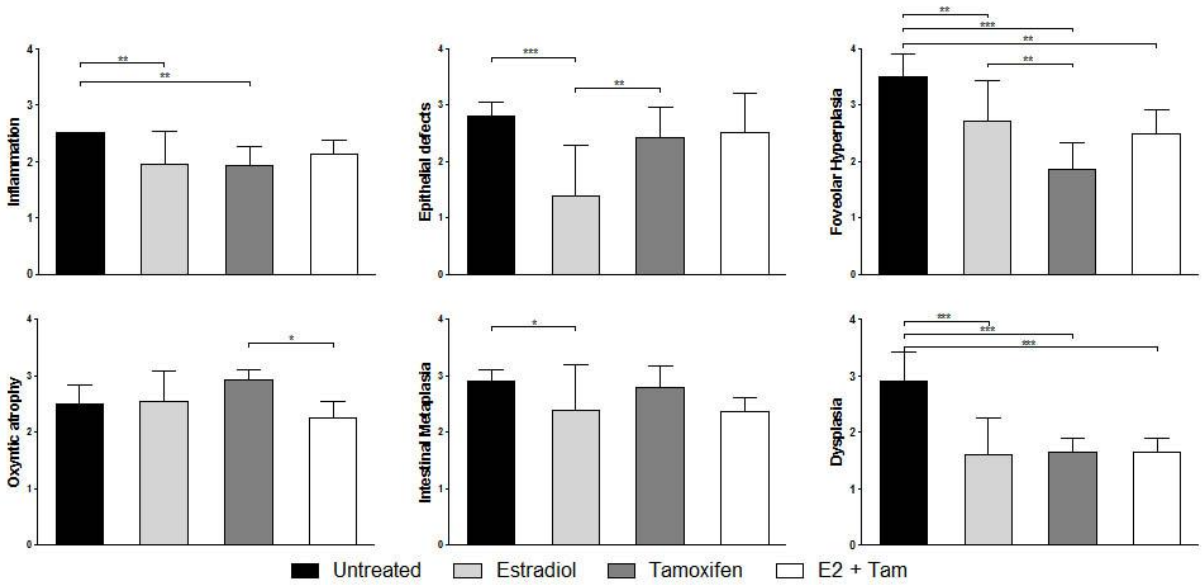

Figure 3.4. Individual histological parameters of corpus pathology after 28 weeks of *H. pylori* infection and 12 weeks of hormone treatment in infected male mice. **P*<0.05, ***P*<0.01, ****P*<0.001. Error bars represent SD.

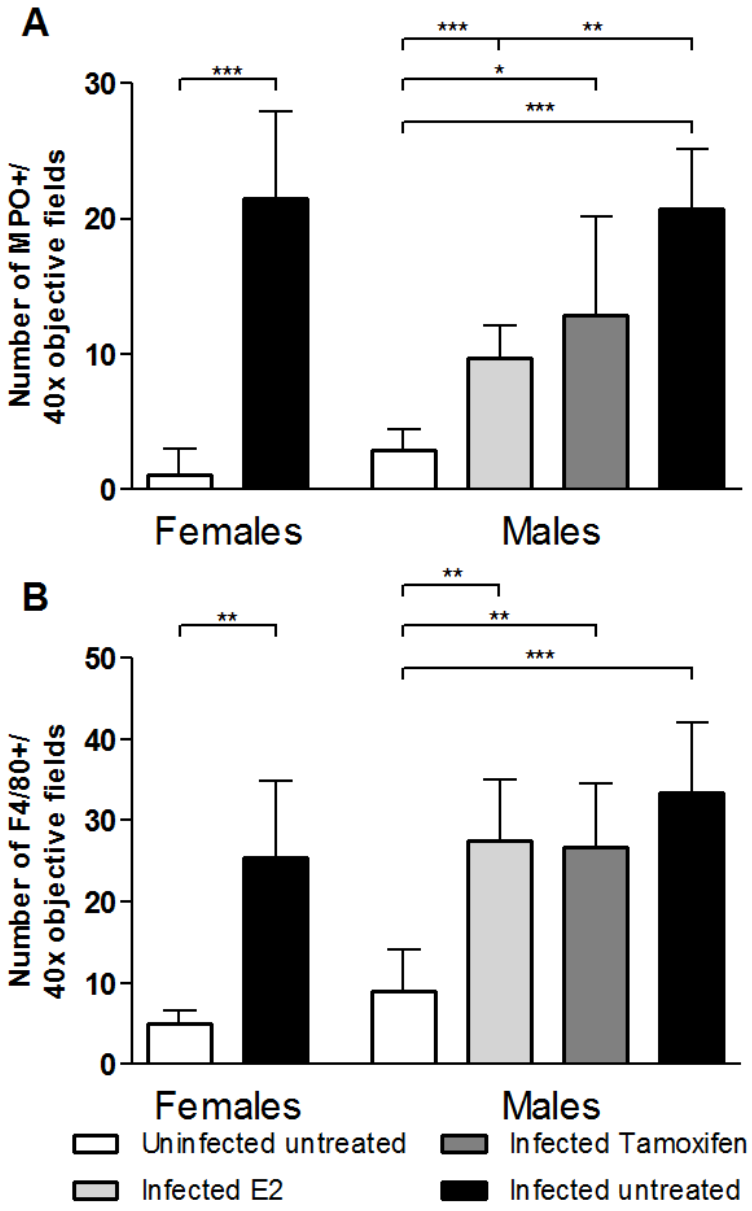

Figure 3.5. Immune cell infiltration of A) MPO+ neutrophils and B) F4/80+ macrophages. Error bars represent SD.

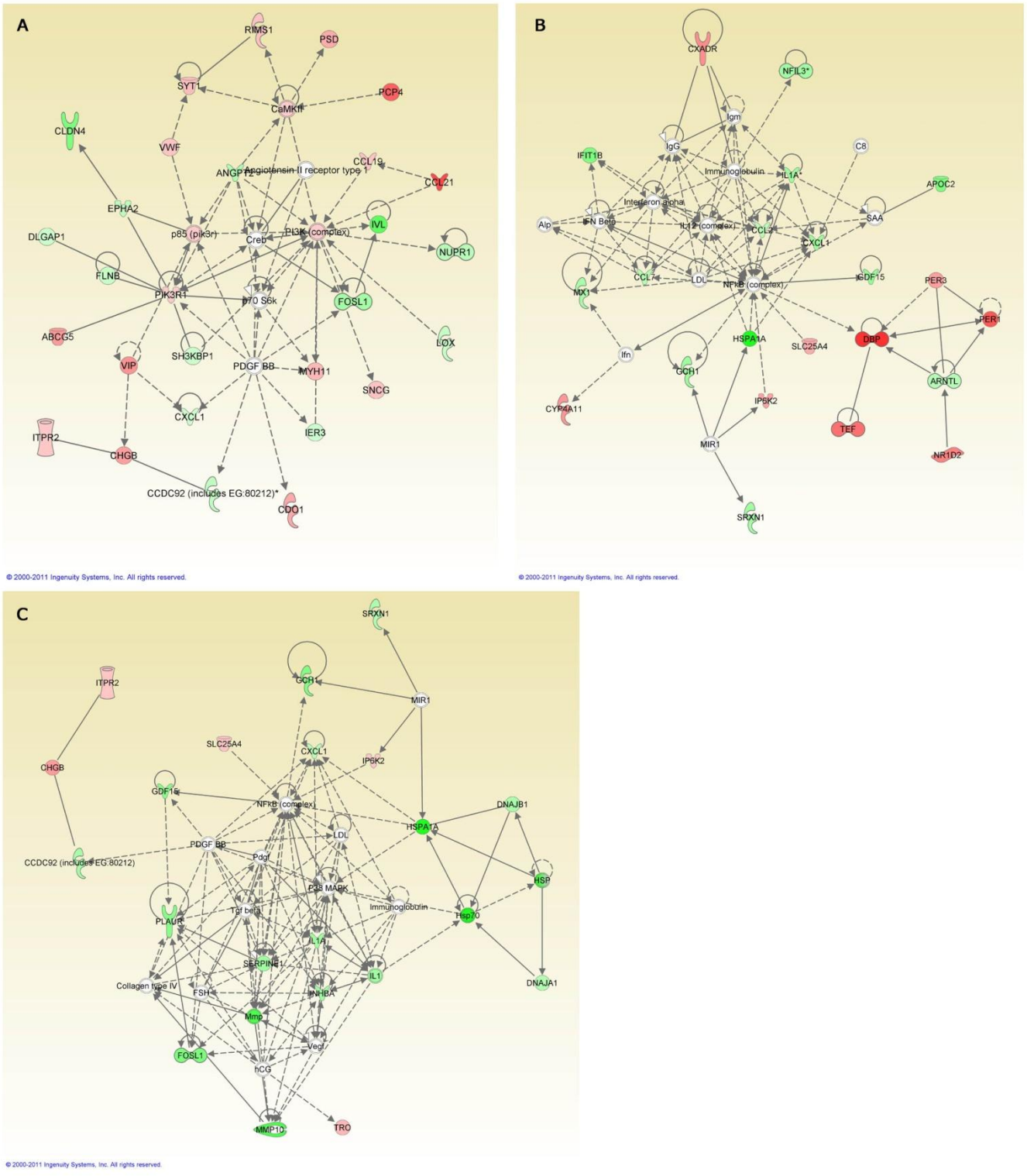

Figure 3.6. Significant molecular networks affected by hormone treatment. Networks display interactions using the gene targets of A. E2 (P=10^{-50}), B. TAM (P=10^{-45}), C. common genes between E2 and TAM (P=10^{-45}). P-values represent the probability of these interactions occurring by chance.

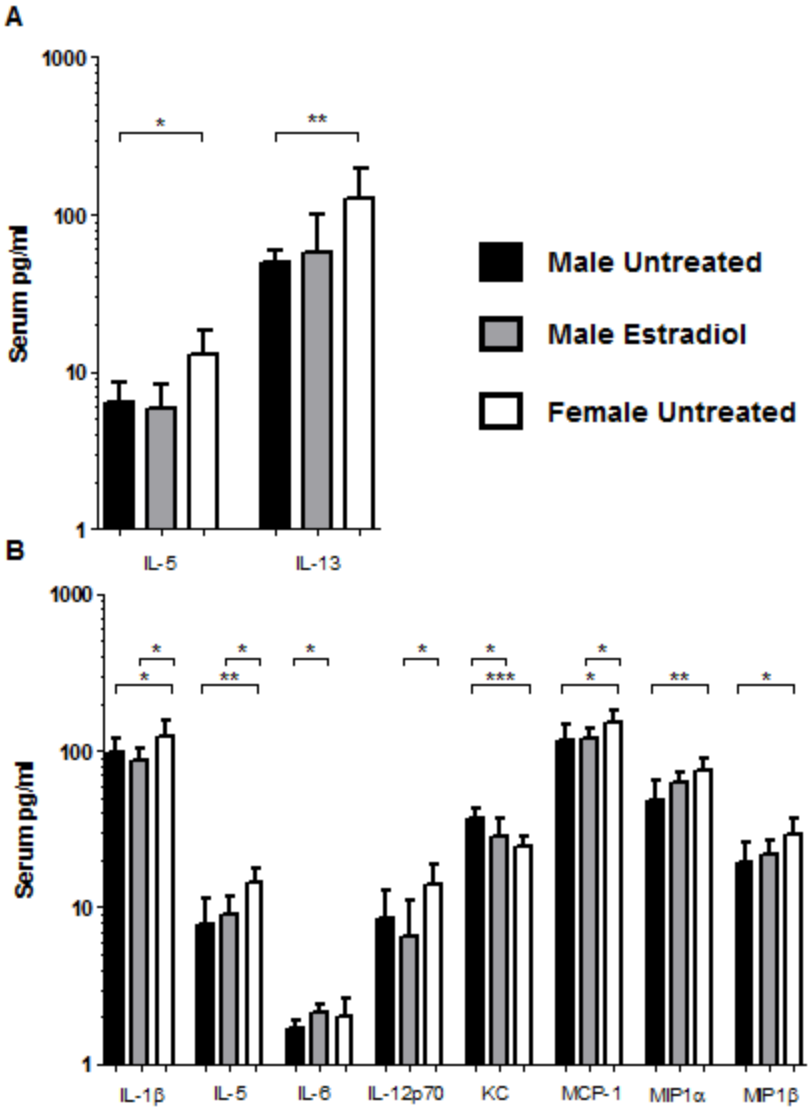

Figure 3.7. Serum levels of cytokines and chemokines in A) uninfected and B) *H. pylori*-infected untreated males, E2 males and untreated females. IL-5 and IL-13 were differentially expressed in uninfected females compared to uninfected males with placebo. IL-1β, IL-5, IL-6, IL-12p70, KC, MCP-1, MIP1α and MIP1β were differentially expressed during infection. **P*<0.05, ***P*<0.01, ****P*<0.001. Error bars represent SD.

3.7 Supplemental Tables

Supplemental Table legends

Table 3.S1. Genes differentially expressed by treatment. A. 169 downregulated and 194 upregulated genes in infected E2 male mice compared to infected untreated male mice. B. 69 downregulated and 75 upregulated genes in infected TAM male mice compared to infected untreated male mice. C. 24 downregulated and 37 upregulated genes in both infected E2 and TAM male mice compared to infected untreated male mice.

Table 3.S2. Networks associated to differentially expressed genes by Ingenuity Pathway Analysis. Genes in capital letters represent differentially expressed genes found within the network. A. Top networks associated with E2 treatment of infected male mice. B. Top networks associated with TAM treatment of infected male mice. C. Top 3 networks associated with commonly induced genes in both E2 and TAM treatments.

Table 3.S3. Biological functions and canonical pathways associated with E2 treatment of infected males and genes associated with function or pathway. A. Diseases and disorders. B. Molecular and Cellular functions. C. Physiological System and Development and Functions. D. Canonical pathways.

Table 3.S4. Biological functions and canonical pathways associated with TAM treatment of infected males and genes associated with function or pathway. A. Diseases and disorders. B. Molecular and Cellular functions. C. Physiological System and Development and Functions. D. Canonical pathways.

Table 3.S5. Biological functions and canonical pathways associated with both E2 and TAM treatment of infected males and genes associated with function or pathway. A. Diseases and disorders. B. Molecular and Cellular functions. C. Physiological System and Development and Functions. D. Canonical pathways.

Table 3.S6. Individual histological parameters in the corpus and antrum at 16 and 28 weeks of *H. pylori* infection. A) Corpus pathology at 16 WPI. B) Corpus pathology at 28 WPI. C) Antrum pathology at 16 WPI. D) Antrum pathology at 28 WPI.

Table 3.S1A. Genes downregulated by E2 treatment

Probe set ID	Gene symbol	Gene title	Log2change	p-value	q-value
A_51_P430259	1700009P17Rik	RIKEN cDNA 1700009P17 gene	-0.70	0.029	0.000
A_51_P225493	1700016C15Rik	RIKEN cDNA 1700016C15 gene	-0.79	0.020	0.000
A_51_P450278	2010003K11Rik	RIKEN cDNA 2010003K11 gene	-0.73	0.018	0.000
A_51_P334318	2010110P09Rik	RIKEN cDNA 2010110P09 gene	-0.87	0.013	0.000
A_51_P281778	2210010C17Rik	RIKEN cDNA 2210010C17 gene	-0.62	0.017	0.000
A_52_P321150	2310016C08Rik	RIKEN cDNA 2310016C08 gene	-0.71	0.004	0.000
A_52_P644479	4930523C07Rik	RIKEN cDNA 4930523C07 gene	-0.70	0.000	0.000
A_51_P445683	4931406C07Rik	RIKEN cDNA 4931406C07 gene	-0.64	0.000	0.000
A_52_P110070	5730416F02Rik	RIKEN cDNA 5730416F02 gene	-0.90	0.004	0.000
A_51_P394354	5730469M10Rik	RIKEN cDNA 5730469M10 gene	-1.03	0.001	0.000
A_52_P747842	9130204L05Rik	RIKEN cDNA 9130204L05 gene	-1.27	0.009	0.000
A_51_P118400	9130404H23Rik	RIKEN cDNA 9130404H23 gene	-1.32	0.029	0.000
A_51_P456113	9930013L23Rik	RIKEN cDNA 9930013L23 gene	-0.75	0.041	0.000
A_52_P349091	A930001A20Rik	RIKEN cDNA A930001A20 gene	-0.82	0.001	0.000
A_51_P116419	Abcc5	ATP-binding cassette, sub-family C (CFTR/MRP), member 5	-0.62	0.004	0.000
A_52_P157450	Abhd1	abhydrolase domain containing 1	-0.71	0.012	0.000
A_51_P440584	Abhd2	abhydrolase domain containing 2	-0.71	0.002	0.000
A_51_P213515	Acnat2	acyl-coenzyme A amino acid N-acyltransferase 2	-1.54	0.004	0.000
A_52_P150851	Adamts12	a disintegrin-like and metallopeptidase (reprolysin type) with thrombospondin type 1 motif, 12	-0.79	0.041	0.000
A_51_P233797	Adh7	alcohol dehydrogenase 7 (class IV), mu or sigma polypeptide	-1.09	0.039	0.000
A_51_P510891	Afp	alpha fetoprotein	-0.77	0.008	0.000
A_52_P87843	Aldh1a3	aldehyde dehydrogenase family 1, subfamily A3	-0.75	0.039	0.000
A_51_P423813	Alpi	alkaline phosphatase, intestinal	-1.93	0.027	0.000
A_52_P368690	Amica1	adhesion molecule, interacts with CXADR antigen 1	-0.64	0.023	0.000
A_51_P201982	Angpt2	angiopoietin 2	-1.00	0.039	0.000
A_51_P338443	Angptl4	angiopoietin-like 4	-1.55	0.014	0.000
A_51_P318618	Anks4b	ankyrin repeat and sterile alpha motif domain containing 4B	-0.62	0.039	0.000
A_52_P620345	Ano10	anoctamin 10	-0.65	0.019	0.000
A_52_P62037	Anxa2	annexin A2	-0.67	0.011	0.000
A_51_P334979	Apoc2	apolipoprotein C-II	-1.08	0.006	0.000
A_51_P503494	Arc	activity regulated cytoskeletal-associated protein	-0.83	0.014	0.000
A_51_P339305	Banp	BTG3 associated nuclear protein	-1.01	0.021	0.000
A_52_P26794	Basp1	brain abundant, membrane attached signal protein 1	-0.87	0.019	0.000
A_52_P575900	Bglap	bone gamma carboxyglutamate protein	-0.92	0.019	0.000
A_51_P167410	Bglap-rs1	bone gamma-carboxyglutamate protein, related sequence 1	-0.85	0.034	0.000
A_51_P213266	Bmp8a	bone morphogenetic protein 8a	-0.62	0.005	0.000
A_51_P488196	Bmper	BMP-binding endothelial regulator	-0.69	0.001	0.000
A_51_P273921	Capg	capping protein (actin filament), gelsolin-like	-0.69	0.014	0.000
A_51_P410430	Ccdc19	coiled-coil domain containing 19	-1.08	0.017	0.000
A_52_P349356	Ccdc92	coiled-coil domain containing 92	-0.67	0.002	0.000
A_51_P360165	Ccng2	cyclin G2	-0.73	0.008	0.000
A_52_P218470	Cdhr2	cadherin-related family member 2	-0.97	0.007	0.000
A_51_P367081	Cdk14	cyclin-dependent kinase 14	-0.93	0.009	0.000
A_51_P234927	Cdk3-ps	cyclin-dependent kinase 3, pseudogene	-0.64	0.009	0.000
A_51_P305843	Chordc1	cysteine and histidine-rich domain (CHORD)-containing, zinc-binding protein 1	-0.62	0.035	0.000
A_51_P199168	Cidea	cell death-inducing DNA fragmentation factor, alpha subunit-like effector A	-1.18	0.000	0.000
A_51_P356467	Cldn4	claudin 4	-1.64	0.024	0.000
A_51_P518001	Creb3l3	cAMP responsive element binding protein 3-like 3	-1.28	0.006	0.000
A_51_P511000	Cwh43	cell wall biogenesis 43 C-terminal homolog (S. cerevisiae)	-0.60	0.012	0.000
A_51_P363187	Cxcl1	chemokine (C-X-C motif) ligand 1	-0.61	0.007	0.000
A_52_P681592	Cybrd1	cytochrome b reductase 1	-0.64	0.003	0.000
A_52_P527775	Cyp2d10	cytochrome P450, family 2, subfamily d, polypeptide 10	-1.03	0.020	0.000
A_51_P247172	D19Ertd652e	DNA segment, Chr 19, ERATO Doi 652, expressed	-0.94	0.021	0.000
A_51_P208603	Dio2	deiodinase, iodothyronine, type II	-0.99	0.049	0.000
A_51_P520650	Dlgap1	discs, large (Drosophila) homolog-associated protein 1	-0.66	0.018	0.000

Table 3.S1A. Genes downregulated by E2 treatment (cont.)

Probe set ID	Gene symbol	Gene title	Log2 change	p-value	q-value
A_51_P303346	Dnaja1	DnaJ (Hsp40) homolog, subfamily A, member 1	-0.65	0.020	0.000
A_51_P153486	Dnajb1	DnaJ (Hsp40) homolog, subfamily B, member 1	-0.75	0.002	0.000
A_52_P141608	E030010A14Rik	RIKEN cDNA E030010A14 gene	-0.65	0.015	0.000
A_51_P462918	Ehhadh	enoyl-Coenzyme A, hydratase/3-hydroxyacyl Coenzyme A dehydrogenase	-0.77	0.010	0.000
A_51_P156222	Elfn1	leucine rich repeat and fibronectin type III, extracellular 1	-0.75	0.027	0.000
A_52_P120037	Emp1	epithelial membrane protein 1	-1.14	0.009	0.000
A_51_P505823	Endod1	endonuclease domain containing 1	-0.73	0.038	0.000
A_52_P518997	Epha2	Eph receptor A2	-0.81	0.036	0.000
A_52_P423424	Ero1l	ERO1-like (S. cerevisiae)	-0.67	0.003	0.000
A_51_P236846	F3	coagulation factor III	-1.02	0.008	0.000
A_51_P336830	Fabp4	fatty acid binding protein 4, adipocyte	-1.06	0.025	0.000
A_52_P19532	Fgd3	FYVE, RhoGEF and PH domain containing 3	-1.02	0.022	0.000
A_52_P286970	Flnb	filamin, beta	-0.70	0.039	0.000
A_52_P476935	Flrt3	fibronectin leucine rich transmembrane protein 3	-0.74	0.030	0.000
A_51_P308796	Fosl1	fos-like antigen 1	-1.14	0.001	0.000
A_52_P501733	Ftl1	ferritin light chain 1	-0.73	0.021	0.000
A_52_P298002	Gch1	GTP cyclohydrolase 1	-0.76	0.000	0.000
A_52_P363216	Gcnt2	glucosaminyl (N-acetyl) transferase 2, I-branching enzyme	-0.60	0.034	0.000
A_52_P532982	Gdf15	growth differentiation factor 15	-1.02	0.001	0.000
A_52_P462657	Gm11545	predicted gene 11545	-1.49	0.000	0.000
A_52_P220933	Gm9758	predicted gene 9758	-1.00	0.000	0.000
A_52_P382067	Gpr55	G protein-coupled receptor 55	-0.65	0.013	0.000
A_51_P461684	Gprc5a	G protein-coupled receptor, family C, group 5, member A	-0.77	0.028	0.000
A_52_P432124	Gsta3	glutathione S-transferase, alpha 3	-0.71	0.009	0.000
A_51_P516133	Hist1h1c	histone cluster 1, H1c	-0.59	0.022	0.000
A_51_P501260	Hist1h1d	histone cluster 1, H1d	-0.83	0.004	0.000
A_51_P182358	Hist1h2bk	histone cluster 1, H2bk	-0.60	0.007	0.000
A_51_P449580	Hmga2-ps1	high mobility group AT-hook 2, pseudogene 1	-0.60	0.016	0.000
A_51_P116039	Hmgcs2	3-hydroxy-3-methylglutaryl-Coenzyme A synthase 2	-0.83	0.030	0.000
A_51_P465292	Hnmt	histamine N-methyltransferase	-0.64	0.020	0.000
A_51_P365152	Hs3st1	heparan sulfate (glucosamine) 3-O-sulfotransferase 1	-0.76	0.019	0.000
A_52_P132165	Hsd17b11	hydroxysteroid (17-beta) dehydrogenase 11	-0.65	0.006	0.000
A_52_P590154	Hsd17b6	hydroxysteroid (17-beta) dehydrogenase 6	-0.76	0.038	0.000
A_51_P117952	Hspa1a	heat shock protein 1A	-2.94	0.011	0.000
A_52_P304902	Hspa1b	heat shock protein 1B	-1.97	0.001	0.000
A_51_P286488	Ier3	immediate early response 3	-0.62	0.003	0.000
A_51_P516826	Igf2	insulin-like growth factor 2	-0.60	0.045	0.000
A_51_P438283	Il1a	interleukin 1 alpha	-0.82	0.001	0.000
A_51_P122321	Il33	interleukin 33	-1.03	0.033	0.000
A_51_P239750	Inhba	inhibin beta-A	-0.83	0.005	0.000
A_51_P413097	Ints2	integrator complex subunit 2	-0.87	0.038	0.000
A_52_P612019	Itga2	integrin alpha 2	-0.70	0.023	0.000
A_51_P475748	Ivl	involucrin	-2.05	0.010	0.000
A_52_P125429	Kif5c	kinesin family member 5C	-0.91	0.032	0.000
A_52_P445360	Krt20	keratin 20	-0.95	0.014	0.000
A_51_P167489	Lama3	laminin, alpha 3	-0.99	0.020	0.000
A_51_P174943	Lamc2	laminin, gamma 2	-0.71	0.007	0.000
A_51_P403564	Lhx5	LIM homeobox protein 5	-1.23	0.000	0.000
A_51_P300493	Lox	lysyl oxidase	-0.71	0.033	0.000
A_51_P257457	Ltbp2	latent transforming growth factor beta binding protein 2	-1.06	0.033	0.000
A_51_P368012	Mdfi	MyoD family inhibitor	-0.63	0.034	0.000
A_51_P390508	Mep1b	meprin 1 beta	-1.11	0.022	0.000
A_51_P266668	Mlec	malectin	-0.61	0.001	0.000
A_51_P120830	Mmp10	matrix metallopeptidase 10	-1.55	0.001	0.000
A_51_P184484	Mmp13	matrix metallopeptidase 13	-1.58	0.013	0.000

Table 3.S1A. Genes downregulated by E2 treatment (cont.)

Probe set ID	Gene symbol	Gene title	Log2 change	p-value	q-value
A_51_P255699	Mmp3	matrix metallopeptidase 3	-0.81	0.035	0.000
A_52_P46085	Mvp	major vault protein	-0.62	0.015	0.000
A_51_P268983	Myom3	myomesin family, member 3	-0.63	0.013	0.000
A_51_P505521	NA	NA	-0.79	0.025	0.000
A_52_P146513	NA	NA	-0.65	0.019	0.000
A_52_P299446	NA	NA	-0.60	0.002	0.000
A_52_P81677	NA	NA	-0.63	0.004	0.000
A_52_P382785	Npnt	nephronectin	-0.63	0.040	0.000
A_52_P359819	Ntf5	neurotrophin 5	-0.63	0.014	0.000
A_51_P519251	Nupr1	nuclear protein 1	-0.89	0.022	0.000
A_51_P253207	Osta	organic solute transporter alpha	-0.70	0.009	0.000
A_51_P280117	Padi2	peptidyl arginine deiminase, type II	-0.61	0.020	0.000
A_52_P37123	Pard6b	par-6 (partitioning defective 6) homolog beta (C. elegans)	-0.59	0.007	0.000
A_51_P450623	Phlda2	pleckstrin homology-like domain, family A, member 2	-0.61	0.016	0.000
A_52_P405465	Piga	phosphatidylinositol glycan anchor biosynthesis, class A	-0.82	0.001	0.000
A_52_P681310	Plaur	plasminogen activator, urokinase receptor	-0.89	0.011	0.000
A_52_P686218	Plb1	phospholipase B1	-0.66	0.001	0.000
A_51_P278163	Plcd3	phospholipase C, delta 3	-0.63	0.045	0.000
A_51_P258150	Plin2	perilipin 2	-0.60	0.020	0.000
A_51_P431107	Pmm1	phosphomannomutase 1	-0.79	0.046	0.000
A_51_P314669	Pnliprp2	pancreatic lipase-related protein 2	-1.39	0.006	0.000
A_51_P375783	Prap1	proline-rich acidic protein 1	-2.85	0.021	0.000
A_52_P540855	Prdx6	peroxiredoxin 6	-0.65	0.026	0.000
A_52_P467930	Prdx6-ps2	peroxiredoxin 6 pseudogene 2	-0.66	0.003	0.000
A_51_P155514	Prl	prolactin	-1.10	0.012	0.000
A_51_P312779	Prl2c3	prolactin family 2, subfamily c, member 3	-2.47	0.031	0.000
A_52_P511450	Prl2c5	prolactin family 2, subfamily c, member 5	-2.29	0.027	0.000
A_51_P146953	Ripply3	ripply3 homolog (zebrafish)	-1.03	0.045	0.000
A_51_P404377	Rnd2	Rho family GTPase 2	-0.66	0.041	0.000
A_51_P432288	Rnf183	ring finger protein 183	-0.80	0.049	0.000
A_51_P406105	Rps4y2	ribosomal protein S4, Y-linked 2	-0.82	0.019	0.000
A_51_P457989	Rragd	Ras-related GTP binding D	-0.91	0.019	0.000
A_52_P488427	Sec14l2	SEC14-like 2 (S. cerevisiae)	-0.67	0.045	0.000
A_51_P457481	Sectm1a	secreted and transmembrane 1A	-0.72	0.011	0.000
A_51_P183571	Serpine1	serine (or cysteine) peptidase inhibitor, clade E, member 1	-0.84	0.020	0.000
A_52_P411296	Sh3kbp1	SH3-domain kinase binding protein 1	-0.65	0.042	0.000
A_52_P196476	Slc11a2	solute carrier family 11 (proton-coupled divalent metal ion transporters), member 2	-0.63	0.024	0.000
A_51_P371311	Slc1a4	solute carrier family 1 (glutamate/neutral amino acid transporter), member 4	-0.63	0.002	0.000
A_51_P265444	Slc28a2	solute carrier family 28 (sodium-coupled nucleoside transporter), member 2	-1.10	0.040	0.000
A_52_P368057	Slc7a11	solute carrier family 7 (cationic amino acid transporter, y+ system), member 11	-0.67	0.034	0.000
A_51_P487487	Speer4d	spermatogenesis associated glutamate (E)-rich protein 4d	-0.61	0.015	0.000
A_52_P400436	Sphk1	sphingosine kinase 1	-0.69	0.007	0.000
A_52_P593200	Srxn1	sulfiredoxin 1 homolog (S. cerevisiae)	-0.67	0.025	0.000
A_51_P281333	St3gal6	ST3 beta-galactoside alpha-2,3-sialyltransferase 6	-0.87	0.001	0.000
A_52_P149380	St8sia6	ST8 alpha-N-acetyl-neuraminide alpha-2,8-sialyltransferase 6	-0.67	0.002	0.000
A_52_P189970	Stc1	stanniocalcin 1	-0.62	0.006	0.000
A_51_P162564	Tceanc	transcription elongation factor A (SII) N-terminal and central domain containing	-0.69	0.017	0.000
A_52_P426952	Tcf23	transcription factor 23	-0.68	0.001	0.000
A_51_P362298	Tmprss3	transmembrane protease, serine 3	-0.91	0.020	0.000
A_52_P351638	Tnfrsf10b	tumor necrosis factor receptor superfamily, member 10b	-0.62	0.023	0.000
A_52_P654161	Trim25	tripartite motif-containing 25	-0.62	0.001	0.000
A_51_P473277	Tspan6	tetraspanin 6	-0.78	0.006	0.000
A_52_P21	Ttc9	tetratricopeptide repeat domain 9	-0.89	0.000	0.000
A_51_P334689	Uts2	urotensin 2	-2.20	0.014	0.000
A_52_P281924	Vamp5	vesicle-associated membrane protein 5	-0.72	0.029	0.000

Table 3.S1A. Genes downregulated by E2 treatment (cont.)

Probe set ID	Gene symbol	Gene title	Log2 change	p-value	q-value
A_52_P278327	Vtcn1	V-set domain containing T cell activation inhibitor 1	-0.70	0.018	0.000
A_52_P537827	Wdr72	WD repeat domain 72	-0.88	0.013	0.000
A_52_P15536	Zfand2a	zinc finger, AN1-type domain 2A	-0.62	0.000	0.000
A_51_P190454	Zfp37	zinc finger protein 37	-0.70	0.002	0.000

Table 3.S1A. Genes upregulated by E2 treatment

Probe set ID	Gene symbol	Gene title	Log2 change	p-value	q-value
A_52_P947	2010007H06Rik	RIKEN cDNA 2010007H06 gene	0.79	0.035	0.000
A_52_P324391	2310058N22Rik	RIKEN cDNA 2310058N22 gene	0.59	0.018	0.000
A_51_P216268	2610001A08Rik	RIKEN cDNA 2610001A08 gene	0.80	0.009	0.000
A_52_P555537	2810008D09Rik	RIKEN cDNA 2810008D09 gene	0.65	0.025	0.000
A_51_P417251	6330403K07Rik	RIKEN cDNA 6330403K07 gene	0.62	0.000	0.000
A_52_P290152	6720401G13Rik	RIKEN cDNA 6720401G13 gene	0.74	0.001	0.000
A_52_P504859	A530020G20Rik	RIKEN cDNA A530020G20 gene	0.61	0.031	0.000
A_51_P256902	Abcg5	ATP-binding cassette, sub-family G (WHITE), member 5	1.17	0.020	0.000
A_52_P306305	Akap2	A kinase (PRKA) anchor protein 2	0.62	0.031	0.000
A_52_P58145	Aldh1a2	aldehyde dehydrogenase family 1, subfamily A2	1.43	0.010	0.000
A_51_P486681	Ap3b2	adaptor-related protein complex 3, beta 2 subunit	0.62	0.005	0.000
A_51_P383524	Art3	ADP-ribosyltransferase 3	1.09	0.009	0.000
A_52_P549985	Asb13	ankyrin repeat and SOCS box-containing 13	0.91	0.012	0.000
A_52_P276412	Atpif1	ATPase inhibitory factor 1	0.66	0.002	0.000
A_52_P12623	Bnipl	BCL2/adenovirus E1B 19kD interacting protein like	0.64	0.047	0.000
A_52_P337126	Bves	blood vessel epicardial substance	0.83	0.007	0.000
A_51_P110301	C3	complement component 3	0.85	0.050	0.000
A_51_P132849	Camk2g	calcium/calmodulin-dependent protein kinase II gamma	0.60	0.001	0.000
A_52_P208649	Cartpt	CART prepropeptide	1.62	0.009	0.000
A_51_P487518	Casp12	caspase 12	0.60	0.005	0.000
A_52_P306845	Cav1	caveolin 1, caveolae protein	0.61	0.038	0.000
A_51_P458258	Ccl19	chemokine (C-C motif) ligand 19	0.69	0.047	0.000
A_51_P129480	Ccl21a	chemokine (C-C motif) ligand 21A (serine)	2.11	0.008	0.000
A_51_P385718	Cd177	CD177 antigen	1.10	0.039	0.000
A_51_P489452	Cdo1	cysteine dioxygenase 1, cytosolic	0.99	0.025	0.000
A_52_P459143	Celf6	CUGBP, Elav-like family member 6	0.75	0.004	0.000
A_51_P413866	Cfb	complement factor B	0.86	0.018	0.000
A_51_P156955	Cfd	complement factor D (adipsin)	4.63	0.049	0.000
A_51_P191669	Chgb	chromogranin B	1.11	0.049	0.000
A_52_P674808	Chrdl1	chordin-like 1	0.62	0.030	0.000
A_51_P241319	Cilp	cartilage intermediate layer protein, nucleotide pyrophosphohydrolase	1.06	0.010	0.000
A_51_P265806	Clca2	chloride channel calcium activated 2	1.25	0.041	0.000
A_51_P189814	Cldn5	claudin 5	0.97	0.017	0.000
A_51_P141413	Clec10a	C-type lectin domain family 10, member A	0.60	0.001	0.000
A_52_P474902	Col20a1	collagen, type XX, alpha 1	0.61	0.021	0.000
A_51_P144160	Colec10	collectin sub-family member 10	1.22	0.012	0.000
A_51_P246001	Cpe	carboxypeptidase E	1.05	0.019	0.000
A_51_P284426	Cstad	CSA-conditional, T cell activation-dependent protein	0.61	0.023	0.000
A_51_P115953	Ctxn3	cortexin 3	1.04	0.002	0.000
A_51_P384187	Cxcl15	chemokine (C-X-C motif) ligand 15	1.08	0.029	0.000
A_51_P334104	Dcn	decorin	0.62	0.022	0.000
A_51_P335969	Des	desmin	0.92	0.047	0.000
A_52_P643375	Dmpk	dystrophia myotonica-protein kinase	1.02	0.030	0.000
A_52_P558259	Dtna	dystrobrevin alpha	0.62	0.050	0.000
A_51_P259029	Dusp26	dual specificity phosphatase 26 (putative)	0.89	0.002	0.000
A_51_P475378	Echdc3	enoyl Coenzyme A hydratase domain containing 3	0.88	0.003	0.000
A_51_P503722	Elavl4	ELAV (embryonic lethal, abnormal vision, Drosophila)-like 4 (Hu antigen D)	0.63	0.000	0.000
A_52_P303274	Epyc	epiphycan	1.85	0.023	0.000
A_51_P167562	Erdr1	erythroid differentiation regulator 1	0.84	0.039	0.000
A_51_P307979	Etv1	ets variant gene 1	0.63	0.013	0.000
A_51_P364391	Fam125b	family with sequence similarity 125, member B	0.59	0.014	0.000
A_51_P283473	Fibin	fin bud initiation factor homolog (zebrafish)	1.09	0.008	0.000
A_52_P644690	Flt3l	FMS-like tyrosine kinase 3 ligand	0.66	0.018	0.000
A_51_P301998	Fmo2	flavin containing monooxygenase 2	0.93	0.000	0.000
A_51_P287001	Fxyd1	FXYD domain-containing ion transport regulator 1	0.66	0.029	0.000

Table 3.S1A. Genes upregulated by E2 treatment (cont.)

Probe set ID	Gene symbol	Gene title	Log2 change	p-value	q-value
A_52_P472302	Fxyd6	FXYD domain-containing ion transport regulator 6	1.07	0.011	0.000
A_52_P217710	Fzd6	frizzled homolog 6 (Drosophila)	0.76	0.004	0.000
A_51_P462428	Galntl2	UDP-N-acetyl-alpha-D-galactosamine:polypeptide N-acetylgalactosaminyltransferase-like 2	0.83	0.001	0.000
A_51_P398766	Gbp1	guanylate binding protein 1	0.90	0.035	0.000
A_52_P675556	Ghrl	ghrelin	0.63	0.002	0.000
A_52_P22611	Gm106	predicted gene 106	0.72	0.023	0.000
A_51_P402583	Gpld1	glycosylphosphatidylinositol specific phospholipase D1	0.73	0.025	0.000
A_51_P152990	Grem2	gremlin 2 homolog, cysteine knot superfamily (Xenopus laevis)	0.66	0.026	0.000
A_51_P356055	Grp	gastrin releasing peptide	1.55	0.012	0.000
A_51_P150489	Gsdmc	gasdermin C	0.76	0.007	0.000
A_52_P87997	Gsdmc2	gasdermin C2	0.73	0.003	0.000
A_52_P498798	Gsdmc3	gasdermin C3	0.82	0.003	0.000
A_51_P249313	Herc3	hect domain and RLD 3	0.75	0.036	0.000
A_51_P124315	Hmcn2	hemicentin 2	1.63	0.000	0.000
A_51_P374571	Igfbp6	insulin-like growth factor binding protein 6	1.37	0.005	0.000
A_51_P215849	Il17b	interleukin 17B	0.73	0.026	0.000
A_52_P78033	Ip6k2	inositol hexaphosphate kinase 2	0.62	0.000	0.000
A_51_P364250	Itih5	inter-alpha (globulin) inhibitor H5	0.60	0.017	0.000
A_51_P147987	Itln1	intelectin 1 (galactofuranose binding)	1.51	0.011	0.000
A_51_P500056	Itpr2	inositol 1,4,5-triphosphate receptor 2	0.63	0.017	0.000
A_51_P338705	Kank1	KN motif and ankyrin repeat domains 1	0.92	0.017	0.000
A_52_P221776	Kif12	kinesin family member 12	0.87	0.001	0.000
A_51_P107020	Kif5a	kinesin family member 5A	0.70	0.006	0.000
A_51_P362698	Klhl24	kelch-like 24 (Drosophila)	0.64	0.026	0.000
A_52_P61273	Leng8	leukocyte receptor cluster (LRC) member 8	0.65	0.025	0.000
A_51_P218091	Lgr5	leucine rich repeat containing G protein coupled receptor 5	0.92	0.003	0.000
A_51_P151862	Lims2	LIM and senescent cell antigen like domains 2	0.76	0.006	0.000
A_51_P173692	Lingo4	leucine rich repeat and Ig domain containing 4	0.59	0.050	0.000
A_51_P429567	Lmod1	leiomodin 1 (smooth muscle)	0.79	0.012	0.000
A_52_P614207	LOC100047222	similar to anti-glycoprotein-B of human Cytomegalovirus immunoglobulin Vl chain	1.09	0.042	0.000
A_52_P49797	LOC100047599	similar to gag protein	1.01	0.003	0.000
A_52_P559957	Macrod1	MACRO domain containing 1	0.83	0.015	0.000
A_51_P451458	Mamdc2	MAM domain containing 2	0.65	0.010	0.000
A_52_P254908	Mcf2l	mcf.2 transforming sequence-like	0.60	0.021	0.000
A_51_P455997	Meg3	maternally expressed 3	1.26	0.030	0.000
A_52_P290211	Meis2	Meis homeobox 2	0.79	0.018	0.000
A_52_P414065	Mgl2	macrophage galactose N-acetyl-galactosamine specific lectin 2	0.64	0.003	0.000
A_51_P426270	Mgp	matrix Gla protein	0.99	0.006	0.000
A_51_P423290	Mmrn1	multimerin 1	0.99	0.025	0.000
A_51_P377620	Mnda	myeloid cell nuclear differentiation antigen	0.83	0.001	0.000
A_51_P206203	Mrgprf	MAS-related GPR, member F	0.72	0.048	0.000
A_51_P375538	Myb	myeloblastosis oncogene	0.61	0.017	0.000
A_51_P362429	Myh11	myosin, heavy polypeptide 11, smooth muscle	0.83	0.017	0.000
A_51_P308298	Myl9	myosin, light polypeptide 9, regulatory	1.03	0.011	0.000
A_52_P575217	Mylk	myosin, light polypeptide kinase	0.93	0.004	0.000
A_51_P122752	NA	NA	2.74	0.022	0.000
A_51_P208490	NA	NA	0.69	0.001	0.000
A_51_P227445	NA	NA	0.79	0.033	0.000
A_51_P266403	NA	NA	1.02	0.004	0.000
A_51_P418884	NA	NA	0.60	0.027	0.000
A_51_P461067	NA	NA	2.71	0.025	0.000
A_52_P1016836	NA	NA	0.65	0.001	0.000
A_52_P1054013	NA	NA	2.64	0.030	0.000
A_52_P186362	NA	NA	0.62	0.037	0.000
A_52_P308875	NA	NA	0.71	0.003	0.000

Table 3.S1A. Genes upregulated by E2 treatment (cont.)

Probe set ID	Gene symbol	Gene title	Log2 change	p-value	q-value
A_52_P346774	NA	NA	0.59	0.035	0.000
A_52_P474528	NA	NA	0.72	0.006	0.000
A_52_P483983	NA	NA	3.82	0.050	0.000
A_52_P575646	NA	NA	0.59	0.002	0.000
A_52_P65524	NA	NA	0.71	0.013	0.000
A_52_P739682	NA	NA	0.69	0.028	0.000
A_52_P236448	Ngfr	nerve growth factor receptor (TNFR superfamily, member 16)	0.63	0.014	0.000
A_51_P454873	Npy	neuropeptide Y	0.80	0.020	0.000
A_51_P296036	Nrbp2	nuclear receptor binding protein 2	0.76	0.004	0.000
A_51_P163953	Nsg2	neuron specific gene family member 2	0.60	0.004	0.000
A_52_P64783	Pabpn1	poly(A) binding protein, nuclear 1	0.65	0.000	0.000
A_51_P220422	Pacsin1	protein kinase C and casein kinase substrate in neurons 1	0.62	0.000	0.000
A_51_P171883	Palmd	palmdelphin	0.69	0.035	0.000
A_51_P253984	Pcp4	Purkinje cell protein 4	1.84	0.009	0.000
A_51_P361150	Pcp4l1	Purkinje cell protein 4-like 1	1.00	0.008	0.000
A_51_P157677	Pdlim3	PDZ and LIM domain 3	1.00	0.023	0.000
A_52_P586928	Pdyn	prodynorphin	0.69	0.012	0.000
A_51_P102987	Penk	preproenkephalin	1.40	0.002	0.000
A_51_P167313	Pgbd5	piggyBac transposable element derived 5	0.64	0.001	0.000
A_51_P451052	Pgm5	phosphoglucomutase 5	0.70	0.022	0.000
A_51_P182572	Phactr1	phosphatase and actin regulator 1	0.70	0.005	0.000
A_51_P357606	Phyhd1	phytanoyl-CoA dioxygenase domain containing 1	0.60	0.003	0.000
A_52_P407239	Pik3r1	phosphatidylinositol 3-kinase, regulatory subunit, polypeptide 1 (p85 alpha)	0.61	0.048	0.000
A_51_P337195	Pipox	pipecolic acid oxidase	0.73	0.004	0.000
A_51_P256632	Pla2g2a	phospholipase A2, group IIA (platelets, synovial fluid)	1.92	0.015	0.000
A_52_P94983	Pla2g5	phospholipase A2, group V	1.01	0.020	0.000
A_51_P141290	Plch2	phospholipase C, eta 2	0.66	0.006	0.000
A_51_P451588	Plekhb1	pleckstrin homology domain containing, family B (evectins) member 1	0.63	0.040	0.000
A_51_P495780	Plin4	perilipin 4	0.69	0.018	0.000
A_52_P340187	Pon2	paraoxonase 2	0.70	0.009	0.000
A_51_P224311	Popdc2	popeye domain containing 2	0.84	0.013	0.000
A_52_P576222	Ppl	periplakin	0.60	0.035	0.000
A_51_P220278	Ppp2r2b	protein phosphatase 2 (formerly 2A), regulatory subunit B (PR 52), beta isoform	1.20	0.000	0.000
A_51_P280455	Prg4	proteoglycan 4 (megakaryocyte stimulating factor, articular superficial zone protein)	1.20	0.025	0.000
A_51_P483280	Prnp	prion protein	0.76	0.013	0.000
A_51_P215438	Prodh	proline dehydrogenase	0.82	0.000	0.000
A_51_P251205	Psd	pleckstrin and Sec7 domain containing	0.99	0.021	0.000
A_52_P10793	Ptn	pleiotrophin	1.14	0.028	0.000
A_52_P11441	Rab6b	RAB6B, member RAS oncogene family	0.91	0.000	0.000
A_51_P394244	Rapgefl1	Rap guanine nucleotide exchange factor (GEF)-like 1	0.64	0.031	0.000
A_52_P557940	Rbm4b	RNA binding motif protein 4B	0.73	0.034	0.000
A_52_P574759	Rbpjl	recombination signal binding protein for immunoglobulin kappa J region-like	0.62	0.006	0.000
A_52_P269334	Rdh13	retinol dehydrogenase 13 (all-trans and 9-cis)	0.59	0.019	0.000
A_51_P365369	Reln	reelin	0.72	0.003	0.000
A_51_P257951	Retnla	resistin like alpha	2.40	0.020	0.000
A_51_P419768	Rgs2	regulator of G-protein signaling 2	0.70	0.023	0.000
A_52_P136782	Rgs5	regulator of G-protein signaling 5	0.64	0.027	0.000
A_52_P192462	Rims1	regulating synaptic membrane exocytosis 1	0.71	0.031	0.000
A_52_P470648	Rnf4	ring finger protein 4	0.61	0.001	0.000
A_51_P142421	Rspo1	R-spondin homolog (Xenopus laevis)	1.41	0.005	0.000
A_51_P444264	Rtn1	reticulon 1	0.61	0.002	0.000
A_51_P221223	Scg5	secretogranin V	0.68	0.012	0.000
A_51_P213691	Scnn1a	sodium channel, nonvoltage-gated 1 alpha	0.61	0.000	0.000
A_51_P277336	Sdpr	serum deprivation response	0.60	0.008	0.000
A_52_P220573	Serpini1	serine (or cysteine) peptidase inhibitor, clade I, member 1	0.70	0.000	0.000

Table 3.S1A. Genes upregulated by E2 treatment (cont.)

Probe set ID	Gene symbol	Gene title	Log2 change	p-value	q-value
A_51_P520849	Sfrp2	secreted frizzled-related protein 2	2.31	0.000	0.000
A_51_P457196	Sfrp4	secreted frizzled-related protein 4	1.42	0.010	0.000
A_51_P108334	Slc25a4	solute carrier family 25 (mitochondrial carrier, adenine nucleotide translocator), member 4	0.65	0.004	0.000
A_51_P194415	Slco3a1	solute carrier organic anion transporter family, member 3a1	0.68	0.005	0.000
A_51_P423880	Smarcd3	SWI/SNF related, matrix associated, actin dependent regulator of chromatin, subfamily d, member 3	1.02	0.027	0.000
A_51_P118300	Sncg	synuclein, gamma	0.70	0.010	0.000
A_51_P369998	Sntg2	syntrophin, gamma 2	0.73	0.006	0.000
A_51_P210510	Sparcl1	SPARC-like 1	0.82	0.017	0.000
A_51_P140690	Stmn3	stathmin-like 3	0.75	0.001	0.000
A_51_P434332	Sycn	syncollin	0.63	0.004	0.000
A_51_P185593	Synm	synemin, intermediate filament protein	0.92	0.007	0.000
A_52_P948080	Synpo2	synaptopodin 2	0.68	0.025	0.000
A_52_P103929	Syt1	synaptotagmin I	0.76	0.001	0.000
A_52_P517683	Tagln	transgelin	0.84	0.041	0.000
A_51_P459944	Tcf21	transcription factor 21	0.71	0.019	0.000
A_52_P485573	Tef	thyrotroph embryonic factor	0.77	0.008	0.000
A_51_P194099	Thrsp	thyroid hormone responsive SPOT14 homolog (Rattus)	1.43	0.010	0.000
A_51_P175303	Tle2	transducin-like enhancer of split 2, homolog of Drosophila E(spl)	0.63	0.045	0.000
A_51_P365008	Tns1	tensin 1	0.62	0.034	0.000
A_51_P505530	Tnxb	tenascin XB	0.94	0.007	0.000
A_52_P315976	Tpm2	tropomyosin 2, beta	1.08	0.021	0.000
A_51_P246924	Tppp3	tubulin polymerization-promoting protein family member 3	0.93	0.035	0.000
A_52_P391624	Trnp1	TMF1-regulated nuclear protein 1	0.67	0.003	0.000
A_51_P433141	Tro	trophinin	0.79	0.023	0.000
A_52_P316712	Ttc19	tetratricopeptide repeat domain 19	0.61	0.002	0.000
A_51_P475049	Uchl1	ubiquitin carboxy-terminal hydrolase L1	0.89	0.013	0.000
A_51_P368313	Vip	vasoactive intestinal polypeptide	1.25	0.017	0.000
A_51_P103397	Vwf	Von Willebrand factor homolog	0.68	0.008	0.000
A_51_P462708	Wfdc15b	WAP four-disulfide core domain 15B	0.91	0.042	0.000

Table 3.S1B. Genes downregulated by Tamoxifen treatment

Probe set ID	Gene symbol	Gene title	Log2 change	p-value	q-value
A_52_P185119	2210010C17Rik	RIKEN cDNA 2210010C17 gene	-0.77	0.003	0.034
A_52_P670766	2210415F13Rik	RIKEN cDNA 2210415F13 gene	-0.67	0.014	0.045
A_52_P110070	5730416F02Rik	RIKEN cDNA 5730416F02 gene	-0.71	0.014	0.045
A_51_P394354	5730469M10Rik	RIKEN cDNA 5730469M10 gene	-0.71	0.045	0.049
A_51_P407660	9630033F20Rik	RIKEN cDNA 9630033F20 gene	-0.61	0.048	0.049
A_51_P456113	9930013L23Rik	RIKEN cDNA 9930013L23 gene	-0.82	0.045	0.049
A_52_P349091	A930001A20Rik	RIKEN cDNA A930001A20 gene	-0.64	0.011	0.045
A_51_P116421	Abcc5	ATP-binding cassette, sub-family C (CFTR/MRP), member 5	-0.59	0.028	0.045
A_52_P24280	Abhd2	abhydrolase domain containing 2	-0.60	0.001	0.034
A_52_P419455	Adora2b	adenosine A2b receptor	-0.70	0.013	0.045
A_51_P510891	Afp	alpha fetoprotein	-0.92	0.033	0.048
A_52_P620345	Ano10	anoctamin 10	-0.61	0.018	0.045
A_51_P165342	Anxa2	annexin A2	-0.68	0.026	0.045
A_51_P334979	Apoc2	apolipoprotein C-II	-1.15	0.041	0.049
A_52_P803082	Apol9a	apolipoprotein L 9a	-0.59	0.040	0.049
A_52_P267651	Arntl	aryl hydrocarbon receptor nuclear translocator-like	-0.65	0.049	0.049
A_51_P146044	Ccdc92	coiled-coil domain containing 92	-0.85	0.003	0.034
A_52_P249514	Ccl12	chemokine (C-C motif) ligand 12	-0.64	0.025	0.045
A_51_P286737	Ccl2	chemokine (C-C motif) ligand 2	-1.09	0.009	0.039
A_51_P436652	Ccl7	chemokine (C-C motif) ligand 7	-0.67	0.019	0.045
A_52_P637199	Chordc1	cysteine and histidine-rich domain (CHORD)-containing, zinc-binding protein 1	-0.76	0.027	0.045
A_51_P199168	Cidea	cell death-inducing DNA fragmentation factor, alpha subunit-like effector A	-1.02	0.006	0.036
A_51_P363187	Cxcl1	chemokine (C-X-C motif) ligand 1	-0.90	0.006	0.036
A_51_P509530	Cybrd1	cytochrome b reductase 1	-0.71	0.006	0.037
A_52_P232637	Dhh	desert hedgehog	-0.67	0.029	0.045
A_51_P208603	Dio2	deiodinase, iodothyronine, type II	-0.77	0.033	0.048
A_51_P303346	Dnaja1	DnaJ (Hsp40) homolog, subfamily A, member 1	-0.96	0.021	0.045
A_51_P153486	Dnajb1	DnaJ (Hsp40) homolog, subfamily B, member 1	-0.74	0.023	0.045
A_51_P308796	Fosl1	fos-like antigen 1	-0.93	0.009	0.040
A_51_P297579	Gch1	GTP cyclohydrolase 1	-0.87	0.009	0.040
A_52_P532982	Gdf15	growth differentiation factor 15	-0.96	0.021	0.045
A_52_P462657	Gm11545	predicted gene 11545	-1.09	0.009	0.039
A_52_P220933	Gm9758	predicted gene 9758	-0.89	0.008	0.039
A_52_P597775	Gprc5a	G protein-coupled receptor, family C, group 5, member A	-0.60	0.039	0.049
A_52_P304902	Hspa1b	heat shock protein 1B	-2.02	0.020	0.045
A_52_P652704	Hspa4l	heat shock protein 4 like	-0.72	0.023	0.045
A_51_P110455	Hsph1	heat shock 105kDa/110kDa protein 1	-1.28	0.043	0.049
A_51_P327751	Ifit1	interferon-induced protein with tetratricopeptide repeats 1	-1.14	0.025	0.045
A_52_P351116	Igf1	insulin-like growth factor 1	-0.68	0.015	0.045
A_52_P100926	Il1a	interleukin 1 alpha	-0.88	0.025	0.045
A_51_P239750	Inhba	inhibin beta-A	-0.74	0.041	0.049
A_51_P394728	Kti12	KTI12 homolog, chromatin associated (S. cerevisiae)	-0.59	0.028	0.045
A_51_P120830	Mmp10	matrix metallopeptidase 10	-1.22	0.020	0.045
A_51_P514085	Mx2	myxovirus (influenza virus) resistance 2	-0.77	0.045	0.049
A_52_P314181	NA	NA	-0.61	0.035	0.049
A_52_P374395	NA	NA	-0.59	0.045	0.049
A_51_P111492	Nfil3	nuclear factor, interleukin 3, regulated	-0.72	0.030	0.046
A_52_P359819	Ntf5	neurotrophin 5	-0.66	0.028	0.045
A_52_P455764	Pard6b	par-6 (partitioning defective 6) homolog beta (C. elegans)	-0.61	0.045	0.049
A_52_P405465	Piga	phosphatidylinositol glycan anchor biosynthesis, class A	-0.60	0.027	0.045
A_52_P681310	Plaur	plasminogen activator, urokinase receptor	-1.05	0.044	0.049
A_51_P314669	Pnliprp2	pancreatic lipase-related protein 2	-0.99	0.019	0.045
A_52_P467930	Prdx6-ps2	peroxiredoxin 6 pseudogene 2	-0.62	0.025	0.045
A_52_P252737	Rangap1	RAN GTPase activating protein 1	-0.59	0.013	0.045
A_51_P340699	Rasl11a	RAS-like, family 11, member A	-0.67	0.013	0.045

Table 3.S1B. Genes downregulated by Tamoxifen treatment (cont.)

Probe set ID	Gene symbol	Gene title	Log2 change	p-value	q-value
A_52_P59318	Rdh10	retinol dehydrogenase 10 (all-trans)	-0.61	0.044	0.049
A_51_P433127	Rdm1	RAD52 motif 1	-0.73	0.042	0.049
A_51_P457481	Sectm1a	secreted and transmembrane 1A	-0.73	0.021	0.045
A_52_P312102	Sema3g	sema domain, immunoglobulin domain (Ig), short basic domain, secreted, (semaphorin) 3G	-0.62	0.042	0.049
A_51_P183571	Serpine1	serine (or cysteine) peptidase inhibitor, clade E, member 1	-0.66	0.036	0.049
A_51_P213940	Sfn	stratifin	-0.59	0.044	0.049
A_51_P371311	Slc1a4	solute carrier family 1 (glutamate/neutral amino acid transporter), member 4	-0.68	0.003	0.034
A_52_P589268	Smg7	Smg-7 homolog, nonsense mediated mRNA decay factor (C. elegans)	-0.60	0.003	0.034
A_52_P381484	Spon2	spondin 2, extracellular matrix protein	-0.75	0.039	0.049
A_51_P330125	Srxn1	sulfiredoxin 1 homolog (S. cerevisiae)	-0.82	0.034	0.049
A_52_P116896	Tinagl1	tubulointerstitial nephritis antigen-like 1	-0.62	0.014	0.045
A_51_P325152	Trmt61a	tRNA methyltransferase 61 homolog A (S. cerevisiae)	-0.65	0.008	0.039
A_51_P473272	Tspan6	tetraspanin 6	-0.61	0.039	0.049
A_52_P21	Ttc9	tetratricopeptide repeat domain 9	-0.63	0.029	0.045

Table 3.S1B. Genes upregulated by Tamoxifen treatment

Probe set ID	Gene symbol	Gene title	Log2 change	p-value	q-value
A_51_P144801	2210403K04Rik	RIKEN cDNA 2210403K04 gene	0.73	0.005	0.036
A_52_P324391	2310058N22Rik	RIKEN cDNA 2310058N22 gene	0.61	0.044	0.049
A_51_P195862	6030487A22Rik	RIKEN cDNA 6030487A22 gene	0.63	0.049	0.049
A_52_P290152	6720401G13Rik	RIKEN cDNA 6720401G13 gene	0.73	0.026	0.045
A_51_P443946	9030607L20Rik	RIKEN cDNA 9030607L20 gene	0.62	0.043	0.049
A_51_P120066	9330151L19Rik	RIKEN cDNA 9330151L19 gene	0.60	0.007	0.039
A_51_P423804	9530010C24Rik	RIKEN cDNA 9530010C24 gene	0.71	0.049	0.049
A_52_P504859	A530020G20Rik	RIKEN cDNA A530020G20 gene	0.75	0.043	0.049
A_51_P239236	Acacb	acetyl-Coenzyme A carboxylase beta	0.75	0.021	0.045
A_52_P549985	Asb13	ankyrin repeat and SOCS box-containing 13	0.85	0.048	0.049
A_52_P83888	Cflar	CASP8 and FADD-like apoptosis regulator	0.61	0.025	0.045
A_51_P191669	Chgb	chromogranin B	0.65	0.005	0.036
A_51_P167292	Chi3l3	chitinase 3-like 3	1.12	0.024	0.045
A_52_P61903	Chka	choline kinase alpha	0.60	0.046	0.049
A_51_P486239	Clec3b	C-type lectin domain family 3, member b	0.61	0.042	0.049
A_51_P115953	Ctxn3	cortexin 3	0.73	0.020	0.045
A_51_P212308	Cxadr	coxsackie virus and adenovirus receptor	0.78	0.006	0.036
A_52_P257774	Cyp4a10	cytochrome P450, family 4, subfamily a, polypeptide 10	0.72	0.037	0.049
A_51_P346715	D4Wsu53e	DNA segment, Chr 4, Wayne State University 53, expressed	0.71	0.033	0.048
A_51_P180492	Dbp	D site albumin promoter binding protein	1.44	0.042	0.049
A_51_P468876	Dixdc1	DIX domain containing 1	0.66	0.002	0.034
A_51_P475378	Echdc3	enoyl Coenzyme A hydratase domain containing 3	0.73	0.041	0.049
A_52_P81533	F730002C09Rik	RIKEN cDNA F730002C09 gene	0.69	0.006	0.036
A_52_P356343	Fam13a	family with sequence similarity 13, member A	0.75	0.004	0.036
A_52_P231075	Fcrls	Fc receptor-like S, scavenger receptor	0.66	0.042	0.049
A_52_P217710	Fzd6	frizzled homolog 6 (Drosophila)	0.72	0.006	0.036
A_51_P462428	Galntl2	UDP-N-acetyl-alpha-D-galactosamine:polypeptide N-acetylgalactosaminyltransferase-like 2	0.62	0.020	0.045
A_51_P292073	Haghl	hydroxyacylglutathione hydrolase-like	0.60	0.002	0.034
A_51_P124315	Hmcn2	hemicentin 2	1.27	0.022	0.045
A_51_P476091	Hnrpdl	heterogeneous nuclear ribonucleoprotein D-like	0.64	0.033	0.048
A_52_P78033	Ip6k2	inositol hexaphosphate kinase 2	0.63	0.003	0.034
A_51_P500056	Itpr2	inositol 1,4,5-triphosphate receptor 2	0.75	0.047	0.049
A_52_P584058	Ivns1abp	influenza virus NS1A binding protein	0.62	0.048	0.049
A_51_P505689	Kifc2	kinesin family member C2	0.78	0.005	0.036
A_52_P118161	Lss	lanosterol synthase	0.63	0.027	0.045
A_52_P432464	Luc7l2	LUC7-like 2 (S. cerevisiae)	0.60	0.027	0.045
A_52_P391505	Meg3	maternally expressed 3	0.93	0.037	0.049
A_52_P4482	NA	NA	0.59	0.040	0.049
A_52_P891818	NA	NA	0.60	0.024	0.045
A_51_P432892	NA	NA	0.62	0.025	0.045
A_51_P208490	NA	NA	0.65	0.008	0.039
A_52_P963820	NA	NA	0.67	0.028	0.045
A_52_P739682	NA	NA	0.77	0.013	0.045
A_51_P279898	NA	NA	0.80	0.023	0.045
A_52_P287811	NA	NA	0.91	0.030	0.046
A_51_P234692	Neat1	nuclear paraspeckle assembly transcript 1 (non-protein coding)	0.71	0.008	0.039
A_51_P233727	Ng23	Ng23 protein	0.66	0.024	0.045
A_52_P303891	Nr1d2	nuclear receptor subfamily 1, group D, member 2	0.87	0.003	0.034
A_51_P296036	Nrbp2	nuclear receptor binding protein 2	0.66	0.014	0.045
A_52_P19606	Osbpl1a	oxysterol binding protein-like 1A	0.69	0.027	0.045
A_52_P64783	Pabpn1	poly(A) binding protein, nuclear 1	0.60	0.005	0.036
A_51_P361150	Pcp4l1	Purkinje cell protein 4-like 1	0.90	0.014	0.045
A_52_P239511	Pde1c	phosphodiesterase 1C	0.62	0.046	0.049
A_52_P79889	Per1	period homolog 1 (Drosophila)	1.17	0.033	0.048
A_51_P258493	Per3	period homolog 3 (Drosophila)	0.66	0.002	0.034

Table 3.S1B. Genes upregulated by Tamoxifen treatment (cont.)

Probe set ID	Gene symbol	Gene title	Log2 change	p-value	q-value
A_51_P150105	Ppnr	per-pentamer repeat gene	0.70	0.034	0.048
A_51_P220278	Ppp2r2b	protein phosphatase 2 (formerly 2A), regulatory subunit B (PR 52), beta isoform	0.76	0.035	0.049
A_51_P273433	Prkg2	protein kinase, cGMP-dependent, type II	0.60	0.044	0.049
A_52_P557940	Rbm4b	RNA binding motif protein 4B	0.91	0.017	0.045
A_52_P195772	Rbmx	RNA binding motif protein, X chromosome	0.72	0.024	0.045
A_52_P209527	Rgs11	regulator of G-protein signaling 11	0.89	0.029	0.045
A_51_P250590	Sbf2	SET binding factor 2	0.64	0.016	0.045
A_51_P319289	Sdr9c7	4short chain dehydrogenase/reductase family 9C, member 7	0.87	0.004	0.034
A_51_P520849	Sfrp2	secreted frizzled-related protein 2	1.25	0.008	0.039
A_51_P108334	Slc25a4	solute carrier family 25 (mitochondrial carrier, adenine nucleotide translocator), member 4	0.59	0.018	0.045
A_51_P296182	Slc43a2	solute carrier family 43, member 2	0.60	0.028	0.045
A_52_P326502	Sox21	SRY-box containing gene 21	0.69	0.003	0.034
A_52_P424308	Sybu	syntabulin (syntaxin-interacting)	0.60	0.048	0.049
A_52_P485573	Tef	thyrotroph embryonic factor	1.00	0.001	0.034
A_52_P115996	Thrap3	thyroid hormone receptor associated protein 3	0.65	0.028	0.045
A_51_P194099	Thrsp	thyroid hormone responsive SPOT14 homolog (Rattus)	0.77	0.020	0.045
A_51_P344770	Tnrc6b	trinucleotide repeat containing 6b	0.60	0.045	0.049
A_51_P433141	Tro	trophinin	0.64	0.027	0.045
A_52_P564625	Ube2b	ubiquitin-conjugating enzyme E2B, RAD6 homology (S. cerevisiae)	0.60	0.045	0.049
A_51_P402160	Zfp750	zinc finger protein 750	0.60	0.017	0.045

Table 3.S1C. Genes downregulated by both E2 and Tamoxifen treatment

Probe set ID	Gene symbol	Gene title
A_52_P110070	5730416F02Rik	RIKEN cDNA 5730416F02 gene
A_51_P394354	5730469M10Rik	RIKEN cDNA 5730469M10 gene
A_51_P456113	9930013L23Rik	RIKEN cDNA 9930013L23 gene
A_52_P349091	A930001A20Rik	RIKEN cDNA A930001A20 gene
A_51_P116419	Abcc5	ATP-binding cassette, sub-family C (CFTR/MRP), member 5
A_51_P510891	Afp	alpha fetoprotein
A_52_P620345	Ano10	anoctamin 10
A_51_P165342	Anxa2	annexin A2
A_51_P334979	Apoc2	apolipoprotein C-II
A_51_P146044	Ccdc92	coiled-coil domain containing 92
A_51_P305843	Chordc1	cysteine and histidine-rich domain (CHORD)-containing, zinc-binding protein 1
A_51_P199168	Cidea	cell death-inducing DNA fragmentation factor, alpha subunit-like effector A
A_51_P363187	Cxcl1	chemokine (C-X-C motif) ligand 1
A_52_P681592	Cybrd1	cytochrome b reductase 1
A_51_P208603	Dio2	deiodinase, iodothyronine, type II
A_51_P303346	Dnaja1	DnaJ (Hsp40) homolog, subfamily A, member 1
A_51_P153486	Dnajb1	DnaJ (Hsp40) homolog, subfamily B, member 1
A_51_P308796	Fosl1	fos-like antigen 1
A_51_P297579	Gch1	GTP cyclohydrolase 1
A_52_P532982	Gdf15	growth differentiation factor 15
A_52_P462657	Gm11545	predicted gene 11545
A_52_P220933	Gm9758	predicted gene 9758
A_52_P304902	Hspa1b	heat shock protein 1B
A_51_P438283	Il1a	interleukin 1 alpha
A_51_P239750	Inhba	inhibin beta-A
A_51_P120830	Mmp10	matrix metallopeptidase 10
A_52_P359819	Ntf5	neurotrophin 5
A_52_P405465	Piga	phosphatidylinositol glycan anchor biosynthesis, class A
A_51_P112405	Plaur	plasminogen activator, urokinase receptor
A_51_P314669	Pnliprp2	pancreatic lipase-related protein 2
A_52_P467930	Prdx6-ps2	peroxiredoxin 6 pseudogene 2
A_51_P457481	Sectm1a	secreted and transmembrane 1A
A_51_P183571	Serpine1	serine (or cysteine) peptidase inhibitor, clade E, member 1
A_51_P371311	Slc1a4	solute carrier family 1 (glutamate/neutral amino acid transporter), member 4
A_51_P330125	Srxn1	sulfiredoxin 1 homolog (S. cerevisiae)
A_51_P473272	Tspan6	tetraspanin 6
A_52_P21	Ttc9	tetratricopeptide repeat domain 9
A_52_P110070	5730416F02Rik	RIKEN cDNA 5730416F02 gene
A_51_P394354	5730469M10Rik	RIKEN cDNA 5730469M10 gene
A_51_P456113	9930013L23Rik	RIKEN cDNA 9930013L23 gene
A_52_P349091	A930001A20Rik	RIKEN cDNA A930001A20 gene

Table 3.S1C. Genes upregulated by both E2 and Tamoxifen treatment

Probe set ID	Gene symbol	Gene title
A_52_P324391	2310058N22Rik	RIKEN cDNA 2310058N22 gene
A_52_P290152	6720401G13Rik	RIKEN cDNA 6720401G13 gene
A_52_P504859	A530020G20Rik	RIKEN cDNA A530020G20 gene
A_52_P549985	Asb13	ankyrin repeat and SOCS box-containing 13
A_51_P191669	Chgb	chromogranin B
A_51_P115953	Ctxn3	cortexin 3
A_51_P475378	Echdc3	enoyl Coenzyme A hydratase domain containing 3
A_52_P217710	Fzd6	frizzled homolog 6 (Drosophila)
A_51_P462428	Galntl2	UDP-N-acetyl-alpha-D-galactosamine:polypeptide N-acetylgalactosaminyltransferase-like 2
A_51_P124315	Hmcn2	hemicentin 2
A_52_P78033	Ip6k2	inositol hexaphosphate kinase 2
A_51_P500056	Itpr2	inositol 1,4,5-triphosphate receptor 2
A_51_P208490	NA	NA
A_52_P739682	NA	NA
A_51_P296036	Nrbp2	nuclear receptor binding protein 2
A_52_P64783	Pabpn1	poly(A) binding protein, nuclear 1
A_51_P361150	Pcp4l1	Purkinje cell protein 4-like 1
A_51_P220278	Ppp2r2b	protein phosphatase 2 (formerly 2A), regulatory subunit B (PR 52), beta isoform
A_52_P557940	Rbm4b	RNA binding motif protein 4B
A_51_P520849	Sfrp2	secreted frizzled-related protein 2
A_51_P108334	Slc25a4	solute carrier family 25 (mitochondrial carrier, adenine nucleotide translocator), member 4
A_52_P485573	Tef	thyrotroph embryonic factor
A_51_P194099	Thrsp	thyroid hormone responsive SPOT14 homolog (Rattus)
A_51_P433141	Tro	Trophinin

Table 3.S2A. Top 5 Networks affected by E2

Associated Network Function	Molecules in Network	Score	# of molecules
Cardiovascular System Development and Function, Antigen Presentation, Cellular Function and Maintenance	ABCG5, Angiotensin II receptor type 1, ANGPT2, CaMKII, CCDC92 (includes EG:80212), CCL19, CCL21, CDO1, CHGB, CLDN4, Creb, CXCL2, DLGAP1, EPHA2, FLNB, FOSL1, IER3, ITPR2, IVL, LOX, MYH11, NUPR1, p70 S6k, p85 (pik3r), PCP4, PDGF BB, PI3K (complex), PIK3R1, PSD, RIMS1, SH3KBP1, SNCG, SYT1, VIP, VWF	50	28
Cell Death, Respiratory Disease, Cardiovascular Disease	ALDH1A3, APOC2, C3, C1q, CAMK2G, CDK14, CFB, CFD, CLEC10A, ETS, GCH1, GDF15, Growth hormone, Hemoglobin, IL33, IL-1R, IL17B, IP6K2, Ldh, MIR1, MYLK, NFkB (complex), PABPN1, PI3, PLIN2, Proinflammatory Cytokine, SAA, SCNN1A, SLC11A2, SLC25A4, SPHK1, SRXN1, TEF, TNFRSF10A (includes EG:8797), XDH	40	25
Behavior, Digestive System Development and Function, Cell-To-Cell Signaling and Interaction	CARTPT, Cytochrome c, Cytokeratin, DES, DTNA, EMP1, FABP4, GHRL, hCG, HIST1H1C, HIST1H1D (includes EG:3007), Histone H1, Histone h3, Insulin, Jnk, KIF5A, KIF5C, KRT20, MAP2K1/2, MCF2L, MEG3 (includes EG:17263), Mlc, MYB (includes EG:4602), MYL9 (includes EG:98932), PDYN, PP2A, PPP2R2B, PRL, RGS2, SFRP2, SFRP4, SNTG2, STC1, SYNM, TRO	38	25
Cell-To-Cell Signaling and Interaction, Renal and Urological System Development and Function, Embryonic Development	Akt, Alp, ANXA2, BGLAP, Calpain, CASP12 (includes EG:12364), Caspase, CAV1, Caveolin, Collagen Alpha1, DNAJA1, DNAJB1, E2f, HIST4H4, Histone h4, HSP, Hsp70, Hsp90, HSPA1A, INHBA, LTBP2, NGFR, PLAUR, PRAP1, PRNP, Raf, Rb, RNF4, SDPR, SEC14L2, SERPINE1, SPARCL1, TAGLN, Tgf beta, TRIM25	33	21
Connective Tissue Disorders, Genetic Disorder, Ophthalmic Disease	ANGPTL4, CELF6, CHP2, CIITA, CLDN4, CYP2D10, ERBB2, EXPI, FLRT3, FOXC2, FSTL3, GCNT2, HNF1A, HNMT, HSD17B6, IGFBP6, INS1, ITPR2, KIAA1199, KIF12, LAMC2, LTBP2, MIR24-1 (includes EG:407012), PAX4, PDHB, PDLIM4, PMM1, PRKCDBP, PRODH, RALB, SCG5, SDPR, SPARCL1, TGFB1, TGFBI	31	20

Table 3.S2B. Top 5 Networks affected by Tamoxifen

Associated Network Function	Molecules in Network	Score	# of molecules
Behavior, Nervous System Development and Function, Cellular Movement	Alp, APOC2, ARNTL, C8, CCL2, CCL7, CXADR, CXCL2, CYP4A11, DBP, GCH1, GDF15, HSPA1A, IFIT1B, Ifn, IFN Beta, IgG, Igm, IL12 (complex), IL1A, Immunoglobulin, Interferon alpha, IP6K2, LDL, MIR1, MX1, NFIL3, NFkB (complex), NR1D2, PER1, PER3, SAA, SLC25A4, SRXN1, TEF	45	22
Nutritional Disease, Organismal Injury and Abnormalities, Neurological Disease	ACACB, ADORA2B, ANXA2, APLNR, ARL2BP, ATXN1, BDKRB1, CCR4, CDC42EP5, CHADL (includes EG:150356), CYBRD1, F2RL3, FNBP1, GPRC5A, GTP, HMGB1L1, HNRPDL, iron, ITPR2, KIAA1199, LSS, MMP10, MSR1, PIGA, RBM7, RBMX, SEMA3G, SLC1A4, SLC43A2, SYBU, TARDBP, TCF3, TGFB1, TNF, ZFP36	32	17
Cellular Growth and Proliferation, Hematological System Development and Function, Nervous System Development and Function	Ap1, CCDC92 (includes EG:80212), CFLAR, CHGB, Collagen Alpha1, Collagen type IV, Collagen(s), Creb, ERK1/2, Fibrinogen, FOSL1, FSH, hCG, IGF1, INHBA, ITPR2, Laminin, Lh, MAP2K1/2, MMP10, NTF4, P38 MAPK, p70 S6k, Pdgf, PDGF BB, PLAUR, PP2A, PPP2R2B, PRKG2, SERPINE1, SMG7, Tgf beta, THRSP, TRO, Vegf	29	16
Cell Death, Dermatological Diseases and Conditions, Connective Tissue Disorders	ABL1, beta-carotene, beta-hydroxyisovaleric acid, C10ORF58, C12ORF5, CHD3, CHI3L3, DBP, FAM173A, HCN2, HMGB1L1, IK, IL6, IL1/IL6/TNF, IL1F8, IVNS1ABP, KIFC2, LUC7L2, MAN2A2, MIR103-1 (includes EG:406895), NEAT1 (includes EG:66961), NFKB1, NFKBIZ, OSBPL1A, PARD6B, PDE1C, PTEN, SOX21, TAC1, TERT, TNRC6B, TP53, TSPAN6, UBE2B, ZCCHC10	26	15
Cellular Compromise, Cell Morphology, Cellular Growth and Proliferation	A2M, ABHD2, ARNTL, ASB13, BAG1, CACNA1B, CARM1, CD7, CEBPA, CEBPG, CHORDC1, CTSL2, DNAJB4, DNAJC3, DNM1, FAM13A, FGR, GBP1 (includes EG:2633), GNAO1, GNB5, HIF1AN, HSP90AA1, LITAF, MEG3 (includes EG:17263), MFGE8, MIR124-1 (includes EG:406907), NOD1, PABPN1, PER3, PRL, RBM4B, RGS11, SECTM1, SFRP2, SMARCA4	21	12

Table 3.S2C. Top 3 Networks affected by both E2 and Tamoxifen

Associated Network Function	Molecules in Network	Score	# of molecules
Tumor Morphology, Cell Morphology, Hair and Skin Development and Function	CCDC92 (includes EG:80212), CHGB, Collagen type IV, CXCL2, DNAJA1, DNAJB1, FOSL1, FSH, GCH1, GDF15, hCG, HSP, Hsp70, HSPA1A, IL1, IL1A, Immunoglobulin, INHBA, IP6K2, ITPR2, LDL, MIR1, Mmp, MMP10, NFkB (complex), P38 MAPK, Pdgf, PDGF BB, PLAUR, SERPINE1, SLC25A4, SRXN1, Tgf beta, TRO, Vegf	45	19
Tissue Development, Cell Death, Drug Metabolism	ABCC5, ANXA2, APOC2, ASB13, BAG4, BAMBI, beta-estradiol, CASP3, CHORDC1, CIDEC, DNAJB4, DNM1, DPM2, FNBP1, GCHFR, HMCN1 (includes EG:83872), HNF4A, HSP90AA1, IL15, KIAA1199, lipoprotein lipase, PABPN1, PCP4L1, PIGA, RBM5, RBM4B, SFRP2, SLC1A4, ST13, TEF, TGFB1, TNF, TSPAN6, TTC9, ZFP36	36	16
Cell Signaling, Molecular Transport, Nucleic Acid Metabolism	13(S)-hydroxyoctadecadienoic acid, ADRB, AFP, Akt, APLNR, C10ORF58, CHGA, CIDEA, DIO2, DSPP, DUSP6, ELK4, ERK, ERK1/2, F2RL3, FZD6, gamma-linolenic acid, GDF15, Histone h3, IL1F8, Insulin, Jnk, lauric acid, Lh, Mac1, MAP3K8, Ncx, NTF4, Pkc(s), PPP2R2B, PPP2R2C, PRKAG1, TERT, THRSP, triiodothyronine, reverse	18	9

Table 3.S3A. Top Biological Functions affected by E2: Diseases and disorders

Biological Function	Molecules in Network	p-value	# of molecules
Cancer	ABCC5, AFP, ALDH1A2, ALDH1A3, ANGPT2, ANGPTL4, ANXA2, BNIPL, C3, C7ORF68, C8ORF84, CAPG, CAV1, CCL19, CCL21, CD177, CDK3, CFB, CFD, CLDN4, CLEC10A, CREB3L3, CXCL2, DCN, DLGAP1, DMPK, DNAJA1, DTNA, EHHADH, EMP1, EPHA2, ETV1, F3, FABP4, FLT3LG, FOSL1, FTL, GCH1, GDF15, GHRL, GPRC5A, GRP, HNMT, HSD17B6, HSD17B11, HSPA1A, IER3, IGF2, IL33, IL17B, IL1A, INHBA, ITGA2, ITIH5, ITLN1, KIAA1199, KRT20, LAMA3, LAMC2, LOX, MGP, MMP3, MMP10, MMP13, MYB (includes EG:4602), MYH11, NGFR, NOS1, NUPR1, PCP4, PDLIM3, PHLDA2, PIK3R1, PIPOX, PLA2G2A, PLAUR, PLEKHB1, PLIN2, POPDC2, PPL, PPP2R2B, PRL, PRNP, PTN, RBM4B, RELN, RETNLA, RGS2, RGS5, RTN1, SCG5, SDPR, SECTM1, SERPINE1, SFRP2, SFRP4, SLC1A4, SLC7A11, SMARCD3, SNCG, SPARCL1, SPHK1, STC1, STMN3, SYNPO2, TAGLN, TCF21, TNFRSF10A (includes EG:8797), TNS1, TNXB, TPM2, TRO, UCHL1, VTCN1, VWF	4.41E-07 - 2.18E-02	115
Reproductive System Disease	ABCC5, AFP, ALDH1A2, ALDH1A3, ANGPT2, ANXA2, APOBEC3B, BNIPL, C3, C7ORF68, C8ORF84, CAV1, CCL19, CCL21, CFB, CLDN4, CLEC10A, DCN, DLGAP1, DTNA, EPHA2, ETV1, F3, FABP4, FOSL1, GDF15, GHRL, GPRC5A, HSD17B6, IER3, IL1A, INHBA, ITLN1, KIAA1199, MGP, MMP3, NOS1, PENK, PIK3R1, PLAUR, PLEKHB1, PRL, RBM4B, SERPINE1, SFRP4, SLC1A4, SMARCD3, STC1, TNXB, TRO, UCHL1, VTCN1	3.82E-04 - 2.18E-02	52
Cardiovascular Disease	ABCC5, ABCG5, ADAMTS12, AMICA1, ANGPT2, ANGPTL4, ANO10, ANXA2, APOC2, ASB13, BGLAP, BMPER, C3, C9ORF71, CAMK2G, CARTPT, CAV1, CDK14, CFB, COLEC10, DES, DIO2, DTNA, F3, FABP4, FGD3, FLT3LG, FOSL1, FXYD6, GDF15, GHRL, HMP19, HNMT, IGF2, IL33, IL1A, ITGA2, ITIH5, ITPR2, KIAA1199, LIMS2, LTBP2, MAMDC2, MCF2L, MEIS2, MGP, MMP3, MYH11, MYLK, NGFR, NOS1, NTF4, PHACTR1, PLA2G5, PLA2G2A, PLEKHB1, PON2, PPL, PPP1R12B, PRL, PRNP, PRODH, RELN, RGS2, RGS5, RIMS1, SCNN1A, SERPINE1, SLC1A4, SNTG2, SYNPO2, SYT1, TNS1, TTC9, UTS2, VIP, VWF, WDR72, XDH	4.73E-04 - 2.18E-02	79
Organismal Injury and Abnormalities	ANGPT2, ANXA2, CAV1, F3, INHBA, ITGA2, LIMS2, NGFR, PLA2G2A, PRNP, SCNN1A, SERPINE1, SERPINI1, SPHK1, UTS2, VWF	4.73E-04 - 2.18E-02	16
Genetic Disorder	ABCG5, ALDH1A2, ALDH1A3, ANGPTL4, ANXA2, C3, CARTPT, CAV1, CFB, CHGB, CIDEA, CLDN5, CPE, DCN, DLGAP1, DTNA, ELAVL4, ETV1, FABP4, FLNB, FTL, FXYD1, FXYD6, GCH1, GDF15, GHRL, GPRC5A, HMGCS2, HSD17B6, IER3, IL1A, KIF5A, LAMA3, LAMC2, MMP13, MYH11, NGFR, NOS1, NPY, NTF4, PCP4, PIK3R1, PLAUR, PLEKHB1, PMM1, PRG4 (includes EG:10216), PRL, PRNP, PRODH, RELN, RTN1, SCG5, SERPINE1, SERPINI1, SLC1A4, SLC7A11, SMARCD3, SYT1, TNXB, UCHL1, XDH	5.30E-04 - 2.18E-02	61

Table 3.S3B. Top Biological Functions affected by E2: Molecular and Cellular functions

Biological Function	Molecules in Network	p-value	# of molecules
Cellular Movement	ABHD2, ANGPT2, ANGPTL4, ANXA2, C3, CARTPT, CAV1, CCL19, CCL21, CFB, CLDN4, CXCL2, CXCL15, DCN, DNAJA1, EPHA2, ETV1, F3, FABP4, FLNB, FLT3LG, FOSL1, GDF15, GHRL, GRP, IGF2, IGFBP6, IL33, IL1A, INHBA, ITGA2, LAMA3, LAMC2, LIMS2, LOX, LTBP2, MCF2L, MGP, MMP3, MMP10, MMP13, MYH11, MYLK, NGFR, NPY, NTF4, PARD6B, PENK, PIK3R1, PLA2G5, PLAUR, PON2, PRAP1, PRL, PRNP, PTN, RELN, RETNLA, SERPINE1, SFRP2, SFRP4, SNCG, SPHK1, STC1, STMN3, SYNM, TAGLN, TNFRSF10A (includes EG:8797), TNS1, UTS2, VIP, VTCN1, VWF, XDH	3.91E-09 - 2.02E-02	74
Cellular Development	ABCC5, ALDH1A2, ANGPTL4, ANXA2, BGLAP, BMPER, BNIPL, BVES, CAPG, CARTPT, CAV1, CCDC92 (includes EG:80212), CCL19, CDO1, CHRDL1, CXCL2, CXCL15, DCN, DES, DIO2, EPHA2, ERO1L, FABP4, FLT3LG, FOSL1, FTL, GDF15, GHRL, GRP, HSPA1A, IER3, IFI16, IGF2, IGFBP6, IL33, IL17B, IL1A, INHBA, ITGA2, IVL, LAMA3, LOX, MGP, MMP3, MMP13, MYB (includes EG:4602), MYH11, MYLK, NGFR, NTF4, PENK, PIGA, PIK3R1, PLAUR, PRG4 (includes EG:10216), PRL, PRNP, PTN, RELN, RETNLA, RGS2, SEC14L2, SERPINE1, SFRP2, SFRP4, SLC7A11, SMARCD3, SNCG, SPHK1, STC1, TCF21, TCF23, TRIM25, UCHL1, UTS2, VIP, XDH	7.48E-06 - 2.18E-02	77
Cell-To-Cell Signaling and Interaction	AFP, AMICA1, ANGPT2, ANXA2, C3, CARTPT, CAV1, CCL19, CCL21, CD177, CLDN4, CLDN5, CLEC10A, CXCL2, DCN, EPHA2, F3, FGD3, FLT3LG, GHRL, GRP, HS3ST1, IFI16, IGF2, IL33, IL1A, INHBA, ITGA2, ITLN1, LAMA3, LOX, MMP13, NGFR, NPY, NTF4, PARD6B, PENK, PIK3R1, PLA2G2A, PLAUR, PRL, PRNP, PTN, RELN, RETNLA, SERPINE1, STC1, TNFRSF10A (includes EG:8797), TNS1, VIP, VTCN1, VWF, XDH	8.25E-06 - 2.18E-02	53
Lipid Metabolism	ABCG5, ADH7, AFP, ALDH1A2, ALDH1A3, ANGPT2, ANGPTL4, ANXA2, APOC2, C3, CARTPT, CAV1, CFD, CIDEA, CPE, DNAJA1, DNAJB1, EHHADH, FABP4, GHRL, GREM2, GRP, IGF2, IL33, IL1A, INHBA, NGFR, NPY, OSTALPHA, PIK3R1, PLA2G5, PLA2G2A, PLCH2, PLIN2, PNLIPRP2, PON2, PRL, PRNP, RGS2, SCG5, SCNN1A, SEC14L2, SERPINE1, SPHK1, ST3GAL6, ST8SIA6, STC1, THRSP, TNXB, VIP, XDH	3.42E-05 - 2.18E-02	51
Molecular Transport	ABCG5, AFP, ANGPT2, ANGPTL4, ANXA2, C3, CAMK2G, CARTPT, CAV1, CCL19, CCL21, CFD, CIDEA, CPE, DCN, DIO2, DNAJB1, FABP4, FXYD1, GCH1, GHRL, GRP, IGF2, IL33, IL1A, INHBA, ITGA2, ITPR2, KRT20, LTBP2, MYB (includes EG:4602), NGFR, NOS1, NPY, OSTALPHA, PIK3R1, PLA2G5, PLA2G2A, PLAUR, PLIN2, PON2, PRL, PRNP, RGS2, SCG5, SCNN1A, SEC14L2, SERPINE1, SLC11A2, SPHK1, STC1, SYT1, UTS2, VIP, XDH	3.42E-05 - 2.18E-02	55

Table 3.S3C. Top Biological Functions affected by E2: Physiological System and Development and Function

Biological Function	Molecules in Network	p-value	# of molecules
Behavior	ARC, CARTPT, CCL21, GCH1, GHRL, GRP, HSPA1A, NGFR, NOS1, NPY, NTF4, PDYN, PENK, PLAUR, PRNP, RGS2, RIMS1,UCHL1	2.55E-05 - 1.90E-02	18
Organismal Development	ALDH1A2, ANGPT2, ANGPTL4, ANXA2, ATPIF1, C3, CARTPT, CAV1, EPHA2, F3, FABP4, FLNB, GCH1, GHRL, HSPA1A, IGF2, IGFBP6, IL17B, IL1A, INHBA, ITGA2, ITPR2, LOX, MEP1B, MMP3, MMP13, MYB (includes EG:4602), NOS1, NPY, NTF4, PIK3R1, PLAUR, PLCD3, PON2, PRL, RGS5, SCNN1A, SERPINE1, SPHK1, STC1, UTS2,VIP	4.52E-05 - 1.90E-02	42
Cardiovascular System Development and Function	ALDH1A2, ANGPT2, ANGPTL4, ANXA2, ATPIF1, C3, CARTPT, CAV1, CXCL15, DCN, DIO2, EMP1, EPHA2, F3, FABP4, GCH1, GHRL, GRP, IFI16, IGF2, IL17B, IL1A, INHBA, ITGA2, LOX, MGP, MMP3, MMP13, MYB (includes EG:4602), MYH11, NOS1, NPY, NUPR1, PIK3R1, PLAUR, PLCD3, PRL, PTN, RGS2, RGS5, SCNN1A, SERPINE1, SPHK1, STC1, UTS2, VIP, VWF	4.91E-05 - 1.90E-02	47
Embryonic Development	ALDH1A2, ALDH1A3, ANXA2, C3, CAV1, EPHA2, GRP, IGF2, INHBA, ITGA2, LIMS2, MYH11, NPNT, PIGA, PIK3R1, PLAUR, PRL, RELN, SFRP4, SPHK1, TCF21, TRO	9.18E-05 - 2.18E-02	22
Hair and Skin Development and Function	ANXA2, CAV1, HSPA1A, INHBA, PLAUR, RELN, SERPINE1	9.18E-05 - 8.86E-03	7

Table 3.S3D. Top Canonical Pathways affected by E2

Canonical Pathway	p-value
LPS/IL-1 Mediated Inhibition of RXR Function	4.43E-03
Coagulation System	4.90E-03
Role of Osteoblasts, Osteoclasts and Chondrocytes in Rheumatoid Arthritis	5.90E-03
Aldosterone Signaling in Epithelial Cells	8.99E-03
Atherosclerosis Signaling	1.11E-02

Table 3.S4A. Top Biological Functions affected by Tamoxifen: Diseases and disorders

Biological Function	Molecules in Network	p-value	# of molecules
Cancer	ABCC5, ADORA2B, AFP, ANXA2, C1ORF63, CCL2, CCL13, CFLAR, CLEC3B, CXADR, CXCL2, CYP4A11, DHH, DNAJA1, FOSL1, GCH1, GDF15, GPRC5A, HNRPDL, HSPA1A, IGF1, IL1A, INHBA, KIAA1199, KIFC2, MMP10, MX1, NFIL3, PER1, PLAUR, PPP2R2B, RBM4B, SECTM1, SERPINE1, SFN, SFRP2, SLC1A4, SPON2, TNRC6B, TRO, UBE2B	1.29E-05 - 1.60E-02	41
Hypersensitivity Response	CCL2, CCL7, CCL13, CHI3L3, PLAUR	2.86E-05 - 8.16E-03	5
Inflammatory Response	ABHD2, ADORA2B, ANXA2, ARNTL, CCL2, CCL7, CCL13, CHI3L3, CXCL2, HSPA1A, IGF1, IL1A, INHBA, MX1, NFIL3, PLAUR, SECTM1, SERPINE1, SPON2	6.15E-05 - 1.63E-02	19
Nutritional Disease	ACACB, ARNTL, CCL13, CIDEA, DIO2, GCH1, HSPA1A, IGF1, NTF4, SERPINE1	8.99E-05 - 1.18E-02	10
Organismal Injury and Abnormalities	CCL2, CCL13, CFLAR, IGF1, IL1A, INHBA, MX1, PLAUR, SERPINE1	1.04E-04 - 1.62E-02	9

Table 3.S4B. Top Biological Functions affected by Tamoxifen: Molecular and Cellular functions

Biological Function	Molecules in Network	p-value	# of molecules
Cellular Movement	ANXA2, CCL2, CCL7, CCL13, CHI3L3, CXCL2, DNAJA1, FOSL1, GDF15, IGF1, IL1A, INHBA, MMP10, MX1, NTF4, PLAUR, SERPINE1, SFRP2	1.51E-05 - 1.62E-02	18
Cell Morphology	ANXA2, CCL2, CCL7, CCL13, CXADR, CXCL2, DHH, FZD6, HSPA1A, IGF1, INHBA, NTF4, OSBPL1A, PARD6B, PIGA, PLAUR, SERPINE1, SFN	2.86E-05 - 1.41E-02	18
Cellular Development	ABCC5, CCDC92 (includes EG:80212), CCL2, CCL7, CCL13, CHKA, CXADR, CXCL2, DHH, DIO2, FOSL1, FZD6, GDF15, HSPA1A, IGF1, IL1A, INHBA, NTF4, PARD6B, PIGA, PLAUR, PRKG2, SERPINE1, SFN, SFRP2	2.86E-05 - 1.62E-02	25
Cell-To-Cell Signaling and Interaction	AFP, ANXA2, CCL2, CCL7, CCL13, CXADR, CXCL2, DHH, HSPA1A, IGF1, IL1A, INHBA, NTF4, PARD6B, PLAUR, SERPINE1, SPON2, SYBU, UBE2B	6.15E-05 - 1.63E-02	19
Antigen Presentation	ANXA2, ARNTL, CCL2, CCL7, CCL13, CXCL2, IGF1, IL1A, INHBA, PLAUR, SPON2	8.29E-05 - 8.16E-03	11

Table 3.S4C. Top Biological Functions affected by Tamoxifen: Physiological System and Development and Function

Biological Function	Molecules in Network	p-value	# of molecules
Hematological System Development and Function	ANXA2, ARNTL, CCL2, CCL7, CCL13, CFLAR, CHI3L3, CXCL2, CYP4A11, HSPA1A, IGF1, IL1A, INHBA, NFIL3, PLAUR, SERPINE1, SPON2	2.86E-05 - 1.63E-02	17
Tumor Morphology	GDF15, IGF1, IL1A, PLAUR, SERPINE1	2.86E-05 - 1.62E-02	5
Immune Cell Trafficking	ANXA2, CCL2, CCL7, CCL13, CHI3L3, CXCL2, HSPA1A, IGF1, IL1A, INHBA, PLAUR, SERPINE1, SPON2	6.15E-05 - 1.63E-02	13
Auditory and Vestibular System Development and Function	DIO2, IGF1	6.59E-05 - 8.16E-03	2
Organ Development	CCL13, DIO2, IGF1, INHBA	6.59E-05 - 1.37E-02	4

Table 3.S4D. Top Canonical Pathways affected by Tamoxifen

Canonical Pathway	**p-value**
LXR/RXR Activation	2.53E-03
Aldosterone Signaling in Epithelial Cells	4.76E-03
Role of Hypercytokinemia/hyperchemokinemia in the Pathogenesis of Influenza	1.62E-02
Chemokine Signaling	1.73E-02
Circadian Rhythm Signaling	2.03E-02

Table 3.S5A. Top Biological Functions affected by both E2 and Tamoxifen: Diseases and disorders

Biological Function	Molecules in Network	p-value	# of molecules
Cancer	ABCC5, AFP, ANXA2, CXCL2, DNAJA1, FOSL1, GCH1, GDF15, HSPA1A, IL1A, INHBA, KIAA1199, MMP10, PLAUR, PPP2R2B, RBM4B, SECTM1, SERPINE1, SFRP2, SLC1A4, TRO	1.89E-05 - 2.77E-02	21
Nutritional Disease	CIDEA, DIO2, GCH1, HSPA1A, NTF4, SERPINE1	5.28E-04 - 2.37E-02	6
Reproductive System Disease	ABCC5, AFP, ANXA2, FOSL1, GDF15, IL1A, INHBA, KIAA1199, PLAUR, SERPINE1, SLC1A4, TRO	5.45E-04 - 2.64E-02	12
Organismal Injury and Abnormalities	ANXA2, IL1A, INHBA, NTF4, PLAUR, SERPINE1	1.44E-03 - 2.56E-02	6
Genetic Disorder	ABCC5, ANO10, APOC2, ASB13, CIDEA, GCH1, GDF15, IL1A, ITPR2, KIAA1199, NTF4, SERPINE1, SLC1A4, SLC25A4, TTC9	2.44E-03 - 2.66E-02	15

Table 3.S5B. Top Biological Functions affected by both E2 and Tamoxifen: Molecular and Cellular functions

Biological Function	Molecules in Network	p-value	# of molecules
Cell Morphology	ANXA2, CXCL2, FOSL1, FZD6, GDF15, HSPA1A, IL1A, INHBA, NTF4, PIGA, PLAUR, SERPINE1	5.16E-05 - 3.13E-02	12
Cell-To-Cell Signaling and Interaction	ANXA2, CXCL2, HSPA1A, IL1A, INHBA, NTF4, PLAUR, SERPINE1	6.94E-05 - 2.92E-02	8
Cell Death	ABCC5, AFP, CIDEA, CXCL2, DNAJA1, DNAJB1, FOSL1, GDF15, HSPA1A, IL1A, INHBA, IP6K2, ITPR2, MMP10, NTF4, PIGA, PLAUR, PPP2R2B, RBM4B, SERPINE1, SFRP2, SLC25A4, SRXN1	1.06E-04 - 2.92E-02	23
Cellular Movement	ANXA2, CXCL2, DNAJA1, FOSL1, GDF15, IL1A, INHBA, MMP10, NTF4, PLAUR, SERPINE1, SFRP2	2.78E-04 - 3.06E-02	12
Drug Metabolism	ABCC5, AFP, ANXA2, DIO2, DNAJA1, DNAJB1, GCH1, IL1A, INHBA	2.78E-04 - 2.92E-02	9

Table 3.S5C. Top Biological Functions affected by both E2 and Tamoxifen: Physiological System and Development and Function

Biological Function	Molecules in Network	p-value	# of molecules
Tumor Morphology	GDF15, IL1A, PLAUR, SERPINE1, SFRP2	2.62E-06 - 2.56E-02	5
Hair and Skin Development and Function	ABCC5, ANXA2, CXCL2, FOSL1, HSPA1A, IL1A, INHBA, NTF4, PLAUR, SERPINE1	5.16E-05 - 2.83E-02	10
Embryonic Development	ABCC5, ANXA2, IL1A, INHBA, PIGA, PLAUR, SERPINE1, SFRP2	6.94E-05 - 1.84E-02	8
Endocrine System Development and Function	AFP, DIO2, DNAJA1, DNAJB1, IL1A, INHBA	3.70E-04 - 2.92E-02	6
Nervous System Development and Function	CXCL2, DIO2, GDF15, IL1A, INHBA, NTF4, PLAUR	4.23E-04 - 2.92E-02	7

Table 3.S5D. Top Canonical Pathways affected by both E2 and Tamoxifen

Canonical Pathway	p-value
Aldosterone Signaling in Epithelial Cells	1.48E-03
Coagulation System	6.19E-03
Wnt/b-catenin Signaling	2.12E-02
Dopamine Receptor Signaling	2.47E-02
LXR/RXR Activation	2.76E-02

Table 3.S6A. Corpus pathology scores at 16 WPI

Treatment	Count	Inflammation	Epithelial defects	Oxyntic atrophy	Foveolar hyperplasia	Intestinal metaplasia	Dysplasia	GHAI
Uninfected female	5	1.0 ± 0.0	0.3 ± 0.4	1.0 ± 0.0	2.6 ± 0.2	0.0 ± 0.0	0.2 ± 0.3	5.1 ± 0.5
Uninfected male	5	0.8 ± 0.3	0.9 ± 0.7	1.4 ± 0.2	2.0 ± 0.0	0.7 ± 0.7	0.7 ± 0.7	6.5 ± 1.8
Infected female	5	1.7 ± 0.3	0.7 ± 0.3	2.4 ± 0.4	3.5 ± 0.0	2.1 ± 0.2	1.0 ± 0.4	11.4 ± 1.2
Infected male	5	1.8 ± 0.3	1.7 ± 0.3	2.4 ± 0.4	3.2 ± 0.3	1.9 ± 0.7	1.2 ± 0.4	12.2 ± 1.9

Table 3.S6B. Corpus pathology scores at 28 WPI

Treatment	Count	Inflammation	Epithelial defects	Oxyntic atrophy	Foveolar hyperplasia	Intestinal metaplasia	Dysplasia	GHAI
Uninfected untreated male	12	0.8 ± 0.3	1.2 ± 0.7	1.2 ± 0.5	1.4 ± 0.5	0.3 ± 0.3	0.9 ± 0.4	5.8 ± 1.8
Uninfected estradiol male	10	0.6 ± 0.4	0.6 ± 0.5	0.5 ± 0.2	1.0 ± 0.5	0.1 ± 0.2	0.3 ± 0.3	3.0 ± 1.1
Uninfected Tamoxifen male	6	0.8 ± 0.3	0.9 ± 0.2	1.1 ± 0.6	0.9 ± 0.2	0.3 ± 0.3	0.6 ± 0.2	4.5 ± 0.9
Uninfected E2 + Tam male	7	0.4 ± 0.2	0.3 ± 0.3	0.3 ± 0.3	0.8 ± 0.5	0.0 ± 0.0	0.0 ± 0.0	1.8 ± 1.0
Infected untreated male	10	2.5 ± 0.0	2.8 ± 0.3	2.5 ± 0.3	3.5 ± 0.4	2.9 ± 0.2	2.9 ± 0.5	17.1 ± 1.2
Infected estradiol male	9	1.9 ± 0.6	1.4 ± 0.9	2.6 ± 0.5	2.7 ± 0.7	2.4 ± 0.8	1.6 ± 0.7	12.6 ± 3.7
Infected Tamoxifen male	7	1.9 ± 0.3	2.4 ± 0.5	2.9 ± 0.2	1.9 ± 0.5	2.8 ± 0.4	1.6 ± 0.2	13.6 ± 0.7
Infected E2 + Tam male	4	2.1 ± 0.3	2.5 ± 0.7	2.3 ± 0.3	2.5 ± 0.4	2.4 ± 0.3	2.1 ± 0.5	13.9 ± 1.9
Uninfected untreated female	9	0.8 ± 0.4	0.3 ± 0.4	1.3 ± 0.3	1.8 ± 0.7	0.0 ± 0.0	0.4 ± 0.2	4.6 ± 1.5
Uninfected Tamoxifen female	1	0.5	0.0	0.5	1.0	0.0	0.0	2.0
Infected untreated female	10	1.3 ± 0.3	0.9 ± 0.5	2.8 ± 0.4	2.3 ± 0.5	2.6 ± 0.6	1.6 ± 0.5	11.4 ± 1.9
Infected Tamoxifen female	9	1.6 ± 0.3	1.2 ± 0.8	2.9 ± 0.2	2.1 ± 0.3	2.8 ± 0.4	1.7 ± 0.4	12.2 ± 1.2

Table 3.S6C. Antrum pathology scores at 16 WPI

Treatment	Count	Inflammation	Epithelial defects	Hyperplasia	Dysplasia	GHAI
Uninfected female	5	0.0 ± 0.0	0.0 ± 0.0	0.7 ± 0.8	0.3 ± 0.3	1.0 ± 0.9
Uninfected male	5	0.1 ± 0.2	0.0 ± 0.0	0.6 ± 0.2	0.3 ± 0.3	1.0 ± 0.5
Infected female	5	0.4 ± 0.2	0.3 ± 0.3	1.3 ± 0.7	0.8 ± 0.6	2.8 ± 1.4
Infected male	5	0.3 ± 0.3	0.2 ± 0.3	1.1 ± 0.5	0.5 ± 0.4	2.1 ± 1.1

Table 3.S6D. Antrum pathology scores at 28 WPI

Treatment	Count	Inflammation	Epithelial defects	Hyperplasia	Dysplasia	GHAI
Uninfected untreated male	12	0.1 ± 0.2	0.0 ± 0.0	0.8 ± 0.3	0.6 ± 0.2	1.4 ± 0.4
Uninfected estradiol male	10	0.0 ± 0.0	0.0 ± 0.0	0.7 ± 0.2	0.5 ± 0.0	1.2 ± 0.2
Uninfected Tamoxifen male	6	0.0 ± 0.0	0.0 ± 0.0	0.7 ± 0.3	0.4 ± 0.2	1.1 ± 0.4
Uninfected E2 + Tam male	7	0.0 ± 0.0	0.0 ± 0.0	0.6 ± 0.2	0.4 ± 0.2	0.9 ± 0.3
Infected untreated male	10	0.7 ± 0.2	0.0 ± 0.0	1.1 ± 0.6	0.8 ± 0.3	2.5 ± 1.1
Infected estradiol male	9	0.0 ± 0.0	0.0 ± 0.0	0.3 ± 0.3	0.1 ± 0.2	0.4 ± 0.2
Infected Tamoxifen male	7	0.0 ± 0.0	0.0 ± 0.0	0.5 ± 0.3	0.1 ± 0.2	0.6 ± 0.4
Infected E2 + Tam male	4	0.1 ± 0.3	0.0 ± 0.0	0.6 ± 0.3	0.4 ± 0.3	1.1 ± 0.5
Uninfected untreated female	9	0.1 ± 0.2	0.0 ± 0.0	0.4 ± 0.2	0.4 ± 0.2	0.9 ± 0.2
Uninfected Tamoxifen female	1	0.0	0.0	0.5	0.5	1.0
Infected untreated female	10	0.4 ± 0.3	0.0 ± 0.0	0.8 ± 0.4	0.3 ± 0.3	1.5 ± 0.7
Infected Tamoxifen female	9	0.3 ± 0.3	0.0 ± 0.0	0.6 ± 0.4	0.2 ± 0.3	1.2 ± 0.6

Chapter 4: Summary

4.1 Summary

This thesis reported studies on gender effects on the pathogenesis of the carcinogenic bacterium *Helicobacter pylori*. To this end, two research goals were planned: 1) characterize the effect of gender, in response to *H. pylori* infection, on somatic mutations in *gpt* delta mice and 2) characterize the effect of estrogen and Tamoxifen, in response to *H. pylori* infection, on carcinogenesis in INS-GAS mice. The first research aim was to investigate if chronic *H. pylori* infection was associated with an increase in mutations in male and female *gpt* delta mice on a C57BL/6 background. Given the ability to detect point mutations and deletions with the *gpt* delta mouse and the robust inflammatory response to *H. pylori* in female C57BL/6 mice, a1.6-fold increase in mutation frequency was observed 12 months post infection in *H. pylori* infected female mice. This result confirmed the mutagenic effects of *H. pylori* infection and led to the realization that the strength of the immune response and the length of exposure are necessary for the induction of point mutations. Increased severity of gastric lesions were observed in female mice at 6 months post infection. Decreased counts of *H. pylori* were also observed in female mice at 6 and 12 months post infection, as well as an increased proinflammatory, Th1 response at 12 months post infection. Altogether, the increased gastric pathology, the decreased *H. pylori* counts and the increased Th1 response were indicative of a more robust immune response to the bacterium in female mice, seen previously in the literature[1], which caused more mutations. Sequencing analysis demonstrated that A:T to G:C transitions and G:C to T:A transversions were the mutations induced by *H. pylori*. The spectrum of mutations point toward oxidative damage as the underlying mechanism of mutagenesis, as had been noted in

other models of chronic inflammation[2] and human gastric cancers[3], indicating that the model closely recapitulates pathogenic processes in humans. Our results show a direct link between *H. pylori* infection, the severity of inflammation and the induction of mutations in C57BL/6 mice.

The second research aim was to characterize the effect of 17β-estradiol (E2) and Tamoxifen (TAM) treatment on *H. pylori*-induced carcinogenesis in INS-GAS FVB mice. INS-GAS mice develop gastric adenocarcinoma in a male-predominant manner making them an ideal mouse model to study the modulatory effects of E2 and TAM in male and female mice. This study led to the discovery of the protective effects of E2 and TAM in this model of gastric cancer, as both compounds prevented the formation of gastric carcinomas in *H. pylori*-infected male mice, and did not exacerbate disease in females. Indeed, this was a surprising result as epidemiological data indicated that TAM might promote the development of gastric cancer in postmenopausal women[4]. Global gene expression analysis revealed evidence of the role of deregulation of cellular movement and oncogenic pathways in mediating protection. Further investigation of the role of cellular movement demonstrated that CXCL1, a potent neutrophil chemokine, was downregulated by E2 or TAM treatment in infected male mice. Serum levels of CXCL1 were also decreased in infected E2 treated males as well as infected untreated females. The downregulation of gastric CXCL1 expression and the lower serum protein levels were supported by significant decreases in neutrophilic infiltration in infected E2-treated males, with a similar decreasing trend in infected TAM-treated males. These results suggest that estrogen signaling may mediate protection in infected males by downregulating trafficking of neutrophils reducing the inflammatory response to *H. pylori* and abrogating cancer formation in our model.

Analysis of genes associated with cancer that were affected by E2 and TAM treatment showed a common downregulation of the receptor for plasminogen activator, urokinase, or *PLAUR*, and several of its immediate regulators (*GDF15* and *SERPINE1*). *PLAUR* serves as a focal point of proteolytic activity during extracellular matrix (ECM) remodeling[5-6]. *PLAUR* overexpression has been associated with increased gastric cancer and poorer survival of gastric cancer patients due to its role in metastasis and invasion[5-7]. Therefore, E2 and TAM may prevent gastric carcinogenesis by decreasing aberrant ECM remodeling. As *PLAUR* is activated by β-catenin[8], genes involved in regulating Wnt/β-catenin signaling were explored. *SFRP2* and *FZD6*, two Wnt signaling repressors, were upregulated by E2 and TAM, suggestive of a possible interaction between estrogen signaling and the Wnt/β-catenin pathway. Further work is necessary to determine the role of *PLAUR* and its regulation by β-catenin. Our results demonstrated that E2 and TAM reduced gastric carcinogenesis in infected INS-GAS male mice by decreasing inflammatory cell recruitment and downregulating oncogenic pathways.

This thesis sought to characterize gender differences in *H. pylori*-mediated gastric cancer using mouse models in order to provide greater insights into inflammation-mediated carcinogenesis in humans. When working with mouse models it is necessary to keep in mind the advantages and disadvantages of the system while determining the translational potential of the data. This final section will attempt to summarize insights into the roles of gender, mutations, cancer, immune cell trafficking and hormone therapy in *H. pylori* pathogenesis gained through this thesis (Table 4.1).

In humans, *H. pylori* promotes male-predominant gastric cancer[9]. Different mouse models have different sexual dimorphisms in gastric disease, e.g. a stronger immune response

in female C57BL/6 mice and male-predominant carcinogenesis in INS-GAS mice. It is of great importance to adequately account for the role of gender in mouse models in relation to the hypothesis queried. The strength of the proinflammatory response, regardless of gender, is a better indicator of *H. pylori*-driven gastric disease in mice. In C57BL/6 mice, female mice had a stronger proinflammatory response to *H. pylori* and had an increased mutation frequency. The A:T to G:C and G:C to T:A mutations are among the top three mutations observed in the mutation spectra of human gastric cancers[3], indicating that the model closely recapitulated the immune response, pathogenic progression and mutation spectra observed in humans in spite of the female predominance in disease. This result is in agreement with current paradigms of gastric carcinogenesis in which *H. pylori* causes gastric cancer development in humans after decades of chronic inflammation. Dampening the proinflammatory response results in protection against gastric cancer in humans and animal models of *H. pylori* infection, as seen in the literature reviewing the antiinflammatory effect of parasitic coinfection[10-11]. E2 and TAM treatment mediated the dampening of the proinflammatory response by deregulating neutrophilic infiltration via CXCL1, which led to prevention of gastric adenocarcimona in the model. Increases in both IL-8 and CXCL1 have been associated to increased gastric cancer incidence in humans[12-15], corroborating the importance of this pathway, and immune cell recruitment, in gastric carcinogenesis. Although the mechanisms by which E2 mediates protection in humans have not been fully clarified, studies in INS-GAS mice have highlighted the importance of decreasing proinflammatory cytokines like IL-1β and increasing antiinflammatory cytokines like IL-10[16-17], as well as decreasing neutrophilic infiltration as seen in the current study, in preventing gastric cancer. The picture is less clear for TAM, as the epidemiological data

is less clear about its role in the induction of gastric cancer[4,18-21]. In the current study, TAM was protective in infected male mice and shared many common features with E2 treatment indicating a similar mechanism. Contrary to our initial hypothesis, TAM did not block estrogen signaling causing more severe gastric lesions. Further studies must be conducted to address this difference between the mouse model and human epidemiological data. These studies will need to focus on the recreating chronic TAM treatment and controlling for the effects of baseline estrogen signaling. The studies presented here have contributed to the understanding of *Helicobacter pylori* mediated mutagenesis and carcinogenesis in the stomach by exploring the role of gender in modulating the inflammatory response to *H. pylori*.

4.2 References

1. Court, M., Robinson, P.A., Dixon, M.F., Jeremy, A.H. & Crabtree, J.E. The effect of gender on Helicobacter felis-mediated gastritis, epithelial cell proliferation, and apoptosis in the mouse model. *J Pathol* **201**, 303-311 (2003).
2. Sato, Y., *et al.* IL-10 deficiency leads to somatic mutations in a model of IBD. *Carcinogenesis* **27**, 1068-1073 (2006).
3. Greenman, C., *et al.* Patterns of somatic mutation in human cancer genomes. *Nature* **446**, 153-158 (2007).
4. Chandanos, E., *et al.* Tamoxifen exposure and risk of oesophageal and gastric adenocarcinoma: a population-based cohort study of breast cancer patients in Sweden. *Br J Cancer* **95**, 118-122 (2006).
5. Beyer, B.C., *et al.* Urokinase system expression in gastric carcinoma: prognostic impact in an independent patient series and first evidence of predictive value in preoperative biopsy and intestinal metaplasia specimens. *Cancer* **106**, 1026-1035 (2006).
6. Kenny, S., *et al.* Increased expression of the urokinase plasminogen activator system by Helicobacter pylori in gastric epithelial cells. *Am J Physiol Gastrointest Liver Physiol* **295**, G431-441 (2008).
7. Kaneko, T., Konno, H., Baba, M., Tanaka, T. & Nakamura, S. Urokinase-type plasminogen activator expression correlates with tumor angiogenesis and poor outcome in gastric cancer. *Cancer Sci* **94**, 43-49 (2003).
8. Mann, B., *et al.* Target genes of beta-catenin-T cell-factor/lymphoid-enhancer-factor signaling in human colorectal carcinomas. *Proc Natl Acad Sci U S A* **96**, 1603-1608 (1999).
9. Sipponen, P. & Correa, P. Delayed rise in incidence of gastric cancer in females results in unique sex ratio (M/F) pattern: etiologic hypothesis. *Gastric Cancer* **5**, 213-219 (2002).
10. Whary, M.T., *et al.* Intestinal helminthiasis in Colombian children promotes a Th2 response to Helicobacter pylori: possible implications for gastric carcinogenesis. *Cancer Epidemiol Biomarkers Prev* **14**, 1464-1469 (2005).
11. Fox, J.G., *et al.* Concurrent enteric helminth infection modulates inflammation and gastric immune responses and reduces helicobacter-induced gastric atrophy. *Nat Med* **6**, 536-542 (2000).
12. Junnila, S., *et al.* Gene expression analysis identifies over-expression of CXCL1, SPARC, SPP1, and SULF1 in gastric cancer. *Genes Chromosomes Cancer* **49**, 28-39 (2010).
13. Jung, J.J., *et al.* Chemokine growth-regulated oncogene 1 as a putative biomarker for gastric cancer progression. *Cancer Sci* **101**, 2200-2206 (2010).
14. Hamajima, N., Naito, M., Kondo, T. & Goto, Y. Genetic factors involved in the development of Helicobacter pylori-related gastric cancer. *Cancer Sci* **97**, 1129-1138 (2006).
15. Gonzalez, C.A., Sala, N. & Capella, G. Genetic susceptibility and gastric cancer risk. *Int J Cancer* **100**, 249-260 (2002).
16. Ohtani, M., *et al.* Protective role of 17 beta -estradiol against the development of Helicobacter pylori-induced gastric cancer in INS-GAS mice. *Carcinogenesis* **28**, 2597-2604 (2007).
17. Ohtani, M., *et al.* 17β-estradiol suppresses Helicobacter pylori-induced gastric pathology in male hypergastrinemic INS-GAS mice. *Carcinogenesis* (Submitted 2010).
18. Rutqvist, L.E., *et al.* Adjuvant tamoxifen therapy for early stage breast cancer and second

primary malignancies. Stockholm Breast Cancer Study Group. *J Natl Cancer Inst* **87**, 645-651 (1995).
19. Curtis, R.E., Boice, J.D., Jr., Shriner, D.A., Hankey, B.F. & Fraumeni, J.F., Jr. Second cancers after adjuvant tamoxifen therapy for breast cancer. *J Natl Cancer Inst* **88**, 832-834 (1996).
20. Chandanos, E. & Lagergren, J. Oestrogen and the enigmatic male predominance of gastric cancer. *Eur J Cancer* **44**, 2397-2403 (2008).
21. Matsuyama, Y., *et al.* Second cancers after adjuvant tamoxifen therapy for breast cancer in Japan. *Ann Oncol* **11**, 1537-1543 (2000).

4.3 Table 4.1. Comparison of *H. pylori* pathogenesis in mice and humans

***H. pylori* & inflammation**	**Mouse models**	**Humans**
Gender	Sexual dimorphisms depend on mouse model	Male predominant disease
Mutations	**A:T>G:C & G:C>T:A** mutations observed associated with oxidative stress and similar to humans	G:C>A:T, **A:T>G:C** & **G:C>T:A** are top mutations in survey of mutation spectra of GC. Associated with oxidative stress.
Cancer	Proinflammatory responses lead to cancer while decreased inflammation may reduce oncogenic pathways.	Dampened proinflammatory responses in humans may prevent gastric cancer
Immune cell trafficking	Deregulation of CXCL1 affected infiltration and decreased cancer	CXCL1 associated to gastric cancer. IL-8 polymorphism also associated with increased GC.
Estrogen	Prophylactic and therapeutic estrogen is protective	Estrogen associated with reduced GC incidence in women. Mechanism?
Tamoxifen	Protective therapeutically in reproductive age females. OVX or postmenopausal mice?	GC studies have large percentage of postmenopausal women. Stronger effect?

Appendix A: Functional classification of *Helicobacter pylori* isolates by gene expression analysis during coculture with gastric epithelial cells

Alexander Sheh, Abhinav Arneja, Forest M. White, Pelayo Correa, James G. Fox

Abstract

While *Helicobacter pylori* infects over 50% of the world's population, the mechanisms involved in the development of gastric disease are not fully understood. Bacterial, host and environmental factors play a role in the outcome of disease. To determine the role of bacterial factors in the outcome of *H. pylori* pathogenesis in vitro, side-by-side comparisons of global gene expression of eight *H. pylori* strains were analyzed. Comparison of two laboratory strains (ATCC43504 and SS1) yielded 6692 of 13469 differentially expressed probes. Clustering analysis of 6 Colombian clinical isolates from a region with low gastric cancer risk and a region with high gastric cancer risk, clustered two low risk strains together and the three high risk strains with the remaining low risk strain. This suggests that a potential signature that may distinguish strains from regions with higher gastric cancer incidence from regions with lesser risk. Interleukin 8 (IL-8) production, cell deformation and activation of Erk and Akt in AGS cells were also measured during coculture with ATCC43504 or SS1. ATCC43504 induced greater IL-8 secretion, more cell deformation and prolonged Erk and Akt activation compared to SS1. Future work will correlate these phenotypes in eukaryotic cells with bacterial pathways to develop a system to distinguish virulence potential among *H. pylori* strains.

A.1 Introduction

Helicobacter pylori infects over 50% of the world's population and has been associated with the development of gastritis, ulcers, and gastric cancer[1]. In spite of its high prevalence, chronic *H. pylori* infection leads to clinical symptoms in approximately 20% of infected individuals, with only 1-2% developing gastric adenocarcinoma. These divergent outcomes suggests that host, environmental and bacterial factors determine the outcome of *H. pylori* infection.

Among these bacterial factors, *H. pylori* genes utilized for motility/chemotaxis[2-4], acid acclimation[5-6], adherence to the mucosa[7] and damaging host epithelial cells[8-9] are necessary for the colonization of the gastric mucosa and have been associated with increased gastric disease[1]. The absence of these virulence factors results in reduced pathogenicity or inability to colonize[2-9]. Early studies comparing diverse *H. pylori* strains indicated that increased virulence correlated with morphological changes and vacuolization of cells in vitro, and specifically to cytotoxin associated gene A (CagA), a 128-140 kDa protein[10-11]. The *CagA* gene is present in 50-70% of *H. pylori* strains and is part of the cytotoxin-associated gene pathogenicity island (CagPAI)[1]. In vitro, isogenic mutants of *H. pylori* lacking the CagPAI region cause very mild, if any, disease and behave similarly to commensals[12]. CagA mediates its pathogenic effects through translocation to the host cell cytoplasm via a type IV secretion system. Upon translocation, CagA is phosphorylated by tyrosine kinases and affects eukaryotic signaling networks by interacting with a variety of host proteins, such as c-Met, SHP-2, PAR1, and Csk, leading to the activation of NF-kB via Erk and signaling linked to hyperproliferation, inflammation, apoptosis and cancer[13-15]. Erk is a member of the MAP kinase family which is involved in signaling cascades affecting

differentiation, cell cycle and cell proliferation in response to extracellular cues and growth factors[16]. Akt, a serine/threonine protein kinase, also activates NF-kB, regulates cell proliferation, apoptosis, cell survival, migration and tumorigenesis and has been found aberrantly expressed in many cancers, including gastric cancer[17-19]. Both of these kinases are activated during *H. pylori*-mediated pathogenesis[15].

Both in vivo and in vitro, *H. pylori*, partly through the effects of CagA, strongly induces the secretion of the proinflammatory cytokine, interleukin-8 (IL-8)[20-23], and the deformation of epithelial cells[24-27]. IL-8 is a potent chemokine that recruits neutrophils to infection site, which release reactive oxygen species (ROS) to eradicate *H. pylori*. The epithelial cells are damaged by the ROS, which in conjunction with *H. pylori*-mediated actin remodeling, allow the flow of nutrients into *H. pylori*-infected gastric mucosa[8]. Constant exposure to ROS due to persistent *H. pylori* infection is the initial step in the pathogenic progression leading to oxyntic gland atrophy, intestinal metaplasia and eventually cancer[28].

Classification of the potential virulence of *H. pylori* strains is normally performed through PCR genotyping of virulence factors such as *CagA*, *VacA*, and *BabA*, due to their importance to human disease[1,9,29]. However, identification of the gene does not guarantee expression in the context of the host, as demonstrated by the lack of CagA translocation in mice of *H. pylori* SS1, a CagA positive strain[30]. Other studies have also demonstrated that IL-8 secretion varies between strains with similar genotypes[23], suggesting that a systems approach would be useful in determining how the interaction of bacterial genes affect phenotypes observed in the host. Previous microarray studies, in vitro and in vivo, have focused on the effects of the environment or the host[31-35] on a single strain of *H. pylori,* or on isogenic

mutants[12], but have not focused on how different isolates of *H. pylori* interact under similar conditions.

Variation between *H. pylori* strains may partly account for differences in gastric cancer incidence rates in different geographical locations worldwide. In Colombia, there is a high prevalence of *H. pylori* infection, but geographically distinct areas differ greatly in gastric cancer risk[36-37]. Colombian populations in the high Andes have a higher incidence of gastric cancer associated with *H. pylori*, while coastal populations have a reduced incidence of gastric cancer[37]. Preliminary Multi Locus Sequence Typing (MLST) analysis of Colombian *H. pylori* strains from these regions have revealed an association between strains from high risk areas and ancestral European strains of *H. pylori* while strains from low risk regions associated phylogenetically with African strains (Pelayo Correa, unpublished results). However, the mechanisms by which these genetic changes mediate greater virulence have not been characterized.

In the present study, Erk and Akt activation, IL-8 secretion and cell deformation were measured in a gastric epithelial cell line (AGS) infected with two laboratory strains of *H. pylori* (SS1 and ATCC43504). Concurrently, early changes in *H. pylori* SS1 or ATCC43504 gene expression during coculture with AGS cells were assessed using a custom *H. pylori* microarray created using the genomes of 7 *H. pylori* strains (26695, J99, P12, HPAG1, B38, Shi470, and G27). After validating the microarray, 6 clinical isolates from areas with low and high incidence of gastric cancer were classified using the system to detect signatures relevant to carcinogenesis. Further work will involve annotating the microarray to determine specific functions involved in virulence and characterizing the induction of cell signaling, IL-8 secretion and cell deformation by the 6 clinical isolates to better assess how *H. pylori* functions correlate

with host phenotypes.

A.2 Materials and Methods

Bacteria and cells. *Helicobacter pylori* strains SS1, ATCC43504, PZ5004, PZ5024, PZ5026, PZ5056, PZ5080 and PZ5086 were cultured on blood agar (TSA with sheep blood, Remel, Lenexa, KS) or Brucella broth with 5% fetal bovine serum under microaerobic conditions (10% H2, 10% CO2, 80% N2). AGS cells (CRL-1739, ATCC, Manassas, VA) were grown in DMEM, Ham's F12-K or a 50:50 mixture with 10% fetal bovine serum. Phenol-red free medium was used for the Western blot and gene expression studies. Confluent AGS cells were infected at an MOI of 100 and incubated at 5% CO2 for the predetermined time.

IL-8 measurements. The supernatant of AGS cells infected with *H. pylori* was collected at 4, 8, and 27 hours. Supernatant was centrifuged to remove cells and frozen at -20C. The BD OPT-EIA human IL-8 kit (BD Biosciences, Franklin Lakes, NJ) was used according to manufacturer's instructions. Briefly, 96-well plates were pre-coated with anti-IL-8 capture antibody. Following blocking, supernatants and standards were incubated in each well. Subsequently, biotinylated anti-IL-8 detection antibody and substrate were added, and the colorimetric signal was detected on a VersaMax spectrophotometer at 450nm with the wavelength correction at 570nm.

Morphology. For the morphology studies, an autoclaved, round coverslip was placed at the bottom of each well of a 12-well plate prior to seeding with AGS cells. AGS cells were not allowed to reach confluency prior to 24-hour infection with *H. pylori* to permit cell elongation. Coverslips were immediately removed and fixed in 10% formalin and stained with hematoxylin and eosin with ethanol and xylene washes. Coverslips were then mounted on a microscope

slide using Permount. Area and perimeter of individual cells were calculated using Zeiss Axiovision software. A dimensionless "aspect ratio" was calculated using the formula: $Aspect\ ratio = 4\pi * AREA/PERIMETER^2$. The aspect ratio allows the quantification of the morphology as a perfect line would have an aspect ratio of 0 while a perfect circle would have a ratio of 1. More than 120 cells were counted from different fields from either uninfected, ATCC43504-infected or SS1-infected AGS cells. Student t-tests were used to calculate statistical significance with $P<0.05$ considered significant.

Western blots. Levels of pERK, pAkt, tubulin and CagA were determined by Western blot analysis. AGS cells infected with *H. pylori* for 0.25, 1, 4 and 8 hours were lysed at 4°C using cell scrapers and RIPA buffer with Phospho-Stop and cOmplete, Mini protease inhibitor cocktail tablets (Roche, Basel, Switzerland). Protein concentration was quantified using a BCA (bicinchoninic acid) protein assay (Thermo Scientific, Waltham, MA). Primary antibodies used were antiphosphotyrosine 4G10 (Upstate Biotechnology, Lake Placid, NY), anti-pERK1/2, anti-Akt S473 and anti-β-Tubulin (Cell Signaling Technologies, Beverly, MA). HRP-conjugated secondary antibodies used were goat anti-rabbit or anti-mouse antibodies (Jackson Immunoresearch, West Grove, PA).

Microarray design. Seven annotated *H. pylori* genomes (26695 [NC_000915], J99 [NC_000921], HPAG1 [NC_008086 & NC_008087], B38 [NC_012973], P12 [NC_011498 & NC_011499], G27 [NC_011333 & NC_011334], and Shi470 [NC_010698]) were utilized to design probes using the Agilent earray software (Agilent Technologies, Santa Clara, CA). Individual 60bp oligonucleotide probes were designed for each gene within a genome. Additionally, 60-mer oligonucleotide probes were designed based on previously published sequences of *H. pylori* probes used by the

Pathogen Functional Genomics Resource Center (pfgrc.jcvi.org). The accuracy of the probes was checked by using BLAST[38] prior to printing by Agilent. 13469 probes for *H. pylori* genes were utilized in creating the array.

Analysis of mRNA expression. Following coculture of *H. pylori* and AGS cells for 1 hour. At the end of the infection, RNAProtect Bacteria (Qiagen, Germantown, MD) was added to the culture media at a 2:1 ratio to prevent RNA degradation. AGS cells were scraped and allowed to incubate prior to collection by centrifugation. RNA was extracted following the RNeasy Mini Kit with RNase-free DNase treatment (Qiagen). Total prokaryotic and eukaryotic RNA was further purified using the Microbenrich kit (Applied Biosystems, Foster City, CA). Quality of the RNA was determined with the Agilent 2100 Bioanalyzer using a RNA 6000 Nano total RNA Kit (Agilent Technologies) before and after the Microbenrich step to determine the removal of eukaryotic RNA. Total RNA was hybridized to the custom Agilent 8x15K *H. pylori* Microarrays following the One-Color Microarray-Based Gene expression Analysis, Low Input Quick Amp Labeling protocol. Briefly, the method utilizes a T7 RNA polymerase that amplifies RNA to cRNA while incorporating cyanine 3-labeled CTP. Cy-3 incorporation and cRNA levels were measured with a NanoDrop ND-1000 UV-Vis Spectrophotometer (NanoDrop Technologies, Inc., Wilmington, DE). Arrays were scanned using an Agilent Microarray Scanner and data was extracted using Feature Extraction 9.1.

Processing of the raw gene expression data was performed using the limma library in R (Vienna, Austria). Microarray data were first corrected for background and then normalized by quantile using the NormalizeBetweenArrays function[39]. Data were log2 transformed, and statistical significance was determined using empirical Bayes statistics for differential expression

and corrected for family-wise error rates using the Benjamini-Hochberg correction. To control the rate of false positives, q-values were calculated as the minimum positive false discovery rate that can occur when identifying significant hypotheses[40]. Significant differential gene expression between groups was defined as a false discovery rate corrected q-value < 0.05. Comparisons were performed between 1) *H. pylori* strain SS1 vs. *H. pylori* strain ATCC43504 2) Colombian strains from a low gastric cancer risk area (PZ5004, PZ5024 and PZ5026) and from a high gastric cancer risk area (PZ5056, PZ5080 and PZ5086). The clustergram function of Matlab (Mathworks, Natick, MA) was used to classify microarray data. Clustering was performed on the entire set of genes prior to analysis of significance and after removal of non-significant genes.

A.3 Results

A.3.1 ATCC43504 elicits greater IL-8 secretion and elongation of AGS cells. ATCC43504 induced higher levels secretion of IL-8 from infected AGS cells compared to SS1 at 4, 8 and 27 hours post-infection (HPI) (ATCC43504 vs. SS1, at 4 hours: 868 vs. 420 pg/ml; at 8 hours: 2774 vs. 52 pg/ml; and at 27 hours, 2130 vs. 269 pg/ml) (Fig. A.1). ATCC43504 ΔCagA elicited slightly lower levels of IL-8 than the parental strain, but at levels higher than SS1 (data not shown). Additionally, ATCC43504 also mediated greater elongation of AGS cells compared to SS1. After 24 hours of coculture of *H. pylori* and AGS cells, AGS cells were formalin fixed and stained with hematoxylin and eosin for better visualization of the cell. Evaluating the elongation of over 120 cells per group, there was no significant difference in elongation between uninfected AGS cells and SS1-infected AGS cells (aspect ratio = 0.58 and 0.57, respectively). ATCC43504 significantly altered the morphology of AGS cells (aspect ratio = 0.41, $P < 0.001$ for both) (Fig. A.2).

A.3.2 ATCC43504 injects more CagA and induces greater phosphorylation of Erk and Akt. Four hours after infection, CagA levels in ATCC43504-infected AGS cells were elevated compared to SS1-infected AGS cells. There was increasing accumulation of CagA noted in both strains of *H. pylori* (Fig. A.3A). pAkt levels were increased 15 minutes post-infection by both strains compared to uninfected AGS cells. Increased pAkt levels were sustained at one hour by both SS1 and ATCC43504. pAkt levels in SS1-infected cells decreased by four hours but were sustained in ATCC43504-infected AGS cells (Fig A.3A). pAkt levels in ATCC43504-infected cells decreased at 8 hours post-infection (data not shown). pErk1/2 levels increased more rapidly upon ATCC43504 infection, with increased phosphorylation from 15 minutes to one hour, which decreased by four hours. SS1 slightly increased the phosphorylation of pErk1/2 at 15 min but this was not seen at later time points (Fig. A.3B).

A.3.3 Microarray Validation. To determine the microarray's ability to detect enriched prokaryotic RNA, AGS cells, before and after eukaryotic RNA removal, as well as AGS cells infected with ATCC43504 or SS1, before and after the Microbenrich step, were hybridized to the custom *H. pylori* microarrays (Fig. A.4). Total RNA from AGS, before and after eukaryotic RNA removal, was hybridized to a custom *H. pylori* microarray, but little hybridization occurred from either eukaryotic sample. Hybridization did occur with samples containing *H. pylori* regardless of microbial enrichment (Fig. A.4). 6692 out of 13469 probes were differentially expressed between ATCC43504 and SS1. Clustering analysis of the entire gene set, clearly separated the replicates of the two strains, distinguishing them from one another (Fig. A.5).

A.3.4 Classification of Colombian strains. To further explore the ability of gene expression profiling to classify virulent and avirulent strains, three *H. pylori* strains from a Colombian region

with high gastric cancer incidence (PZ5056, PZ5080 and PZ5086) and three strains from a Colombian region with low gastric cancer incidence (PZ5004, PZ5024 and PZ5026) were analyzed (n = 3 for each strain). Classification by clustering separated the six strains into two main clusters with two strains from the area of low incidence (PZ5004 and PZ5024) clustering very similarly while the three strains from the area of high incidence (PZ5026) as well as PZ5026 were clustered in the other group (Fig. A.6). The second cluster was subdivided into two closely clustered high risk strains (PZ5080 and PZ5086) and a group with a low risk strain (PZ5026) and a high risk strain (PZ5056). Both PZ5026 and PZ5056 show similarities and differences to the other two strains from the area they belong to. Analysis of all the low risk strains vs. all the high risk strains yielded 4349 of 13469 probes differentially expressed based on the geographic location of patients from which the strains were isolated.

Analysis of differentially expressed genes between one low risk (PZ5004) and one high risk (PZ5080) strain reduced the probe set from 13469 to 7198. This reduced probe set was used to classify the remaining four isolates (Fig. A.7). Similar to the previous classification attempt, PZ5056 clustered with the strains from the higher risk region. The reduced probe set from the SS1 and ATCC43504 comparison was used to determine if a more virulent lab strain would cluster with isolates from a high cancer risk area, while a less virulent lab strain would cluster with low risk isolates (Fig. A.8). Interestingly, ATCC43504 did not cluster closely with any Colombian strains, and SS1 was clustered most closely with a subgroup of high strains (PZ5080 and PZ5086). The remaining Colombian strains clustered as before with PZ5056 and PZ5026 clustering closely while PZ5004 and PZ5024 clustered tightly with one another.

A.4 Discussion

Helicobacter pylori has infected human hosts for many millennia[41]. Due to the plasticity of its genome, this protracted association, along with laterally acquired genes from bacterial donors in the environment, has allowed *H. pylori* to adapt to its niche in the gastric mucosa and develop an extensive array of virulence factors that facilitate its survival in the harsh gastric environment[8,42]. However, some strains of *H. pylori* elicit a mild immune response and can effectively act as commensals[12]. The existence of non-virulent strains may be explained by concurrent infection with multiple strains of *H. pylori* if virulence is presumed to be necessary for persistent infection[8]. However, the coexistence of a virulent strain in the gastric mucosa of every patient with a non-virulent isolate has not been determined systematically, and animal studies have demonstrated that less virulent strains can persistently infect the host[43], suggesting that less pathogenic strains can adequately inhabit the niche. A better understanding of the intricate pathogenic mechanisms developed by *H. pylori* will improve our ability to treat chronic inflammatory conditions, while the ability to functionally classify strains will increase our knowledge of the nature of *H. pylori* pathogenesis.

Using laboratory strains, ATCC43504 and SS1, we demonstrated that ATCC43504 is a more virulent strain as it induces greater IL-8 secretion, cell deformation and prolonged Erk and Akt activation. Increased IL-8 secretion has been associated with increased virulence of *H. pylori* strains. East Asian CagA motifs, which are highly associated with gastric carcinoma[13,44], induce greater IL-8 release from epithelial cells compared to Western CagA motifs[23]. As IL-8 recruits neutrophils to the site of infection, increased IL-8 leads to higher concentrations of reactive oxygen and nitrogen species and increased adhesion, migration and invasion in gastric

cells[45]. Indeed, a single nucleotide polymorphism associated with the IL-8 promoter region, which increases IL-8 protein levels, is correlated with increased gastric cancer risk[46-47].

Cell deformation is an in vitro representation of tight junction deregulation in vivo; strains that robustly induce this phenotype may promote epithelial-to-mesenchymal transitions[48]. The gastric epithelium is the interface that separates the host's cells from the lumen. In order to achieve adequate separation of the host and the external environment, adjacent epithelial cells form tight junctions that limit the diffusion of molecules from the host to the environment, and vice versa[13]. The deregulation of these tight junctions is necessary for *H. pylori* survival as it causes the release of nutrients unavailable in the gastric mucosa[8]. Highlighting the importance of disrupting tight junctions and cell polarity, two key bacterial virulence factors, VacA and CagA, mediate structural changes in epithelial cells[1]. As we demonstrated in this study, the ability to mediate this changes in epithelial cells is variable among strains, and we propose that the ability to induce greater deformation is a proxy of the strain's virulence.

Another measure of *H. pylori*'s pathogenicity is the bacterium's ability to hijack host signaling pathways. Increased Erk and Akt activation are associated with increased IL-8 secretion and other cell responses to *H. pylori*; therefore, aberrant activation may mediate oncogenic processes such as deregulated proliferation, apoptosis, and tumorigenesis[15]. Both ATCC43504 and SS1 affected the phosphorylation of Erk and Akt in epithelial cells. However, the perturbations in host signaling had different kinetics with ATCC43504 eliciting a prolonged activation of the two signaling proteins. As CagA is greatly associated with changes in host cell signaling, the higher levels of ATCC43504's CagA in the AGS cells may be responsible for the

sustained stimulation of Erk and Akt. Other possibilities include a different CagA variant or a lesser immunogenic potential in SS1. Further work is needed to elucidate the mechanisms by which diverse *H. pylori* strains modulate the duration of host signals, but characterization of the level and duration of pathway activation may be useful in determining the degree of pathogen-host interactions.

6692 probes were differentially expressed between ATCC43504 and SS1. This probe set will be analyzed to determine the differences in bacteria-host interactions between the more virulent ATCC43504 and the less immunogenic SS1. Further work needs to be done to annotate the microarray, but our initial analysis demonstrates that it can be useful to distinguish strains that have markedly different phenotypes in vitro and in vivo. *H. pylori* strain 26695 has 1630 genes[49], so we expect that the differentially expressed probes will be greatly reduced (at least 7-fold). Similarly, classification of the Colombian strains showed a potential signature for low and high strains as 2 of the strains evaluated from each region displayed very similar gene expression. While Multi Locus Sequence Typing (MLST) has provided a platform to characterize the origins of *H. pylori* strains[50-52] and their putative virulence by association with their geographic origin, gene expression analysis will provide a mechanistic understanding of how variations in the bacterial genome affect pathogenicity. In the present study, we propose a systems level approach that studies the *H. pylori* pathways involved in the generation of the pathological phenotypes associated with *H. pylori* infection. Upon completion, these results will provide a comprehensive view of the information flow from *H. pylori* infection to generation of the pathological phenotypes and help probe the differences between commensals and pathogens.

A.5 References

1. Kusters, J.G., van Vliet, A.H. & Kuipers, E.J. Pathogenesis of Helicobacter pylori infection. *Clin Microbiol Rev* **19**, 449-490 (2006).
2. Williams, S.M*., et al.* Helicobacter pylori chemotaxis modulates inflammation and bacterium-gastric epithelium interactions in infected mice. *Infect Immun* **75**, 3747-3757 (2007).
3. Croxen, M.A., Sisson, G., Melano, R. & Hoffman, P.S. The Helicobacter pylori chemotaxis receptor TlpB (HP0103) is required for pH taxis and for colonization of the gastric mucosa. *J Bacteriol* **188**, 2656-2665 (2006).
4. Ottemann, K.M. & Lowenthal, A.C. Helicobacter pylori uses motility for initial colonization and to attain robust infection. *Infect Immun* **70**, 1984-1990 (2002).
5. Bauerfeind, P., Garner, R., Dunn, B.E. & Mobley, H.L. Synthesis and activity of Helicobacter pylori urease and catalase at low pH. *Gut* **40**, 25-30 (1997).
6. Wen, Y., Feng, J., Scott, D.R., Marcus, E.A. & Sachs, G. The HP0165-HP0166 two-component system (ArsRS) regulates acid-induced expression of HP1186 alpha-carbonic anhydrase in Helicobacter pylori by activating the pH-dependent promoter. *J Bacteriol* **189**, 2426-2434 (2007).
7. Gerhard, M*., et al.* Clinical relevance of the Helicobacter pylori gene for blood-group antigen-binding adhesin. *Proc Natl Acad Sci U S A* **96**, 12778-12783 (1999).
8. Tan, S., Tompkins, L.S. & Amieva, M.R. Helicobacter pylori usurps cell polarity to turn the cell surface into a replicative niche. *PLoS Pathog* **5**, e1000407 (2009).
9. Gonzalez, C.A*., et al.* Helicobacter pylori cagA and vacA Genotypes as Predictors of Progression of Gastric Preneoplastic Lesions: A Long-Term Follow-Up in a High-Risk Area in Spain. *Am J Gastroenterol* (2011).
10. Leunk, R.D., Johnson, P.T., David, B.C., Kraft, W.G. & Morgan, D.R. Cytotoxic activity in broth-culture filtrates of Campylobacter pylori. *J Med Microbiol* **26**, 93-99 (1988).
11. Covacci, A*., et al.* Molecular characterization of the 128-kDa immunodominant antigen of Helicobacter pylori associated with cytotoxicity and duodenal ulcer. *Proc Natl Acad Sci U S A* **90**, 5791-5795 (1993).
12. Guillemin, K., Salama, N.R., Tompkins, L.S. & Falkow, S. Cag pathogenicity island-specific responses of gastric epithelial cells to Helicobacter pylori infection. *Proc Natl Acad Sci U S A* **99**, 15136-15141 (2002).
13. Hatakeyama, M. SagA of CagA in Helicobacter pylori pathogenesis. *Curr Opin Microbiol* **11**, 30-37 (2008).
14. Yamaoka, Y*., et al.* Role of interferon-stimulated responsive element-like element in interleukin-8 promoter in Helicobacter pylori infection. *Gastroenterology* **126**, 1030-1043 (2004).
15. Tabassam, F.H., Graham, D.Y. & Yamaoka, Y. Helicobacter pylori activate epidermal growth factor receptor- and phosphatidylinositol 3-OH kinase-dependent Akt and glycogen synthase kinase 3beta phosphorylation. *Cell Microbiol* **11**, 70-82 (2009).
16. Keshet, Y. & Seger, R. The MAP kinase signaling cascades: a system of hundreds of components regulates a diverse array of physiological functions. *Methods Mol Biol* **661**, 3-38 (2010).

17. Han, Z*., et al.* Reversal of multidrug resistance of gastric cancer cells by downregulation of Akt1 with Akt1 siRNA. *J Exp Clin Cancer Res* **25**, 601-606 (2006).
18. Manning, B.D. & Cantley, L.C. AKT/PKB signaling: navigating downstream. *Cell* **129**, 1261-1274 (2007).
19. Sizemore, N., Leung, S. & Stark, G.R. Activation of phosphatidylinositol 3-kinase in response to interleukin-1 leads to phosphorylation and activation of the NF-kappaB p65/RelA subunit. *Mol Cell Biol* **19**, 4798-4805 (1999).
20. Boughan, P.K*., et al.* Nucleotide-binding oligomerization domain-1 and epidermal growth factor receptor: critical regulators of beta-defensins during Helicobacter pylori infection. *J Biol Chem* **281**, 11637-11648 (2006).
21. Brandt, S., Kwok, T., Hartig, R., Konig, W. & Backert, S. NF-kappaB activation and potentiation of proinflammatory responses by the Helicobacter pylori CagA protein. *Proc Natl Acad Sci U S A* **102**, 9300-9305 (2005).
22. Al-Ghoul, L*., et al.* Analysis of the type IV secretion system-dependent cell motility of Helicobacter pylori-infected epithelial cells. *Biochem Biophys Res Commun* **322**, 860-866 (2004).
23. Argent, R.H., Hale, J.L., El-Omar, E.M. & Atherton, J.C. Differences in Helicobacter pylori CagA tyrosine phosphorylation motif patterns between western and East Asian strains, and influences on interleukin-8 secretion. *J Med Microbiol* **57**, 1062-1067 (2008).
24. Segal, E.D., Cha, J., Lo, J., Falkow, S. & Tompkins, L.S. Altered states: involvement of phosphorylated CagA in the induction of host cellular growth changes by Helicobacter pylori. *Proc Natl Acad Sci U S A* **96**, 14559-14564 (1999).
25. Mimuro, H*., et al.* Grb2 is a key mediator of helicobacter pylori CagA protein activities. *Mol Cell* **10**, 745-755 (2002).
26. Backert, S., Moese, S., Selbach, M., Brinkmann, V. & Meyer, T.F. Phosphorylation of tyrosine 972 of the Helicobacter pylori CagA protein is essential for induction of a scattering phenotype in gastric epithelial cells. *Mol Microbiol* **42**, 631-644 (2001).
27. Backert, S*., et al.* Functional analysis of the cag pathogenicity island in Helicobacter pylori isolates from patients with gastritis, peptic ulcer, and gastric cancer. *Infect Immun* **72**, 1043-1056 (2004).
28. Fox, J.G. & Wang, T.C. Inflammation, atrophy, and gastric cancer. *J Clin Invest* **117**, 60-69 (2007).
29. Hatakeyama, M. Helicobacter pylori CagA -- a bacterial intruder conspiring gastric carcinogenesis. *Int J Cancer* **119**, 1217-1223 (2006).
30. Crabtree, J.E., Ferrero, R.L. & Kusters, J.G. The mouse colonizing Helicobacter pylori strain SS1 may lack a functional cag pathogenicity island. *Helicobacter* **7**, 139-140; author reply 140-131 (2002).
31. Merrell, D.S., Goodrich, M.L., Otto, G., Tompkins, L.S. & Falkow, S. pH-regulated gene expression of the gastric pathogen Helicobacter pylori. *Infect Immun* **71**, 3529-3539 (2003).
32. Merrell, D.S*., et al.* Growth phase-dependent response of Helicobacter pylori to iron starvation. *Infect Immun* **71**, 6510-6525 (2003).
33. Thompson, L.J*., et al.* Gene expression profiling of Helicobacter pylori reveals a growth-phase-dependent switch in virulence gene expression. *Infect Immun* **71**, 2643-2655

(2003).
34. Gancz, H., Jones, K.R. & Merrell, D.S. Sodium chloride affects Helicobacter pylori growth and gene expression. *J Bacteriol* **190**, 4100-4105 (2008).
35. Scott, D.R., Marcus, E.A., Wen, Y., Oh, J. & Sachs, G. Gene expression in vivo shows that Helicobacter pylori colonizes an acidic niche on the gastric surface. *Proc Natl Acad Sci U S A* **104**, 7235-7240 (2007).
36. Bravo, L.E., van Doom, L.J., Realpe, J.L. & Correa, P. Virulence-associated genotypes of Helicobacter pylori: do they explain the African enigma? *Am J Gastroenterol* **97**, 2839-2842 (2002).
37. Whary, M.T*., et al.* Intestinal helminthiasis in Colombian children promotes a Th2 response to Helicobacter pylori: possible implications for gastric carcinogenesis. *Cancer Epidemiol Biomarkers Prev* **14**, 1464-1469 (2005).
38. Altschul, S.F*., et al.* Gapped BLAST and PSI-BLAST: a new generation of protein database search programs. *Nucleic Acids Res* **25**, 3389-3402 (1997).
39. Team, R.D.C. R: A Language and Environment for Statistical Computing. (ed. Computing, R.F.f.S.) (Vienna, Austria, 2008).
40. Storey, J.D. The Positive False Discovery Rate: A Bayesian Interpretation and the q-Value. *The Annals of Statistics* **31**, 23 (2003).
41. Linz, B*., et al.* An African origin for the intimate association between humans and Helicobacter pylori. *Nature* **445**, 915-918 (2007).
42. Ahmed, N., Tenguria, S. & Nandanwar, N. Helicobacter pylori--a seasoned pathogen by any other name. *Gut Pathog* **1**, 24 (2009).
43. Franco, A.T*., et al.* Activation of beta-catenin by carcinogenic Helicobacter pylori. *Proc Natl Acad Sci U S A* **102**, 10646-10651 (2005).
44. Naito, M*., et al.* Influence of EPIYA-repeat polymorphism on the phosphorylation-dependent biological activity of Helicobacter pylori CagA. *Gastroenterology* **130**, 1181-1190 (2006).
45. Ju, D*., et al.* Interleukin-8 is associated with adhesion, migration and invasion in human gastric cancer SCG-7901 cells. *Med Oncol* (2010).
46. Lu, W*., et al.* Genetic polymorphisms of interleukin (IL)-1B, IL-1RN, IL-8, IL-10 and tumor necrosis factor {alpha} and risk of gastric cancer in a Chinese population. *Carcinogenesis* **26**, 631-636 (2005).
47. Taguchi, A*., et al.* Interleukin-8 promoter polymorphism increases the risk of atrophic gastritis and gastric cancer in Japan. *Cancer Epidemiol Biomarkers Prev* **14**, 2487-2493 (2005).
48. Bagnoli, F., Buti, L., Tompkins, L., Covacci, A. & Amieva, M.R. Helicobacter pylori CagA induces a transition from polarized to invasive phenotypes in MDCK cells. *Proc Natl Acad Sci U S A* **102**, 16339-16344 (2005).
49. Tomb, J.F*., et al.* The complete genome sequence of the gastric pathogen Helicobacter pylori. *Nature* **388**, 539-547 (1997).
50. Wirth, T*., et al.* Distinguishing human ethnic groups by means of sequences from Helicobacter pylori: lessons from Ladakh. *Proc Natl Acad Sci U S A* **101**, 4746-4751 (2004).
51. Falush, D*., et al.* Traces of human migrations in Helicobacter pylori populations. *Science*

299, 1582-1585 (2003).
52. McClain, M.S., Shaffer, C.L., Israel, D.A., Peek, R.M., Jr. & Cover, T.L. Genome sequence analysis of Helicobacter pylori strains associated with gastric ulceration and gastric cancer. *BMC Genomics* **10**, 3 (2009).

A.6 Figures

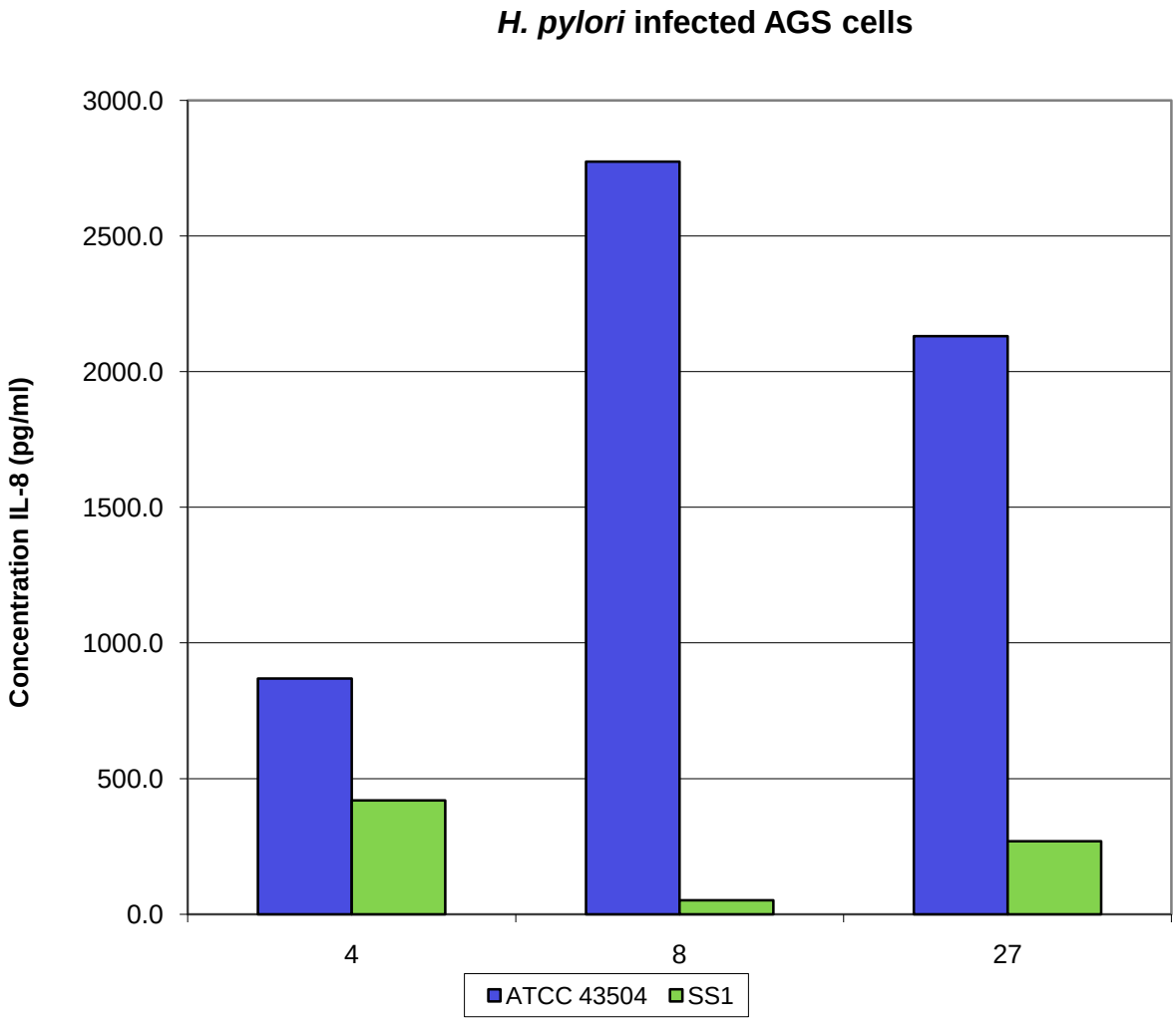

Figure A.1. IL-8 secretion was higher in AGS cells cocultured with ATCC43504 at 4, 8 and 27 hours post-infection (n=2).

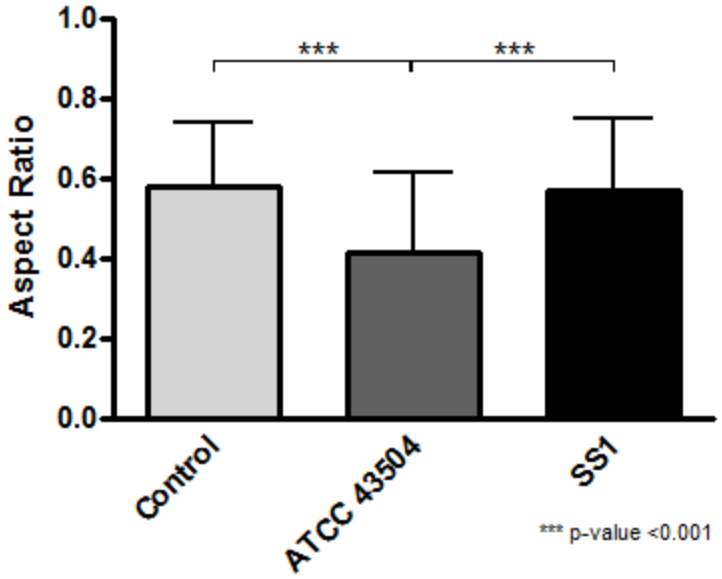

Figure A.2. ATCC43504 significantly deformed AGS cells compared to uninfected and SS1-infected AGS cells (*P*<0.001). A dimensionless ratio based on the area and perimeter of AGS cells was calculated for over 120 cells per group.

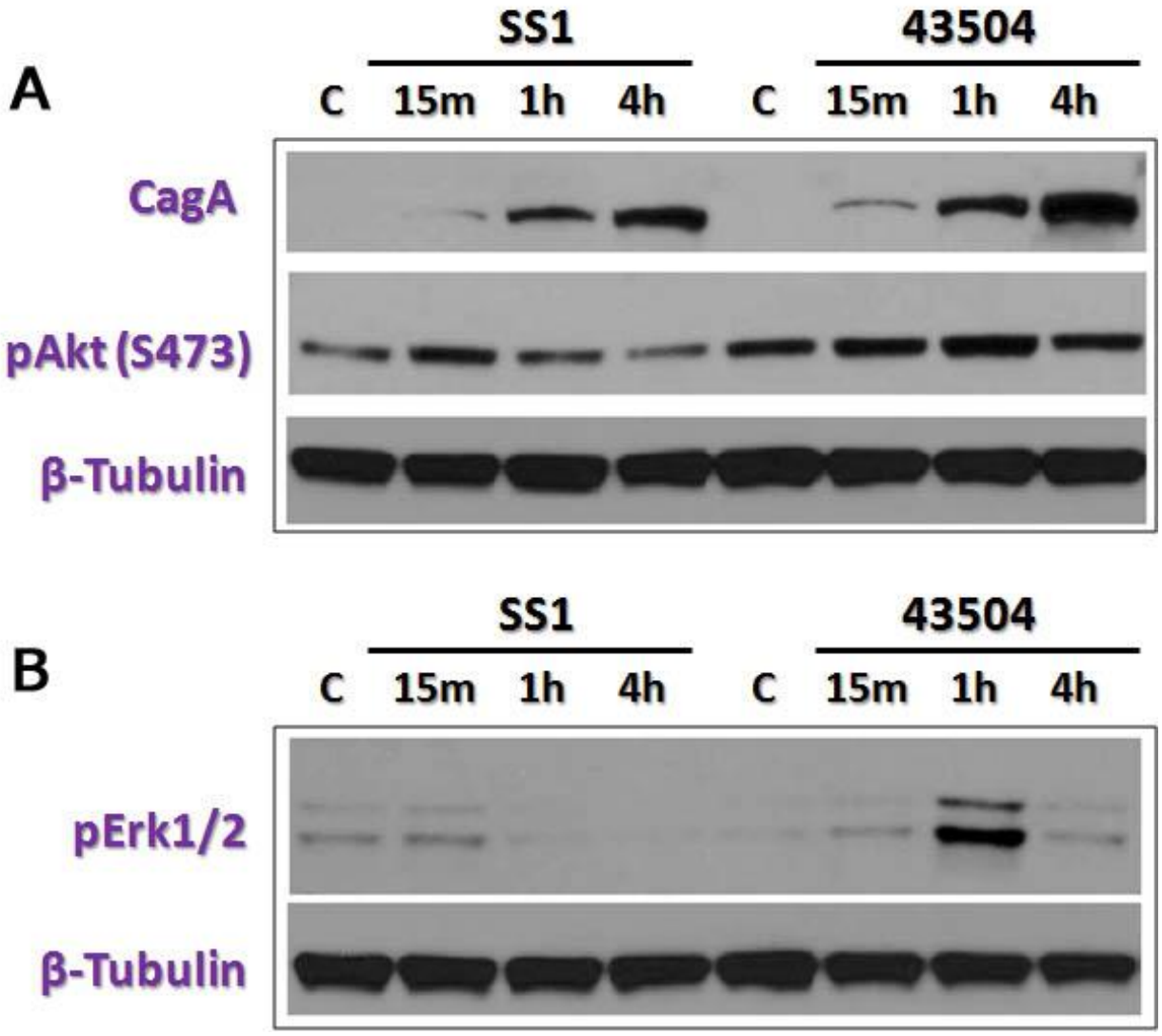

Figure A.3. ATCC43504 also injects more CagA than SS1 (3A). Akt (3A) and Erk1/2 (3B) are phosphorylated for a greater time by ATCC43504 compared to SS1.

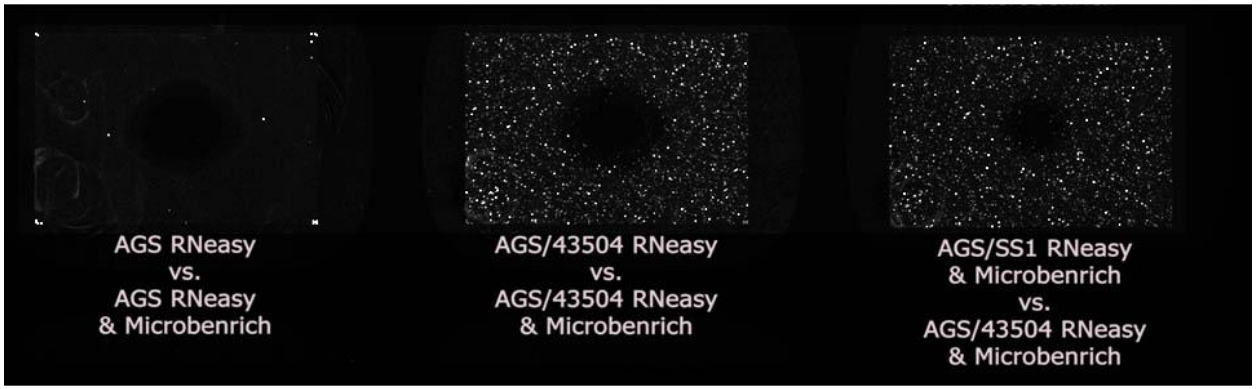

Figure A.4. Eukaryotic RNA does not bind to custom *H. pylori* microarrays (*left),* but hybridization is observed in samples containing bacterial RNA, with or without Microbenrich purification (*middle and right*).

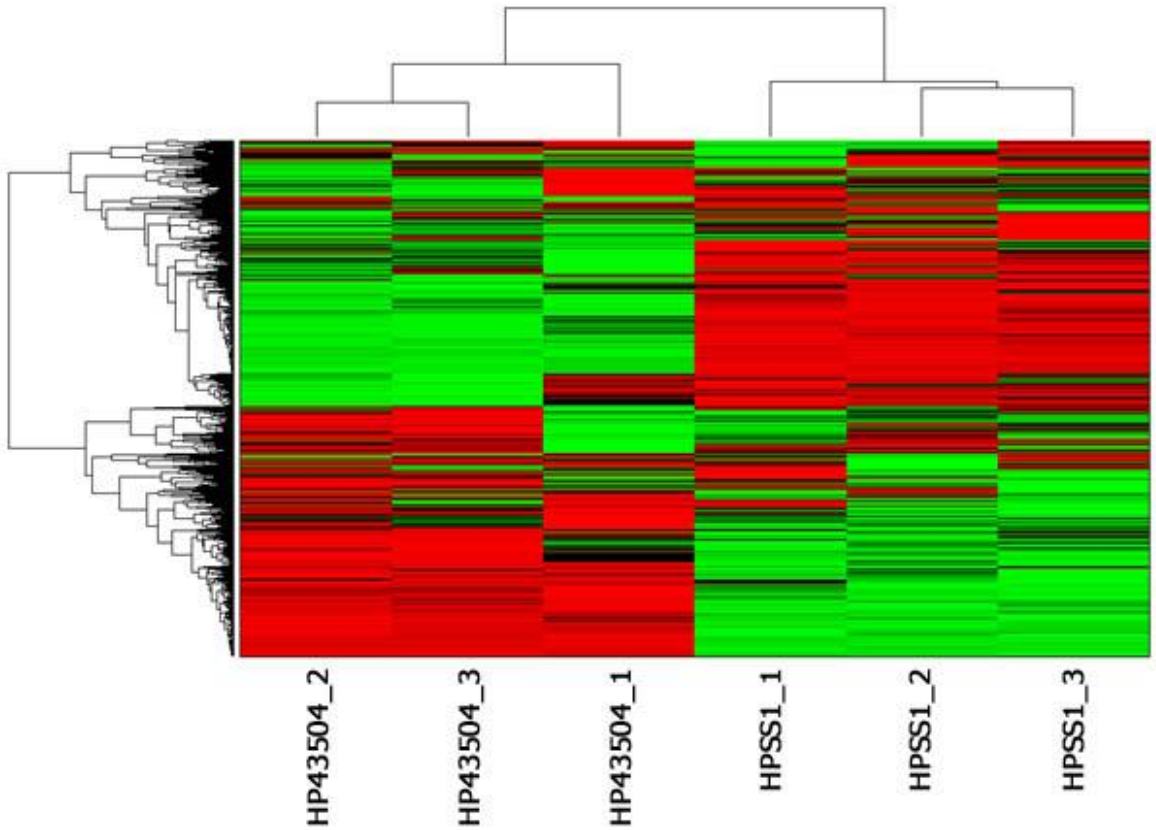

Figure A.5. Clustering analysis of bacterial RNA isolated from coculture system. ATCC43504 (n=3) and SS1 (n=3) samples were separated by clustering analysis and demonstrated different gene expression signatures.

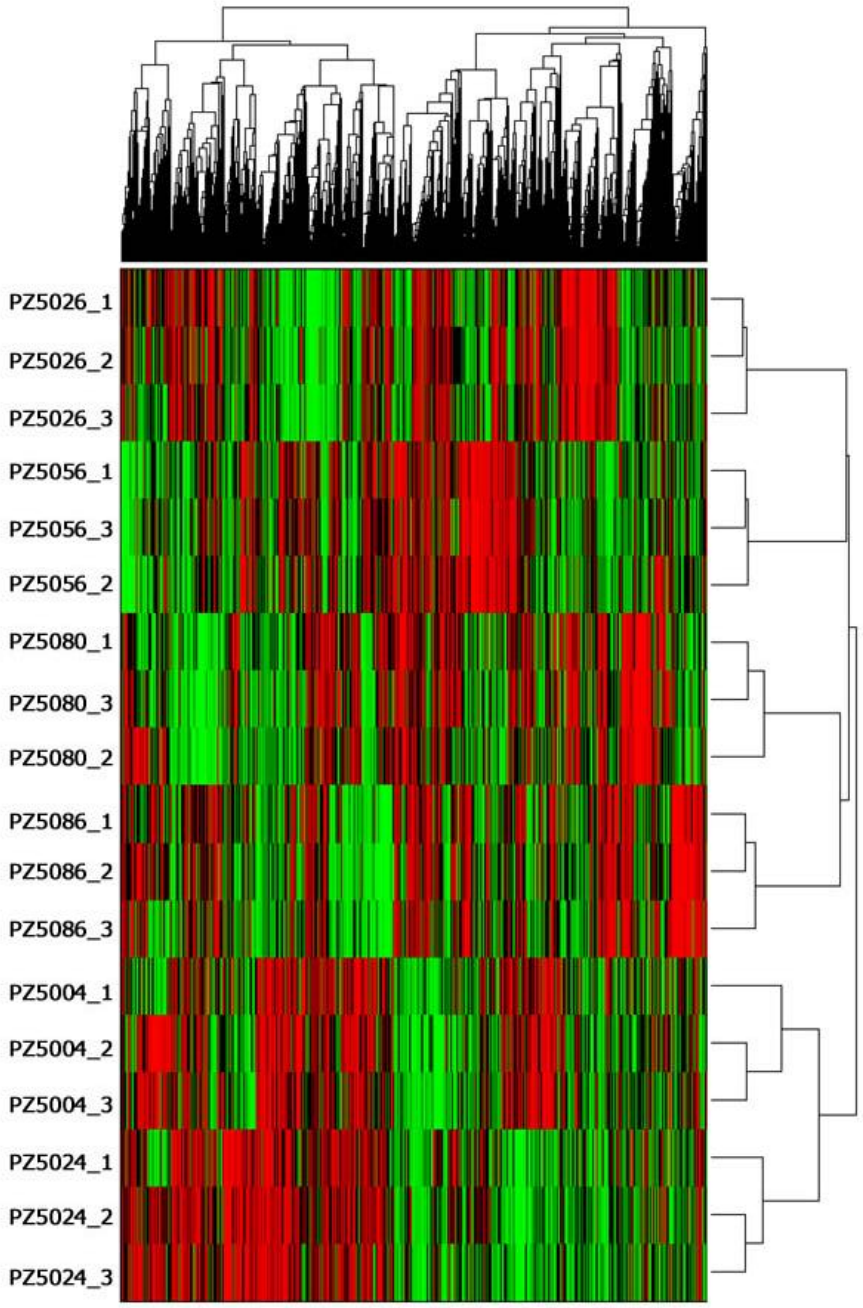

Figure A.6. Clustering analysis of 6 Colombian isolates. Three strains from a low gastric cancer risk area and three strains for a high gastric cancer risk area were assessed (all n=3). Clustering analysis created to main clusters composed of 1) 2 low risk strains and 2) 3 high risk strains and 1 low risk strain.

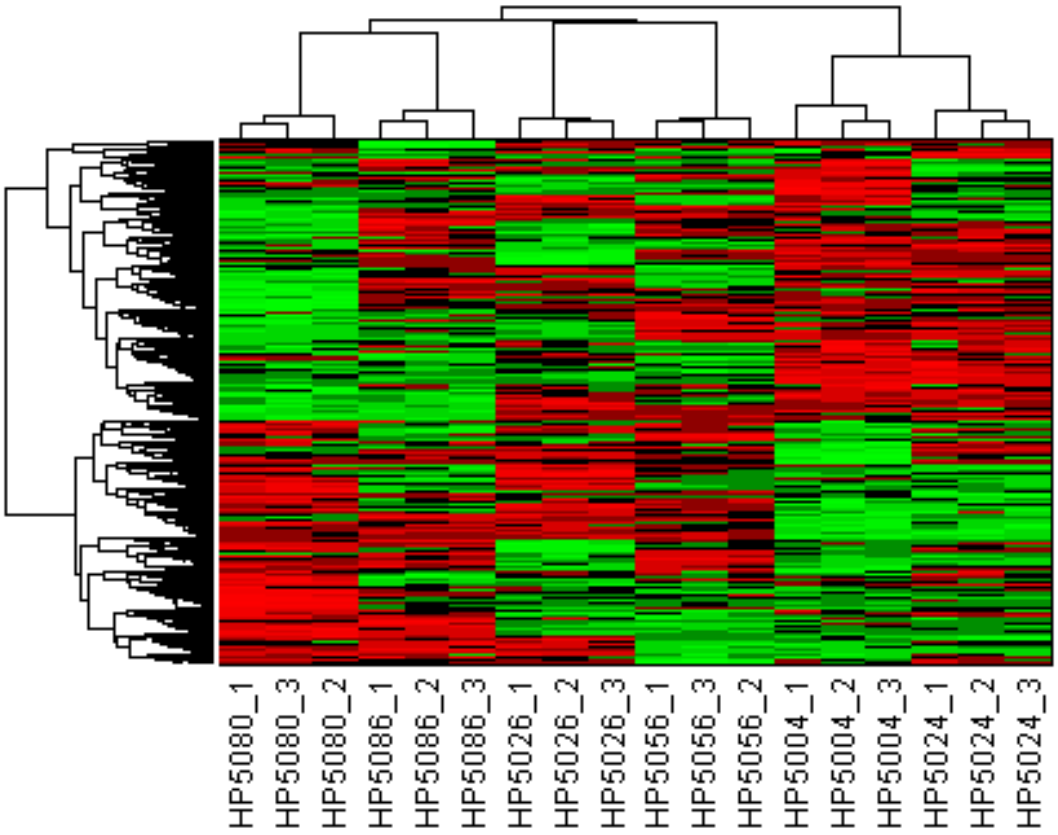

Figure A.7. Clustering analysis of 6 Colombian strains after reduction of probe set to differentially expressed genes between low risk strain PZ5004 and high risk strain PZ5080. Two low risk strains still composed one cluster, while 3 high risk strains and 1 low risk strain composed the second cluster.

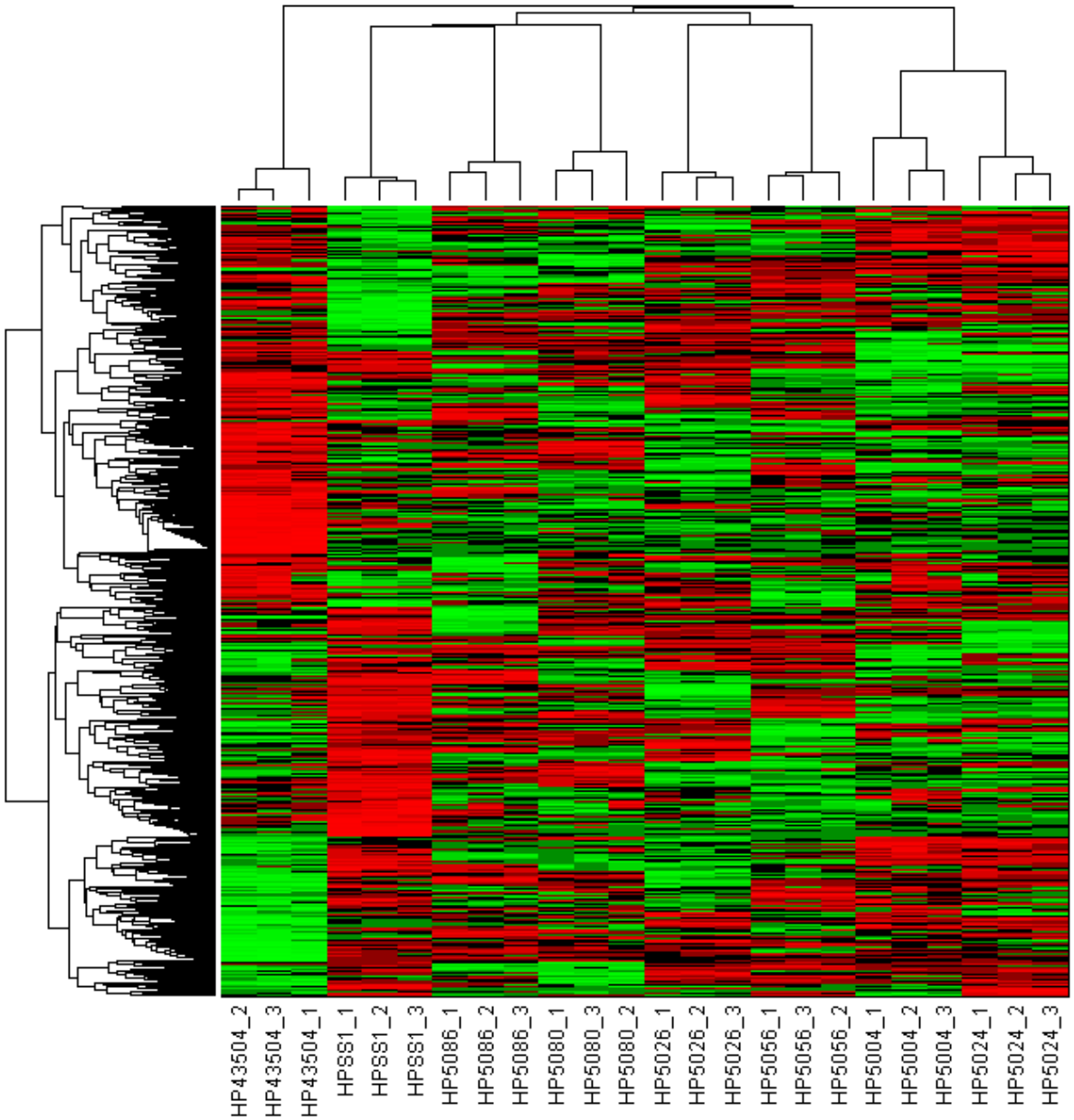

Figure A.8. Using the reduced probe set from comparing ATCC43504 and SS1, the 6 Colombian strains were classified to determine if virulence in laboratory strains correlated with gastric cancer risk. ATCC43504 had little similarity to other strains, while SS1 clustered most closely with 2 high risk strains.

Appendix B: Published version of Chapter 2: Sheh et al. "Mutagenic potency of Helicobacter pylori in the gastric mucosa of mice is determined by sex and duration of infection." PNAS *August 24, 2010 vol. 107 no. 34, 15217-15222.*

Mutagenic potency of *Helicobacter pylori* in the gastric mucosa of mice is determined by sex and duration of infection

Alexander Sheh[a], Chung Wei Lee[a,b], Kenichi Masumura[c], Barry H. Rickman[b], Takehiko Nohmi[c], Gerald N. Wogan[a,1], James G. Fox[a,b,2], and David B. Schauer[a,b,2]

[a]Department of Biological Engineering, Massachusetts Institute of Technology, Cambridge, MA 02139; [b]Division of Comparative Medicine, Massachusetts Institute of Technology, Cambridge, MA 02139; and [c]Division of Genetics and Mutagenesis, National Institute of Health Sciences, Tokyo 158-8501, Japan

Contributed by Gerald N. Wogan, July 19, 2010 (sent for review April 27, 2010)

***Helicobacter pylori* is a human carcinogen, but the mechanisms evoked in carcinogenesis during this chronic inflammatory disease remain incompletely characterized. We determined whether chronic *H. pylori* infection induced mutations in the gastric mucosa of male and female *gpt* delta C57BL/6 mice infected for 6 or 12 mo. Point mutations were increased in females infected for 12 mo. The mutation frequency in this group was 1.6-fold higher than in uninfected mice of both sexes ($P < 0.05$). A:T-to-G:C transitions and G:C-to-T:A transversions were 3.8 and 2.0 times, respectively, more frequent in this group than in controls. Both mutations are consistent with DNA damage induced by oxidative stress. No increase in the frequency of deletions was observed. Females had more severe gastric lesions than males at 6 mo postinfection (MPI; $P < 0.05$), but this difference was absent at 12 MPI. In all mice, infection significantly increased expression of *IFNγ*, *IL-17*, *TNFα*, and *iNOS* at 6 and 12 mo, as well as *H. pylori*–specific IgG1 levels at 12 MPI ($P < 0.05$) and IgG2c levels at 6 and 12 MPI ($P < 0.01$ and $P < 0.001$). At 12 MPI, IgG2c levels in infected females were higher than at 6 MPI ($P < 0.05$) and also than those in infected males at 12 MPI ($P < 0.05$). Intensity of responses was mediated by sex and duration of infection. Lower *H. pylori* colonization indicated a more robust host response in females than in males. Earlier onset of severe gastric lesions and proinflammatory, Th1-biased responses in female C57BL/6 mice may have promoted mutagenesis by exposing the stomach to prolonged oxidative stress.**

gpt delta mouse | *Helicobacter* | inflammation | mutagenesis | sexual dimorphism

Acting through multiple, complex mechanisms that are incompletely understood, chronic inflammation is a significant risk factor for several major human malignancies, including stomach cancer. Chronic inflammation induced by *Helicobacter pylori* infection increases lifetime risk of developing gastritis, duodenal and gastric ulcers, mucosa-associated lymphoid tissue lymphoma, mucosal atrophy, and gastric carcinoma (1, 2). Indeed, *H. pylori* has been classified by International Agency for Research on Cancer as a group I human carcinogen on the basis of its impact on gastric cancer incidence, the second most frequent cause of cancer-related death worldwide (3). Among postulated mechanisms through which infection may contribute to increased cancer risk are overproduction of reactive oxygen and nitrogen species (RONS) by inflammatory cells, and the consequent induction of mutations critical for tumor initiation in cells of inflamed tissues (4). The inflammatory response to infection results in increased production of RONS, including superoxide ($O_2^{-}\cdot$), hydrogen peroxide (H_2O_2), nitric oxide (NO), peroxynitrite (ONO_2^{-}), and nitrous anhydride (N_2O_3), in vitro (5, 6) and in vivo (7–9). *H. pylori* can also directly activate RONS-producing enzymes, such as inducible NO synthase (iNOS) and spermine oxidase, in gastric epithelial cells, causing DNA damage and apoptosis (5, 6). Chronic inflammatory states increase levels of DNA adducts, such as etheno adducts, 8-oxoG, and other mutagenic precursors, in vitro and in vivo (10–12), but tend not to alter the frequency of deletions (13). RONS also can damage DNA indirectly by creating adduct-forming electrophiles via lipid peroxidation (14, 15). RONS have been shown to induce mutations in *H. pylori* by inducing a hypermutation state in the bacteria (16).

A widely used experimental model is the *H. pylori* SS1-infected C57BL/6 mouse, which is susceptible to chronic infection and develops robust gastritis and premalignant lesions similar to those occurring in humans (17, 18). To date, limited investigation has focused on genetic damage associated with infection in these animals, but available data are still incomplete. Enhanced DNA fragmentation was observed in gastric cells of infected mice (19), in which dsDNA breaks were also detected by TUNEL assay (20, 21). Mutagenicity in reporter genes recovered from gastric DNA of male and female Big Blue transgenic mice 6 mo after infection with *H. pylori* or *Helicobacter felis* has also been reported (22). In *H. pylori*-infected male mice, point mutation frequency was increased at 6 mo post infection (MPI), but decreased to control levels by 12 MPI, suggesting that the animals may have adapted to infection (22). Female mice infected with *H. felis* also had an increased frequency of point mutations at 7 MPI, compared with uninfected controls (23). Mutagenesis resulting from infection has also been associated with p53 status. Mutations were found in the *lacI* reporter genes of a small number of *H. felis*-infected female TSG-p53/Big Blue mice harboring either one ($p53^{+/-}$) or two ($p53^{+/+}$) WT p53 alleles (23). A 2-fold increase in mutations was found in DNA from the gastric mucosa of infected $p53^{+/+}$ mice, and also in uninfected $p53^{+/-}$ mice; the mutation frequency in infected $p53^{+/-}$ mice was further increased by approximately threefold. The intensity of inflammation was estimated to be significantly higher in infected $p53^{+/-}$ mice than in infected $p53^{+/+}$ animals, and gastric epithelial proliferation was similarly increased with infection in both latter treatment groups. By contrast, in another study, infection of Big Blue transgenic mice (sex not specified) with the SS1 strain of *H. pylori* for 3.5 mo resulted in no significant increase in gastric mutations over uninfected controls (13).

We used the *gpt* delta mouse to measure the accumulation of gastric mutations associated with *H. pylori* SS1 infection in male and female animals at 6 and 12 MPI. This experimental system comprises λ-EG10–based transgenic C57BL/6 mice harboring tandem arrays of 80 copies of the bacterial *gpt* gene at a single site on chromosome 17. The model was specifically designed to facilitate the in vivo detection of point mutations by 6-thioguanine

Author contributions: A.S., C.W.L., J.G.F., and D.B.S. designed research; A.S., C.W.L., and B.H.R. performed research; K.M. and T.N. contributed new reagents/analytic tools; A.S., B.H.R., G.N.W., J.G.F., and D.B.S. analyzed data; and A.S., G.N.W., and J.G.F. wrote the paper.

The authors declare no conflict of interest.

[1]To whom correspondence should be addressed. E-mail: wogan@mit.edu.

[2]J.G.F. and D.B.S. contributed equally to this work.

This article contains supporting information online at www.pnas.org/lookup/suppl/doi:10.1073/pnas.1009017107/-/DCSupplemental.

MICROBIOLOGY

(6-TG) selection, and deletions up to 10 kb in length by selection based on sensitivity to P2 interference (Spi$^-$) (24). When phage DNA rescued from mouse tissues is introduced into appropriate *Escherichia coli* strains, both point mutations and large deletions can be efficiently detected (24). We also characterized histopathologic changes, expression of inflammatory cytokines, and expression of iNOS in gastric mucosa 6 and 12 mo after initial infection. In addition, we compared responses of male and female mice to assess the influence of sex. We found that *H. pylori* infection induced significant increases in the frequency of point mutations in the gastric mucosa of female, but not male, *gpt* delta mice. The accumulation of point mutations was therefore sex-dependent and was mediated by the duration of infection and the severity of disease.

Results and Discussion

Pathology, Cytokine and iNOS Expression, and Serologic Responses to *H. pylori* Infection and *H. pylori* Levels. Inflammatory histopathologic changes resulting from *H. pylori* infection were evaluated (Fig. S1) and gastric histological activity index (GHAI) scores calculated, with the following results. Scores were significantly increased in infected animals of both sexes at 6 and 12 MPI (female, $P < 0.001$ and $P < 0.01$, respectively; and male, $P < 0.05$ and $P < 0.001$, respectively; Fig. 1). Regarding specific types of lesions represented in the GHAI, infected females experienced higher levels of hyperplasia ($P < 0.05$), epithelial defects ($P < 0.001$), and dysplasia ($P < 0.05$) compared with infected males at 6 MPI, and thus had correspondingly higher ($P < 0.05$) GHAI scores at this time point. At 6 MPI, infected animals of both sexes displayed mild to moderate inflammation, comprised chiefly of submucosal and mucosal infiltrates of mononuclear and granulocytic cells. In addition, in infected males, mucous metaplasia, intestinal metaplasia, oxyntic gland atrophy, and hyalinosis were all significantly elevated compared with controls (all $P < 0.01$; intestinal metaplasia, $P < 0.001$); no significant increases occurred in foveolar hyperplasia, epithelial defects, or dysplasia. In infected females, inflammation ($P < 0.05$), epithelial defects ($P < 0.001$), mucous metaplasia ($P < 0.01$), hyalinosis ($P < 0.001$), as well as premalignant lesions of oxyntic gland atrophy ($P < 0.001$), intestinal metaplasia ($P < 0.05$), and dysplasia ($P < 0.05$) were significantly elevated compared with uninfected controls. At 12 MPI, there were no differences in gastric lesion severity between infected males and females; both groups had similar mucosal changes. Infected male mice at 12 MPI displayed significantly increased epithelial defects but decreased intestinal metaplasia than infected males at 6 MPI ($P < 0.01$ and $P < 0.001$).

H. pylori infection significantly increased transcription profiles at 6 and 12 MPI as follows (details in Fig. S2): *IFNγ* (males, $P < 0.001$; females, $P < 0.01$ at 6 and 12 MPI); *TNF-α* (males, $P < 0.01$ at 6 and 12 MPI; females, $P < 0.01$ and $P < 0.05$); *IL-17* (males, $P < 0.05$ and $P < 0.001$; females, $P < 0.05$ and $P < 0.01$). *iNOS* expression was increased in male and female mice at 6 and 12 MPI (males, $P < 0.05$ and $P < 0.01$; females, $P < 0.01$ and $P < 0.001$) compared with controls at 12 mo. *IL-10* expression was not significantly affected by infection in animals of either sex ($P > 0.05$).

H. pylori infection also resulted in a Th1-predominant IgG2c response in infected mice as previously reported (25, 26) (Fig. 2). *H. pylori*-specific IgG2c levels were higher in infected than in uninfected animals at 6 and 12 MPI ($P < 0.01$ and $P < 0.001$, respectively). At 12 MPI, infected females had significantly higher

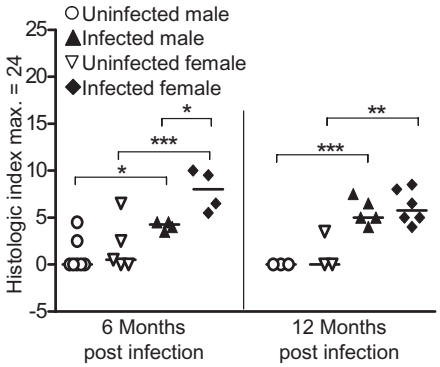

Fig. 1. *H. pylori* infection elicits more gastric pathologic processes in female mice at 6 mo. *H. pylori* infection increased the GHAI in both male and female C57BL/6 mice at 6 and 12 mo. At 6 mo of infection, infected females had significantly more pathologic processes than infected males. Uninfected males (○; 6 MPI, $n = 7$; 12 MPI, $n = 3$), uninfected females (▽; 6 MPI, $n = 5$; 12 MPI, $n = 3$), infected males (▼; 6 MPI, $n = 4$; 12 MPI, $n = 5$) and infected females (◆; 6 MPI, $n = 4$; 12 MPI, $n = 6$). Bar represents the mean. $*P < 0.05$, $**P < 0.01$, and $***P < 0.001$.

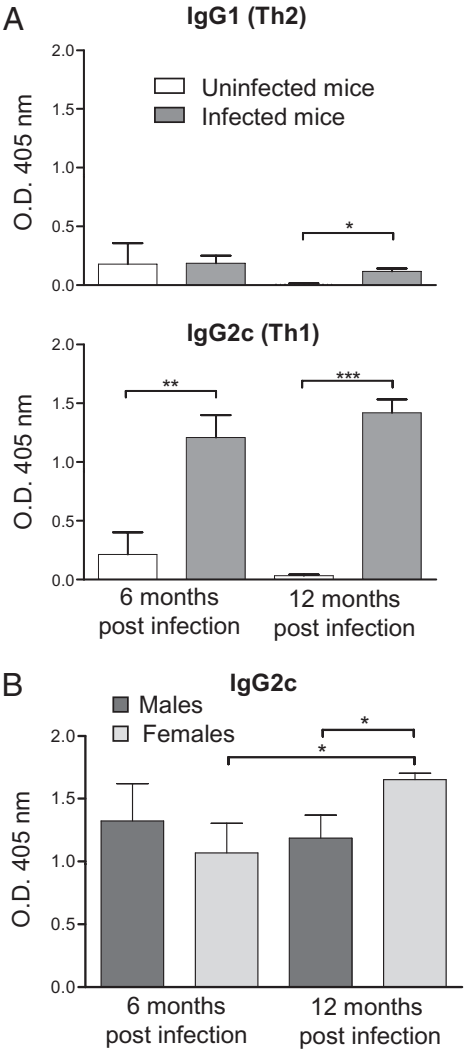

Fig. 2. The effect of *H. pylori* infection on *H. pylori*–specific IgG1 and IgG2c. Serum levels of IgG were measured by ELISA in uninfected and *H. pylori*–infected mice. (*A*) *H. pylori*–infected mice (gray bars; 6 MPI, $n = 9$; 12 MPI, $n = 12$) developed a greater IgG1 response after 12 mo of infection compared with uninfected mice (white bars; 6 MPI, $n = 6$; 12 MPI, $n = 6$; $P < 0.05$). *H. pylori*–infected mice developed a greater IgG2 response after 6 and 12 mo of infection ($P < 0.01$ and $P < 0.001$, respectively). (*B*) At 12 mo, infected female mice (light gray bars; 6 MPI, $n = 4$; 12 MPI, $n = 6$) had substantially increased IgG2c compared with infected males (dark gray bars; 6 MPI, $n = 5$; 12 MPI, $n = 6$) at 12 mo and infected females at 6 mo ($P < 0.05$, both). Data are mean (SE) of mice in different treatment groups. $*P < 0.05$, $**P < 0.01$, and $***P < 0.001$.

IgG2c levels than infected males ($P < 0.05$). Duration of infection also increased IgG2c levels in infected females, with higher levels noted at 12 versus 6 MPI ($P < 0.05$). *H. pylori*-specific IgG1 (Th2) levels were higher in infected than in uninfected animals at 12 MPI ($P < 0.05$). Females had higher Th1/Th2 ratios than males: at 6 MPI, 8.58 vs. 4.01; and at 12 MPI, 12.9 vs. 7.51.

We and others have demonstrated that *H. pylori* levels are inversely correlated with the degree of pathology and the immune response as measured by antibody and cytokine production (25, 27). At 6 MPI, *H. pylori* was detectable by quantitative PCR in all infected males, but not in one female. At 12 MPI, there was a salient difference in levels of *H. pylori* colonization between males and females; *H. pylori* was undetectable in four infected females, but undetectable in only one male (Fig. 3).

Frequency and Nature of Mutations. We determined the frequency of *gpt* point mutations in gastric DNA isolated from infected and uninfected mice by selection of mutants based on 6-TG resistance. Recognizing the possible confounding effect of clonal expansion of sibling mutants (i.e., jackpot mutations), we sequenced the *gpt* genes from all 566 recovered mutants. Any mutation found to duplicate another at the same site within an individual sample was excluded from subsequent frequency calculations. After this adjustment, at 12 MPI the *gpt* mutation frequency in infected females ($7.5 \pm 2.0 \times 10^{-6}$; $P < 0.05$) was significantly (1.6-fold) higher than that in all control animals ($4.7 \pm 1.1 \times 10^{-6}$), whereas the frequency in infected males ($6.3 \pm 5.4 \times 10^{-6}$; $P = 0.49$) was not. At 6 MPI, *gpt* mutation frequency in infected animals of either sex (females, $5.6 \pm 2.0 \times 10^{-6}$, $P = 0.72$; males, $7.2 \pm 2.2 \times 10^{-6}$, $P = 0.57$) was not significantly different from that of controls ($6.2 \pm 3.0 \times 10^{-6}$; Fig. 4).

After sequencing and accounting for clonal expansion, 236 from infected and 156 mutants from uninfected mice were used to identify effects of *H. pylori* infection on types of mutations causing loss of *gpt* function, with the results summarized in Table 1 and Table S1. G:C-to-A:T transitions and G:C-to-T:A transversions were the most prevalent types of mutations in both infected and uninfected animals, representing 33% to 50% and 17% to 31%, respectively, of total mutations in various treatment groups; mutant frequencies varied from 2.1 to 3.0×10^{-6} in these transitions and 0.9–1.8×10^{-6} in the transversions. The 1.6-fold higher total mutations observed in infected females compared with age-matched controls at 12 MPI was attributable mainly to two types of mutations: 3.8 times more A:T-to-G:C transitions ($P < 0.05$) and 2.0 times more G:C-to-T:A transversions ($P < 0.05$). These two mutations are consistent with the expected mutational spectrum induced by RONS (28) and have been found elevated in another animal model of chronic inflammation (13). An increase in G:C-to-T:A transversions was also reported in a previous study documenting *H. pylori*-induced mutations (22).

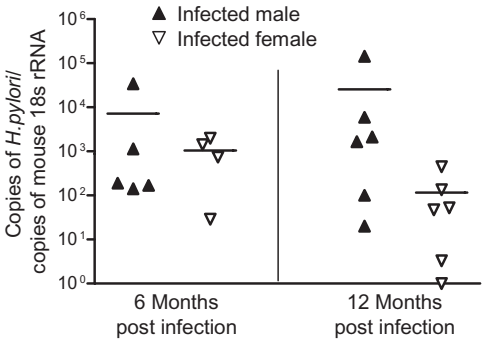

Fig. 3. *H. pylori* levels in the stomach were lower in infected females at 12 MPI. Values represent the number of *H. pylori* organisms per copies of mouse 18s rRNA. At 6 MPI, one infected female mouse was under the threshold of detection (15 copies of *H. pylori*). At 12 MPI, four infected females and one infected male were undetectable. Infected males (▼; 6 MPI, $n = 5$; 12 MPI, $n = 6$) and infected females (▽; 6 MPI, $n = 4$; 12 MPI, $n = 6$). Bar represents the mean.

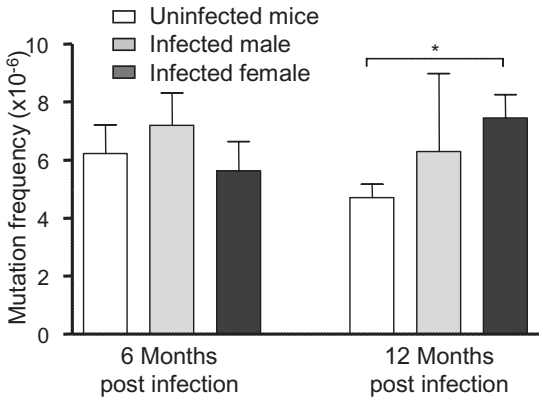

Fig. 4. Twelve-month infection with *H. pylori* increases the frequency of point mutations in female mice. The mutation frequency of point mutations was determined by the *gpt* assay in uninfected mice (white bars; 6 MPI, $n = 13$; 12 MPI, $n = 15$), *H. pylori*-infected males (light gray bars; 6 MPI, $n = 4$; 12 MPI, $n = 5$) and *H. pylori*-infected females (dark gray bars; 6 MPI, $n = 9$; 12 MPI, $n = 11$). Control mice of both sexes were grouped for this analysis. Data are mean (SEM) of mutation frequency of mice in different treatment groups. $*P < 0.05$.

A:T-to-G:C transitions can be formed by deamination of adenine to hypoxanthine or creation of ethenoadenine. Deamination is mediated by N_2O_3, the autoxidation product of NO·, which directly nitrosates primary amines on DNA bases (28, 29). Hypoxanthine resembles guanine and mispairs with cytosine, resulting in the observed mutation. Alternatively, A:T-to-G:C transitions can also be created indirectly by lipid peroxidation by RONS, forming etheno adducts in DNA such as highly mutagenic ethenoadenine (30, 31). G:C-to-T:A transversions have also been associated with increased *iNOS* expression levels, pointing to the involvement of RONS (32). Cells cocultivated with activated macrophages predominantly develop G:C to T:A transversions caused by exposure to NO·, O_2^{-}·, and H_2O_2 (33). G:C-to-T:A transversions are also caused by adducts produced by oxidative stress or lipid peroxidation, such as 8-oxodG, εdC, and M1G (34, 35). The presence of 8-oxodG, a major product of oxidative damage to DNA, results in mispairing of guanine with adenine during replication, thus inducing transversions (36). Although 8-oxodG is believed to be the main cause of this mutation, etheno adducts formed by lipid peroxidation may also play a significant role in mutagenesis observed in vivo (37).

Fig. S3 shows the mutation spectrum detected in the *gpt* gene, of which the following features are noteworthy. In both uninfected and infected mice, hotspots occurred at nucleotides C64, G110, G115, and G418; C64, G110, and G115 are CpG sites and are known hotspots in this assay (38, 39). Hotspots occurring in infected mice were located at A8, G116, and G143; A8 and G116 were found predominantly in infected females at both 6 and 12 mo, whereas G143, located at a CpG site, was a hotspot in infected animals of both sexes. Uninfected mice had hotspots at G406, G416, and A419, one of which (G416) occurred mainly in males. Mutations in infected males were concentrated mainly in hotspots common to both uninfected and infected animals, whereas in infected females there was an increase in mutations throughout the *gpt* gene at non-G:C sites. This result suggests that the chemistry of DNA damage in mice with a stronger host response to infection may have differed from that in mice with mild or minimal gastritis.

Table 1. Twelve months of *H. pylori* infection increases the mutation frequency of A:T-to-G:C transitions and G:C-to-T:A transversions in female mice

Effect	6 mo			12 mo		
	Uninfected all (n = 6)	Infected male (n = 4)	Infected female (n = 8)	Uninfected all (n = 14)	Infected male (n = 5)	Infected female (n = 11)
Transition						
G:C to A:T	3.02 (2.07)	2.41 (2.64)	2.74 (1.07)	2.13 (0.87)	2.66 (1.70)	2.69 (0.97)
A:T to G:C	0.27 (0.61)	0.00	0.16 (0.22)	0.23 (0.19)	0.08 (0.16)	0.88 (0.59)*
Transversion						
G:C to T:A	1.30 (1.34)	1.64 (1.29)	0.89 (0.68)	0.85 (0.62)	1.69 (2.43)	1.75 (0.54)*
G:C to C:G	0.29 (0.66)	0.36 (0.71)	0.40 (0.60)	0.19 (0.27)	0.84 (1.25)	0.09 (0.14)
A:T to T:A	0.34 (0.47)	0.00	0.37 (0.37)	0.31 (0.41)	0.00	0.53 (0.89)
A:T to C:G	0.00	0.36 (0.71)	0.18 (0.22)	0.05 (0.12)	0.00	0.25 (0.46)
Deletion						
1-bp deletion	0.84 (0.94)	2.44 (3.99)	0.66 (0.43)	0.53 (0.35)	0.67 (0.54)	0.88 (0.73)
≥2-bp deletion	0.04 (0.12)	0.00	0.44 (0.57)	0.22 (0.20)	0.18 (0.36)	0.22 (0.34)
Insertion	0.00	0.00	0.08 (0.16)	0.20 (0.23)	0.00	0.11 (0.17)
Complex mutation	0.14 (0.31)	0.00	0.04 (0.08)	0.00	0.18 (0.36)	0.12 (0.29)
Total	6.23 (2.98)	7.20 (2.21)	5.95 (1.54)	4.71 (1.13)	6.29 (5.37)	7.51 (1.91)*

Data are mean (SD) of mutation frequency data from 411 mutants recovered from the *gpt* assay after excluding 155 mutants considered siblings. Control mice of both sexes were grouped for this analysis. The mutation frequency of A:T-to-G:C transitions and G:C-to-T:A transversions was significantly elevated in female mice infected with *H. pylori* for 12 mo.
*$P < 0.05$.

Mutation analysis using the Spi$^-$ assay revealed that the frequency of deletion mutations in *gpt* of gastric tissue DNA was not significantly affected by *H. pylori* infection (Fig. 5). Analyses of 57 samples from 32 mice showed that Spi$^-$ mutant frequencies in infected mice (females at 6 MPI, $4.8 \pm 2.5 \times 10^{-6}$, $P = 0.09$; females at 12 MPI, $5.0 \pm 2.6 \times 10^{-6}$, $P = 0.30$; males at 6 MPI, $6.3 \pm 2.5 \times 10^{-6}$, $P = 0.87$; and males at 12 MPI, $5.2 \pm 1.4 \times 10^{-6}$, $P = 0.17$) were not significantly different from those of age-matched controls at either time point (all mice at 6 MPI, $2.9 \pm 1.3 \times 10^{-6}$; all mice at 12 MPI, $3.6 \pm 1.8 \times 10^{-6}$).

Current models of inflammation-driven carcinogenesis are based on chronic inflammation inducing mutations that lead to cancer (40, 41). Female mice at 6 MPI had more hyperplasia, epithelial defects, and dysplasia than infected males and age-matched controls, but this increase in pathologic findings was not accompanied by increased frequency of mutations. This was detected only in infected female mice at 12 MPI, which had experienced more severe gastritis for a longer period, suggesting that gastritis is necessary but not sufficient to induce mutagenesis. Similarly, duration of infection in itself was insufficient, as mutation frequency was not increased in male mice at 12 MPI. Based on the GHAI, infected male mice had a weaker response at 6 MPI compared with infected females, whereas by 12 MPI, the level of pathologic process was similar in both sexes. These data suggest that the delayed onset of severe gastric lesions in males reduced the duration of their exposure to chronic gastritis, protecting them from mutagenesis, highlighting the importance of severity and duration of the inflammatory response.

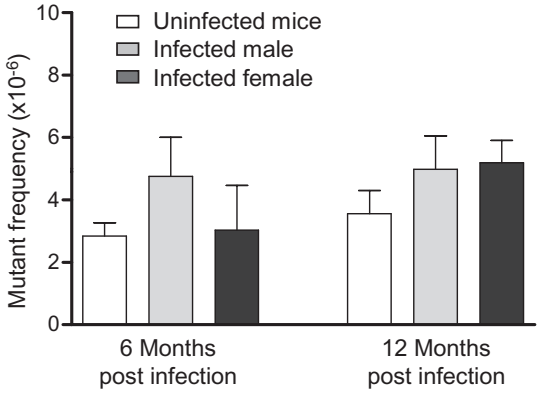

Fig. 5. Mutant frequency of deletions was unchanged by *H. pylori* infection. *H. pylori* infection did not alter the levels of deletions detected by the Spi$^-$ assay in uninfected mice (white bars; 6 MPI, n = 12; 12 MPI, n = 16), *H. pylori*-infected males (light gray bars; 6 MPI, n = 3; 12 MPI, n = 5) and *H. pylori*-infected females (dark gray bars; 6 MPI, n = 9; 12 MPI, n = 12). Control mice of both sexes were grouped for this analysis. Data are mean (SEM) of mutant frequency of mice in different treatment groups.

Our findings agree with current paradigms for the role of inflammation in carcinogenesis (4) and with the more severe pathology induced in female versus male C57BL/6 mice infected with *Helicobacter* spp. (42). Our observations in female *gpt* delta mice are consistent with previously reported data from female C57BL/6 Big Blue mice infected with *H. felis*, which induces more severe gastritis at earlier time points than *H. pylori*, effectively increasing the amount of DNA damage inflicted after infection (23, 43, 44). The higher mutation frequency found at 7 MPI in *H. felis*-infected female C57BL/6 Big Blue mice may be comparable to that occurring at 12 MPI in female *gpt* delta mice infected with *H. pylori*, based on increased inflammation and epithelial proliferation. In contrast, another study of DNA point mutations induced by *H. pylori* in male Big Blue mice reported that, although mutant frequency was increased at 6 MPI, it returned to control levels by 12 MPI (22). The decrease between 6 and 12 MPI was accompanied by loss of *iNOS* expression and reversion of the mutation spectrum to one indistinguishable from that of uninfected mice (22). Two possible explanations for these results are that (*i*) the increase in mutations at 6 MPI may have reflected jackpot mutations, because clonal expansion was not assessed or (*ii*) loss of infection resulted in absence of iNOS expression and reversion of the mutation spectrum. An additional factor pertinent to comparisons of previous mutagenesis studies involving gastric infection by *Helicobacter* spp. is the endogenous *Helicobacter* status of the mouse colony (45). We recently reported that concurrent, subclinical infection in C57BL/6 mice with non-gastric *Helicobacter bilis* significantly reduced *H. pylori*-associated premalignant gastric lesions at 6 and 11 MPI (46). This immunomodulatory effect could affect observed mutagenic responses,

and it is unknown whether Big Blue mice used in previous studies were free of enteric *Helicobacter* spp.

Our observed sex-based effects on mutagenesis induced by *H. pylori* in mice has not been reported previously, but sex bias has been found in other responses to infection. In *H. pylori*–infected Mongolian gerbils, immune responses and cytokine production were reported to be affected by sex (47), and *H. pylori* preferentially induced cancer in male INS-GAS mice (48). Greater female susceptibility to gastric *Helicobacter* infections has been noted previously in WT C57BL/6 mice (42), whereby females infected with *H. felis* experience an earlier onset of gastric inflammation, epithelial hyperplasia, atrophy, and apoptosis (42). Mechanisms responsible for the observed sex-based effects are incompletely understood, but findings to date collectively indicate that sex is an important variable, affecting strength of the host response to *H. pylori* infection, which in turn determines disease outcome.

The typical host response to *Helicobacter* infection is a proinflammatory Th1 response that causes chronic gastritis (49, 50). However, mouse strains such as BALB/c, which mount a strong antiinflammatory Th2 humoral immune response to *H. pylori* infection, develop less severe disease (51). We have previously shown that modulation of the Th1 response by an increased Th2 response reduces pathology associated with concurrent helminth infections (27). In the current study, the immune response of females to *H. pylori* infection was biased toward a greater Th1/Th2 ratio compared with males at both 6 and 12 mo. Higher Th1/Th2 ratios reflect a stronger inflammatory response to *H. pylori* infection. Furthermore, proinflammatory Th17 cells and regulatory T cells have been recently shown to modulate host responses to *H. pylori* (52, 53). *H. pylori*-specific Th17 immunity, mediated by IL-17 (54), increases inflammation unless it is suppressed by regulatory T cells, which are up-regulated by TGF-β and IL-10 (53). Higher levels of inflammation, epithelial defects, and atrophy were indeed observed in infected females at 6 MPI. At 12 MPI, the level of serum IgG2c was significantly elevated in infected females, reflective of increased proinflammatory cytokines in the gastric mucosa, and is consistent with the reduction in *H. pylori* colonization levels. The earlier onset of severe pathologic process caused by the Th1- and Th17-biased response to *H. pylori* was also associated with the increase in point mutations seen at 12 MPI.

In summary, we have shown that chronic *H. pylori* infection can cause premalignant gastric lesions and induce point mutations consistent with inflammatory processes. As our data are derived from analysis of nontranscribed DNA, it serves as an indicator of unbiased mutations reflecting genetic changes during the early stages of tumor initiation in inflamed tissues. At 12 mo, *H. pylori*-infected female C57BL/6 mice accumulate more inflammation-mediated point mutations compared with males as a result of a greater Th1-biased response to infection inducing earlier and more severe pathology. The sex-biased increase in premalignant gastric lesions and induction of mutations highlights the importance of taking into account sex-based effects in future studies of inflammation-driven disease.

Materials and Methods

Bacteria and Animals. *H. pylori* strain SS1 was grown on blood agar or *Brucella* broth with 5% FBS as described in *SI Materials and Methods*. Specific pathogen-free (including *Helicobacter* spp.) male and female C57BL/6 *gpt* delta mice (24) were infected by oral gavage with *H. pylori* SS1 or sham-dosed. At the indicated times, mice were euthanized, gastric tissue collected for histopathology and DNA and RNA extraction, and sera were collected for cytokine and Ig analysis. Gastric lesions were scored for inflammation, epithelial defects, atrophy, hyperplasia, mucous metaplasia, hyalinosis, intestinal metaplasia, and dysplasia using previously published criteria (55). The GHAI is the sum of inflammation, epithelial defects, atrophy, hyperplasia, intestinal metaplasia, and dysplasia scores. A detailed description of the husbandry, treatment, and histopathology is provided in *SI Materials and Methods*.

DNA Isolation and in Vitro Packaging. Genomic DNA was extracted from gastric tissue using RecoverEase DNA Isolation Kit (Stratagene) following the manufacturer's recommendations. λ-EG10 phages were packaged in vitro from genomic DNA using the Transpack Packaging Extract (Stratagene) following the instructions.

***gpt* Assay and Sequencing Analysis.** The 6-TG selection assay was performed as previously described (24, 56). Briefly, phages rescued from murine genomic DNA were transfected into *E. coli* YG6020 expressing Cre recombinase. Infected cells were cultured on plates containing chloramphenicol (Cm) and 6-TG for 3 d until 6-TG–resistant colonies appeared. To confirm the 6-TG–resistant phenotype, colonies were restreaked on plates containing Cm and 6-TG. Confirmed 6-TG–resistant colonies were cultured, and a 739-bp DNA product containing the *gpt* gene was amplified by PCR. DNA sequencing of the *gpt* gene was performed by the Biopolymers Facility at Harvard Medical School (Boston, MA) with AMPure beads (Agencourt) and a 3730xL DNA Analyzer (Applied Biosystems). Sequences were aligned with the *E. coli gpt* gene (GenBank M13422.1) (57) using Geneious (Biomatters). Mutations were classified as transitions, transversions, deletions, insertions, or complex (multiple changes). Duplicate mutations at the same site within an individual tissue were excluded to account for clonal expansion of sibling mutations. More information on primers and methods is provided in *SI Materials and Methods*.

Spi$^-$ Assay. The Spi$^-$ assay was performed as described in *SI Materials and Methods*. Briefly, phages rescued from murine genomic DNA were transfected into *E. coli* strains with or without P2 lysogen. Infected cells were cultured overnight on λ-trypticase agar plates to allow plaque formation. The inactivation of *red* and *gam* genes was confirmed by respotting plaques on another *E. coli* strain with P2 lysogen (24).

mRNA Expression. RNA was extracted from gastric tissue and reverse-transcribed to cDNA. Quantitative real-time PCR was performed using TaqMan Gene Expression Assays (Applied Biosystems). TaqMan primers and analysis methods are described in *SI Materials and Methods*.

***H. pylori* Detection.** *H. pylori* levels in the gastric mucosa were quantified by real-time quantitative PCR assay of gastric DNA as described in *SI Materials and Methods*. A threshold of 15 copies of the *H. pylori* genome was set as the lower limit for a positive sample.

Serum IgG Isotype Measurement. Sera were analyzed for *H. pylori*-specific IgG2c and IgG1 by ELISA. Additional information on the measurements is provided in *SI Materials and Methods*.

Statistical Analysis. Two-way ANOVA followed by Bonferroni posttests were used to analyze GHAI and mRNA expression values. Student two-tailed *t* tests were used to analyze mutant and mutation frequency data and serum IgG isotypes. Poisson distribution analysis was used to determine hotspots at a 99% confidence level (58). For some analyses, age-matched controls of both sexes were grouped when no statistical differences were detected between sexes. Analyses were done with GraphPad Prism, version 4.0, or Microsoft Excel 2002. $P < 0.05$ was considered significant.

ACKNOWLEDGMENTS. We thank Sureshkumar Muthupalani for help with the histological images and Laura J. Trudel for assistance with the manuscript and figures. This study is dedicated in loving memory of David Schauer, a mentor and a friend, for his contribution in the design and analysis of this work. This work was supported by National Institutes of Health Grants R01-AI037750 and P01-CA026731 and Massachusetts Institute of Technology Center for Environmental Health Sciences Program Project Grant P30-ES02109.

1. Fox JG, Wang TC (2007) Inflammation, atrophy, and gastric cancer. *J Clin Invest* 117: 60–69.
2. Suerbaum S, Michetti P (2002) Helicobacter pylori infection. *N Engl J Med* 347:1175–1186.
3. International Agency for Research on Cancer (1994) Schistosomes, liver flukes and Helicobacter pylori. IARC Working Group on the Evaluation of Carcinogenic Risks to Humans. Lyon, 7-14 June 1994. *IARC Monogr Eval Carcinog Risks Hum* 61:1–241.
4. Coussens LM, Werb Z (2002) Inflammation and cancer. *Nature* 420:860–867.
5. Obst B, Wagner S, Sewing KF, Beil W (2000) Helicobacter pylori causes DNA damage in gastric epithelial cells. *Carcinogenesis* 21:1111–1115.
6. Xu H, et al. (2004) Spermine oxidation induced by Helicobacter pylori results in apoptosis and DNA damage: Implications for gastric carcinogenesis. *Cancer Res* 64: 8521–8525.

7. Davies GR, et al. (1994) Relationship between infective load of Helicobacter pylori and reactive oxygen metabolite production in antral mucosa. *Scand J Gastroenterol* 29: 419–424.
8. Davies GR, et al. (1994) Helicobacter pylori stimulates antral mucosal reactive oxygen metabolite production in vivo. *Gut* 35:179–185.
9. Mannick EE, et al. (1996) Inducible nitric oxide synthase, nitrotyrosine, and apoptosis in Helicobacter pylori gastritis: Effect of antibiotics and antioxidants. *Cancer Res* 56: 3238–3243.
10. Meira LB, et al. (2008) DNA damage induced by chronic inflammation contributes to colon carcinogenesis in mice. *J Clin Invest* 118:2516–2525.
11. Nair J, et al. (2006) Increased etheno-DNA adducts in affected tissues of patients suffering from Crohn's disease, ulcerative colitis, and chronic pancreatitis. *Antioxid Redox Signal* 8:1003–1010.
12. Zhuang JC, Lin C, Lin D, Wogan GN (1998) Mutagenesis associated with nitric oxide production in macrophages. *Proc Natl Acad Sci USA* 95:8286–8291.
13. Sato Y, et al. (2006) IL-10 deficiency leads to somatic mutations in a model of IBD. *Carcinogenesis* 27:1068–1073.
14. Bartsch H, Nair J (2004) Oxidative stress and lipid peroxidation-derived DNA-lesions in inflammation driven carcinogenesis. *Cancer Detect Prev* 28:385–391.
15. Nair U, Bartsch H, Nair J (2007) Lipid peroxidation-induced DNA damage in cancer-prone inflammatory diseases: a review of published adduct types and levels in humans. *Free Radic Biol Med* 43:1109–1120.
16. Kang JM, Iovine NM, Blaser MJ (2006) A paradigm for direct stress-induced mutation in prokaryotes. *FASEB J* 20:2476–2485.
17. Crabtree JE, Ferrero RL, Kusters JG (2002) The mouse colonizing Helicobacter pylori strain SS1 may lack a functional cag pathogenicity island. *Helicobacter* 7:139–140, author reply 140–141.
18. Lee A, Mitchell H, O'Rourke J (2002) The mouse colonizing Helicobacter pylori strain SS1 may lack a functional cag pathogenicity island: Response. *Helicobacter* 7:140–141.
19. Miyazawa M, et al. (2003) Suppressed apoptosis in the inflamed gastric mucosa of *Helicobacter pylori*-colonized iNOS-knockout mice. *Free Radic Biol Med* 34:1621–1630.
20. Jang J, et al. (2003) Malgun (clear) cell change in *Helicobacter pylori* gastritis reflects epithelial genomic damage and repair. *Am J Pathol* 162:1203–1211.
21. Lee H, et al. (2000) "Malgun" (clear) cell change of gastric epithelium in chronic *Helicobacter pylori* gastritis. *Pathol Res Pract* 196:541–551.
22. Touati E, et al. (2003) Chronic Helicobacter pylori infections induce gastric mutations in mice. *Gastroenterology* 124:1408–1419.
23. Jenks PJ, Jeremy AH, Robinson PA, Walker MM, Crabtree JE (2003) Long-term infection with Helicobacter felis and inactivation of the tumour suppressor gene p53 cumulatively enhance the gastric mutation frequency in Big Blue transgenic mice. *J Pathol* 201:596–602.
24. Nohmi T, et al. (1996) A new transgenic mouse mutagenesis test system using Spi- and 6-thioguanine selections. *Environ Mol Mutagen* 28:465–470.
25. Ihrig M, Whary MT, Dangler CA, Fox JG (2005) Gastric helicobacter infection induces a Th2 phenotype but does not elevate serum cholesterol in mice lacking inducible nitric oxide synthase. *Infect Immun* 73:1664–1670.
26. Lee CW, et al. (2008) Helicobacter pylori eradication prevents progression of gastric cancer in hypergastrinemic INS-GAS mice. *Cancer Res* 68:3540–3548.
27. Fox JG, et al. (2000) Concurrent enteric helminth infection modulates inflammation and gastric immune responses and reduces helicobacter-induced gastric atrophy. *Nat Med* 6:536–542.
28. De Bont R, van Larebeke N (2004) Endogenous DNA damage in humans: A review of quantitative data. *Mutagenesis* 19:169–185.
29. Burney S, Caulfield JL, Niles JC, Wishnok JS, Tannenbaum SR (1999) The chemistry of DNA damage from nitric oxide and peroxynitrite. *Mutat Res* 424:37–49.
30. Kadlubar FF, et al. (1998) Comparison of DNA adduct levels associated with oxidative stress in human pancreas. *Mutat Res* 405:125–133.
31. Pandya GA, Moriya M (1996) 1, N6-ethenodeoxyadenosine, a DNA adduct highly mutagenic in mammalian cells. *Biochemistry* 35:11487–11492.
32. Ambs S, et al. (1999) Relationship between p53 mutations and inducible nitric oxide synthase expression in human colorectal cancer. *J Natl Cancer Inst* 91:86–88.
33. Kim MY, Wogan GN (2006) Mutagenesis of the supF gene of pSP189 replicating in AD293 cells cocultivated with activated macrophages: roles of nitric oxide and reactive oxygen species. *Chem Res Toxicol* 19:1483–1491.
34. Dedon PC, Plastaras JP, Rouzer CA, Marnett LJ (1998) Indirect mutagenesis by oxidative DNA damage: formation of the pyrimidopurinone adduct of deoxyguanosine by base propenal. *Proc Natl Acad Sci USA* 95:11113–11116.
35. Jackson AL, Loeb LA (2001) The contribution of endogenous sources of DNA damage to the multiple mutations in cancer. *Mutat Res* 477:7–21.
36. Wood ML, Esteve A, Morningstar ML, Kuziemko GM, Essigmann JM (1992) Genetic effects of oxidative DNA damage: comparative mutagenesis of 7,8-dihydro-8-oxoguanine and 7,8-dihydro-8-oxoadenine in Escherichia coli. *Nucleic Acids Res* 20: 6023–6032.
37. Pang B, et al. (2007) Lipid peroxidation dominates the chemistry of DNA adduct formation in a mouse model of inflammation. *Carcinogenesis* 28:1807–1813.
38. Masumura K, et al. (2003) Low dose genotoxicity of 2-amino-3,8-dimethylimidazo[4,5-f]quinoxaline (MeIQx) in gpt delta transgenic mice. *Mutat Res* 541:91–102.
39. Masumura K, et al. (2000) Characterization of mutations induced by 2-amino-1-methyl-6-phenylimidazo[4,5-b]pyridine in the colon of gpt delta transgenic mouse: novel G:C deletions beside runs of identical bases. *Carcinogenesis* 21:2049–2056.
40. Balkwill F, Coussens LM (2004) Cancer: An inflammatory link. *Nature* 431:405–406.
41. Clevers H (2004) At the crossroads of inflammation and cancer. *Cell* 118:671–674.
42. Court M, Robinson PA, Dixon MF, Jeremy AH, Crabtree JE (2003) The effect of gender on Helicobacter felis-mediated gastritis, epithelial cell proliferation, and apoptosis in the mouse model. *J Pathol* 201:303–311.
43. Fox JG, et al. (2002) Germ-line p53-targeted disruption inhibits helicobacter-induced premalignant lesions and invasive gastric carcinoma through down-regulation of Th1 proinflammatory responses. *Cancer Res* 62:696–702.
44. Lee A, Fox JG, Otto G, Murphy J (1990) A small animal model of human Helicobacter pylori active chronic gastritis. *Gastroenterology* 99:1315–1323.
45. Taylor NS, et al. (1995) Long-term colonization with single and multiple strains of Helicobacter pylori assessed by DNA fingerprinting. *J Clin Microbiol* 33:918–923.
46. Lemke LB, et al. (2009) Concurrent Helicobacter bilis infection in C57BL/6 mice attenuates proinflammatory *H. pylori*-induced gastric pathology. *Infect Immun* 77: 2147–2158.
47. Crabtree JE, et al. (2004) Gastric mucosal cytokine and epithelial cell responses to Helicobacter pylori infection in Mongolian gerbils. *J Pathol* 202:197–207.
48. Fox JG, et al. (2003) Host and microbial constituents influence Helicobacter pylori-induced cancer in a murine model of hypergastrinemia. *Gastroenterology* 124:1879–1890.
49. Bamford KB, et al. (1998) Lymphocytes in the human gastric mucosa during Helicobacter pylori have a T helper cell 1 phenotype. *Gastroenterology* 114:482–492.
50. Mohammadi M, Czinn S, Redline R, Nedrud J (1996) Helicobacter-specific cell-mediated immune responses display a predominant Th1 phenotype and promote a delayed-type hypersensitivity response in the stomachs of mice. *J Immunol* 156: 4729–4738.
51. Sakagami T, et al. (1996) Atrophic gastric changes in both Helicobacter felis and Helicobacter pylori infected mice are host dependent and separate from antral gastritis. *Gut* 39:639–648.
52. Lee CW, et al. (2007) Wild-type and interleukin-10-deficient regulatory T cells reduce effector T-cell-mediated gastroduodenitis in Rag2-/- mice, but only wild-type regulatory T cells suppress Helicobacter pylori gastritis. *Infect Immun* 75:2699–2707.
53. Kao JY, et al. (2010) Helicobacter pylori immune escape is mediated by dendritic cell-induced Treg skewing and Th17 suppression in mice. *Gastroenterology* 138:1046–1054.
54. Xu S, Cao X (2010) Interleukin-17 and its expanding biological functions. *Cell Mol Immunol* 7:164–174.
55. Rogers AB, et al. (2005) Helicobacter pylori but not high salt induces gastric intraepithelial neoplasia in B6129 mice. *Cancer Res* 65:10709–10715.
56. Masumura K, et al. (1999) Spectra of gpt mutations in ethylnitrosourea-treated and untreated transgenic mice. *Environ Mol Mutagen* 34:1–8.
57. Nüesch J, Schümperli D (1984) Structural and functional organization of the gpt gene region of Escherichia coli. *Gene* 32:243–249.
58. Kim MY, Dong M, Dedon PC, Wogan GN (2005) Effects of peroxynitrite dose and dose rate on DNA damage and mutation in the supF shuttle vector. *Chem Res Toxicol* 18: 76–86.